

GAMMA FUNCTION AND ITS APPLICATION

Aisyah Amirah binti Ahmad Senusi & En. Che Lokman Jaafar

Abstract

Special functions occur quite frequently in mathematical analysis and lend itself rather frequently in physical and engineering applications. Among the special functions, gamma function seemed to be widely used. The purpose of this thesis is to analyse the various properties of gamma function and use these properties and its definition to derive and tackle some integration problem which occur quite frequently in applications. It should be noted that if elementary techniques such as substitution and integration by parts were used to tackle most of the integration problems, then we will end up with frustration. Due to this, importance of gamma function cannot be denied.

Keywords: Special function, Gamma function, integrals

Introduction

In mathematics, a function is a relation between a set of inputs and a set of permissible outputs with the property that each input is related to exactly one output. A basic example is the function that relates each real number x to its square x^2 . The output of a function f corresponding to an input x is denoted by $f(x)$. (Read as " f of x "). Functions of various kinds are "the central objects of investigation in most fields of modern mathematics. There are many ways to describe or represent a function. Some functions may be defined by a formula or algorithm that tells how to compute the output for a given input. Others are given by a picture, called the graph of the function. In science, functions are sometimes defined by a table that gives the outputs for selected inputs. A function also could be described implicitly.

In analogy with arithmetic, it is possible to define addition, subtraction, multiplication, and division of functions, in those cases where the output is a number. Another important operation defined on functions is function composition, where the output from one function becomes the input to another function. Special function is a particular mathematical functions which have more or less established names and notations due to their importance in mathematical analysis, functional analysis, physics, or other applications. It usually named after an early investigator of its properties. Some examples of special function include the gamma function, beta function, hyper geometric function, elliptic function, and geometric function.

By year 1720, Euler started his major industrial drive into the world of calculus. And he started talking about lots of other standard special functions. He found the gamma function as a continuation of factorial. He also defined Bessel functions for investigating circular drums. Then, he looked systematically at elliptic integrals. He usually didn't give the functions any names. But gradually more and more of the functions he talked about started being used by several people. And after a few iterations, he started having definite notations, and definite names.

Literature Review

The gamma function $\Gamma(x)$ is applied in exact sciences almost as often as the well-known factorial symbol $x!$. It was introduced by the famous mathematician L. Euler (1729) as a natural extension of the factorial operation $x!$ from positive integers x to real and even complex values of this argument. The gamma function $\Gamma(x)$ has a long history of development and numerous applications since 1729 when Euler derived his famous integral representation of the factorial function. The history of the gamma function is described in the subsection "General" of the section "Gamma function". Since the famous work of J. Stirling (1730) who first used series for $\log(x!)$ to derive the asymptotic formula for $x!$, mathematicians have used the logarithm of the gamma function $\log(\Gamma(x))$ for their investigations of the gamma function $\Gamma(x)$. Investigators of mention include: C. Siegel, A. M. Legendre, K. F. Gauss, C. J. Malmstén, O. Schlömilch, J. P. M. Binet (1843), E. E. Kummer (1847), and G. Plana (1847). M. A. Stern (1847) proved convergence of the Stirling's series for the derivative of $\log(\Gamma(x))$. C. Hermite (1900) proved convergence of the Stirling's series for $\log(\Gamma(x + 1))$ if x is a complex number.

During the twentieth century, the function $\log \Gamma(x)$ was used in many works where the gamma function was applied or investigated. The appearance of computer systems at the end of the twentieth century demanded more careful attention to the structure of branch cuts for basic mathematical functions to support the validity of the mathematical relations everywhere in the complex plane. This led to the appearance of a special log-gamma function $\log \Gamma(x)$, which is equivalent to the logarithm of the gamma function $\log(\Gamma(x))$ as a multivalued analytic function, except that it is conventionally defined with a different branch cut structure and principal sheet. The loggamma function $\log \Gamma(x)$ was introduced by J. Keiper (1990) for *Mathematica*. It allows a concise formulation of many identities related to the Riemann zeta function, $\zeta(x)$.

[Arpad, 2000] The gamma function $\Gamma(x)$ is defined by:

$$\Gamma(x) = \int_0^{\infty} t^{x-1} e^{-t} dt$$

where $x > 0$.

Clearly $\Gamma(1) = 1$ as can be seen by

$$\Gamma(1) = \int_0^{\infty} e^{-t} dt = [-e^{-t}]_0^{\infty} = 1$$

A recurrence formula for the gamma function is:

$$\Gamma(x + 1) = x \Gamma(x)$$

Using this recurrence formula, x can be extended to $x < 0$.

This is possible by referring the recurrence formula as

$$\Gamma(x) = \frac{\Gamma(x + 1)}{x}$$

This remarkable function leads many applications, particularly those concerning evaluating improper integrals.

To apply this function we need some properties of this function. One of the famous properties is the Euler Duplication formula which state:

$$\Gamma(x)\Gamma(1-x) = \frac{\pi}{\sin \pi x}$$

where $0 < x < 1$.

Properties of gamma function can be used to derive or proved many results of difficult improper integrals particularly those of the first kind. Often, the case in calculus course we try to evaluate improper integral using the standard technique such as substitution, partial fraction, integration by parts and etc. However, when the integrals become more involved, the standard techniques are inferior. Gamma function can be employed to tackle some of these integrals.

Gamma function is also known as Factorial function this is because if x is positive integer. Then we can show that

$$\Gamma(x+1) = x! \quad , x = 1, 2, 3, \dots$$

Methodology

In completing the research, we will use two methods to solve our problem. The first one is basic method for example integration, where integral is one of the main method used to solve gamma function. In integration, we have some techniques that we need to know in order to solve integration such as integration by substitutions, integration by tabular method, integration by parts and also integration using partial fractions. Besides, we also need to study about a few integration methods for different function for example, integration of trigonometric functions, hyperbolic functions, irrational functions and also for the inverse of both three functions. This knowledge in integration is needed for us to solve the gamma function.

Besides, we also will use gamma function itself as a method to solve the mathematical problem and the physics application. When we have some problem to be solved, a gamma function can be used to derive the solution for the problem. Furthermore, in solving certain problem of gamma function, we will use other special function such as Beta function.

There are some techniques of integration that can be used in solving gamma function problem. The first is integration by substitution. This method is the first to be considered when we to solve any integral problem. By using this method, we need to change the integrand into an expression of basic integral forms.

The Next is the integration by parts. This is another important method to solve integrals, especially when the problem involve is product of algebraic and transcendental function. Integration by parts is derived from these formulas, which is

$$\frac{d}{dx}(uv) = u \frac{dv}{dx} + v \frac{du}{dx}$$

Then integrate with respect to x , it becomes

$$uv = \int u \frac{dv}{dx} dx + \int v \frac{du}{dx} dx$$

Then,

$$\int u dv = uv - \int v du.$$

This formula expresses an integral $\int u dv$ in term of a second integral $\int v du$.

In this method, the evaluation of integrals needs repeated integrations and differentiation. The calculation is monotonous and the stages are too long and complicated. But, we can get over this by using tabular method. After solving the forms of integrals before using $\int u dv$, then we now shall solve using $\int uv' dx$ where $dv = v' dx$. For this to be feasible, the integrals must satisfy the following condition. First, u can be differentiated repeatedly with respect to x until become 0. Next, v' can be integrated repeatedly with respect to x easily.

Since the definition of gamma function is in form of improper integral, we need some results on improper integrals of the form $\int_0^\infty f(x)dx$. First,

$$\int_0^\infty f(x)dx = \lim_{b \rightarrow \infty} \int_a^b f(x)dx$$

First,

$$\int_a^\infty e^{tx} dx,$$

where t is a constant, converges if $t > 0$ and diverges if $t \leq 0$

Secondly,

$$\int_a^\infty \frac{dx}{x^p}$$

where $a > 0$, p is a constant, converges if $p > 1$ and diverges if $p < 1$

The next is, quotient test for integrals with non-negative integrands.

- i. If $f(x) \geq 0$ and $g(x) \geq 0$ and if $\lim_{x \rightarrow \infty} \frac{f(x)}{g(x)} = A$, $A \neq 0$ or $A \neq \infty$, then $\int_a^\infty f(x)dx$ and $\int_a^\infty g(x)dx$ with both converges or both diverges.
- ii. If $A = 0$ in (i), $\int_a^\infty g(x)dx$ converges, then $\int_a^\infty f(x)dx$ also converges.
- iii. If $A = \infty$ in (i), $\int_a^\infty g(x)dx$ diverges, then $\int_a^\infty f(x)dx$ also diverges.

The method used next is differentiation under the integral sign. Leibnitz's Rule for differentiating under the integrals sign states that:

Let

$$\phi(x) = \int_u^v f(x, \alpha) dx,$$

$a \leq x \leq b$. u and v may depends on x . Then

$$\frac{d\phi}{dx} = \int_u^v \frac{df}{dx} dx + f(v, x) \frac{dv}{dx} - f(u, x) \frac{du}{dx}$$

Result and Discussion

Definition of gamma function:

$$\Gamma(x) = \int_0^{\infty} t^{x-1} e^{-t} dt, \quad x > 0$$

The gamma function converges for $x > 0$

Here are some properties of Gamma Function:

1. $\Gamma\left(\frac{1}{2}\right) = \sqrt{\pi}$
2. If x is a positive integer, then $\Gamma(x + 1) = x!$
3. $\Gamma(x + 1) = x \Gamma(x)$,
4. $\Gamma(x) = 2 \int_0^{\infty} e^{-t^2} t^{2x-1} dt$
5. $\int_0^{\frac{\pi}{2}} \cos^{2x-1} \theta \sin^{2y-1} \theta d\theta = \frac{\Gamma(x)\Gamma(y)}{2\Gamma(x+y)}$
6. $\Gamma(2x) = \frac{2^{2x-1}}{\sqrt{\pi}} \Gamma(x)\Gamma\left(x + \frac{1}{2}\right)$
7. $\Gamma(x)\Gamma(1-x) = \frac{\pi}{\sin \pi x}$

By using the properties of gamma function, we can solve some of integrals problem. For example,

- Evaluate

$$\int_0^a y^4 \sqrt{a^2 - y^2} dy$$

Solution:

Let $y^2 = a^2 x$ or $y = a\sqrt{x}$

Since $y = 0$, $x = 0$ and $y = a$, $x = 1$

Then the integrals become

$$\begin{aligned} \frac{a^6}{2} \int_0^1 x^{\frac{3}{2}} (1-x)^{\frac{1}{2}} dx &= \frac{a^6}{2} B\left(\frac{5}{2}, \frac{3}{2}\right) \\ &= \frac{a^6 \Gamma\left(\frac{5}{2}\right) \Gamma\left(\frac{3}{2}\right)}{2\Gamma(4)} \\ &= \frac{a^6 \pi}{32} \end{aligned}$$

- Evaluate

$$\int_0^1 \frac{dx}{\sqrt{-\ln x}}$$

Solution:

Let $-\ln x = u$ so, $x = e^{-u}$ and $dx = e^{-u} du$
 since $x = 1$, $u = 0$. and $x = 0$, $u = \infty$

$$\begin{aligned} & \int_0^1 \frac{dx}{\sqrt{-\ln x}} \\ &= \int_0^\infty \frac{e^{-u}}{\sqrt{u}} du \\ &= \int_0^\infty e^{-u} u^{-\frac{1}{2}} du \end{aligned}$$

$$\begin{aligned} n - 1 &= -\frac{1}{2} \\ n &= \frac{1}{2} \end{aligned}$$

$$\begin{aligned} &= \Gamma\left(\frac{1}{2}\right) \\ &= \sqrt{\pi} \end{aligned}$$

- Evaluate

$$\int_0^\infty x^m e^{-ax^n} dx$$

where m, n, a are positive constants.

Solution:

Let $ax^n = y$

$$\begin{aligned} \int_0^\infty x^m e^{-ax^n} dx &= \int_0^\infty \left\{ \left(\frac{y}{a} \right)^{\frac{1}{n}} \right\}^m e^{-y} d \left\{ \left(\frac{y}{a} \right)^{\frac{1}{n}} \right\} \\ &= \frac{1}{na^{\frac{m+1}{n}-1}} \int_0^\infty y^{\frac{m+1}{n}-1} e^{-y} dy \\ &= \frac{1}{na^{\frac{m+1}{n}}} \Gamma\left(\frac{m+1}{n}\right) \end{aligned}$$

Conclusion

At the beginning of this research, we have introduced the gamma function as one of the important special function that is well known in the worldwide. This special function also had been used widely in mathematics. In beginning, we had introduced the special function itself. As for further research, we decided to choose the gamma function. Then, we introduced the history of gamma function and some brief explanation of gamma function. After a while, we managed to understand the properties and some theorem involved in the gamma function. Besides, having good understanding on basic integration and differentiation

of equation will help in solving problem of gamma function. By using the properties and theorems, it will easier to understand and solve problem of the function. Finally, we managed to solve problem analytically and some of it had been successfully proved.

References

Abd Wahid Md. Raji, Hamisan Rahmat, Ismail Kamis, Mohd Nor Mohamad, Ong Chee Tiong (2011), *Engineering Mathematics 1*, Comtech Marketing Sdn Bhd.

Andrews, G.E, Askey, R. and Roy, R (1999), *Special Function*, Cambridge University Press, Cambridge.

Arpad Elbert and Andrea LaForgia (2000), *Proceeding of the American Mathematical Society, On Some Properties of the Gamma Function*, 128.

B.C. Carlson (1977), *Special Functions of Applied Mathematics*, Academic Press Inc, New York.

Emil Artin (1964), *The Gamma Function*, Holt, Rinehart and Winston Inc.

Erdelyi, A., Magnus, W., Oberhettinger, F. and Tricomi, F.G.(1991), *The Gamma Function,* " Ch. 1 in *Higher Transcendental Functions*, Vol. 1, Krieger, New York.

Freeden, W; Gutting, M (2013), *Special Functions of Mathematical Physics*, Birkhauser Basel.

Luis A. Medina, Victor H. Moll (2009), *The Integrals in Gradshteyn and ryzhik. Part 10: The Digamma Function*, Scientia Universidad Técnica Fed. Santa María, 45-66.

Mark W. Coffey (2010), *Integral and series representations of the digamma and polygamma functions*, Department of Physics, Colorado School of Mines.

Murray R. Spiegel (1983), *Theory and Problems of Advanced Mathematics for Engineers and Scientist*, McGraw-Hill Book Co, Singapore.

V. Moll.(2007), *The integrals in Gradshteyn and Ryzhik. Part 4: The gamma function.* Scientia, 15:37–46.

Mathematical Analysis for Tumor Growth Model of Ordinary Differential Equations

Amira Fadina Ahmad Fadzil and Normah Maan

1.1 INTRODUCTION

In mathematics, an ordinary differential equation (ODE) is an equation containing a function or functions of one independent variable and its derivatives. There are two types of ordinary differential equations which are linear or nonlinear in the form of first order, second order and even higher order. A system of differential equation could be in the form of a two dimensional system, a three dimensional systems or nth dimensional system.

The use of differential equations have been applied in many real field areas such as in engineering, physics, economics, biology and other sciences. For instances, in biology there are lots of dynamical populations involving differential equations which indicates the rate of change of the population. The system of differential equations in biological perspective is also known as a dynamical system.

In biology, the studies of mathematical modelling of a dynamical system often involve medical field applications. One of the mathematical biology applications that have been studied by many researchers is related to the tumor growth population models. Some of them are Buric, N. and Todorovic, D. [1], Villasana, M., and Radunskaya, A. [2], D'Onofrio, A. *et al.* [3], Rihan, F. A. *et al.* [4], Borges, F. S. *et al.* [5] and Dong, Y, *et al.* [6].

In understanding the tumor cases, except for Borges, F. S. *et al.* [5], all of them have studied the stability of the steady state solution of the tumor-immune interaction and all include delay in their study to check the effect of delays regarding the response of immune system to the tumor cells. For Dong, Y, *et al.* [6] only, they introduce two types of delay

which are the immune activation delay for effector cells and activation delay for helper T cells.

Besides adding a delay, some of them also study bifurcation of the steady state solution of the model as Buric, N. and Todorovic, D. [1], Villasana, M., and Radunskaya, A. [2], D'Onofrio, A. *et al.* [3] and Rihan, F. A. *et al.* [4]. They considered the change of stability of the steady state via Hopf bifurcation. Other than that, Borges, F. S. *et al.* [5] examined the drug effect on the model. Their model exposes the domination of tumor cells when either continuous or pulsed treatment is applied and they show that the tumor cells were exponentially decline when patients are treated with the drug.

In this study, two types of tumor growth model from Villasana, M., and Radunskaya, A. [2] are studied. The first model considered a tumor interphase and mitosis interaction and the second model considered a tumor-immune interaction. The stability of the steady state is found by analysing the characteristic equation and the stability maps created for both systems are compared to show the influence of adding immune suppression to the tumor growth.

1.2 BACKGROUND OF STUDY

Before studying the models and understanding the tumor growth, the basic of how a normal cell and immune system is necessary.

1.2.1 Cell Cycle of A Normal Cell

Cell cycle is also known as cell division. For a cell cycle to be successfully and completely divides, it needs to go through four discrete phases referred to as phase G_1 , phase S, phase G_2 and phase M [7]. The first phase is the first of interphase which is G_1 . G_1 phase is a resting phase which occurs after a cell has gone through mitosis and it is the longest phase of the cycle which might last for two days. It is also known as pre-synthetic phase. This phase give a gap period for the cell to decide whether to continue to divide.

Next is the second phase called the S phase or the synthetic phase which often last for 8 to 20 hours at most. During S phase, the Deoxyribonucleic Acid (DNA) replicates and once it is done the cycle enters the next phase which is G_2 phase. The duration time for the S phase may take longer than usual if there is DNA damage. G_2 phase is also a resting phase which

the cell prepares for the division or mitosis. It also called post-synthetic phase as it offers a break to the cell to complete the DNA replication process from S phase.

Lastly, the mitosis or division of cell is the last phase before the cell goes through mitosis again. For a normal cell, it takes only about one hour in order for the cell to complete mitosis. During this phase, the cell separates the duplicated sets of chromosomes between daughter cells. Then again, a cell may leave this cycle during G_1 and become a non-dividing or quiescent cell [2].

1.2.2 Factors of Tumor Development

Cancer or tumor cells often described as loss of control of the cell cycle. Generally, all tumor cells share one major characteristic. They are abnormal cells in which the processes of regulating a normal cell cycle are interrupted. The tumor cells may develop from the changes of mutations or some environmental factors such as Ultraviolet light, X-rays, chemicals, tobacco products and viruses. Normally, the tumor cells were not caused from only one factor.

Since the abnormalities in cancer cells usually caused from mutations, so over time more genes will become mutated. This is because the already mutated genes that normally repair DNA damage are not functioning well. Later, mutations begin to increase in the cell, causing further abnormalities. It is true that some of the mutated cells may die but the remaining abnormal cell left will continue to multiply.

Therefore, it does not necessarily that the cells proliferate rapidly than normal cells but it is because of there exist an abnormality in regulating the cell cycle which causes an uncontrollable proliferation. Similar to normal cells, tumor cells too might cycle again or not after they have gone through mitosis. So, as long as the tumor cells stay in their original location, they are considered benign but if they become aggressive, they are considered malignant.

Therefore, our body cell is the most important things that need to be taken care of but since the cells is unseen, people cannot recognize if the cell does not function well in their bodies until there is symptoms showed up. In this case, the dangerous tumor cells may have developed and proliferated.

1.2.3 Humans Immune System

In our body, our immune system is comprises of many type of cells with various functions. Some of the important cell type is the lymphocytes which have a subset called T cells. The T cells have two subcategories which are the helper T cells and the cytotoxic T lymphocytes cells (CTL). These CTL cells function dynamically in fighting or restricting the tumor cells. In our case, we take CTL cells as the main representation of the immune system and consider only one form of interactions which is one to one binding of CTL cells to tumor cells [2].

In finding the cure of the disease, it is true that there are many specific drugs used by scientists that would have restrict the proliferation of the cancer cells. However, in this paper we are interested in studying the model of a drug free systemspecifically in a non-delay case. For a better understanding and as a comparison, this study considers two cases of a drug free model which include and exclude the immune response factor.

1.2.4 Tumor Growth Model of Ordinary Differential Equations

In this research the two models from Villasana, M., and Radunskaya, A. [2] discussedhere are the drug-free ordinary differential equation model for tumor growth in a non-delay case without immune suppression

$$\frac{dT_I}{dt} = 2a_4T_M - (d_2 + a_1)T_I \quad (1.1a)$$

$$\frac{dT_M}{dt} = a_1T_I - dT_M \quad (1.1b)$$

and the drug-free differential equation model for tumor growth in a non-delay case in the presence of immune response

$$\frac{dT_I}{dt} = 2a_4T_M - (c_1I + d_2)T_I - a_1T_I \quad (1.2a)$$

$$\frac{dT_M}{dt} = a_1T_I - d_3T_M - a_4T_M - c_3T_MI \quad (1.2b)$$

$$\frac{dI}{dt} = k + \frac{\rho I(T_I + T_M)^n}{\alpha + (T_I + T_M)^n} - c_2IT_I - c_4T_MI - d_1I \quad (1.2c)$$

where T_I denote the population of tumor cells during interphase at time t , T_M denote the population of tumor cells during mitosis at time t and $I(t)$ denote the immune system population at time t . The terms $T_M I$ and $T_I I$ indicates the standard competition terms which represents losses due to encounters among different type of cells.

The terms $d_2 T_I$, $d T_M$ and $d_1 I$ represent proportions of natural cell death or apoptosis while a_1 and a_4 represent the different rates of cell reproduction. Meanwhile, the term c_i indicate the losses from encounters of tumor cells with T cells of immune system and lastly, the term $\frac{\rho I(T_I+T_M)^n}{\alpha+(T_I+T_M)^n}$ represents the nonlinear growth of the T cells immune population due to stimulus by the tumor cells. The parameters ρ , α and n is influenced by the type of tumor and the condition of the immune system specially its capability to create cytokinesis.

For a deeper understanding in the behavior of this model, the parameter values and ranges from Villasana, M., and Radunskaya, A.[2] have been set in Table 1.1.

Table 1.1 Estimated parameters value for the models

Parameters	Estimated Value
a_1	0.8470 day ⁻¹
a_4	0.9159 day ⁻¹
$c_1 = c_3$	2.16×10^{-7} cell day ⁻¹
$c_2 = c_4$	3.422×10^{-10} cell day ⁻¹
d_1	0.04 day ⁻¹
d_2	0.1145 day ⁻¹
d_3	0.6641 day ⁻¹
k	1.3×10^4 cell day ⁻¹

ρ 0.2day⁻¹

α (0.3 × 10⁶ cell)³

n 3

METHOD OF SOLUTION

The tumor growth model that needs to be solved is of a two dimensional system of ordinary differential equations and three dimensional system which have the form

$$\begin{aligned}\frac{dN_1}{dt} &= f_1(N_1, N_2, \dots, N_k) \\ \frac{dN_2}{dt} &= f_2(N_1, N_2, \dots, N_k) \\ \frac{dN_3}{dt} &= f_3(N_1, N_2, \dots, N_k)\end{aligned}\tag{1.3}$$

where the f_i can be nonlinear functions and the right-hand-side of the ODEs may depend only on the independent variable t . Since this study involved solving the stability analysis of the solution, then the earliest step is to find the steady state of both systems.

1.2.1 The Drug-Free Ordinary Differential Equation Model for Tumor Growth in A Non-Delay Case without Immune Suppression

For the two dimensional system of the first case in Equations(1.1a) and (1.1b), the steps to find the stability of the steady state of the system are as follows:

Step 1: Find the steady state solution of Equations (1.1a) and (1.1b) by equating the equations to zero.

$$\frac{dT_I}{dt} = 0\tag{1.4a}$$

$$\frac{dT_M}{dt} = 0\tag{1.4b}$$

The steady state found in the system is

$$(T_I, T_M) = (0,0)\tag{1.5}$$

Step 2: Find the Jacobian of the system.

$$J = \begin{pmatrix} T_{II} & T_{IM} \\ T_{MI} & T_{MM} \end{pmatrix} \quad (1.6)$$

Step 3: Find the trace and determinant of the system.

The trace of this system is

$$\begin{aligned} \tau &= -(d_2 + a_1) + (-d) \\ &= -(d_2 + a_1 + d) \end{aligned} \quad (1.7)$$

$$\therefore \tau < 0$$

The determinant of this system is

$$\begin{aligned} \Delta &= -d(-(d_2 + a_1)) - a_1(2a_4) \\ &= d(d_2 + a_1) - 2a_1a_4 \end{aligned} \quad (1.8)$$

Step 4: Find the necessary condition for the system.

$$\therefore d < \frac{2a_1a_4}{(d_2 + a_1)} \quad (1.9)$$

So that the steady state is an unstable point using the following cases.

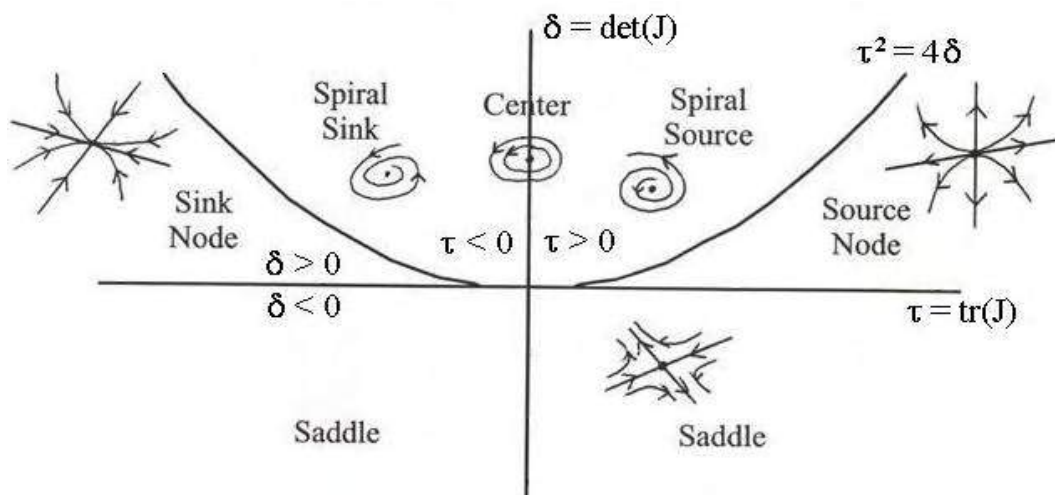


Figure 1.1 Determinant-trace plane [8]

Step 5: Check the ranges of parameters for the necessary condition by manipulating the parameters in the phase portrait.

Step 6: Create a stability map for the necessary condition.

1.2.2 The Drug-Free Ordinary Differential Equation Model for Tumor Growth in A Non-Delay Case with Immune Suppression

For the three dimensional system of the second case in Equations (1.2a), (1.2b) and (1.2c), the steps to find the stability of the steady state of the system is much similar to the first case which as follows:

Step 1: Find the steady state solution of Equations (1.2a), (1.2b) and (1.2c) by equating the equations to zero.

$$\frac{dT_I}{dt} = 0 \quad (1.10a)$$

$$\frac{dT_M}{dt} = 0 \quad (1.10b)$$

$$\frac{dI}{dt} = 0 \quad (1.10c)$$

The steady state found in the system is

$$(T_I, T_M, I) = \left(0, 0, \frac{k}{d_1}\right) \quad (1.11)$$

Step 2: Find the Jacobian of the system.

$$J = \begin{pmatrix} T_{IT_I} & T_{IT_M} & T_{II} \\ T_{MT_I} & T_{MT_M} & T_{MI} \\ I_{T_I} & I_{T_M} & I_I \end{pmatrix} \quad (1.12)$$

Step 3: Find the trace and determinant of the system.

The trace of this system is

$$\bar{\tau} = -(a_1 + d_2 + (c_1 + c_3)d_1 + d) \quad (1.13)$$

$$\therefore \bar{\tau} < 0$$

The determinant of this system is

$$\bar{\Delta} = (c_1 + c_3)d_1 + \Delta \tag{1.14}$$

Step 4: Find the necessary condition for the system.

$$\therefore d < \frac{-(c_1 + c_3)d_1 + 2a_1a_4}{(d_2 + a_1)} \tag{1.15}$$

So that the steady state solution is an unstable point using Routh-Hurwitz criteria.

Routh-Hurwitz Criteria [8]

Form matrices as follows:

$$H_n = \begin{pmatrix} a_1 & 1 & 0 & \dots & 0 \\ a_3 & a_2 & a_1 & \dots & 0 \\ a_5 & a_4 & a_3 & \dots & 0 \\ \vdots & \vdots & \vdots & \ddots & \vdots \\ a_{2n-1} & a_{2n-2} & a_{2n-3} & \dots & a_n \end{pmatrix} \tag{1.16}$$

where (l, m) term in matrix H_n is

$$a_{2l-m} \quad \text{for } 0 < 2l - m < n$$

$$1 \quad \text{for } 2l = m$$

$$0 \quad \text{for } 2l < m \text{ or } 2l > n + m$$

Then, the steady state \bar{N} of the system is stable if and only if the determinants of all Hurwitz matrices are positive that is

$$\det H_n > 0 (n = 1, 2, \dots, k) \tag{1.17}$$

Step 5: Check the ranges of parameters for the necessary condition by manipulating the parameters in the phase portrait.

Step 6: Create a stability map for the necessary condition.

1.3 SIMULATION AND DATA ANALYSIS

To check the ranges of parameters for the necessary condition, the ranges of parameters is manipulated to get an unstable phase portrait as Figure 1.2 below.

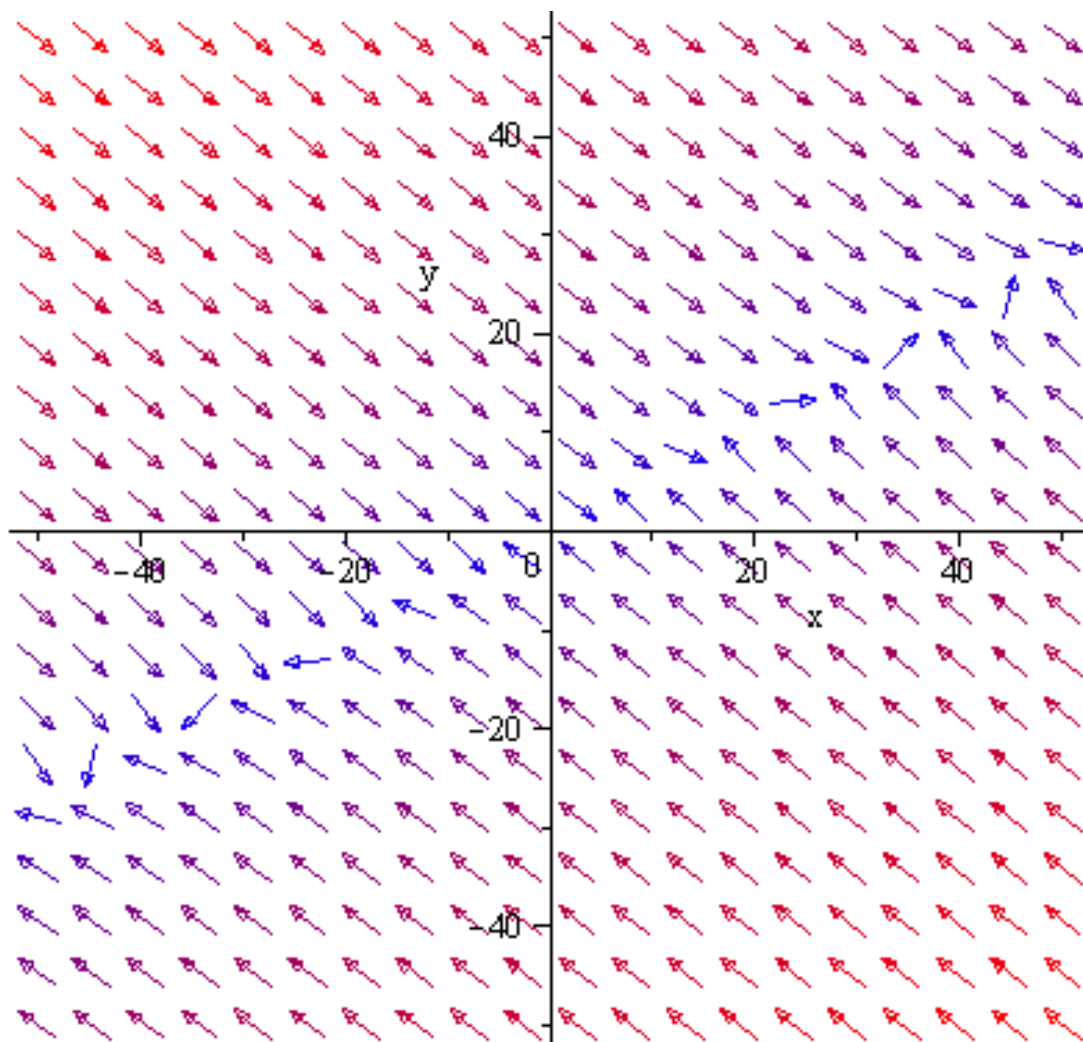


Figure 1.2 Phase portrait for the case of absence in immune response for an unstable condition

Based on the necessary conditions of both system, stability maps were created using Maple 12 software via DEtools package. The range of y -axis which is the natural cell death or apoptosis is set between $0 < d < 2$ and the range of x -axis which is the rate of cell reproduction is set between $0 < a_1 < 1$.

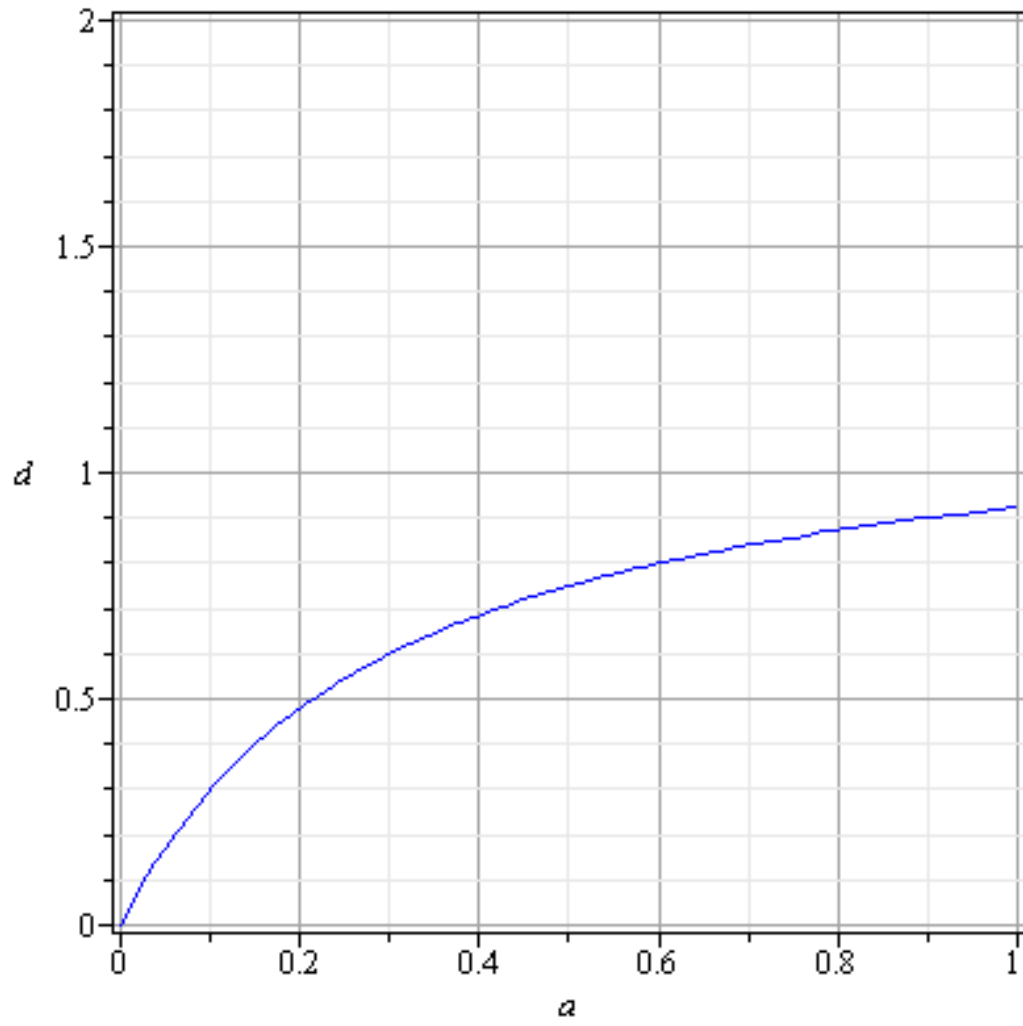


Figure 1.3 Stability map for the case in absence of immune response where the parameters d is the tumor cell death rates and a is the tumor cell cycle rates.

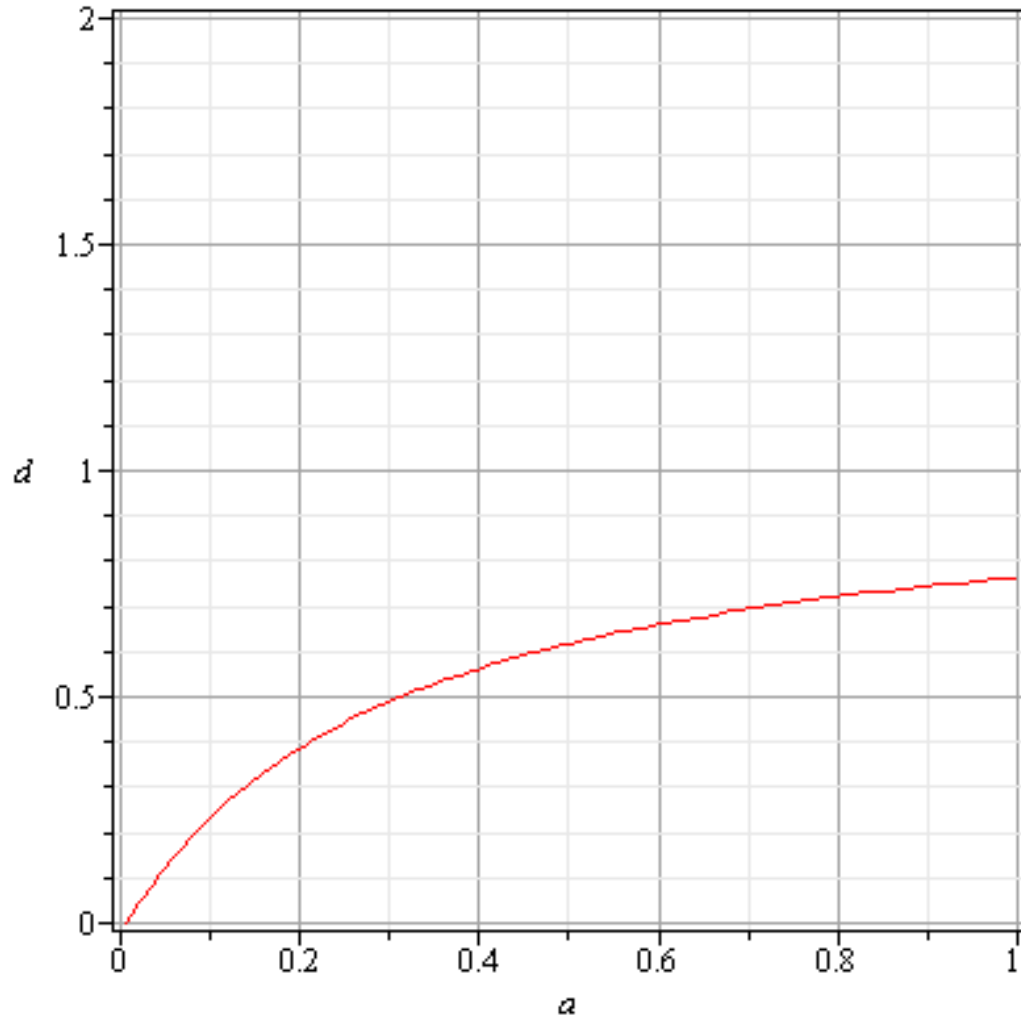


Figure 1.4 Stability map for the case in the presence of immune response where the parameters d is the tumor cell death rates and a is the tumor cell cycle rates.

Combining both stability maps in Figure 1.3 and Figure 1.4, we get Figure 1.5 as below.

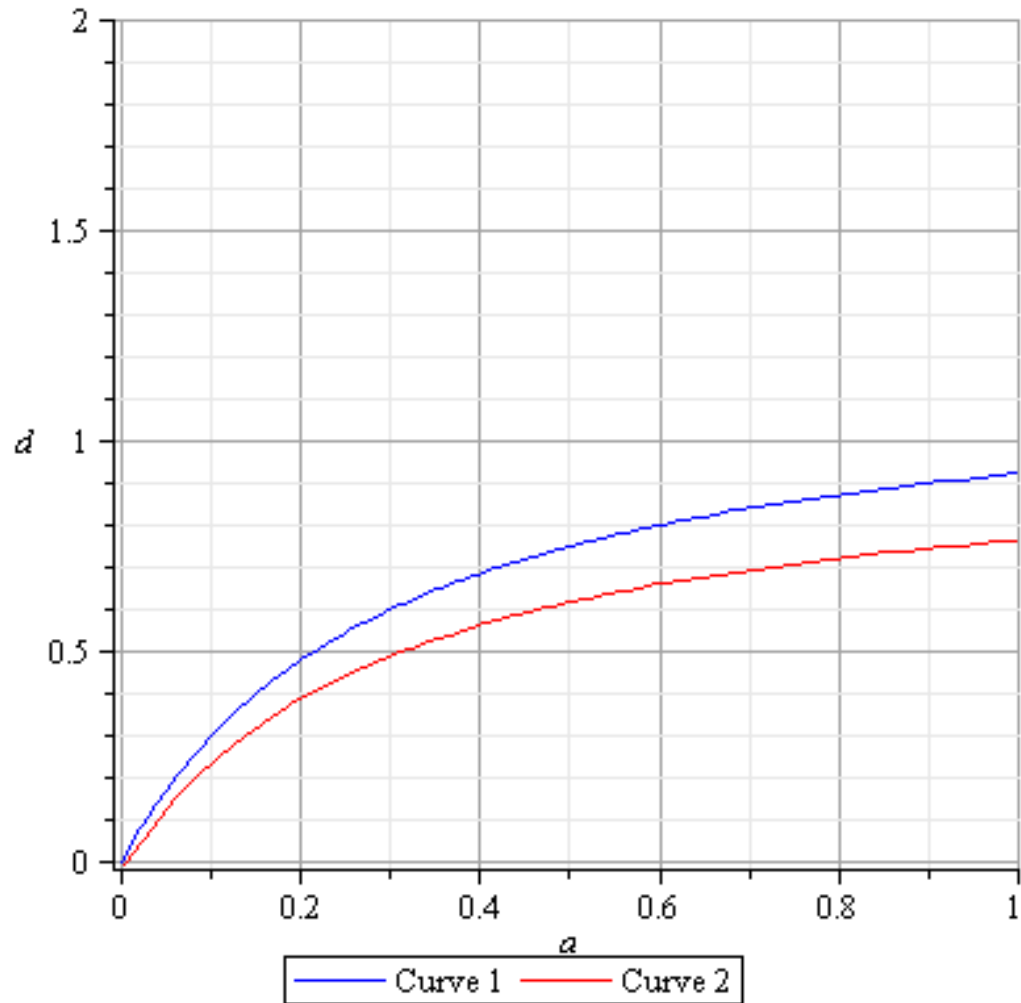


Figure 1.4 Stability map for both cases in absence and in presence of immune response where Curve 1 indicates the curve limits for tumor growth region when there is no immune suppression and Curve 2 indicates the curve limits for tumor growth region when immune suppression is present.

1.4 CONCLUSION

Based on the stability map in Figure 1.4, there is a slight difference on the necessary conditions found in Equations (1.9) and (1.15). These necessary conditions built curves in the stability maps and the curves limit the tumor growth region. There are two regions split up by the two curves. In our case which is a non-delay, the region covered under the curves

indicates the region of tumor growth and the complement which is covered above the curves indicates the region of tumor decay.

With the slight different of necessary conditions applied, the region of tumor growth system with immune suppression is reduced compared to the region of tumor growth system without immune suppression. Therefore, it can be concluded that the system in presence of immune response system is more stable than in absence of immune response system.

However, the model solved in this research is very simple such that there were no drug effects, no delay in the cell cycle and only two phases of cell division were considered. Of course there are significant sorts that can be involved in this model for better results. For instances, since we separated the cell cycle phases to be more clear, the outcome of adding a delay or drugs factors to the model could be seen more aggressively and clear.

Relating to the immune response system, the scope touched in this research regarding the immune system is still at the surface but we know that the immune system is complex. We also just considered only one type of cell in the immune system that is cytotoxic T cells (CTL). Therefore, a deeper research is needed to see how the immune could affect more on a certain disease or cell population.

REFERENCES

- [1] Buric, N., and Todorovic, D. (2002). *Dynamics of delay-differential equations modelling immunology of tumor growth*, *Chaos, Solitons & Fractals*, 645-655.
- [2] Villasana, M., and Radunskaya, A. (2003). A Delay Differential Equation Model for Tumor Growth. *Journal of Mathematical Biology*, 47(3), 270-294.
- [3] D’Onofrio, A. *et al.* (2010). *Delay-induced oscillatory dynamics of tumour-immune system interaction*, 572-591.
- [4] Rihan, F.A. *et al.* (2014). *A Time Delay Model of Tumour-immune System Interactions: Global Dynamics, Parameter Estimation, Sensitivity Analysis*, 606-623.
- [5] Borges, F.S. *et al.*(2014). *Model For Tumour Growth With Treatment By Continuous And Pulsed Chemotherapy*, 43-48.
- [6] Dong, Y., *et al.* (2015). *Dynamics in a Tumor Immune System With Time Delays*, 99-113.
- [7] Bury, J., and Cross, S. (2003). *Molecular Biology in Diagnostic Histopathology. Part 1- The Cell Cycle, Current Diagnostic Pathology*, 266-275.
- [8] Edelstein-Keshet, L. (1988). *Mathematical Models in Biology*. New York: Random House.

BOX-BEHNKEN EXPERIMENTAL DESIGN FOR MODELING AND OPTIMIZING THE OXIDATION OF ARSENITE

Ang June Leong & Assoc. Prof. Dr. Robiah Adnan

Abstract

Response Surface Methodology is an experimental method that is used to find the optimal response with some specified ranges of the variables. Some of the major designs are like Central Composite Design and Box-Behnken Design. The objective of Box-Behnken Designs is to study the effects of variables and find the optimal solution for all the factors in order to yield optimal response. This design requires at least three levels, coded as -1 , 0 , and $+1$. One of the advantages of designs is they does not contain the combination of all factors in either highest or lowest levels. This is useful when the extreme levels of the factor combinations that are prohibitively expensive or impossible to test because of the physical process constraints. In the case study, a second order polynomials model was proposed to fit the data in order to study the main effects and the interactions. Through this model, the optimal solutions for the oxidation of arsenite were found to be $235.9596 \text{ W L}^{-1}$ power density of ultrasound, 0.5 mg L^{-1} of initial concentration of arsenite and $72.52524 \text{ mg L}^{-1}$ of H_2O_2 concentration. 88.97% of oxidation efficiency was predicted by Box-Behnken Design and a confirmation test of the optimal solution verified the validity of the model, which gives an oxidation efficiency of 90.1%.

Keywords: Box-Behnken, Response Surface Methodology, Oxidation of Arsenite

Introduction

Response Surface Methodology (RSM) is a collection of statistical and mathematical techniques for empirical model building. The objective of Response Surface Methodology is to optimize a response (output variable) which is influenced by several independent input variables. This experiment is a series of tests which was called as runs, where changes are made in the input variables in order to identify the reasons for changes in the output response.

Box-Behnken design was created by George E. P. Box and Donald Behnken in 1960. Box-Behnken design is a type of response surface design that the design points does not fall at the high or low factor levels which were the vertices for the figure below. This design requires at least three levels, coded as -1 , 0 , and $+1$. This design is all about the midpoint. Therefore this design has treatment combinations that are at the midpoints of the edges of the experimental space and require at least three factors. This will be an advantage when the points on the corners of the cube represent factor level combinations that are prohibitively expensive or impossible to test because of physical process constraints. However, Box-Behnken designs can only have 3 levels per factor, unlike Central Composite designs which can have up to 5 levels per factor. Also unlike central composite designs, Box-Behnken designs never include runs where all factors are at their extreme levels, such as all in the low level or high level.

Arsenic is often found in two oxidation states: Arsenite, As (III) and Arsenate, As(V). These different states of arsenic have different chemical behaviours, bio-availabilities and toxicities. Arsenate, As(V) is less mobile and less toxic than arsenite, As (III), which make up about 42% of the total Arsenic in groundwater systems. To oxidize Arsenite, As (III) to Arsenate, As(V), a typical combination of ultrasound & hydrogen peroxide (H_2O_2) is used.

It shows that the combined process could be an effective method to oxidizing Arsenite with the right ratio, which is instead of using only ultrasonic or only hydrogen peroxide (H₂O₂).

Literature Review

George E. P. Box and Donald Behnken proposed three level designs for fitting response surfaces. These designs are formed by combining 2k factorials with incomplete block designs. The figure below illustrates the three variables Box-Behnken design. It can be noticed that the Box-Behnken design is a spherical design with all points lying on a sphere. Also the Box-Behnken design does not contain any point at the vertices of the cubic region created by the upper and lower limits for each variable

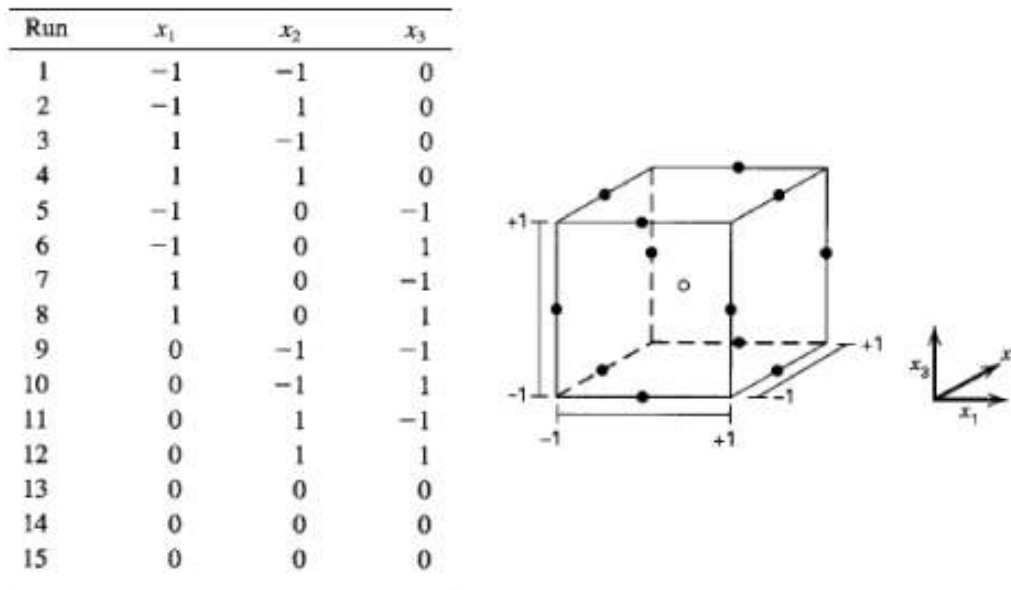


Figure 1: Box-Behnken Design with 3 Factors

This could be advantageous when the points on the corners of the cube represent factor level combinations that are impossible to test due to physical process constraints or prohibitively expensive. Its "missing corners" may be useful when the researcher should avoid combined factor extremes. This property prevents a potential loss of data in those cases.

Box-Behnken designs require fewer treatment combinations than a Central Composite Design, in problems involving 3 or 4 factors. The Box-Behnken design is rotatable (or nearly so) but it contains regions of poor prediction quality like the Central Composite Design. Table 2.1 below shows the number of designs runs required by Box-Behnken Design and Central Composite Design for certain number of factors.

Table 1: Comparison of the Number of Design Runs of Box-Behnken Design and Central Composite Design for Certain Number of Factors.

Number of Factors	Central Composite Design	Box-Behnken Design
2	13 (5 center points)	-

3	20 (6 centerpoint runs)	15
4	30 (6 centerpoint runs)	27
5	33 (fractional factorial) or 52 (full factorial)	46
6	54 (fractional factorial) or 91 (full factorial)	54

We can see that Box-Behnken Design will required less number of run than Central Composite Design. Box-Behnken Design is beneficial for those who do not have too much capital to undergo the experiment or the experiments material is too expensive or unfordable.

Methodology

Response Surface Methodology is an experimental method created to find the optimal response within specified ranges of the factors. The purpose of response surface methodology is to build an approximate regression model that is closest to the true regression model. The true regression model is usually never known. The model to be built is based on observation data and the empirical model. Multiple regression analysis is used in response surface methodology.

This experiment was performed using the Box–Behnken experimental design and the effects of the three variables can be model using a second-order polynomial model equation, as shown below

$$Y = \beta_0 + \sum_{i=1}^3 \beta_i x_i + \sum_{i=1}^3 \sum_{j=1}^3 \beta_{ij} x_i x_j + \sum_{i=1}^3 \beta_{ii} x_i^2 + \varepsilon \tag{1}$$

Or

$$Y = \beta_0 + \beta_1 x_1 + \beta_2 x_2 + \beta_3 x_3 + \beta_{12} x_1 x_2 + \beta_{13} x_1 x_3 + \beta_{23} x_2 x_3 + \beta_{11} x_1^2 + \beta_{22} x_2^2 + \beta_{33} x_3^2 + \varepsilon$$

Where,

Y is the oxidation efficiency,

$x_i (i= 1, 2, 3)$ and $x_j (j = 1, 2, 3)$ are independent variables,

$\beta_0, \beta_i (i= 1, 2, 3), \beta_{ij} (i= 1, 2, 3 \ \& \ j = 1, 2, 3), \beta_{ii} (i= 1, 2, 3)$ are the coefficient of the model,

ε is the random error.

In matrix form,

$$Y = \beta X + \varepsilon \tag{2}$$

And β can be approach from the equation below,

$$\beta = (X^T X)^{-1} X^T Y \tag{3}$$

Assumption for the model

- (i) The mathematical form of the relation, thus $E(\varepsilon_i) = 0$ for all i .
- (ii) $Var(\varepsilon_i) = \sigma_\varepsilon^2$ for all i .
- (iii) The ε_i 's are independent.
- (iv) ε_i is normally distributed.

Hypothesis testing for the significance of the regression coefficient

$$H_0 : \beta_0 = \beta_i = \beta_{ij} = \beta_{ii} = 0$$

v.s.

H_1 : At least one β is not equal to zero.

Hypothesis testing for the Lack-of-fit of model

H_0 : The model is not significant; the lack of fit is good.

H_1 : The model is significant; the lack of fit is bad.

The analysis is undergoing at a level of significance 95%. ($\alpha = 0.05$)

Table 2: Analysis of variance (ANOVA) Table.

Source	Sum of Squares	Degree of Freedom	Mean Squares	F
Regression	SS_R	$k-1$	$MS_R=[SS_R/(k-1)]$	$F_1=MS_R/MS_r$
Residual Error	SS_r	$n-k$	$MS_r=[SS_r/(n-k)]$	
Lack-of-fit	SS_{lof}	$m-k$	$MS_{lof}= [SS_{lof}/(m-k)]$	$F_2=MS_{lof}/MS_{pe}$
Pure error	SS_{pe}	$n-m$	$MS_{pe}=[SS_{pe}/(n-m)]$	
Total	SS_T	$n-1$		

Where,

n is the total number of observations,

n_i is the number of replicate at the i^{th} level,

k is the number of parameters in the model,

m is the number of distinct levels of the independent variables.

$$SS_R = \sum_i^m \sum_j^{n_i} (\hat{y}_i - \bar{y})^2 \tag{4}$$

$$SS_r = \sum_i^m \sum_j^{n_i} (y_{ij} - \hat{y}_i)^2 \tag{5}$$

$$SS_{lof} = \sum_i^m \sum_j^{n_i} (\hat{y}_i - \bar{y}_i)^2 \tag{6}$$

$$SS_{pe} = \sum_i^m \sum_j^{n_i} (y_{ij} - \bar{y}_{ij})^2 \tag{7}$$

$$SS_T = \sum_i^m \sum_j^{n_i} (y_{ij} - \bar{y})^2 \tag{8}$$

Table 3: Experimental Response of oxidation efficiencies under different conditions.

Run	Coded Variables			Real Variables			Experimental Response
	x_1	x_2	x_3	X_1	X_2	X_3	
1	-1	-1	0	160	0.5	60	71.6
2	1	-1	0	240	0.5	60	85.1
3	-1	1	0	160	1.5	60	64.6
4	1	1	0	240	1.5	60	74.8
5	-1	0	-1	160	1.0	20	55.2
6	1	0	-1	240	1.0	20	69.7
7	-1	0	1	160	1.0	100	53.6
8	1	0	1	240	1.0	100	83
9	0	-1	-1	200	0.5	20	75.9
10	0	1	-1	200	1.5	20	63.2
11	0	-1	1	200	0.5	100	78.3
12	0	1	1	200	1.5	100	70.2
13	0	0	0	200	1.0	60	79.2
14	0	0	0	200	1.0	60	79.1
15	0	0	0	200	1.0	60	79.2

Results and Discussion

Table 3: Analysis of variance (ANOVA) Table.

Source	Sum of Squares	Degree of Freedom	Mean Squares	f	P-value
Regression	1217.44	9	135.271	12.71	0.006
Residual Error	53.20	5	10.641		
Lack-of-Fit	53.20	3	17.732	5319.75	0
Pure Error	0.01	2	0.003		
Total	1270.64	14			

$$Y = 79.17 + 8.45x_1 - 4.76x_2 + 2.64x_3 - 0.83x_1x_2 + 3.73x_1x_3 + 1.15x_2x_3 - 5.83x_1^2 + 0.69x_2^2 - 7.96x_3^2 \tag{9}$$

Table 4: Analysis of variance result for acquired model.

Source	Sum of squares	Degrees of freedom	Mean square	F-value	p-value	Characteristics
Model	1217.44	9	135.271	12.71	0.006	Significant
X_1	571.22	1	571.22	53.68	0.001	Significant
X_2	181.45	1	181.451	17.05	0.009	Significant
X_3	55.65	1	55.651	5.23	0.071	Slightly Significant
$X_1 X_2$	2.72	1	2.722	0.26	0.634	Not Significant
$X_1 X_3$	55.50	1	55.502	5.22	0.0713	Slightly Significant
$X_2 X_3$	5.29	1	5.290	0.50	0.512	Not Significant
X_1^2	105.44	1	125.641	11.81	0.019	Significant
X_{22}	6.31	1	1.766	0.17	0.701	Not Significant
X_{32}	233.85	1	233.853	21.98	0.005	Significant
Residuals	53.20	5	10.641			

After the significance of the parameters has been evaluated, the model can be improved by eliminating the terms that are not very significant. The final model for describing the relationship between the oxidation efficiency and the US power density, initial concentration of arsenite, and H₂O₂ concentration is shown as below

$$Y = 79.59 + 8.45x_1 - 4.76x_2 + 2.64x_3 + 3.73x_1x_3 - 5.88x_1^2 - 8.01x_3^2 \quad (10)$$

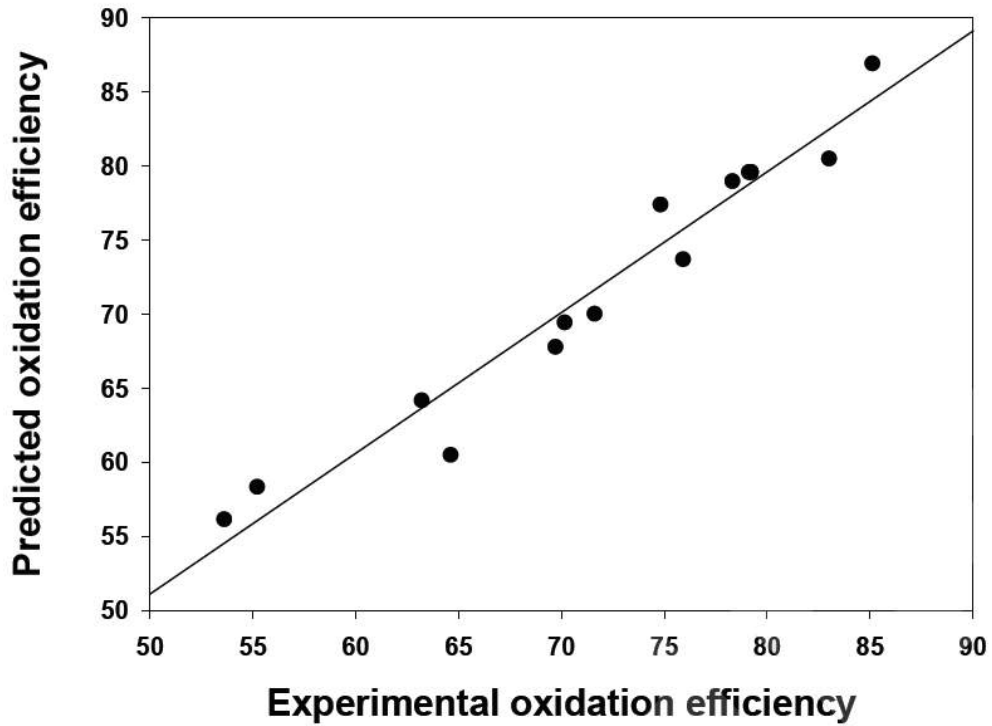


Figure 2: Comparison of predicted and experimental oxidation efficiencies.

From Figure 2, a line of best-fit can be drawn which means that the model is fitting the data quite well

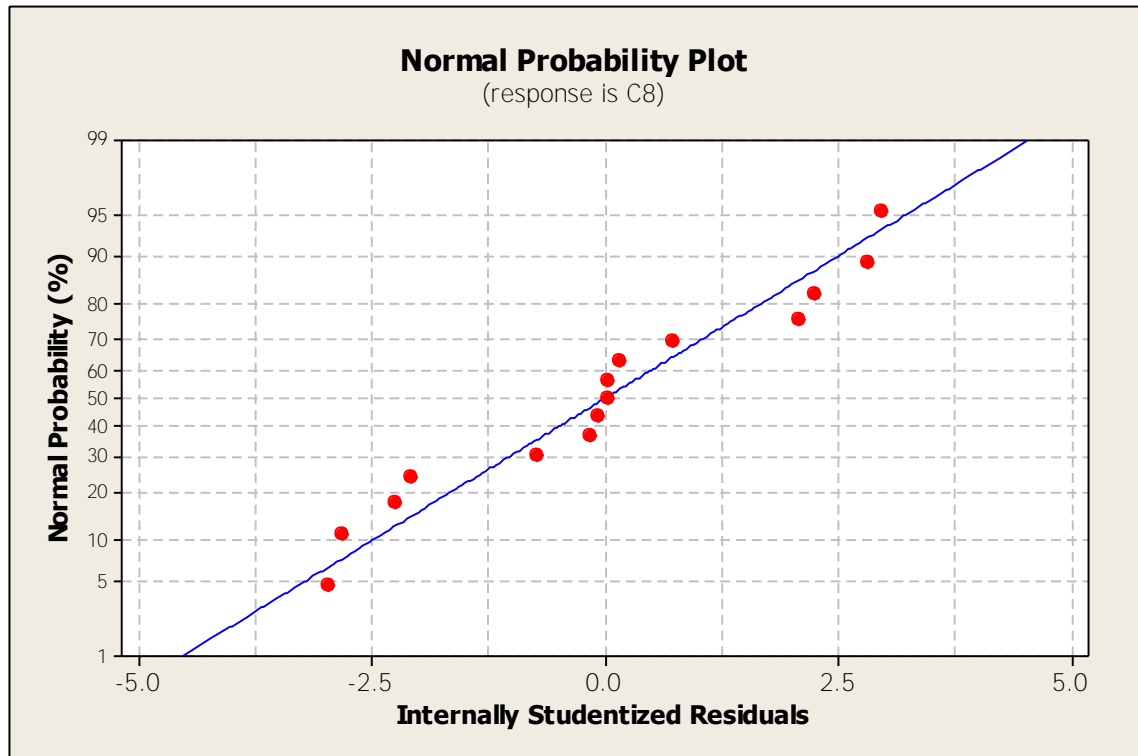


Figure 3: Normal Probability Plot.

The figure above shows that the relationship between normal probability (%) and internally studentized residuals. The straight line shows that there is no response transformation was required and that there was no apparent problem with normality

The optimization function in Minitab was used to obtain the optimal conditions for the experiment. Results are shown as below.

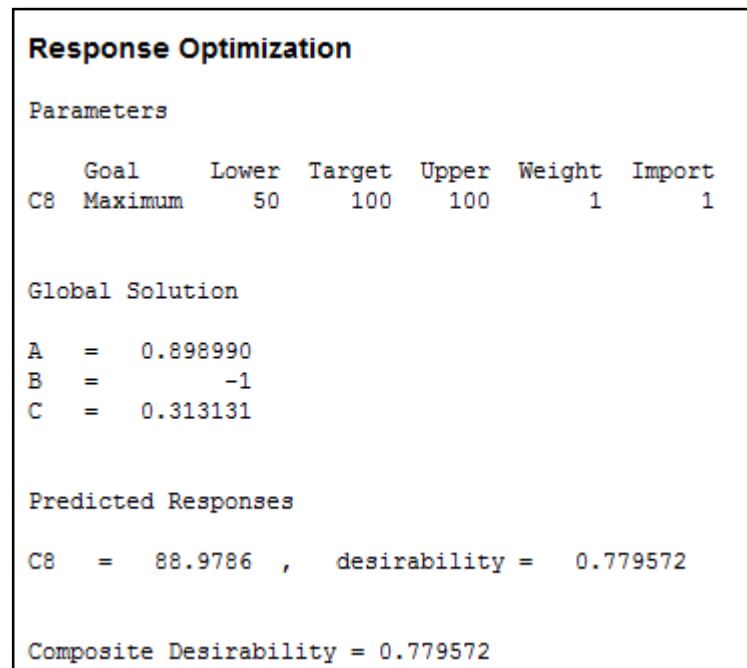


Figure 4: Response Optimization

Table 4.7: Optimal Solution

Variable	Coded Unit	Uncoded Unit
Power density (W L ⁻¹)	0.89899	235.9596
Initial concentration of arsenite (mg L ⁻¹)	-1	0.5
H ₂ O ₂ concentration (mg L ⁻¹)	0.313131	72.52524

The optimize value we get from Minitab is 88.97% which can be achieved by using the optimal solution of 235.9596 W L⁻¹ power density, 0.5 mg L⁻¹ of initial concentration of arsenite and 72.52524 mg L⁻¹ of H₂O₂ concentration. After we obtain the theoretical value, 3 more experiment is conducting again by using the optimal solution and we found that the average removal oxidation efficiency was 90.1% which is very near to what Box-Behnken have predicted.

Conclusion

In conclusion, we are able to optimize the oxidation efficiency by using Box-Behnken Design, yielding 88.97% the theoretical or predicted value which is very close to the experimental value after we obtain the optimal solution for all the 3 factor which were 235.9596 W L⁻¹ power density of ultrasound, 0.5 mg L⁻¹ of initial concentration of arsenite and 72.52524 mg L⁻¹ of H₂O₂ concentration. This implies that Box-Behnken Design is a very good method for optimization. They are very useful when it comes to evaluating and assessing product performance. Especially to those experiment where the points on the corners of the cube represent factor level combinations that are impossible to test due to physical process constraints or prohibitively expensive. Box-Behnken designs require fewer treatment combinations than a Central Composite Design, but only involving 3 or 4 factors. In shorts, Box-Behnken Design Response Surface Methodology is an effective and powerful method to optimize individual's factors.

References

- Box, G. E. P., and Draper, N. R. *Empirical Model Building and Response Surfaces*. New York. John Wiley & Sons.; 1987
- Douglas C. Montgomery. *Design and Analysis of Experiments 7th (seventh) edition*. 2009
- Gary W. Dehlert. *A First Course in Design and Analysis of Experiments* W. H. Freeman. pp 522-523; 2000
- Giunta, A. A., Balabanov, V., Haim, D., Grossman, B., Mason, W.H. and Watson, L. T. *Wing Design for a High-Speed Civil Transport Using a Design of Experiments Methodology*, "Bellevue, WA, AIAA, Inc., Vol. 1, pp. 168-183; 1996
- Jacqueline K. Telford. *A Brief Introduction to Design of Experiments*. Johns Hopkins APL Technical Digest. 2007. Volume 27 pp 224-232
- L. Eriksson, E. Johansson, N. Kettaneh-Wold, C. Wikström, and S. Wold. *Design of Experiments: Principles and Applications*. Umetrics company; 2008
- Minitab Release 12, User Guide: Data Analysis and Quality Tools, Minitab Inc.; 1997
- Montgomery, D.C. *Design and analysis of Experiments*. United State of Amerika, John Wiley & Sons, Inc; 2005

Myers, R.H., Montgomery DC, *Response surface methodology process and product optimization using designed experiments*. A Wiley-Interscience Publication; 2002

Pengpeng Chiu, Mingcan Cui, Kyounglim Kang, Beomguk Park, Yonggyu Son, EunkyungKhim, Min Jang and JeehyeongKhim. *Application of Box-Behnken design with response surface methodology for modelling and optimizing ultrasonic oxidation of arsenite with H₂O₂*. 2013

Robiah Adnan and MaizahHura Ahmad. *Design of Experiments*. Department of Mathematics Sciences, Faculty of Science, University Technology Malaysia. Desktop Publisher; 2014

Sergio Luis Costa Ferreira, Roy Edward Bruns, Erik GalvãoParanhos da Silva, Walter Nei Lopes dos Santos, Cristina Maria Quintella, Jorge Mauricio David, JailsonBittencourt de Andrade, Marcia Cristina Breikreitz, Isabel Cristina Sales FontesJardim and Benicio Barros Neto. *Statistical designs and response surface techniques for the optimization of chromatographic systems*. ScienceDirect; 2007

Van Campen, D.H., Nagtegaal, R. and Schoofs, A.J.G. (), *Approximation methods in structural optimization using experimental designs for multiple response*, ISpringer-Verlag, Berlin, Heidelberg, New York, pp. 205-228; 1990

Numerical Computations and Conditioning in Solving System of Linear Equations

Aqilah farhana binti Abdul Rahman and Nor'ainiAris

1.1 INTRODUCTION

Numerical computation is one of the branches of mathematics which is used to find the approximations of difficult problems such as solving differential equations, finding the roots of non-linear equations and integration involving complex expressions. Solving linear systems of equations and computing eigenvalues and eigenvectors of matrices are mainly two types of matrix computations, but only solving linear systems of equations is discussed.

In numerical computation, there are some factors that need to be considered such as floating point arithmetic, rounding errors, types of errors, norm of matrices, stability, accuracy and conditioning properties in solving linear systems. Floating point arithmetic is necessary to be used in numerical computation since computers cannot represent real or complex number exactly. Thus, computers can approximate real numbers by a system of floating point arithmetic, which in a digital equivalent of scientific notation, each number is represented so that the scale does not matter unless the number is tiny or so huge as to cause underflow or overflow (Trefethen and Lloyd N., 2006). The standard computer representation of non-integer numbers is as floating point numbers with a fixed number of bits. Most calculations with floating point numbers will induce further round-off errors and error can be measured in two ways which are relative error and absolute error.

Besides, the numerical analyst should be aware of the possible sources of error in each stages of the computational process which these errors can affect in final answer in analyzing the accuracy of numerical results. It is convenient to be able to associate with any vector or matrix a nonnegative scalar that in some sense measures its magnitude for the purpose of quantitatively discussing errors. Thus, matrix and vector norm is used in numerical computation.

When solving linear systems numerically, conditioning is important for the stability and sensitivity to rounding errors and it is related to the perturbation behavior of a mathematical problem. In a condition of a mathematical problem, if a small change in the coefficient matrix or a small change in the right hand side results in a small change in the solution vector, a system of equations is considered to be well-conditioned. Meanwhile, a system of equations is said to be ill-conditioned if a small change in the right hand side or a small change in the coefficient matrix results in a large change in the solution vector.

In order to solve a system of linear equations more rapidly, the problem of interest can be transformed so that the properties of the matrix involved can be improved drastically. Thus, the process of preconditioning is introduced and essential to most successful applications of iterative methods. A ‘preconditioner’ is used to solve the linear system more efficiently than solving the linear system with an ill-conditioned matrix A . Hence, this research direction is focused on studying the notion and the method of preconditioning in solving systems of linear equations.

1.2 LITERATURE REVIEW

1.2.1 Condition Number

In numerical analysis, the condition number of a function measures how much output value of the function can change for a small change in the input argument. The purpose of the condition number is to measure how sensitive a function is to change or errors in the input, and how much error in the output results from an error in the input.

The idea of the condition number of a matrix is introduced by Alan Turing in 1948, in which the same Turing who founded the theoretical computer science, and predicted the possibility of chemical waves long before its discovery in the laboratory and the eminent researcher who had contributed to the “Enigma” code-breaking effort that helped end the control of the Atlantic by German submarines in the World War II.

Based on Anna *et al.* (2011) study, G. Dahilquist and A. Bjorck stated that the condition number of a matrix decides the convergence of the approximate solution obtained in the iteration process, to the correct solution of the equation system. The condition number is defined as $\kappa(A) = \|A\| \|A^{-1}\|$ and the value of the condition number depends on the choice of the matrix norm, but indirectly on the choice of a vector norm.

BiswaNath (1995) stated that in the perturbation analysis, the condition number is the deciding factor. This indicates that if the condition number is large, then a small perturbation in the input data may cause a large relative error in the computed solution. In this problem, the system is called an ill-conditioned system, otherwise it is well conditioned. Anna *et al.* (2011) in her study mentioned that the condition number measures the sensitivity of the solution of a problem to the perturbations in the data and provides an approximate upper bound on the error in the computed solution.

1.2.2 Method to Improve Ill-Conditioned Matrix

According to Joong Kim *et al.* (1996), Rice has studied about the numerical properties of the ill-conditioned linear systems. He stated that “if the problem is ill-conditioned, then no amount of effort, trickery, or talent used in the computation can produce accurate answers except by chance”. To produce reliable solution, most of the algorithm approaches have failed. Besides, Kaczmarz has been first suggested to use the simplest projection method to solve rank-deficient or ill-conditioned large scale linear systems. Unfortunately, it converges very slowly.

Other than that, according to Laurene (2008), iterative refinement is a technique for improving an approximate solution to the system of linear equations. This is due to the fact that the errors in the solutions may be the result of round-off in the computations, besides the effect of such errors may be more extreme if the coefficient matrix is ill-conditioned. Farooq and Salhi (2011) used the approach to construct a new matrix and a new right-hand side that constitute an instance of an equivalent system linear equation (SLE) to the one given which is ill-conditioned. The construction of a new matrix has a small condition number compared with the matrix of the initial SLE. That means by solving this equivalent system is much better than solving the original equation by virtue of the difference in the magnitude of the condition numbers of their matrices. They have mentioned that near-parallelism is what exacerbates inaccuracy by creating a potentially very large set of solutions from which to pick. So by removing the parallelism in a matrix reduces its condition number and hence ill-conditioning.

In Zahra and Behrouz (2013) study, they proposed a novel technique to modify a given ill-conditioned matrix in order to make it a better conditioned one. They found two invertible diagonal matrices D_1 and D_2 by Simulating Annealing method, which is

$$\text{cond}(D_1AD_2) = \inf_{\Delta_1, \Delta_2 \in \gamma} \text{cond}(\Delta_1A\Delta_2),$$

wherey denoting the set of all diagonal matrices, relative to the given norm. Simulating annealing (SA) is proposed by Gelatt and Vecchi in 1983 and Cerny in 1985 for finding the global minimum of an objective function that may possess several local minima.

1.2.3 Method of Preconditioning in Solving Linear Systems

The concept of preconditioning is a way of transforming a difficult problem into the easier one has a long history. According to Massimiliano (2012), Trefethen and Bau stated that the

term “preconditioning” refers to “the art of transforming a problem that appears intractable into another whose solution can be approximated rapidly” while the “preconditioner” is the mathematical operator that is responsible for such a transformation.

The preconditioning which reduces the condition number in order to improve the convergence of an iterative process have first considered by Cesari in 1937. The idea of Cesari is to use a low degree polynomial $p(A)$ in A as a preconditioner for a Richardson-type iteration applied to the preconditioned system $p(A)Ax = p(A)b$. He showed how to determine the coefficients of the polynomial for A symmetric and positive definite so that the condition number of the preconditioned matrix $p(A)A$ was small as possible. However, it is well known that the earliest tricks to solve a linear system numerically were already developed in the 19th century.

For these reasons, research on the construction of effective preconditioners has significantly grown over the last two decades, while the advances on the Krylov subspace methods have progressively faded. The preconditioning appears to be much more effective and promising research field than either iterative or direct solution methods recently.

In this research, some preconditioning methods are investigated. The aim is to improve the condition property of the ill-conditioned system $Ax = b$ by reducing the condition number of A . A linear system $Ax = b$ with ill-conditioned matrix A can be solved effectively by solving the equivalent linear system using a preconditioner matrix C such that $C^{-1}Ax = C^{-1}b$ with $C^{-1}A$ better conditioned than A (Gregoire and Sidi, 2008). According to Massimilano (2012), preconditioning means transforming the system of equations into an equivalent mathematical problem which is expected to converge faster using an iterative solver. For example, by multiplying the system of equations with M^{-1} giving $M^{-1}Ax = M^{-1}b$ and if matrix $M^{-1}A$ is better conditioned than A for a Krylov subspace method, then M^{-1} is the preconditioner. In this approach, the system is known as a left preconditioned system. Besides, M^{-1} can be applied on the right, where

$$AM^{-1}y = b, \quad x = M^{-1}y$$

produces a right preconditioned system.

From this motivating, this research will focus on three types of preconditioning, which are polynomial preconditioning, diagonal preconditioning and split preconditioning (right and left preconditioning) that will be applied to improve the ill-conditioned problem, followed by solving the better conditioned problem using Gaussian elimination with partial pivoting and matrix inversion. Therefore, the preconditioning in this research is not about to improve the convergence of an iterative solver, but to reduce the condition number of the system, such that any direct known methods can be applied to give a good approximate

solution compared to the situation when the problem is solved directly without preconditioning

1.3 BASIC CONCEPTS UNDERLYING THE THEORETICAL BASIS ON NUMERICAL COMPUTATION

1.3.1 Floating-Point System

When doing numerical computation, it is well known that computers cannot represent real or complex numbers exactly (Lloyd N. Trefethen, 2006). Thus, floatingpoint numbers are commonly used when approximating real numbers. Floating-point numbers can be define as real numbers of the form

$$\pm(0.d_1 \cdots d_p) \times b^n$$

1.3.2 Sources of Errors

According to Germund and Bjorck (1974), numerical results are influenced by many types of errors. Johnson and Riess (1977) stated that there are three types of errors which occur in computation. First, there are errors which are called “initial data” errors. These errors arise when the equations of the mathematical model are formed, due to the sources such as the idealistic assumptions made to simplify the model, inaccurate measurements of data, miscopying of figures, the inaccurate representation of mathematical constants.

Another class of errors, “truncation” errors occurs when we are forced to use mathematical techniques which give approximate, rather than exact answers. This error usually occur because many numerical methods are iterative in nature, with the approximations theoretically becoming more accurate as more iterations were taken and the iteration need to be stop after a finite number of steps. Lastly, “round-off” or “rounding” errors, is due to the fact that a computer has a finite word length. Hence, most numbers and the results of arithmetic operations on most numbers cannot be represented exactly on a computer.

1.3.3 Absolute and Relative Error

Most of real numbers have undergoes rounding process in order to be presented as t-digit floating point number. The difference between the floating point number x' and the original number x is called the round off error. According to BiswaNath (1995), the errors in a computation are measured either by absolute error or relative error, where the relative errors make more sense than absolute error. In analyzing the error of computation, the absolute error can be defined to be $(x - \check{x})$ and the relative error can be defined to be $(x - \check{x}) / x$ if \check{x} represent the “computed solution” to the “true solution” x (Johnson and Riess, 1977).

1.3.4 Vector and Matrix Norms

1.3.4.1 Vector Norm

The special cases of the Holder norms are the most commonly used vector norms in numerical linear algebra, which is

$$\|x\|_p = \left(\sum_{i=1}^n |x|^p \right)^{1/p}$$

The cases $p=1$, $p=2$ and $p=\infty$ indicate to this important norms.

1. $\|x\|_1 = |x_1| + |x_2| + \dots + |x_n|$,
2. $\|x\|_2 = [|x_1|^2 + |x_2|^2 + \dots + |x_n|^2]^{1/2}$,
3. $\|x\|_\infty = \max_{i=1 \dots n} |x_i|$.

1.3.4.2 Matrix Norm

According to BiswaNath (1995), a nonnegative number defined by:

$$\|A\|_p = \max_{x \neq 0} \frac{\|Ax\|_p}{\|x\|_p}$$

given a matrix A and a vector norm $\|\cdot\|$. This norm represents the matrix norm subordinate to the vector norm. Note that the two most easily computable p -norms are:

$$\|A\|_1 = \max_{1 \leq j \leq n} \sum_{i=1}^m |a_{ij}| \quad (\text{maximum column-sum norm})$$

$$\|A\|_\infty = \max_{1 \leq i \leq m} \sum_{j=1}^n |a_{ij}| \quad (\text{maximum row-sum norm})$$

1.3.5 Matrix Conditioning

The condition number plays an important role in the numerical linear algebra. Here, condition number is introduced to measure the sensitivity of a linear system $Ax = b$ to the perturbations in the coefficients of matrix A or vector b . The condition number associated with the linear equation $Ax = b$ provides an approximate upper bound on the error in a computed solution. Beside, conditioning is a property of the matrix, not the floating point accuracy of the computer or algorithm used to solve the corresponding system; note that this is before the effects of round-off error are taken into account.

$$\frac{\|x_1 - x_2\|}{\|x_1\|} \leq \|A\| \|A^{-1}\| \frac{\|b_1 - b_2\|}{\|b_1\|}$$

The coefficient $\|A\| \|A^{-1}\|$ depends on the matrix in the problem, not the right-hand side vector, thus it shows up as an amplifier to the relative change in the right-hand side vector. Therefore, the condition number of a nonsingular matrix A is defined as $\text{cond}(A) = \|A\| \|A^{-1}\|$.

Definition 1.3(Gregoire, 2008) The condition number of a matrix $A \in M_n(\mathbb{K})$, relative to subordinate matrix norm $\|\cdot\|$, is the quantity defined by

$$\text{cond}(A) = \|A\| \|A^{-1}\|$$

A matrix A is said to be “well-conditioned” if for a given norm, $\text{cond}(A) \approx 1$, and it is “ill-conditioned” if $\text{cond}(A) \gg 1$.

1.3.6 Conditioning of a System of Equations

According to Anna *et al.* (2011), the condition number measures the sensitivity of the solutions to the perturbation in the data. This sensitivity of linear equation is related with the performance on producing the exact solutions. When the floating point is introduced in the system, such problem may arise. There will be effects in determining the solutions for the linear problem due to the existence of rounding off number since the system is exposed to the floating point environment which will defect the result leading to a less accurate solution. This condition is said to be perturbed where a small change in the data could lead to changes in the final solution which are less accurate toward the exact solution. The effect of perturbations can be classified into 3 cases.

1.3.6.1 Effect of Perturbation in the Vector b

Theorem 1.3.1 (BiswaNath, 1995): Right Perturbation Theorem If δb and δx , are, respectively, the perturbations of b and x in the linear system $Ax = b$ and A is assumed to be nonsingular and $b \neq 0$, then

$$\frac{\|\delta b\|}{\text{Cond}(A)\|b\|} \leq \frac{\|\delta x\|}{\|x\|} \leq \text{Cond}(A) \frac{\|\delta b\|}{\|b\|}$$

1.3.6.2 Effect of Perturbation in the Coefficient Matrix

Theorem 1.3.2 (BiswaNath, 1995): Left Perturbation Theorem Assume matrix A is nonsingular and $b \neq 0$. Suppose that δx and ΔA are the perturbations of A and x respectively in the linear system

$$Ax = b.$$

Besides, assume that ΔA is such that $\|\Delta A\| < \frac{1}{\|A^{-1}\|}$.

$$\frac{\|\delta x\|}{\|x\|} \leq \text{Cond}(A) \frac{\|\Delta A\|}{\|A\|} / \left(1 - \text{Cond}(A) \frac{\|\Delta A\|}{\|A\|}\right)$$

1.3.6.3 Effect of Perturbation in Both Matrix A and Vector b

Theorem 1.3.3 (BiswaNath, 1995): General Perturbation Theorem By assuming that A is nonsingular, $b \neq 0$ and $\|\Delta A\| < \frac{1}{\|A^{-1}\|}$. Then

$$\frac{\|\delta x\|}{\|x\|} \leq \left(\frac{\text{Cond}(A)}{1 - \text{Cond}(A) \frac{\|\Delta A\|}{\|A\|}} \right) \left(\frac{\|\Delta A\|}{\|A\|} + \frac{\|\delta b\|}{\|b\|} \right)$$

1.3.7 Stability of the Algorithm and Accuracy of the Solution

In order to solve a given problem, an appropriate algorithm and its numerical implementation is observed. The stability of the algorithm is an important thing in determining the accuracy of the computed solution converging to the desired solution. When a system has a good conditioning and stable algorithm is used, this criterion guarantees that the solutions will be accurate. According to BiswaNath (2010), the stability of the algorithm and the conditioning of the problem will effects the accuracy of the solution computed by the algorithm.

- Stable algorithm + Well conditioned problem = Accurate solution
- Stable algorithm + Ill-conditioned problem = Accuracy not guaranteed.

1.4 PRECONDITIONING

Preconditioning is the application of a transformation, which is called the preconditioner that will condition a given problem into a form that are suitable for numerical solving methods. The objective of preconditioning is to reduce the condition number of the problem. Gregoire and Sidi (2008) stated that it may be more efficient to solve the equivalent linear system $C^{-1}Ax = C^{-1}b$ with a nonsingular matrix C that is easily invertible and $C^{-1}A$ is said to be a better conditioned than A rather than solving a linear system $Ax = b$ with an ill-conditioned matrix A . The matrix C is called a preconditioner and the best choice of $C^{-1}A$ is that $C^{-1}A$ is close to the identity where the conditioning is minimal, equal to 1, that is C is close to A .

1.4.1 Polynomial Preconditioning

In this section, the algorithm to compute polynomial preconditioning as a worked out problem is illustrated.

The idea of this preconditioning is to define $C^{-1} = p(A)$, where p is polynomial such that $cond(C^{-1}A) \ll cond(A)$. A good choice of $C^{-1} = p(A)$ is by truncate the expansion in power series of A^{-1} , where

$$A^{-1} = (I - (I - A))^{-1} = I + \sum_{k \geq 1} (I - A)^k$$

which will converges if $\|I - A\| < 1$. In other words, the polynomial $p(x) = 1 + \sum_{k=1}^d (1 - x)^k$ is chosen (Gregoire and Sidi, 2008).

Example 1.4.1

Consider the Hilbert matrix of size 2x2 given by

$$A = \begin{pmatrix} 1.0000 & 0.5000 \\ 0.3333 & 0.3333 \end{pmatrix}$$

Let $C = I - A$, where $I = \begin{pmatrix} 1 & 0 \\ 0 & 1 \end{pmatrix}$

The preconditioning $C^{-1} = p(A)$ converges when $\|I - A\| < 1$. This condition is satisfied when the largest modulus of the eigenvalues of C denoted as $\| \max C \| < 1$.

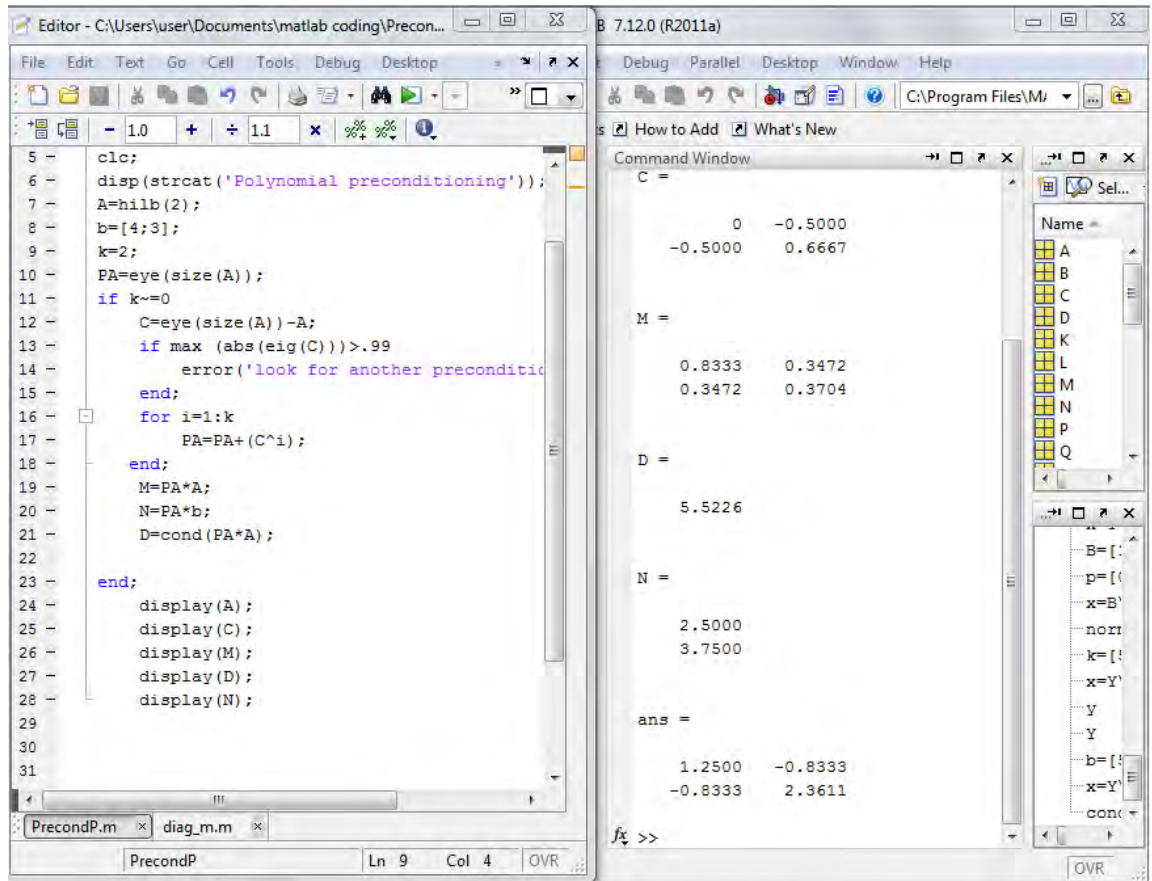


Figure 1.4.1: Method on the polynomial preconditioning with $k = 2$

From the results obtained in Figure 1.4.1, the condition number of the matrix M is reduced to 1.0656 when $k = 40$ as compared with the condition number when $k = 2$ which is 5.5226. Thus, as the value of k increases, the better is the conditioning.

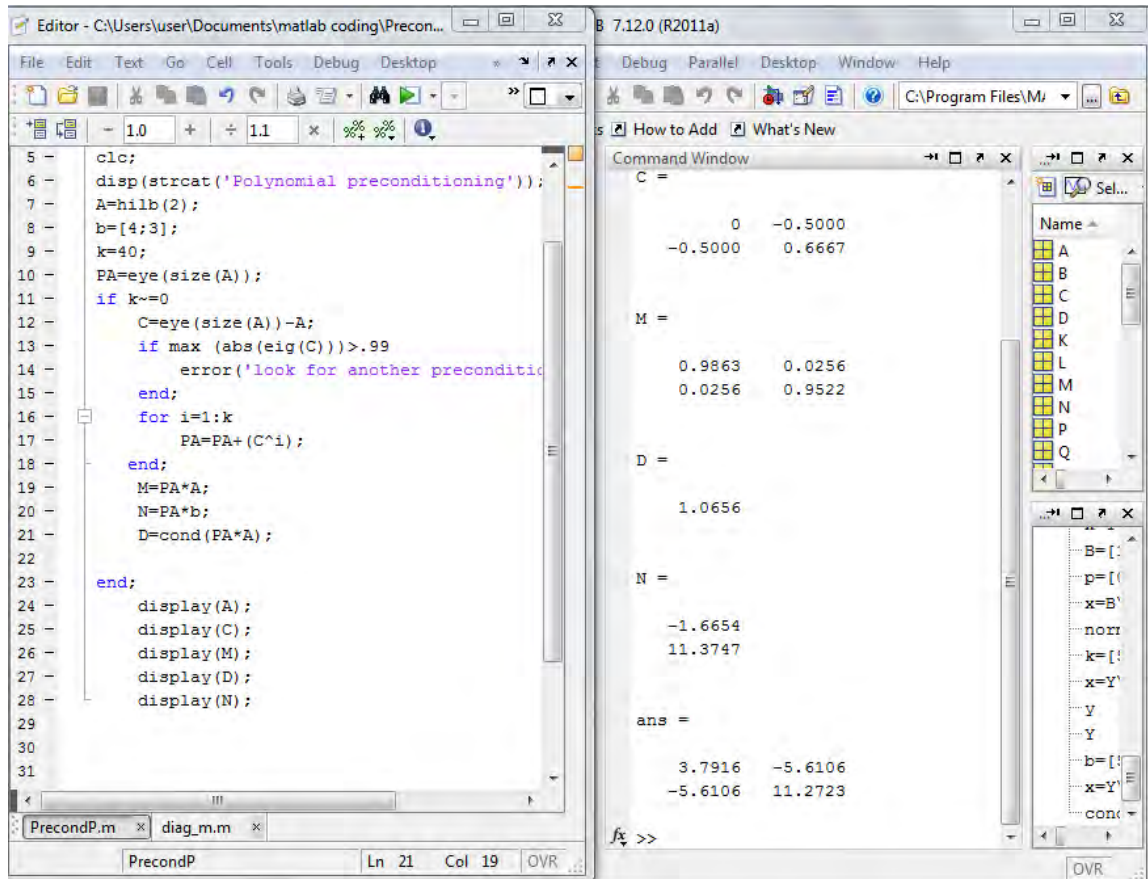


Figure 1.4.2: Method on the polynomial preconditioning with $k = 40$

By solving the preconditioned system, the solution obtained is $x = \begin{pmatrix} -2.0000 \\ 11.9995 \end{pmatrix}$ and the value of residual is $1.5452e - 016 = 1.7389 \times 10^{-7}$. Since the condition number of the preconditioned system is small, therefore the solution obtained is accurate as the product of both $Cond(M)$ and the relative residual are small, which is 1.8529×10^{-7} .

1.4.2 Diagonal Preconditioning

The diagonal preconditioner (or Jacobi preconditioner) is one of the simplest forms of the preconditioning, in which the preconditioner is chosen to be the diagonal of matrix $P = diag(A)$. By assuming that the diagonal entries of matrix $A \neq 0$, then $P_{ij}^{-1} = \frac{d_{ij}}{A_{ij}}$. This type of preconditioning is said to be very efficient when the matrix A is diagonally dominant matrix, where

$$|a_{ii}| > \sum_{j \neq i} |a_{ij}|$$

for all i , where a_{ij} is the entry in the i th row and j th column.

Example 1.4.2

Solve the ill-conditioned linear problem

$$A = \begin{pmatrix} 1.0000 & 0.5000 & 0.3333 \\ 0.5000 & 0.3333 & 0.2500 \\ 0.3333 & 0.2500 & 0.2000 \end{pmatrix} \text{ and } b = \begin{pmatrix} 0.1002 \\ 1.0001 \\ 0.0020 \end{pmatrix}$$

Solution:

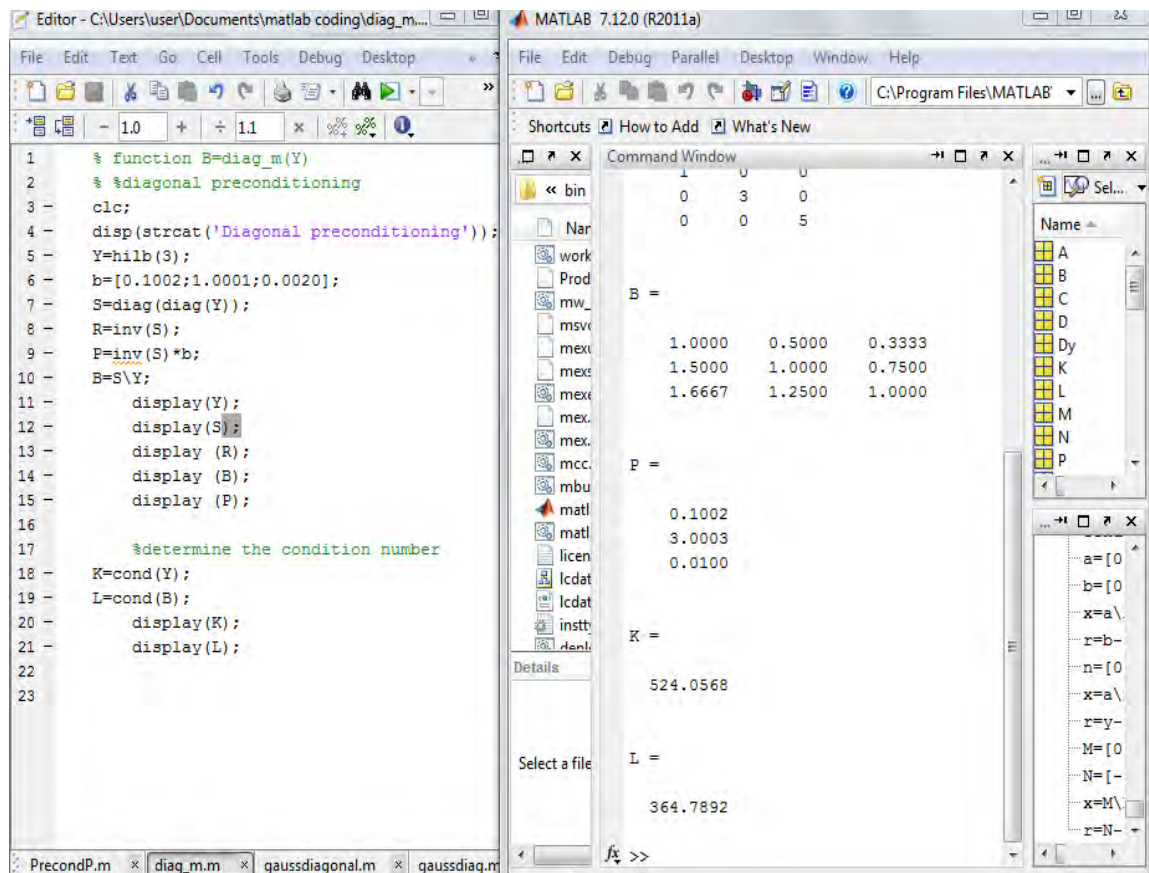


Figure 1.4.3: Solution on diagonal preconditioning

Based on the results shown in Figure 1.4.3, the condition number of 3x3 Hilbert matrix is reduced from 524.0568 to 364.7892. Although the value of condition number is still large, the system is better conditioned compared to the original system of equations. Hence, by using diagonal preconditioning to this ill conditioned problem, diagonal preconditioning has reduced the value of the condition number of the matrix, but the value is still greater than 1.

1.4.3 Right Preconditioning

Besides using polynomial and diagonal preconditioning, another idea is by transforming the system of equation $Ax = b$ into $AD^{-1}y = b$ with $x = D^{-1}y$ in which D (easily invertible) is called a right preconditioner. Instead of that, by replacing the system $Ax = b$ by $C^{-1}Ax = C^{-1}b$, the system is called left preconditioning. According to Gregoire and Sidi (2008), these two kinds of preconditioning can be mixed together and solving $C^{-1}AD^{-1}y = C^{-1}b$, then compute x by $D^{-1}y = x$. If the matrix A is symmetric, then choose $C = D^t$ due to the symmetric of matrix $C^{-1}AD^{-1}$. Benzi (2002) stated that split preconditioning is also possible, where

$$M_1^{-1}AM_2^{-1}y = M_1^{-1}b, \quad x = M_2^{-1}y$$

where the preconditioner $M = M_1M_2$ and $M_1 = M_2^t$. Therefore this preconditioning is efficient when the condition number, $\text{cond}(C^{-1}AD^{-1}) \ll \text{cond}(A)$, hence solving $Dx = y$ become easy.

Example 1.4.3

Solve the ill-conditioned linear problem

$$A = \begin{pmatrix} 0.3330 & 0.2500 & 0.2000 \\ 0.5000 & 0.3330 & 0.2500 \\ 1.0000 & 0.5000 & 0.3330 \end{pmatrix} \quad \text{and the vector } b = \begin{pmatrix} 0.2000 \\ 0.3330 \\ 0.3330 \end{pmatrix}$$

The given exact value of $x = \begin{pmatrix} -3 \\ 16 \\ -14 \end{pmatrix}$

Solution:

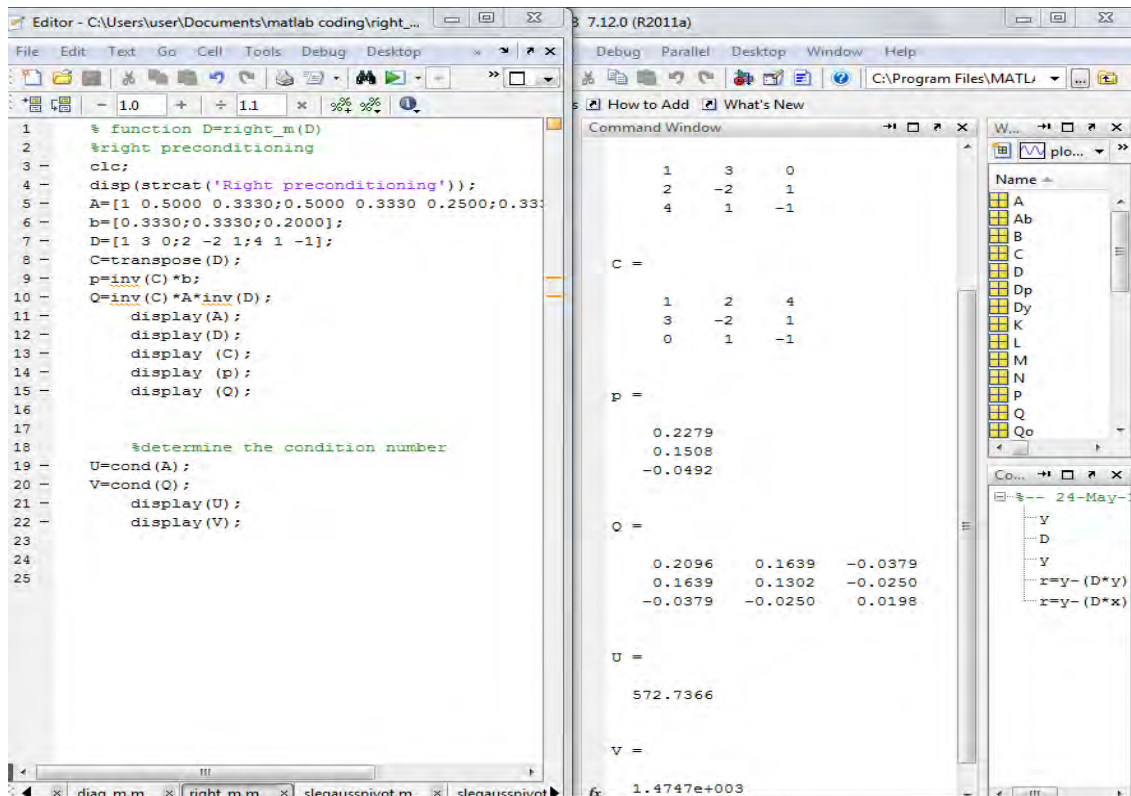


Figure 1.4.4: Solution on split preconditioning

Figure 1.4.4 shows the computation for finding the matrix $Q = C^{-1}AD^{-1}$ in split preconditioning. The matrix

$$D = \begin{pmatrix} 1 & 3 & 0 \\ 2 & -2 & 1 \\ 4 & 1 & -1 \end{pmatrix}$$

is chosen since this matrix is invertible. The condition number of matrix A is reduced from 572.7366 into 1.4747e+003 which is equal to 29.6201. This indicates that the matrix become a better conditioned compare to the original problem and solving the equation by using Gaussian elimination with partial pivoting.

1.5 CONCLUSION

The concepts of preconditioning is used in order to reduce the condition number of an ill-condition system whereby the condition number of the coefficient matrix A is large and is sensitive to the perturbations of data either in A , vector b or both. Instead of solving the linear system with an ill-conditioned matrix, a ‘preconditioner’ is used to solve the linear system more efficiently.

Three types of preconditioning techniques have been discussed and applied to observe the effects of conditioning on the condition number of a matrix. For polynomial preconditioning, if the convergence criteria is not satisfied then other preconditioning techniques have to be sought. Besides this, diagonal preconditioning (or Jacobi preconditioning) is also applied to improve the condition number of ill-conditioned systems. However, diagonal preconditioning allows reducing the condition number for certain problems. This is due to the condition number after the preconditioned is larger than the condition number of matrix A , which do not reduce after undergo preconditioning process. Lastly, split preconditioning may be regarded as a compromise between left and right preconditioning. This preconditioning is efficient when $cond(C^{-1}AD^{-1}) \ll cond(A)$, hence solving $Dx = y$ is easy.

Conditioning of a system of equations can be used to determine the conditioning behavior of the coefficient matrix and predict the accuracy of the solutions. When the system is well conditioned or ill-conditioned, conditioning of the system will have influence on the stability and accuracy of the system because the condition number of the system has some effects towards the perturbation which can increase or reduce the accuracy of the solutions.

REFERENCES

- Anna Pyzara, BeataBylna and JaroslawBylina.(2011). The Influence of a Matrix Condition Number on Iterative Method's Convergence.*Proceeding of the Federated Conference on Computer Science and Information System*.Lubin Poland.459-464.
- BiswaNathDatta. (1995). *Numerical Linear Algebra and Application*. Brooks.
- Che Rahim CheTeh. Algorithm and Matlab Programming Numerical Method July 2009. (2009). Desktop Publisher.
- Ferronato, M. Preconditioning for Sparse Linear Systems at the Dawn of the 21st Century: History, Current Developments, and Future Perspectives. (2012). *International Scholarly Research Notices*. Vol. 2012, 49.
- GermundDahlquist and AkeBjorck.(1974). *Numerical Methods*. Englewood Cliffs, N.J.: Prentice-Hall.
- GregoireAllaire, Sidi Mahmoud Kaber. (2008). *Numerical Linear Algebra*. New York, NY: Springer-Verlag.
- HyoungJoong Kim, Kyung Choi, H.B. Lee, H.K. Jung and S. Y. Hahn.(1996). A New Algorithm for Solving Ill-Conditioned Linear Systems.*IEEE Transactions On Magnetics*. Vol. 32, No. 3, May, Korea. 1373 -1376.
- James F. Epperson. (2007)..*An Introduction To Numerical Methods And Analysis*: Revised Edition.
- Kubicek, M., Janovská, D., &Dubcová, M.(2005).*Numerical Methods and Algorithms*.Praha.
- Laurene V. Fausett. (2008). *Applied Numerical Analysis Using MATLAB*. (2nded.).Texas A&M University-Commerce: Pearson Prentice Hall.
- Lee W. Johnson and R. Dean Riess (1977).*Numerical Analysis*. Addison-Wesley Longman Incorporated.
- Michele Benzi (2002). Preconditioning Techniques for Large Linear Systems: A Survey.*Journal of Computational Pyhsics*. 182, 418-477.

Muhammad Farooq and AbdellahSalhi (2011).Improving The Solvability of Ill-Conditioned Systems of Linear Equations by Reducing The Condition Number of Their Matrices. J. Korean Math. Soc. 48, No. 5, pp. 939-952.

Rizwan Butt. (2008). *Introduction to Numerical Analysis Using MATLAB*. Hingham, Massachusetts New Delhi:Infinity Science Press LLC.

Trefethen, Lloyd N. (2006) IV. 21 Numerical Analysis.

YousefSaad (2003). *Iterative Methods for Sparse Linear Systems*. (2nded.) Philadelphia PA, SIAM.

Yu Liang (2005). *The Use of Parallel Polynomial Preconditioners in the Solution of Systems of Linear Equations*.Doctor Philosophy, University of Ulster.

Zahra Vahedipour and BehrouzDaneshian (2013).On the Solution of Ill-Conditioned Systems of Linear Equations..*Journal of Expert Systems*, Vol.2, No. 1, pp. 119-122.

A Study Of The Dynamics Of Hand, Foot, And Mouth Disease (Hfmd) Using A System Of Ordinary Differential Equations

Aufa A'qilahbinti A Hamid & Dr. Fuaada Mohd Siam

Abstract

Hand, foot and mouth disease (HFMD) is a mild infectious disease with no specific treatment to cure. Since it has no specific treatment to cure, thus the study of the dynamics of the disease is needed. S (Susceptible), I (Infected), R (Recovered) model is introduced by Ross and Hudson in 1916 in order to study the probabilities of a prior pathometry. Since 1926, SIR model becomes famous especially in order to study the disease transmission between susceptible and infective individuals. By using the framework of SIR model, we investigate the dynamics of HFMD. We also extend the model by taking into account the latent class in the model developed. We analyse the dynamics process by using system of Ordinary Differential Equations and also the analysis of multivariable stability analysis. For both models, we consider the disease free equilibrium and endemic equilibrium.

Keywords : HFMD, SIR model, latent class, system of ODEs, multivariable stability analysis, disease free equilibrium, endemic equilibrium.

Introduction

Hand, foot and mouth disease (HFMD) is a mild illness caused by Coxsackie virus (A16) and human enteroviruses (HEV71). HFMD usually affected the children who is below 5 years old. However, adults and older children can also got infected. This illness commonly occurs in countries with temperature climates in summer and early autumn (Roy, 2012). There are many symptoms of HFMD whereas feeling vaguely unwell (fever, poor appetite, malaise), sores (ulcers) in mouth and rashes or blisters on the palms and feet and sometimes on the buttocks. However, some infected people may only have a rash and others may only have mouth sores and some does not show any symptoms (Roy, 2012). HFMD usually caused mild infections but not a serious illness because the symptoms of HFMD usually gone within 7-10 days without medical treatment. Rarely, HFMD caused by HEV71 can cause complications such as polio-like paralysis or encephalitis (inflammation of the brain) and this complication may be fatal (James, 2014). HFMD can be spread by; (i) fecal-oral route. For example is food and water that was prepared in the presence of fecal matter and poor cleaning after handling feces or anything that has been in contact with it; (ii) contact with skin lesions; (iii) oral secretions; (iv) contact with toy's surfaces that contaminated with HFMD.

Most of children are infected by hand, foot and mouth disease (HFMD) in their early ages. Unfortunately, there is no specific treatment to cure HFMD. Owing to that, much attention have been focused on devising method for preventing the spread of HFMD. However, we need further understanding on the dynamics of HFMD. Therefore, in this work,

we study the dynamics of HFMD using the framework of SIR model (S =Susceptible, I =Infected), R =Recovered). The objectives of the research are; (i) to analyse the dynamics of HFMD follow the framework of SIR model; (ii) to extent the SIR model by allowing the latent variable; and (iii) to understand the behaviour of both system's dynamics through the stability analysis of the system using Jacobian matrix and its eigenvalues. The scope of the study is only focus on SIR model that determine the number of people infected with HFMD in a closed population over time. Then, the model is expanded by taking into account the latent class of infected individuals. The model was derived from a system of ODEs for HFMD. Next, the dynamics of the system and the stability at the equilibrium of the system was analysed by using Jacobian matrix and also eigenvalues. From this study, we can enhance our understanding on HFMD. Besides that, the results provided will help us to suggest a new therapeutic protocol in order to cure HFMD.

Literature Review

In 1906, Hamer has developed one of the earliest epidemic model. He try to apply post-germ-theory thinking towards the solution of two specific quantitative problems whereas the relationship between numbers mosquitoes regarding incidence of malaria; and the regular recurrence of measles epidemic (Anderson & May, 1992). From the work of Hamer, then in 1916-1917, the classical SIR model originated from the papers of Ross and Ross and Hudson. (Magal & Ruan, 2014). After year of 1926, SIR model become famous since fundamental contribution of Kermack and Mckendrick which describes the transmission of infectious disease between susceptible and infective individuals and provides the basic framework for almost all later epidemic models they also include stochastic epidemic models using Monte Carlo simulations or known as individual-based models (IBM) in their paper. (Magal & Ruan, 2014). The model categorizes population into Susceptible, Infected and Recovered. In this model, susceptible individuals in S-stage have chance to be infected and progress to infection I-stage until recovery to R-stage. The flow is shown in figure 1 (Chong & Zee, 1927).



Figure 1 Flow of SIR model

SIR model have been used in various fields of modelling and mathematical problems. For example, Jiang, He, & Cheng (2009) used SIR model to study the stability and bifurcation with time delays. Wang and his co-workers (2010) prepared the application of the Lambert W Function (an inverse of ωe^ω) to the SIR model. Tian (2012) extended the SIR model to SIRS model to study the stability of a delayed SIRS model with vaccination and nonlinear incidence. Liu, Wang, Xu, & Li (2013) used SIR model to study the dynamic of the model with stochastic process perturbations and Grigorieva & Khailov (2014), the

researcher study about the optimal vaccination, treatment and preventive campaign in regard to the SIR model.

Research Methodology

To study the dynamics of the disease outbreak, we apply the system of Ordinary Differential Equations (ODE) and stability analysis of the system. ODE is a differential equation that involving only derivatives with respect to one independent variable. Then, a system of ODE is a combination of two or more ODEs that treated simultaneously. For example,

$$\frac{d^n y}{dx^n} = F\left(x, y, \frac{dy}{dx}, \frac{d^2 y}{dx^2}, \dots, \frac{d^{n-1} y}{dx^{n-1}}\right). \quad (1)$$

After having a system of ODE, we find the basic reproduction number, R_0 to know the critical density of susceptible population to occur an epidemic. R_0 is an expected number of secondary cases produced by a single infection in a completely susceptible population (Jones, 2007). R_0 is a dimensionless number and not a rate. Suppose that

$$R_0 \propto \left(\frac{\text{infection}}{\text{contact}}\right) \cdot \left(\frac{\text{contact}}{\text{time}}\right) \cdot \left(\frac{\text{time}}{\text{infection}}\right). \quad (2)$$

Note that, if $R_0 < 1$, infected individual will die out and disease eliminated. Otherwise, if $R_0 > 1$, infected individuals grows and spread in a population (Kodaira, 2010).

Next, we will use stability analysis of ODE system to interpret the dynamics of a system. Stability of the system can be analysed using system of ODE by finding its Jacobian and eigenvalues at equilibrium points (Roussel, 2005). The Jacobian matrix of a system of ODE can be written as

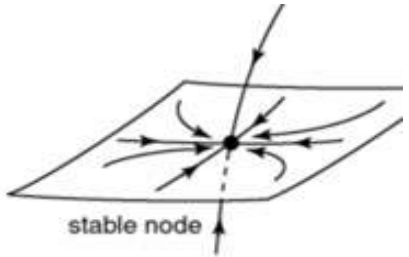
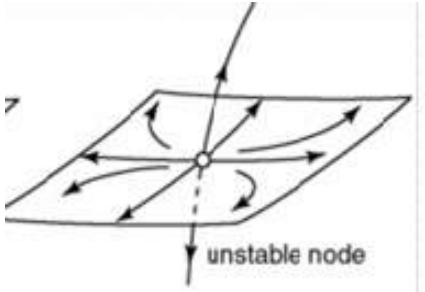
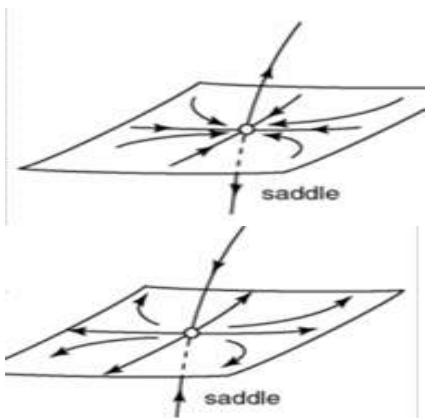
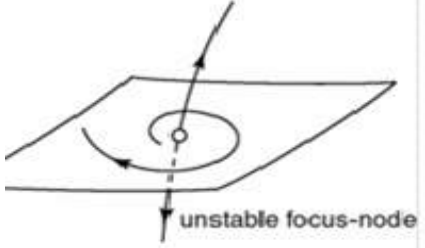
$$J = \begin{bmatrix} \frac{\partial F_1}{\partial x_1} & \frac{\partial F_1}{\partial x_2} & \dots & \frac{\partial F_1}{\partial x_n} \\ \frac{\partial F_2}{\partial x_1} & \frac{\partial F_2}{\partial x_2} & \dots & \frac{\partial F_2}{\partial x_n} \\ \vdots & \vdots & \ddots & \vdots \\ \frac{\partial F_m}{\partial x_1} & \frac{\partial F_m}{\partial x_2} & \dots & \frac{\partial F_m}{\partial x_n} \end{bmatrix}, \quad (3)$$

and the eigenvalues can be obtained by using

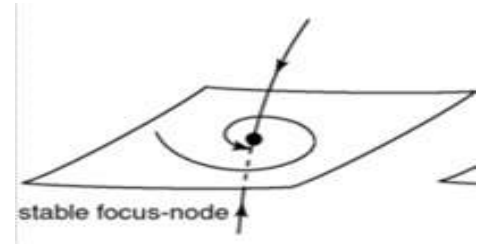
$$\det(\lambda I - A) = 0, \quad (4)$$

where I is an identity matrix, λ is an eigenvalue and A is a Jacobian matrix at an equilibrium point. Then, the eigenvalues is analysed using table 1 to check the stability of the system.

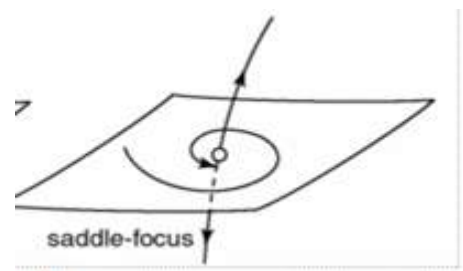
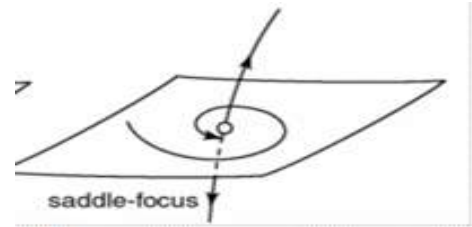
Table 1: Stability analysis of three-dimensional system (Sprott, 2000)

Category	Stability	Type of critical point	Sketches
All eigenvalues are negative	Stable	Node	 <p>stable node</p>
All eigenvalues are positive	Unstable	Node	 <p>unstable node</p>
All eigenvalues are real and at least one of them is positive and at least one is negative	Unstable	Saddle	 <p>saddle</p> <p>saddle</p>
one real eigenvalue and a pair of complex-conjugate eigenvalues (all eigenvalues have positive sign for the real parts)	Unstable	Focus-Node	 <p>unstable focus-node</p>

one real eigenvalue and a pair of complex-conjugate eigenvalues (all eigenvalues have negative sign for the real parts) Stable Focus-Node



one real eigenvalue and a pair of complex-conjugate eigenvalues (all eigenvalues have an opposite sign for the real parts) Unstable Saddle-Focus



Furthermore, we are using resultant and discriminant for dealing with multivariate polynomials. Resultant is also known as an eliminant. The resultant $R(f, g)$ of f and g with respect to y is the determinant of the $(m + n) \times (m + n)$ Sylvester matrix of f and g .

$$R(f, g) = \begin{vmatrix} a_n(x) & a_{n-1}(x) & a_{n-2}(x) & \cdots & a_1(x) & a_0(x) & \cdots & 0 \\ \vdots & \vdots & \ddots & \vdots & \vdots & \vdots & \ddots & \vdots \\ 0 & 0 & \cdots & a_n(x) & a_{n-1}(x) & \cdots & \cdots & a_0(x) \\ b_m(x) & b_{m-1}(x) & \cdots & b_1(x) & b_0(x) & 0 & \cdots & \cdots \\ \vdots & \vdots & \ddots & \cdots & \vdots & \vdots & \ddots & \vdots \\ 0 & 0 & \cdots & \cdots & b_m(x) & b_{m-1}(x) & \cdots & b_0(x) \end{vmatrix}. \quad (5)$$

From equation (5), we get a polynomial in terms of x . Resultants are applied for solving simultaneous systems of polynomial equations and allow one to eliminate a variable from a system of equations.

Next, suppose that $Q(x)$ is a one-variable polynomial (one-variable of characteristic polynomial) given by

$$Q(x) = c_r x^r + c_{r-1} x^{r-1} + c_{r-2} x^{r-2} + \cdots + c_1 x + c_0. \quad (6)$$

The discriminant Δ of $Q(x)$ is given by

$$\Delta = (-1)^{\frac{1}{2}r(r-1)} \frac{1}{c_r} R(Q, Q'), \tag{7}$$

where $R(Q, Q')$ is known as the resultant of $Q(x)$ and the derivative Q with respect to x , $Q'(x)$. Then, the graph of discriminant, Δ is plotted several possible cases is distinguished depending on the discriminant, Δ ; (i) if $\Delta < 0$, then the equation has one real root and a pair of a complex conjugate roots; (ii) if $\Delta > 0$, then all roots (three roots) are real and unequal; (iii) if $\Delta = 0$, then the equation has three real roots and at least two are equal.

Results and Discussion

For SIR model, the system of linear ODE given by; (i) $\frac{dS}{dt} = \alpha - \beta SI + \lambda R$; (ii) $\frac{dI}{dt} = \beta SI - \delta I - \rho I$; (iii) $\frac{dR}{dt} = \rho I - \lambda R$. The calculated R_0 is given as $R_0 = \frac{\beta}{(\delta + \rho)}$ and the Jacobian matrix is given as

$$J = \begin{pmatrix} -\beta I & -\beta S & \lambda \\ \beta I & \beta S - \delta - \rho & 0 \\ 0 & \rho & -\lambda \end{pmatrix}. \tag{8}$$

At disease free equilibrium points (DFEP), we have point $(S, I, R) = (1, 0, 0)$. We substitute the point into Jacobian matrix (8) and the eigenvalues obtained are $a_1 = 0$, $a_2 = -\lambda$, $a_3 = \beta - \delta - \rho$. Note that, DFE only exists if all the eigenvalues are negative (Roy, 2012). Therefore, a_3 must be less than zero. Hence, we obtain $\frac{\beta}{\delta + \rho} < 1$. This shown that $R_0 < 1$ which implies that at $(S, I, R) = (1, 0, 0)$, infected individual will die out and disease will be eliminated. Furthermore, the stability of HFMD at DFEP is stable based on eigenvalues that we found (by referring table 1).

At endemic equilibrium point (EEP), we have point $(S, I, R) = (\frac{(\delta + \rho)}{\beta}, \frac{\alpha}{\delta}, \frac{\alpha \rho}{\lambda \delta})$. However, both points I and R are not so important and it depends on the parameter values. (i.e, can be any numbers). Thus, we substitute point $(S, I, R) = (\frac{(\delta + \rho)}{\beta}, I, R)$ in Jacobian matrix (8) and the characteristic polynomial obtained is

$$a^3 + (\lambda + \beta I)a^2 + (\lambda \beta I + \delta \beta I + \rho \beta I)a + \delta \lambda \beta I = 0. \tag{9}$$

From (9), the eigenvalues obtained could be negative, positive, zero or any combinations of the three alternatives, depend on the parameter values provided. Therefore, we use the characteristic polynomial to check the stability of the EEP. Next, we obtain the resultant and

discriminant, Δ to know the condition for characteristic polynomial (9) to have one, two and three roots. The discriminant is given as

$$\Delta = -3 + 6\lambda - 9\lambda^2 + 6\lambda^3 - 3\lambda^4 - 10\rho + 12\lambda^2\rho + 2\lambda^3\rho - 11\rho^2 - 10\lambda\rho^2 + \lambda^2\rho^2 - 4\rho^3. \quad (10)$$

Then, by the aid of MATHEMATICA, we plot the graph of the discriminant as shown in figure 2.

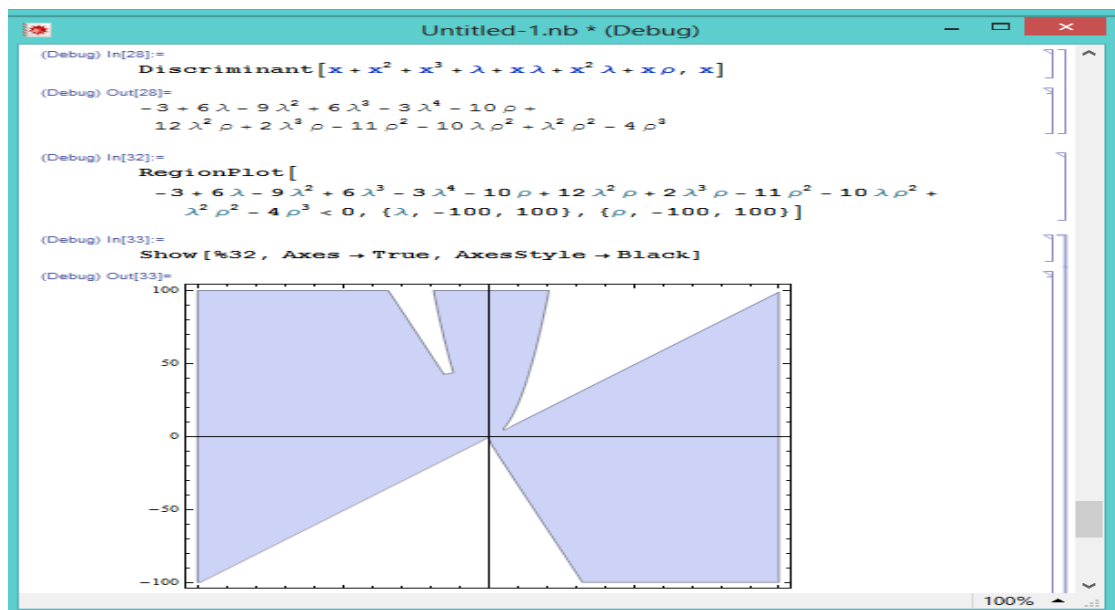


Figure 2 The domain of the equation (10) having four, three and one real root

From figure 2; (i) if $-3 + 6\lambda - 9\lambda^2 + 6\lambda^3 - 3\lambda^4 - 10\rho + 12\lambda^2\rho + 2\lambda^3\rho - 11\rho^2 - 10\lambda\rho^2 + \lambda^2\rho^2 - 4\rho^3 < 0$ (Shaded region), the equation having one real root and a pair of complex conjugate roots; (ii) if $-3 + 6\lambda - 9\lambda^2 + 6\lambda^3 - 3\lambda^4 - 10\rho + 12\lambda^2\rho + 2\lambda^3\rho - 11\rho^2 - 10\lambda\rho^2 + \lambda^2\rho^2 - 4\rho^3 > 0$ (Unshaded region), the equation has all real and unequal roots; (iii) if $-3 + 6\lambda - 9\lambda^2 + 6\lambda^3 - 3\lambda^4 - 10\rho + 12\lambda^2\rho + 2\lambda^3\rho - 11\rho^2 - 10\lambda\rho^2 + \lambda^2\rho^2 - 4\rho^3 = 0$ the equation has three real roots and at least two are equal.

For SLIR model, latent class (L) is added into SIR model to check the dynamic of HFMD. Latent class is a latent period of an infectious disease. Latent period is a time interval between a susceptible individual to become an infected individual (Roy, 2012). It is happen because we assumed that susceptible individual do not immediately become infected individual when susceptible contact with infected individuals. The system of ODE is given

as; (i) $\frac{dS}{dt} = \alpha - \beta SI + \lambda R$; (ii) $\frac{dL}{dt} = \beta SI - \gamma L$; (iii) $\frac{dI}{dt} = \gamma L - \delta I - \rho I$; (iv) $\frac{dR}{dt} = \rho I - \lambda R$.
 The calculated R_0 is given as $R_0 = \frac{\beta}{(\delta + \rho)}$ and the Jacobian matrix is given as

$$J = \begin{pmatrix} -\beta I & 0 & -\beta S & \lambda \\ \beta I & -\gamma & \beta S & 0 \\ 0 & \gamma & -\delta - \rho & 0 \\ 0 & 0 & \rho & -\lambda \end{pmatrix}. \tag{11}$$

At disease free equilibrium point (DFEP), we have point $(S, L, I, R) = (1, 0, 0, 0)$. The point is substituted into Jacobian matrix 2 and the eigenvalues obtained are $a_1 = 0$, $a_2 = -\lambda$, $a_3 = \frac{1}{2}(-\gamma - \delta - \rho - \sqrt{(\gamma + \delta + \rho)^2 - 4(-\beta\gamma + \gamma\delta + \gamma\rho)})$ and $a_4 = \frac{1}{2}(-\gamma - \delta - \rho + \sqrt{(\gamma + \delta + \rho)^2 - 4(-\beta\gamma + \gamma\delta + \gamma\rho)})$.

At endemic equilibrium point (EEP), we have point $(S, L, I, R) = (\frac{\delta + \rho}{\beta}, (\frac{\delta + \rho}{\gamma})(\frac{\alpha}{\delta}), \frac{\alpha}{\delta}, \frac{\rho\alpha}{\lambda\delta})$. The point will be substituted into Jacobian matrix 2 and obtain the eigenvalues that could be negative, positive, zero or any combinations of the three alternatives. Hence, to check the dynamics of HFMD at EEP using SLIR model, we plot the graph of characteristic polynomial by the aids of MATHEMATICA. The characteristic polynomial is given as

$$[a + \beta(\frac{\alpha}{\delta})](a + \gamma)(a + \delta + \rho)(a + \lambda) = 0. \tag{12}$$

At parameters value $\alpha = -8, \beta = -2, \gamma = -2, \delta = -2, \lambda = -2, \rho = -2$, we get two real roots and two complex conjugate roots and the eigenvalues obtained are $a_1 = 3.1520 - 2.1240i$, $a_2 = 0.8480 + 2.1240i$, $a_3 = -3.5193$ and $a_4 = 5.2153$.

At parameters value $\alpha = 8, \beta = -2, \gamma = -10, \delta = -2, \lambda = -10, \rho = -2$, we have two real roots and two complex conjugate roots and the eigenvalues obtained are $a_1 = 5.8852 - 2.3304i$, $a_2 = 5.8852 + 2.3304i$, $a_3 = 0.6923$, and $a_4 = 11.5374$.

At parameters value $\alpha = -8, \beta = 2, \gamma = -10, \delta = -2, \lambda = -10, \rho = -2$, we get two real roots and two complex conjugate roots and the eigenvalues obtained are $a_1 = 7.0942 - 8.1915i$, $a_2 = 7.0942 + 8.1915i$, $a_3 = -7.9107$ and $a_4 = 1.7224$.

At parameters value $\alpha = -8, \beta = -2, \gamma = 10, \delta = -2, \lambda = -2, \rho = -2$, we get two real roots and two complex conjugate roots and the eigenvalues obtained are $a_1 = 6.8980 - 7.9288i$, $a_2 = 6.8980 + 7.9288i$, $a_3 = -7.6818$ and $a_4 = 1.8858$.

At parameters value $\alpha = -8, \beta = -2, \gamma = -10, \delta = 2, \lambda = -2, \rho = -2$, we get four real roots and the eigenvalues obtained are $a_1 = 7.0942 - 8.1915i, a_2 = 7.094 + 8.192i, a_3 = -7.9107$ and $a_4 = 1.722$.

At parameters value $\alpha = -8, \beta = -2, \gamma = -10, \delta = -2, \lambda = 10, \rho = -2$, we get four real roots and the eigenvalues obtained are $a_1 = 4.5120 - 2.0182i, a_2 = 4.512 + 2.018i, a_3 = -11.93$ and $a_4 = -1.0983$.

At parameters value $\alpha = -8, \beta = -2, \gamma = -10, \delta = -2, \lambda = -10, \rho = 2$, we get two real roots and two complex conjugate roots and the eigenvalues obtained are $a_1 = 6.7198 - 5.548i, a_2 = 6.7199 + 5.5480i, a_3 = -11.304$ and $a_4 = 1.864$.

For SLIR model, the number of roots for the characteristic equation obtained is four. These could be positive, negative, real or imaginary values, where these roots might give stable or unstable equilibrium points. Due to time constraints, we limit ourselves only on the characteristic polynomial graph plotting using some values of parameters. Further analysis can be done in future.

Conclusion

In this study, we presented the dynamics of HFMD by using the system of ODEs of SIR model and the extended of SIR model which is called SLIR model. The dynamics of HFMD at disease free equilibrium and endemic equilibrium were studied in this work.

For SIR model, HFMD is stable at DFEP. Furthermore, at DFEP, the infected individuals of HFMD will die out and the disease will be eliminated from the population. However, at EEP, HFMD may have stable and unstable equilibrium depending on the various values of the model parameters.

Next, for SLIR model, we add latent variable into simple SIR model. By adding this variable, the model become more realistic since we assume that not all susceptible individual will become infected individual and there is a time gap between susceptible individual to get infected. We presented the dynamic of HFMD using SLIR model by plotting the graph of characteristic polynomial at DFEP and EEP by the aid of MATHEMATICA.

From the graphs, we can see the pattern of the graphs is almost the same at various values of parameters for DFEP and EEP. However, we can't provide the stability of the equilibrium. We need to have some further works since we have to analyse the stability of the system with four roots.

References

- Anderson, R. M., & May, R. M. (1992). *Infectious Diseases of Humans: Dynamics and Control*. Oxford University Press. Retrieved from <https://books.google.com/books?id=HT0--xXBguQC&pgis=1>
- Chong, K. C., & Zee, B. C. (1927). PharmaSUG China Compartmental Models in SAS : Application to Model Epidemics, 1–9.
- Grigorieva, E. V., & Khailov, E. N. (2014). Optimal Vaccination, Treatment, and Preventive Campaigns in Regard to the SIR Epidemic Model. *Mathematical Modelling of Natural Phenomena*, 9(4), 105–121. doi:10.1051/mmnp/20149407
- James, K. (2014). Hand, Foot, and Mouth Disease | Features | CDC. Retrieved October 27, 2014, from <http://www.cdc.gov/features/handfootmouthdisease/>
- Jiang, Z., He, C., & Cheng, G. (2009). Stability and Bifurcation Analysis of a Stage-Structured Sir Model With Time Delays. *International Journal of Biomathematics*, 03(03), 337–350. doi:10.1142/S1793524510001045
- Jones, J. H. (2007). Notes On R 0, 1–19.
- Kodaira, J. Y. (2010). THE BASIC REPRODUCTION NUMBER IN SIR MODELS – A PROBABILISTIC APPROACH, 226–231.
- Liu, Z., Wang, J., Xu, Y., & Li, G. (2013). Dynamic Analysis of an Sir Model With Stochastic Perturbations. *International Journal of Biomathematics*, 06(06), 1350041. doi:10.1142/S1793524513500411
- Magal, P., & Ruan, S. (2014). Susceptible-infectious-recovered models revisited: From the individual level to the population level. *Mathematical Biosciences*, 250(1), 26–40. doi:10.1016/j.mbs.2014.02.001
- Roussel, M. R. (2005). Stability Analysis for ODEs, 1–13.
- Roy, N. (2012). Mathematical Modeling of Hand-Foot-Mouth Disease : Quarantine as a Control Measure, 34–44.
- Sprott, J. C. (2000). Dynamical Systems Theory - Chaos and Time-Series Analysis. Retrieved May 29, 2015, from <http://sprott.physics.wisc.edu/phys505/lect04.htm>

TWO DIMENSIONAL STEADY STATE HEAT EQUATION USING FINITE ELEMENT METHOD

Carrie Tan Shiau Ying & Dr.Yeak Su Hoe

Abstract

The purpose of this study is to investigate the application of numerical method toward steady state of heat diffusion equation in two dimensional geometry by applying Finite Element Method (FEM). FEM involves the finding of approximate solutions on boundary value problems for partial differential equations and it is well known as a tool in solving complicated problem such as irregular geometry. In FEM, variational method is used in order to minimize the error in energy function. The FEM calculation is coded in MATLAB language which is ideal for large scale iterations. The calculated results are compared with a well-known numerical method such as Finite Difference Method (FDM). FDM able to solve the same problem but limited to regular geometry and simple irregular geometry problems. The differences of these two methods lie in their error functions produce by respective equations. In conclusion, FEM generally will produce more accurate results compared to FDM.

Keywords: Finite Element Method(FEM), heat diffusion equation, regular geometry , irregular geometry

Introduction

Heat is a form of energy in transit due to a temperature difference (Rathore & Raul R. A. Kapuno, 2011). This variation in temperature is governed by the principle of energy conservation, which when applied to a control volume or a control mass, states that the sum of the flow of energy and heat across the system, the work done on the system, and the energy stored and converted within the system, is zero. Numerical method is a technique for obtaining approximate solutions. Numerical method is well known due to its applications to the industries especially in sciences and engineering field. In the reality the analytical solutions a not exist. Thus, this method is being used to calculate the approximation to the analytical solutions. Finite Element Method (FEM) and Finite Difference Method (FDM) are the examples of numerical methods that can be used to solve this kind of problems. FEM is useful for problems with complicated geometries, loadings and material properties where analytical solutions cannot be obtained. It is a numerical technique in finding approximate solutions to boundary value for differential equations problems of engineering and mathematical physics. This research is focusing on solving a two-dimensional irregular geometry heat transfer equation by applying the finite element method. Computations of this method will be performed using MATLAB program due to large scale problem. It is also to assure the accuracy of the solution.

Methodology

There are two type of heat transfer problem will be solve which are regular geometry heat transfer problem and irregular geometry heat transfer problem where the problem are time independent. Both problems will be chose using Poisson equation.

Below are the mathematical model of regular geometry heat transfer problem.

$$T_{xx} + T_{yy} = f(x, y)$$

$$T = u = x^2(1 + y)$$

$$u_{xx} + u_{yy} = -f(x, y)$$

$$-2 - 2y = f(x, y)$$

and the boundary conditions are

$$\begin{aligned} BC1 : u(x,0) &= x^2 \\ BC2 : u(1, y) &= 1 + y \\ BC3 : u(x,2) &= 3x^2 \\ BC4 : u(0, y) &= 0 \end{aligned}$$

Range of x and y is given as $0 \leq x \leq 1, 0 \leq y \leq 2$

And below are the mathematical model of irregular geometry heat transfer problem where they are heat source provided.

$$\begin{aligned} \nabla^2 T + Q &= 0 \\ \nabla^2 T &= -Q \\ \frac{\partial^2 T}{\partial x^2} + \frac{\partial^2 T}{\partial y^2} &= -Q. \end{aligned}$$

Range of x and y is given as

$$0 \leq x \leq 3, 0 \leq y \leq 2.$$

Equation Q and boundary conditions given as

$$Q = f \frac{1}{(x - x_Q)^2 + (y - y_Q)^2 + 0.1}$$

$$\begin{aligned} \frac{\partial T}{\partial x} &= 0 & \text{for} & \text{ B2 and B6 (right \& left)} \\ T &= 0 & \text{for} & \text{ B3, B4 and B5 (above \& slant)} \\ T &= 100 & \text{for} & \text{ B1 (bottom)} \end{aligned}$$

where

B represents the boundary conditions

Q is an additional heat source that is set at the coordinate (X_Q, Y_Q)

$$f = -100$$

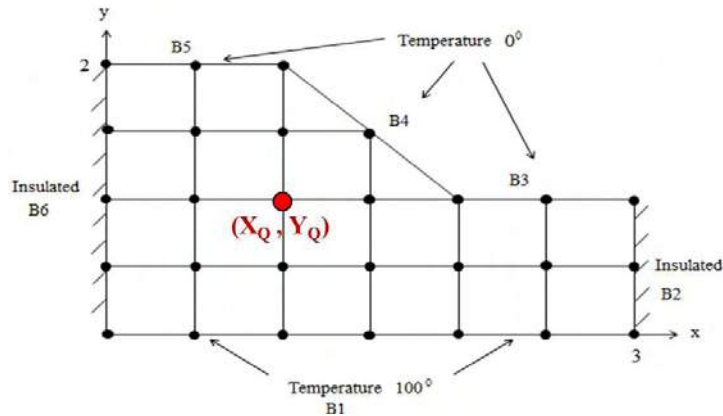


Figure 1: 2D simple irregular geometry heat transfer problem

Finite Element Method (FEM) are a powerful tool to solve complex and irregular geometry problem. Below are the FEM formula.

Based on Pepper and Heinrich (1992), the heat conduction problem is shown as below

$$\frac{\partial}{\partial x} \left(k \frac{\partial T}{\partial x} \right) + \frac{\partial}{\partial y} \left(k \frac{\partial T}{\partial y} \right) + Q = 0. \quad (1)$$

where T is temperature

Q represents an equation for heat source.

The given boundary conditions are

$$T = T_0 \text{ on } S_T, q_n = q_0 \text{ on } S_q, q_n = h(T - T_\infty) \text{ on } S_c.$$

where S_T is specified temperature, S_q specified heat flux and S_c is convection.

Let

$$\iint_A \phi \left[\frac{\partial}{\partial x} \left(k \frac{\partial T}{\partial x} \right) + \frac{\partial}{\partial y} \left(k \frac{\partial T}{\partial y} \right) \right] dA + \iint_A \phi Q dA = 0$$

using product rule, we get

$$\phi \frac{\partial}{\partial x} \left(k \frac{\partial T}{\partial x} \right) = \frac{\partial}{\partial x} \left(\phi k \frac{\partial T}{\partial x} \right) - k \frac{\partial \phi}{\partial x} \frac{\partial T}{\partial x}$$

then we have,

$$\iint_A \left\{ \left[\frac{\partial}{\partial x} \left(\phi k \frac{\partial T}{\partial x} \right) + \frac{\partial}{\partial y} \left(\phi k \frac{\partial T}{\partial y} \right) \right] - \left[k \frac{\partial \phi}{\partial x} \frac{\partial T}{\partial x} + k \frac{\partial \phi}{\partial y} \frac{\partial T}{\partial y} \right] \right\} dA + \iint_A \phi Q dA = 0$$

using notation

$$q_x = -k\left(\frac{\partial T}{\partial x}\right), q_y = -k\left(\frac{\partial T}{\partial y}\right)$$

and divergence theorem for first term we get

$$-\iint_A \left[\frac{\partial}{\partial x} (\phi q_x) + \frac{\partial}{\partial y} (\phi q_y) \right] dA = -\int_s \phi [q_x n_x + q_y n_y] dS = -\int_s q_n dS.$$

Here n_x and n_y are the direction cosines of the unit normal \mathbf{n} to the boundary and

$q_n = q_x n_x + q_y n_y = \mathbf{q} \cdot \mathbf{n}$ is the normal heat flow along the unit outward normal.

Since

$$S = S_T + S_q + S_c, \phi = 0 \text{ on } S_T, q_n = q_0 \text{ on } S_q, \text{ and } q_n = h(T - T_\infty) \text{ on } S_c,$$

Then will yield,

$$\iint_A \left\{ \left[\frac{\partial}{\partial x} \left(\phi k \frac{\partial T}{\partial x} \right) + \frac{\partial}{\partial y} \left(\phi k \frac{\partial T}{\partial y} \right) \right] - \left[k \frac{\partial \phi}{\partial x} \frac{\partial T}{\partial x} + k \frac{\partial \phi}{\partial y} \frac{\partial T}{\partial y} \right] \right\} dA + \iint_A \phi Q dA = 0$$

which turns into

$$-\int_s \phi q_0 dS - \int_s \phi h(T - T_\infty) dS - \iint_A \left(k \frac{\partial \phi}{\partial x} \frac{\partial T}{\partial x} + k \frac{\partial \phi}{\partial y} \frac{\partial T}{\partial y} \right) dA + \iint_A \phi Q dA = 0 \quad (2)$$

The same interpolation of geometry coordinate and variable function or also known as isoparametric relations are introduced for triangular element $T=NT^e$. Denote global virtual temperature since

$$\begin{bmatrix} \partial T / \partial x \\ \partial \phi / \partial y \end{bmatrix} = B_T T^e .$$

Then

$$\nabla \phi = \begin{bmatrix} \partial T / \partial x \\ \partial \phi / \partial y \end{bmatrix} = (\nabla N) \psi = B_T \psi .$$

Now consider the first term of equation (3.2),

$$\int_{S_q} \phi q_0 dS = \int_{S_q} N \psi q_0 dS = \int_{S_q} \psi^T N^T q_0 dS = \sum_e \int_e \psi^T N^T q_0 dS.$$

Consider Figure 3.3 below as an example of heat transfer problem,

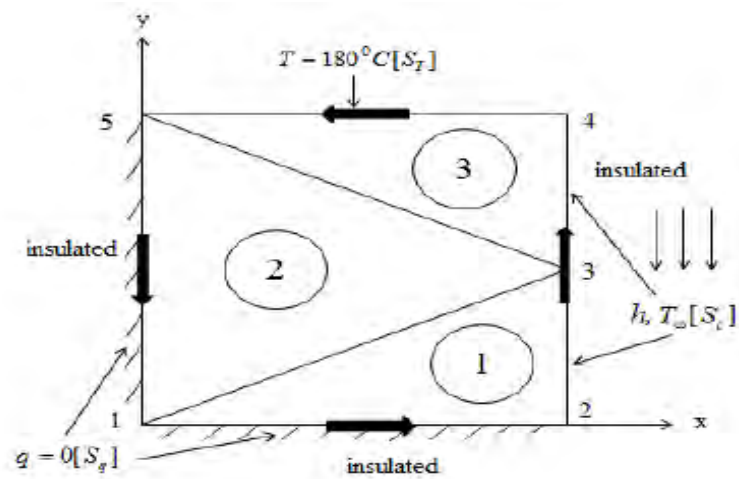


Figure 2: The example of 2D heat transfer problem

Then refer to Figure 3.3, if edge 2-3 is on the boundary, so

$$N = [0, \eta, 1 - \eta], \quad dS = l_{2-3} d\eta, \quad (l_{2-3} = \text{length edge } 2 - 3)$$

and get equation

$$\int_{S_q} \phi q_0 dS = \sum_e \int_e \psi^T N^T q_0 dS = \sum_e \psi^T q_0 l_{2-3} \int_0^1 N^T d\eta = \sum_e \psi^T r_Q \quad (3)$$

where
$$r_Q = \frac{q_0 l_{2-3}}{2} \begin{bmatrix} 0 \\ 1 \\ 1 \end{bmatrix}.$$

Next, consider

$$\int \phi h(T - T_\infty) dS = \int \phi h T dS - \int \phi h T_\infty dS$$

and get

$$\int \phi h(T - T_\infty) dS = \int \psi^T N^T h N T^e dS - \int \psi^T N^T h T_\infty dS.$$

If edge 2-3 is the convection edge of the element, then

$$\int \phi h(T - T_\infty) dS = \sum_e \psi^T \left[hl_{2-3} \int_0^1 N^T N d\eta \right] T^e - \sum_e \psi^T hT_\infty l_{2-3} \int_0^1 N^T d\eta \quad (4)$$

$$= \sum_e \psi^T h_T T^e - \sum_e \psi^T r_\infty$$

Substituting for $N = [0, \eta, 1 - \eta]$ thus,

$$h_T = hl_{2-3} \int \begin{bmatrix} 0 \\ \eta \\ 1 - \eta \end{bmatrix} [0 \ \eta \ 1 - \eta] d\eta = \frac{hl_{2-3}}{6} \begin{bmatrix} 0 & 0 & 0 \\ 0 & 2 & 1 \\ 0 & 1 & 2 \end{bmatrix}$$

and

$$r_\infty = hT_\infty l_{2-3} \int \begin{bmatrix} 0 \\ \eta \\ 1 - \eta \end{bmatrix} d\eta = \frac{hT_\infty l_{2-3}}{2} \begin{bmatrix} 0 \\ 1 \\ 1 \end{bmatrix}.$$

Next,

$$\iint_A k \left(\frac{\partial \phi}{\partial x} \frac{\partial T}{\partial x} + \frac{\partial \phi}{\partial y} \frac{\partial T}{\partial y} \right) dA = \iint_A k \left(\frac{\partial \phi}{\partial x} \frac{\partial \phi}{\partial y} \right) \cdot \begin{pmatrix} \partial T / \partial x \\ \partial T / \partial y \end{pmatrix} dA \quad (5)$$

$$= \sum_e \psi^T \left[k_e \int_e B_T^T B_T dA \right] T^e = \sum_e \psi^T k_T T^e$$

where

$$k_T = k_e \int_e B_T^T B_T dA = k_e B_T^T B_T \int dA = k_e A_e B_T^T B_T.$$

If $Q = Q^e$ is a constant within the element, hence

$$\iint_A \phi Q dA = \sum_e \psi^T Q_e \int_e N^T dA = \sum_e \psi^T r_Q \quad (6)$$

where

$$r_Q = Q_e \int_e \begin{bmatrix} \xi \\ \eta \\ 1 - \xi - \eta \end{bmatrix} dA = Q_e 2A_e \int_{\eta=0}^1 \int_{\xi=0}^{1-\eta} \begin{bmatrix} \xi \\ \eta \\ 1 - \xi - \eta \end{bmatrix} d\xi d\eta = \frac{Q_e A_e}{3} \begin{bmatrix} 1 \\ 1 \\ 1 \end{bmatrix}.$$

Then the final equation is

$$- \sum_A \psi^T r_q - \sum_e \psi^T h_T T^e + \sum_e \psi^T r_\infty - \sum_e \psi^T T^e + \sum_e \psi^T r_Q = 0$$

Or can be written as

$$\psi^T R_\infty - \psi^T R_q + \psi^T R_Q - \psi^T H_T T + \psi^T K_T T = 0$$

and can be simplified into

$$\psi^T (R_\infty - R_q + R_Q) - \psi^T (H_T + K_T) T = 0. \quad (7)$$

Results and Discussion:

Below are the figures yield from MATLAB of FDM and FEM in regular geometry heat transfer problem.

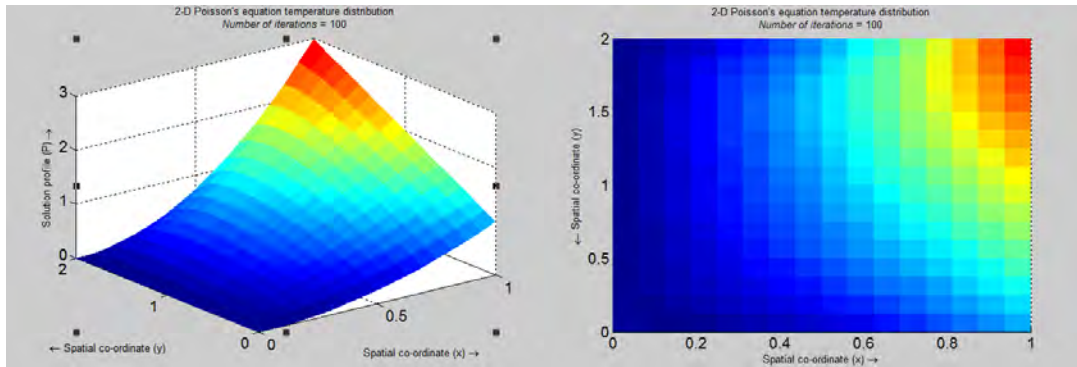
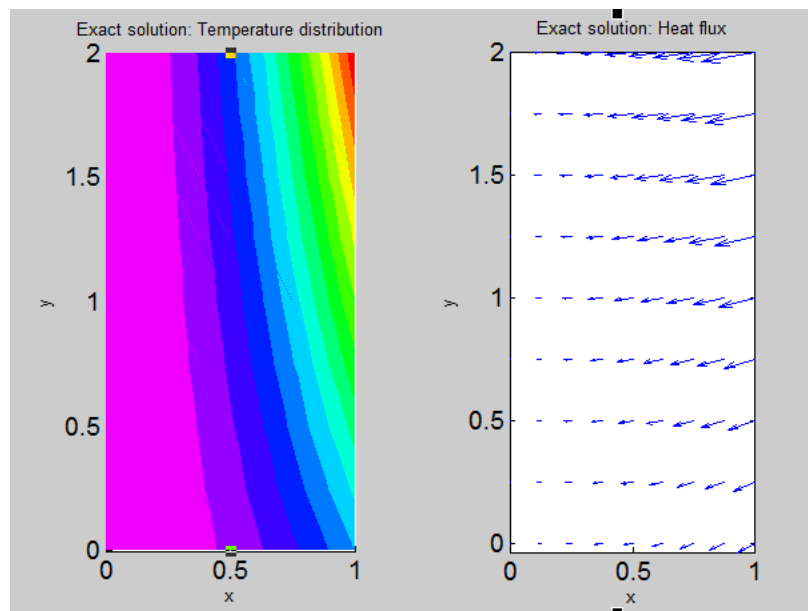
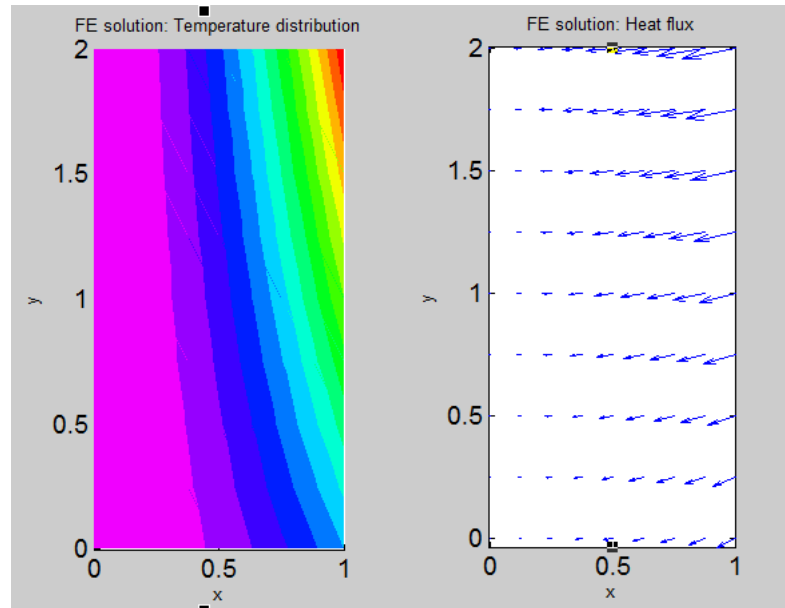


Figure 3: 3D plotting and upper view of temperature distribution of FDM with number of elements = 16



(Left) Figure 4(a): Temperature distributions of exact solution

(Right) Figure 4(b): Heat flux of exact solution



(Left) Figure 5(a): Temperature distributions of FEM solution

(Right) Figure 5(b): Heat flux of FEM solution

In the temperature distribution figures, cold colour represent smaller values where warm colour represent bigger values. Figure 3 shows the temperature distribution of the problem. The temperature are increasing as closer to coordinate (1,2). From the figures 4(a), 4(b), 5(a) and 5(b), the temperature distribution between the exact solution and FEM solution are almost similar. Same goes to the directions of the heat flux which is toward the left. Similar to Figure 3, the temperature increasing as it approach coordinate of (1,2). This shown that the FEM solution computed in MATLAB is the correct results. By comparing both FDM and FEM results in Poisson's equation problem, FEM is more persuasive to be more accurate results due to the similar outcome to the exact solutions. Based on Figure 3 and 5(a), the results of FEM also seem more accurate. Although there are only slight difference between both figure but FEM figure are closer to the exact solution figure 4(a). In short FEM calculation proved to be more accurate than FDM in 2D regular geometry heat diffusion problem.

For the irregular geometry heat transfer problem, the results are displayed below. The figures of FDM and FEM are displayed in colour form where the warm colour represent the higher temperature meanwhile the cold colour represent lower temperature.

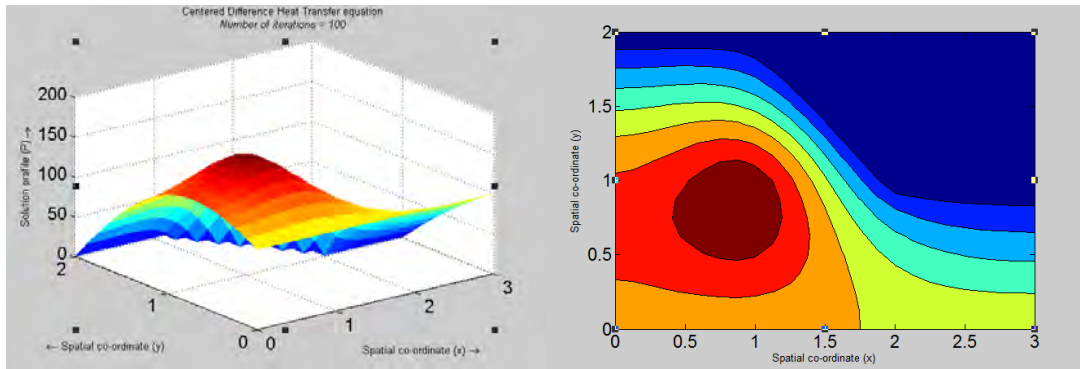
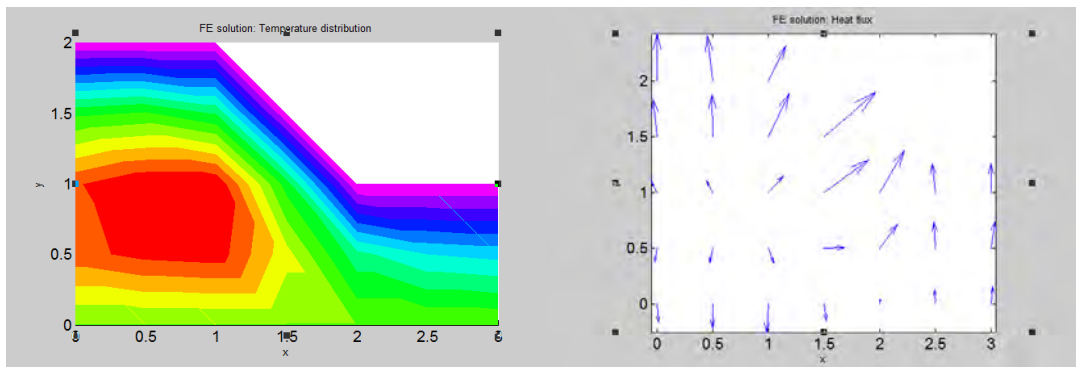


Figure 6: 3D plotting and contour of temperature distribution of FDM with number of element = 8



(Left) Figure 7(a): Contour plot of temperature distribution of FEM solution

(Right) Figure 7(b): Heat flux of FEM solution

In irregular geometry case, exact solution is either too hard or complicated and it is impossible to produce analytically. By comparison of both methods, FEM will yield more accurate results although in irregular geometry heat transfer problem, the figures produce by FDM (Figure 8) and FEM (Figure 7(a)) are almost similar. This is can be support by previous findings in results of two dimensional regular geometry heat transfer problem. In section 4.3, FEM is more accurate than FDM due to the similar results with exact solution's result. This implies that FEM will did the same to two dimensional heat diffusion irregular geometry. Besides, the strong form of FEM equations (Integration equation) also produce smaller error value compare to the weak form of FDM equation (Differential equation). Not only that, FEM also known to produce more accurate outcomes. In short, FEM outcomes are more accurate than FDM.

CONCLUSION

FEM and FDM are legible to solve heat diffusion problem based on the results and discussion. FEM prove to be more useful due to FDM unable or difficult to solve complex geometry problems. Roylance(2001) also said that FEM can be used to solve complex geometry approximately and frequently used in industry. Based on Kailani (2014), the solution for two dimensional simple irregular geometry heat transfer problem using FEM is more stable and consistent compared to FDM. In short, FEM are more effective than FDM in solving irregular geometry heat transfer problems.

REFERENCE

1. Kailani, N. H. (2014). *The Application of Finite Element Method in 2D Heat Distribution Problem for Irregular Geometry*. UniversitiTeknologi Malaysia.
2. Rathore, M. M., & Raul R. A. Kapuno, J. (2011). Two-Dimensional Steady-State Heat Conduction. In M. M. Rathore, & J. Raul R. A. Kapuno, *Engineering Heat Transfer* (pp. 1,151- 155). United States of America: Jones & Bartlett Learning, LLC.
3. Pepper, D. W. (1992). *The Finite Element Method Basic Concepts and Applications*. Hemisphere Publishing Corporation.
4. Roylance, D. (28 February, 2001). *Finite Element Analysis*. Retrieved from MIT Open Courseware Massachusetts Institute of Technology Cambridge: <http://ocw.mit.edu/courses/materials-science-and-engineering/3-11-mechanics-of-materials-fall-1999/modules/fea.pdf>

A Farthest Insertion Heuristic Algorithm For The Distance-Constrained Capacitated Vehicle Routing Problem

Chai Jin Sian & Dr. Farhana Johar

Abstract

The vehicle routing problem (VRP) under distance and capacity constraints involves the design of a set of delivery routes which originate and terminate at a central depot after satisfying the customer demands. Each customer must be served exactly once and by one vehicle, where vehicle capacity and distance limit become the constraints of the problem. In this study of Distance-Constrained Capacitated Vehicle Routing Problem (DCVRP), farthest insertion method is used to construct the initial solution. The method focuses on choosing the farthest customer from the route and then inserting the selected customer into the nearest path which will give the smallest increment of length without violating the distance and capacity constraints. C++ numerical programming is used to code the proposed algorithm in order to solve DCVRP which involves large groups of data. Three categories of data which are cluster, random and random cluster data are being analyzed by considering different amount of distance and capacity constraints. By utilizing the farthest insertion method, the number of routes participated and the total distance travelled by the vehicles can be obtained. Based on the computational results acquired, the increasing value of capacity and distance will reduce the number of routes formed as well as the total distance travelled. Further research should be done to improve the initial solution for DCVRP by using metaheuristics methods such as simulated annealing, tabu search and genetic algorithms.

Keywords: Distance-Constrained Capacitated Vehicle Routing Problem (DCVRP), farthest insertion method, initial solution.

Introduction

The rapid improvement of transportation technology in recent centuries has make the transportation sector becomes a vital component for the economic development. This is because transport availability contributes to the growth of industrial productivity, market size and business investment. Hence, transportation plays an important role to meet the requirement of people as well as the transport requirement of goods in transportation sector. Mostly, transportation companies will plan and organize the road path taken while deliver the goods to their customers in order to maximize the profit gained by minimizing the total distance travelled by the vehicles. In 1941, the transportation problem was introduced by F.L. Hitchcock with the objectives to minimize the total transportation cost and total delivery time as well as to maximize the profit gained (Gangadwala & Dhodiya, 2012). Therefore, the solution for the transportation problem was developed to find out the most efficient and effective way to deliver the goods to the customers.

According to Liong *et al.* (2008), Vehicle Routing Problem (VRP) is one of the most widely studied among the combinatorial optimization transportation problems. VRP can be defined as the problem of finding the optimal routes to distribute the goods for a number of customers from one or several depots with the consideration of some constraints such as vehicle capacity, distance travelled, time window and so forth. Basically, VRP can be divided into several important variants like Capacitated VRP, VRP with Time Window and VRP with Pickup and Delivery. To obtain a solution for VRP, the algorithms used can be classify into two categories which are exact algorithms and heuristic algorithms. Exact algorithms are often developed to obtain global optimal solution. However, these algorithms

can only solve relatively small problems. As for the heuristics, these approximate algorithms are able to produce near-optimal solutions to large problems. This explains why most of the research effort has been directed to heuristic algorithms. Heuristic algorithms can be categorized into construction heuristics, improvement heuristics and metaheuristics. Construction heuristics concern about the construction of a feasible solution with a main interest on the cost and not improvement. Hence, construction heuristics is usually being used to generate an initial solution for VRP that can be improved upon by improvement heuristics or metaheuristics. There are three main types of construction heuristics which are insertion heuristics, savings heuristics and clustering heuristics (Ropke, 2006).

The Clarke and Wright savings algorithm is the most famous saving heuristic. According to Cordeau *et al.* (2011), although this algorithm is easy to implement and code, but it cannot encounter various types of constraints and usually results in low quality results. On the other hand, insertion heuristics are able to handle many types of constraints efficiently and effectively compared to the Clarke and Wright savings algorithm. Therefore, insertion heuristics are usually being selected to solve VRP with different restrictions.

This research concerns on the generation of an initial solution for Distance-Constrained Capacitated Vehicle Routing Problem (DCVRP), a variation of VRP with the consideration of distance and capacity constraints. Construction heuristics is chosen to solve DCVRP due to its efficiency in handling various types of constraints. Different value of capacity and distance constraints will be tested in this research in order to determine their effects towards the number of routes formed and the total distance travelled by the vehicles for three large groups of data which involve 100 customers. C++ numerical programming is applied to perform numerical calculations for the construction of an initial solution for DCVRP.

Literature Review

Vehicle Routing Problem (VRP) was introduced in order to find a set of routes at a minimal cost that satisfies all customer demands. Many mathematical models have been proposed to find out the optimal solution for the distribution problems that happened in real-world applications such as solid waste collection, street cleaning, school bus routing, dial-a-ride system and routing of salespeople. Since VRP deals with the management of pickup and delivery activities, therefore it is important to design an optimal set of routes for a fleet of vehicles to serve the customers. As mentioned by Toth and Vigo (2002), there are several components that need to be considered for the typical characteristics of the routing and scheduling problems such as the road network, customer, depots, vehicles, drivers and operational constraints.

There are several important variants of VRP like the Capacitated Vehicle Route Problem (CVRP), Vehicle Routing Problem with Backhauls (VRPB), Vehicle Routing Problem with Time Window (VRPTW) as well as Vehicle Routing Problem with Pickup and Delivery (VRPPD). Combinations of these variants can be made to form more complex variants of the VRP such as Vehicle Routing Problem with Backhauls and Time Windows (VRPBTW) and Vehicle Routing Problem with Pickup Delivery and Time Windows (VRPPDTW). On the other hand, Distance-Constrained Capacitated Vehicle Routing Problem (DCVRP) is the extension of CVRP with the consideration of distance constraint.

There are many algorithms that can be used to produce a solution for VRP and its variants. The most widely used is the heuristic algorithms in VRP. Heuristics make use of greedy approach to generate a good initial solution efficiently and then utilized the neighborhood exchanges or local search to improve the solution obtained. Normally, heuristics are used to construct the solutions for VRP but they do not guarantee that the

solution found is optimal. These heuristics usually begin with an empty solution and then iteratively select a facility and allocate it to a free location (Burkard, Amico & Martello, 2009). The advantages of using heuristics in VRP are short running time, easy to implement, flexible and simple. As reported by Ropke (2006), heuristic algorithms can be divided into three categories which are construction heuristics, improvement heuristics and metaheuristics. Construction heuristics are used to generate an initial solution for VRP. However, the solution obtained can be improved upon by improvement heuristics or metaheuristics.

Paschos (2010) mentioned that the construction algorithms are similar to greedy algorithms since they consist of choosing an optimal route among a set of routes with each iteration. These algorithms are easy to implement and also fast to obtain solution. Two types of solution constructions are applied in VRP, sequential construction which builds one route at a time and parallel construction which builds many or all routes simultaneously. There are several types of construction heuristics that can be used to generate an initial solution for VRP. They are insertion heuristics, savings heuristics and clustering heuristics.

Methodology

Model formulation of single depot DCVRP is defined as follows:

- i. Central depot is assigned as an origin.
- ii. A group of customers with known demands, D and a homogenous fleet of vehicles with fixed capacity, Q .
- iii. The demand for each customer does not exceed the capacity of the vehicles.
- iv. Total distance travelled for each vehicle does not exceed the maximum distance of vehicle, T .
- v. Distance travelled, d_{ij} and transportation cost, C from customer i to customer j are symmetric such that $d_{ij} = d_{ji}$ and $C_{ij} = C_{ji}$.

Parameters involved:

- | | |
|------------|--|
| N | The number of customers. |
| P | Total number of vehicle. |
| D_i | The demand of customer i . |
| Q | The capacity of vehicle. |
| T | The maximum distance of vehicle. |
| C_{ij}^p | The transportation cost from customer i to customer j by vehicle p . |
| d_{ij}^p | The distance travelled by vehicle p from customer i to customer j . |
| X_{ij}^p | The travel distance from customer i to customer j by vehicle p . |

Decision variables:

If vehicle p travels from customer i to customer j

$$X_{ij}^p = \begin{cases} 1 \\ 0 \end{cases} \quad \text{Otherwise}$$

The objective is to minimize

$$\sum_{p=1}^P \sum_{i=0}^N \sum_{j=0}^N C_{ij}^p X_{ij}^p \quad (1)$$

subject to

$$\sum_{p=1}^P \sum_{i=0}^N X_{ij}^p = 1 \quad j = 0,1,2,\dots,N \quad (2)$$

$$\sum_{j=1}^N X_{0j}^p \leq 1 \quad p = 1,2,3,\dots,P \quad (3)$$

$$\sum_{i=1}^N X_{i0}^p \leq 1 \quad p = 1,2,3,\dots,P \quad (4)$$

$$d_{ij}^p \leq T \quad \begin{matrix} i = 0,1,2,\dots,N; j = 0,1,2,\dots,N \\ p = 1,2,3,\dots,P \end{matrix} \quad (5)$$

$$\sum_{j=0}^N D_j \left(\sum_{i=0}^N X_{ij}^p \right) \leq Q \quad p = 1,2,3,\dots,P \quad (6)$$

From the formulation presented, the objective function (1) is to minimize the total cost consumed by all the vehicles used. Equation (2) imposes that every customer is served exactly once whereas equations (3) and (4) require that each customer is served exactly by one vehicle. Moreover, equation (5) restricts that the distance travelled between any two distinct customers must not exceed the maximum distance fixed for each vehicle. Lastly, equation (6) shows that the total demand of customers for any route must not exceed the vehicle capacity.

For this research, we focus on the generation of an initial solution for DCVRP by using sequential farthest insertion method. First and foremost, we obtain the input data which consists of the information about the locations and demands for each node. Next, we need to calculate the distance between each pair of nodes by using the Euclidean distance. After that, we apply the farthest insertion method to generate an initial solution for DCVRP. The sequential farthest insertion method works as follows:

Step 1: Set the depot as the origin with node 0.

Step 2: Find the farthest unrouted node m from the depot. Then, form a subtour.

$$R = 0 - m - 0$$

Step 3: Find the nearest distance between unrouted nodes, x and the subtour nodes, R .

$$\min_{x \notin R} d_{xR}$$

Step 4: Find an unrouted node k which is farthest from the subtour nodes, R .

$$d_{kR} = \max \left\{ \min_{x \notin R} d_{xR} \right\}$$

Step 5: Find an edge $[i, j]$ of the subtour for which the insertion of the node k will gives the smallest increment of length, Δf .

$$\Delta f = d_{ik} + d_{kj} - d_{ij}$$

Step 6: Test whether the insertion of the selected node k between the edge $[i, j]$ will satisfy both of the capacity and distance constraints. If yes, insert node k between node i and node j . If no, reject node k and choose for other unrouted nodes by repeating Step 4 to 5.

Step 7: Examine whether all the nodes have been tested. If yes, a complete vehicle route is formed. If no, repeat Step 3 until 6.

Step 8: Investigate whether all the nodes have been assigned to one vehicle route. If yes, an initial solution for DCVRP is obtained. If no, start a new route and repeat Step 2 until 7.

Case Study

For this research, we are going to generate an initial solution for DCVRP which involves a depot and 100 customers with different locations and demands. There are three types of data that need to be solved which are cluster, random and random cluster. By the application of C++ numerical programming, the initial solutions for these data are calculated and tabulated in Table 1, Table 2 and Table 3, respectively. After that, the data are analyzed based on the number of routes formed, average number of customers per route as well as total distance travelled when different amount of distance and capacity constraints are applied on the vehicles used.

Table 1: Results for cluster data

Maximum Distance (Units)	Vehicle Capacity (Units)	Number of Routes	Average Number of Customers	Total Distance (Units)
	150	14	7	2027.61
150	300	13	8	1830.54
	450	13	8	1830.54
	150	13	8	2775.96
300	300	7	14	1735.43
	450	6	17	1593.15
	150	13	8	2885.67
450	300	7	14	1933.59
	450	5	20	1467.60

Table 2: Results for random data

Maximum Distance (Units)	Vehicle Capacity (Units)	Number of Routes	Average Number of Customers	Total Distance (Units)
	150	12	8	1614.61
150	300	10	10	1487.84
	450	10	10	1487.84
	150	10	10	2066.14
300	300	6	17	1471.57
	450	5	20	1241.76
	150	10	10	2072.86
450	300	5	20	1391.07
	450	4	25	1180.74

Table 3: Results for random cluster data

Maximum Distance (Units)	Vehicle Capacity (Units)	Number of Routes	Average Number of Customers	Total Distance (Units)
	150	16	6	2275.14
150	300	14	7	1960.27
	450	14	7	1960.27
	150	12	8	2941.89
300	300	7	14	1974.79
	450	6	17	1730.81
	150	12	8	3284.86
450	300	6	17	2187.20
	450	4	25	1616.54

Overall, the results obtained for cluster, random and random cluster data show similar outcomes when the amount of distance and capacity constraints fixed on each vehicle are increased. The increasing of the values of maximum distance and vehicle capacity at the

same time will lead to a reduction on the number of routes participated as well as the total distance travelled by the vehicles. This is because vehicle with larger capacity and maximum distance has greater opportunity to satisfy more customer demands within one route.

When the maximum distance travelled by a vehicle is fixed, the increasing in the value of vehicle capacity will reduce the number of routes participated and the total distance travelled. The reason is the vehicle with larger capacity is able to carry more goods to be distributed to the customers. So, the average number of customers for each route increases and less routes will be used to satisfy all customer demands. Consequently, the total distance travelled is also decreases. On the other hand, if the maximum distance is increased but the vehicle capacity is kept constant, then the vehicle has more chance to go further to satisfy more customers within a route. Thus, the average number of customers per route increases and fewer routes will be used to satisfy all the customer demands. While the total distance travelled has a tendency to increase or vice versa based on the routes formed. This is because farthest insertion method selects the farthest customer to be inserted into the route. Hence, vehicles with larger maximum distance tend to satisfy the customers that far away from the routes formed.

Note that random data has the smallest total distance travelled if compared to cluster and random cluster data. For example, when both the maximum distance and vehicle capacity are set to be 450 units, the total distance travelled for random data is the smallest with 1180.74 units and then followed by cluster data with 1470.60 units. Random cluster data has the largest value which is 1616.54 units. This may due to the farthest insertion method that we used to generate the initial solution for DCVRP. Instead of choosing the nearest customer from the route, farthest customer is selected to be added into the vehicle route. Therefore, the vehicle will not deliver the goods to the next customer who is close to the current route but tends to go to the customer that far apart. This is the reason why cluster data has larger total distance compared to random data. Hence, farthest insertion method is more suitable to be used to generate an initial solution for random data which contains evenly distributed customers around the depot.

Conclusions and Recommendations

There are some conclusions that can be drawn from this research. Firstly, the values of distance and capacity constraints for each vehicle do affect the number of routes and total distance travelled. The greater the maximum distance and the vehicle capacity, the smaller the number of routes participated and the total distance travelled by the vehicles. Next, the computational results obtained using C++ numerical programming showed that random data has the shortest total distance travelled compared to cluster and random cluster data with the same amount of distance and capacity constraints. This is because farthest insertion method concerns on the selection of farthest customer to be added into the vehicle route. Hence, this method is beneficial to random data which contains evenly distributed customers around the depot.

This research focuses on farthest insertion method to generate an initial solution for DCVRP. Hence, it is recommended that further research should be carried out by using

other insertion heuristic methods such as nearest insertion method, cheapest insertion method and random insertion method. Then, the results obtained from those methods can be used for comparisons on the number of routes formed as well as the total distance travelled by the vehicles.

Other than the heuristics methods, there are many types of metaheuristics that can be applied to improve the initial solutions obtained in this research such as simulated annealing, tabu search and genetic algorithms. Hence, it is recommended that further research should be done to improve the initial solutions for DCVRP by utilizing the metaheuristics methods.

References

- Burkard, R., Amico, M. D. and Martello, S. (2009). *Assignment Problems*. United States of America: Society for Industrial and Applied Mathematics.
- Cordeau, J. F., Gendreau, M., Laporte, G., Potvin, J. Y. and Semet, F. (2002). A Guide to Vehicle Routing Problem. *Journal of the Operational Research Society*. 13, 512-522.
- El-Sherbeny, N. A. (2010). Vehicle Routing with Time Windows: An Overview of Exact, Heuristic and Metaheuristic Methods. *Journal of King Saud University (Science)*. 22, 123-131.
- Gangadwala, H. A. and Dhodiya, J. M. (2012). Transportation Problem Issues and solutions with a Technological Approach. *International Journal of Application or Innovation in Engineering & Management (IJAEM)*. Volume 1 (Issue 2), 134 – 140.
- Joubert, J. W. and Claasen, S. J. (2006). A Sequential Insertion Heuristic for the Initial Solution to A Constrained Vehicle Routing Problem. *ORiON*. Volume 22(1), 105 -116.
- Laporte, G. and Nobert, Y. (1983). A Branch and Bound Algorithm for the Capacitated Vehicle Routing Problem. *OR Spektrum*. 5:77-85.
- Liang, D. Y. (2010) *Introduction to Programming with C++*. United States of America: Pearson Higher Education.
- Liong, C. Y., Wan Rosmanira Ismail, Khairuddin Omar and Zirour, M. (2008). Vehicle Routing Problem: Models and Solutions (Masalah Perjalanan Kendaraan: Model dan Penyelesaian). *Journal of Quality Measurement and Analysis (Jurnal Pengukuran Kualiti dan Analisis)*. JQMA 4(1), 205-218.
- Mehrjerdi, Y. Z. (2012). Vehicle Routing Problem: Meta-heuristic Approaches. *International Journal of Applied Operational Research*. Vol. 2, No. 3, 55-68.
- Paschos, V. T. (2010). *Paradigms of Combinatorial Optimization*. United States of America: ISTE Ltd and John Wiley & Sons, Inc.
- Pichpibul, T. and Kawtummachai, R. (2012). An Improved Clarke and Wright Savings Algorithm for the Capacitated Vehicle Routing Problem. *Research Article*. 38, 307-318.
- Rand, G. K. (2009). The Life and Times of the Savings Method for Vehicle Routing Problems. *ORiON*. Volume 25(2), 125-145.
- Ropke, S. (2006). *Heuristic and Exact Algorithms for Vehicle Routing Problems*. Doctor Philosophy. University of Copenhagen (DIKU).
- Schulze, J. and Fahle, T. (1999). A Parallel Algorithm for the Vehicle Routing Problem with Time Window Constraints. *Annals of Operations Research*. 86, 585-607.

- Shaharuddin Salleh (2012). *C++ Numerical Programming*. Malaysia: Universiti Teknologi Malaysia.
- Toth, P. and Vigo, D. (2002). *The Vehicle Routing Problem*. United States of America: Society for Industrial and Applied Mathematics.
- Tzoreff, T. E. Granot, D., Granot, F. and Sošić, G. (2002). The Vehicle Routing Problem with Pickups and Deliveries on Some Special Graphs. *Discrete Applied Mathematics*. 116, 193-229.
- Wade, A. C. and Salhi, S. (2002). An Investigation into A New Class of Vehicle Routing Problem with Backhauls. *The International Journal of Management Science*. Omega 30, 479-487.
- Yaw, C. and Lin, C. (2007). Solve the Vehicle Routing Problem with Time Windows Via A Genetic Algorithm. *Discrete And Continuous Dynamical Systems Supplement*. 240-249.

Mathematical Modelling of Inputs and Outputs for Rotating Disc Contactor Column using Particle Swarm Optimization Technique

Chan Poh Ching & Assoc. Prof. Dr. KhairilAnuar bin Arshad

Abstract

Particle swarm optimization (PSO) is a randomized search method inspired by principles of social interaction. It has been extensively used in mathematical modelling for solving optimization problems in both engineering and scientific research. In this research, numerous studies on concepts of PSO have been done to ease the process of modelling for example explanations on the background of PSO, its algorithm and parameter setting as well as its benefits and drawbacks. This research concerns the modelling of inputs and outputs of RDC column using the PSO technique. RDC column is one of the tools used to perform liquid-liquid extraction which involves separating compounds into two distinct immiscible liquids, most often comprised of water and organic solvents. Data on RDC column consist of four inputs namely, rotor speed, dispersed phase flow rate, concentration of continuous and dispersed phase inlets, and four outputs which include hold-up, Sauter mean diameter (d_{32}), concentration of continuous and dispersed phase outlets. These data are collected and prepared to be modelled using the PSO technique. In addition, a code based on the PSO algorithm is developed using Matlab version R2013a. The PSO algorithm is employed to perform prediction on RDC column outputs. Various analyses using the percentage of error, mean squared error and the Pearson correlation coefficient are carried out as well to test the performance of the PSO algorithm based on the accuracy of predictions obtained.

Keywords: Particle swarm optimization, Rotating disc contactor column, Prediction, Matlab.

1 Introduction

Liquid-liquid extraction is a method of separating compounds into two distinct immiscible liquids, most often comprised of water and organic solvents. This method consists of movement of a soluble component from one liquid phase into another liquid phase. Liquid-liquid extraction can be performed at low temperature and is suitable for thermally fragile solutes. Nowadays, this important chemical technique is widely applied in a number of major current industries such as in the field of biotechnology, pharmaceuticals, perfumes and food products. There are a variety of apparatus and equipment available for liquid-liquid extraction for examples, separatory funnel, mixer-settler and rotating disc contactor column. Column type extraction using rotating disc contactor (RDC) is the major concern in this research. According to Haderer et al. (2004), the rotating disc contactor column is an extractor with the low density dispersed phase and the continuous phase which moves from bottom to the top and top to bottom of the column respectively. The process occurred in these two phases can be mathematically modelled to effectively predict the output of rotating disc contactor column.

Mathematical modelling is the simulation of a model that involves mathematical concepts and terms. It is performed to study the effects or characteristics of a system and to optimize or make predictions of a certain event or process. Many mathematicians, scientists and economists use mathematical modelling to understand the way a process works or to analyse trends and movements in the financial market. One of the major advantages of mathematical modelling is that it can greatly save costs and increase profits by optimizing a certain process in business or industry. As such, this research concentrated on the modelling of inputs and

outputs for rotating disc contactor column using particle swarm optimization technique to analyse data of the object being studied.

The objectives of this research comprise (i) to study and understand concepts of particle swarm optimization; (ii) to model the inputs and outputs of rotating disc contactor column by using the particle swarm optimization technique; and (iii) to predict outputs of the rotating disc contactor column by using the particle swarm optimization technique. The data employed in this research is divided into four inputs and four outputs. The four input data are namely, rotor speed (nr), dispersed phase flow rate (fd), concentration of the continuous phase inlet ($cc-in$) and concentration of the dispersed phase inlet ($cd-in$). On the other hand, the four output data consist of hold-up ($c-holdup$), Sauter mean diameter ($d32$) ($c-d32$), concentration of the continuous phase outlet ($cc-out$) and concentration of the dispersed phase outlet ($cd-out$).

1.1 Particle Swarm Optimization (PSO)

PSO is a randomized search method inspired by principles of social interaction. According to Chong and Zak (2013), a randomized search method also known as probabilistic search method is an algorithm that considers randomized samples of candidate points in the search for feasible set of an optimization problem. The technique of randomized search method involves in updating only a single candidate solution represented by $x^{(k)}$ at each iteration. However, Chong and Zak (2013) stated that the PSO algorithm is different from the usual randomized search method. They explained that in PSO algorithm, a population or in another word, a set of candidate solutions called a swarm is updated at each iteration. Each candidate solution in the swarm is known as a particle.

According to Venter and Sobieszczanski-Sobieski (2003), PSO applies a velocity vector, \mathbf{v}_i to update i th particle's current position, \mathbf{x}_i in the swarm. The update of i th particle's position is based on the social behaviour that the swarm adapts to its environment by returning to previously discovered regions. The process is stochastic and uses the memory of each particle including the knowledge gained by the swarm as a whole.

Van den Bergh and Engelbrecht (2005) stated that,

$$x_{ij}(t+1) = x_{ij}(t) + v_{ij}(t+1) \quad (1)$$

for $i = 1, \dots, n_s$ and $j = 1, \dots, n_x$, where

n_s is the total number of particles in the swarm,

n_x is the dimension of the problem that is the number of parameters used,

$\mathbf{x}_i(t)$ is the position of particle i at time step t ,

$\mathbf{v}_i(t)$ is the velocity of particle i at time step t .

In order to successfully apply PSO, researchers have to familiarise themselves with basic algorithms and parameters of PSO. Two algorithms developed under PSO are the gbest PSO and the lbest PSO. Kennedy and Mendes (2002) defined the global best PSO or the gbest PSO as an algorithm which treated the entire population or swarm as the neighbourhood for each particle. Meanwhile, the local best PSO or also known as lbest PSO has a neighbourhood which consists of adjacent members in the array of population.

The velocity of particle i in gbest PSO (Engelbrecht, 2005) is calculated as

$$v_{ij}(t+1) = v_{ij}(t) + c_1 r_{1j}(t)[y_{ij}(t) - x_{ij}(t)] + c_2 r_{2j}(t)[\hat{y}_i(t) - x_{ij}(t)] \quad (2)$$

for $i = 1, \dots, n_s$ and $j = 1, \dots, n_x$, where

n_s	is the total number of particles in the swarm,
n_x	is the dimension of the problem,
$x_{ij}(t)$	is the position of particle i in dimension j at time step t ,
$v_{ij}(t)$	is the velocity of particle i in dimension j at time step t ,
c_1 and c_2	are positive acceleration constants,
$r_{1j}(t), r_{2j}(t) \sim U(0,1)$	are random values from a uniform distribution with range $[0, 1]$,
$y_i(t)$	is the personal best position of particle i at time step t ,
$\hat{y}(t)$	is the global best position discovered by any particles in the swarm at time step t ,
$c_1 r_{1j}(t)[y_{ij}(t) - x_{ij}(t)]$	is the cognitive component,
$c_2 r_{2j}(t)[\hat{y}(t) - x_{ij}(t)]$	is the social component.

The velocity of particle i in lbest PSO (Engelbrecht, 2005) is calculated as

$$v_{ij}(t+1) = v_{ij}(t) + c_1 r_{1j}(t)[y_{ij}(t) - x_{ij}(t)] + c_2 r_{2j}(t)[\hat{y}_{ij}(t) - x_{ij}(t)] \quad (3)$$

for $i = 1, \dots, n_s$ and $j = 1, \dots, n_x$, where $\hat{y}_{ij}(t)$ is the local best position of particle i in the neighbourhood N_i at time step t .

1.2 Rotating Disc Contactor (RDC) Column

According to Ritcey and Ashbrook (1979), the RDC is a type of rotary-agitated column patented by Reman of Royal Dutch Shell. Attarakih et al. (2013) stated that RDC column has higher conduct and efficiency in its operation when compared to non-agitated columns such as spray, packed and perforated plate columns.

The RDC column comprises a cylindrically shaped column of 12m tall with a diameter between 0.5m to 2.5m. As shown in Figure 1, there are a series of stator rings in RDC column that forms numerous compartments with each consisting of a rotating disc located at the center. A common rotating shaft holds the central rotating discs in place. Ismail et al. (2014) explained that these horizontal rotating discs are employed in RDC column as agitating elements. The shearing action produced by the rapidly rotating discs is used to inter-disperse phases in order to form drops of smaller diameter size. The mixer discs placed on the column's vertical shaft are applied to control the size of droplets. Besides, back-mixing in RDC column can be effectively reduced after the cross-section between each mixer disc is lessened by compartmentalizing RDC column with rings. This also means that the mixing process of each disc happens in its individual compartment.

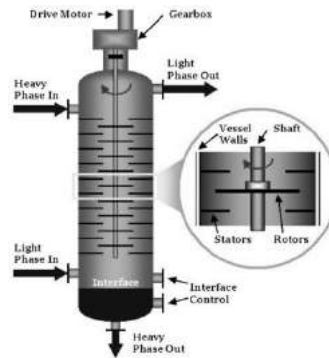


Figure 1 The RDC column

The two phases in RDC column which consist of the light and heavy phase can each be set as either dispersed or continuous phase. Flow rates, viscosities and wetting characteristics are several features that influence the choice of the dispersed phase. Some common characteristics of RDC column are it is applicable for fouling and viscous materials, and is rather sensitive to emulsions due to high shear mixing. Other than that, although axial back-mixing limited its efficiency, it possesses both reasonable capacity and turndown of 20 - 30 m^3/m^2 - hr and 40% respectively.

2 Methodology

The data to be used are prepared by normalizing or standardizing it to ensure all variables are proportionate with one another. In normalization, each variable's coefficient is scaled accordingly to the range of (0, 1) so that inequity in the variable sizes can be adjusted. Before the modelling process begins, the fitness function for the data that forms a part of the PSO algorithm has to be predetermined. The selected model to be used for the fitness function in this research is the multiple linear regression model. A multiple linear regression model is a linear regression model with more than one independent variable which is implemented in this research. After that, the process continues with problem formulation of the PSO algorithm to analyse the data and to predict the outputs of RDC column. A Matlab code developed using the mathematical software, Matlab version R2013a is applied to solve the PSO algorithm.

The PSO algorithm begins with the initialization of parameters according to the data such as number of particles, dimension and acceleration coefficients which can be adjusted in the Matlab code. Then, the position and velocity of particles are randomly generated before starting the iteration that follows. The value of the objective function or also known as the fitness function is calculated. The fitness function is formulated by using the multiple linear regression model. After the calculation of the fitness function, the position and velocity of particles are updated as shown in equation (1) and equation (2) respectively. In this research, the stopping condition is fulfilled if the mean square error between the actual and predicted value of output converges to a constant number. As such, if the stopping condition is satisfied, the iteration ends. Otherwise, the iteration will start again until the stopping condition is reached.

The following illustrated the pseudo code (Kamrani, 2010) used in Matlab to solve the PSO model.

```

for each particle
    Initialize particle;
end
do
    for each particle

```

```

        Calculate fitness value;
        if the fitness value is better than the best fitness value (pbest) in history then
        Set current value as the new pbest;
    end
    Choose the particle with the best fitness value of all the particles as the gbest
    for each particle
        Calculate particle velocity using equation (2);
        Update particle position using equation (1);
    end
until stopping condition is true;

```

Results obtained in this research will be analysed for accuracy which can be used as a benchmark for performance measure of the employed PSO technique. According to Engelbrecht (2005), the performance of PSO can be measured based on a few criteria which include accuracy, coherence, diversity, efficiency, reliability and robustness. This research applies the percentage of error for each solution, the mean squared error (MSE) and the Pearson correlation coefficient, r to evaluate the performance of PSO used.

3 Result and Discussion

Three datasets used in this research are collected from the experimentation of liquid-liquid extraction in RDC column. Two of the datasets which are data of cumeneisobutyric acid with fast rotor speed and data of cumeneisobutyric acid with slow rotor speed have 256 data each. Meanwhile, data of butanol acid with fast rotor speed consists of 243 data. Each data is divided into four input variables and four output variables. In this section, only the analysis for data of cumeneisobutyric acid with fast rotor speed is discussed in detail as same analyses are carried out on the other two data as well. There are in total four output variables for the data of cumeneisobutyric acid with fast rotor speed to be predicted individually using PSO with the help of Matlab. These output variables include hold-up ($c - holdup$), Sauter mean diameter (d_{32}) ($c - d_{32}$), concentration of continuous phase outlet ($cc - out$) and concentration of dispersed phase outlet ($cd - out$).

10 outputs out of the total 256 outputs of each hold – up, Sauter mean diameter (d_{32}), concentration of continuous phase outlet and concentration of dispersed phase outlet are selected for analysis of percentage of error obtained after prediction. Table 1, 2, 3 and 4 show the percentages of error attained for each predicted outputs.

Table 1: Percentages of error obtained for the predicted hold-up in cumeneisobutyric acid with fast rotor speed

No.	Actual <i>c-holdup</i>	Predicted <i>c-holdup</i>	Absolute Error	Percentage of Error (%)
1	0.581736587	0.57875	0.0030	0.5134
2	0.582236148	0.5788	0.0034	0.5902
3	0.581736587	0.57869	0.0030	0.5237
4	0.582236148	0.57874	0.0035	0.6005
5	0.581736587	0.57879	0.0029	0.5065

6	0.582236148	0.57884	0.0034	0.5833
7	0.581736587	0.57874	0.0030	0.5151
8	0.582236148	0.57879	0.0034	0.5919
9	0.581736587	0.57884	0.0029	0.4979
10	0.582236148	0.57889	0.0033	0.5747

Table 2: Percentages of error obtained for the predicted Sauter mean diameter (d32) in cumeneisobutyric acid with fast rotor speed

No.	Actual <i>c-d32</i>	Predicted <i>c-d32</i>	Absolute Error	Percentage of Error (%)
1	0.921715334	0.85588	0.0658	7.1427
2	0.921715334	0.85577	0.0659	7.1546
3	0.921715334	0.85565	0.0661	7.1677
4	0.921715334	0.85554	0.0662	7.1796
5	0.923413198	0.85148	0.0719	7.7899
6	0.928026521	0.85137	0.0767	8.2602
7	0.928026521	0.85126	0.0768	8.2720
8	0.928026521	0.85114	0.0769	8.2849
9	0.928026521	0.85137	0.0767	8.2602
10	0.928026521	0.85125	0.0768	8.2731

Table 3: Percentages of error obtained for the predicted concentration of continuous phase outlet in cumeneisobutyric acid with fast rotor speed

No.	Actual <i>cc-out</i>	Predicted <i>cc-out</i>	Absolute Error	Percentage of Error (%)
1	0.527333335	0.57429	0.0470	8.9045
2	0.604106374	0.65427	0.0502	8.3038
3	0.486757983	0.51979	0.0330	6.7861
4	0.564974799	0.59977	0.0348	6.1587
5	0.642849663	0.67974	0.0369	5.7386
6	0.720073987	0.75972	0.0396	5.5058
7	0.615579792	0.62524	0.0097	1.5693

8	0.675308103	0.70522	0.0299	4.4294
9	0.752744641	0.7852	0.0325	4.3116
10	0.829989352	0.86518	0.0352	4.2399

Table 4: Percentages of error obtained for the predicted concentration of dispersed phase outlet in cumeneisobutyric acid with fast rotor speed

No.	Actual <i>cd-out</i>	Predicted <i>cd-out</i>	Absolute Error	Percentage of Error (%)
1	0.336785668	0.35577	0.0190	5.6369
2	0.406127792	0.41422	0.0081	1.9925
3	0.477867895	0.47267	0.0052	1.0877
4	0.551591657	0.53112	0.0205	3.7114
5	0.481509572	0.51372	0.0322	6.6895
6	0.533997361	0.57217	0.0382	7.1485
7	0.609146117	0.63062	0.0215	3.5252
8	0.686743596	0.68907	0.0023	0.3388
9	0.340549769	0.31471	0.0258	7.5877
10	0.409422396	0.37317	0.0363	8.8545

As shown in Table 1, percentages of error obtained for the selected 10 predicted outputs of hold – up in cumeneisobutyric acid with fast rotor speed are all very much less than 10%. Same observations are noticed in Table 2, Table 3 and Table 4 for predictions of Sauter mean diameter (d_{32}), concentration of continuous and dispersed phase outlets. These indicate that the predictions for the four outputs are close to the actual output and exhibit a rather high accuracy since any percentages of error less than 10% are deemed acceptable. These indications can be further proven by looking at scatterplots of the four predicted outputs in Figure 2, Figure 3, Figure 4 and Figure 5 with correlation coefficients of 0.9403, 0.9695, 0.9825 and 0.9873 respectively. These figures depict all actual and predicted points are distributed quite near to the regression line and correlation coefficients acquired are close to 1. These imply a reasonably strong relationship between the actual and the predicted outputs. Hence, predictions of the four outputs for cumeneisobutyric acid with fast rotor speed using PSO are up – to – par and display a satisfactory performance. Fitting performances of PSO are also found in predictions of four outputs for cumeneisobutyric acid with slow rotor speed and butanol acid with fast rotor speed when similar analyses are performed on these two data.

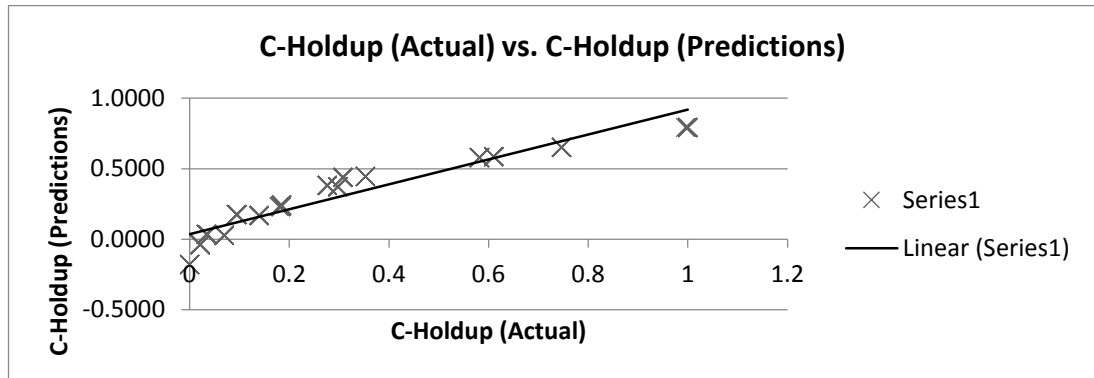


Figure 2 Scatterplot of actual versus predicted hold – up for cumeneisobutyric acid with fast rotor speed

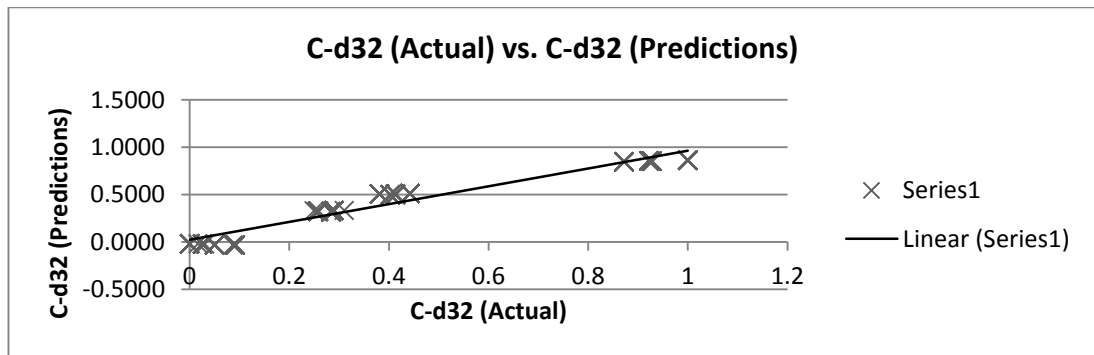


Figure 3 Scatterplot of actual versus predicted Sauter mean diameter (d32) for cumeneisobutyric acid with fast rotor speed

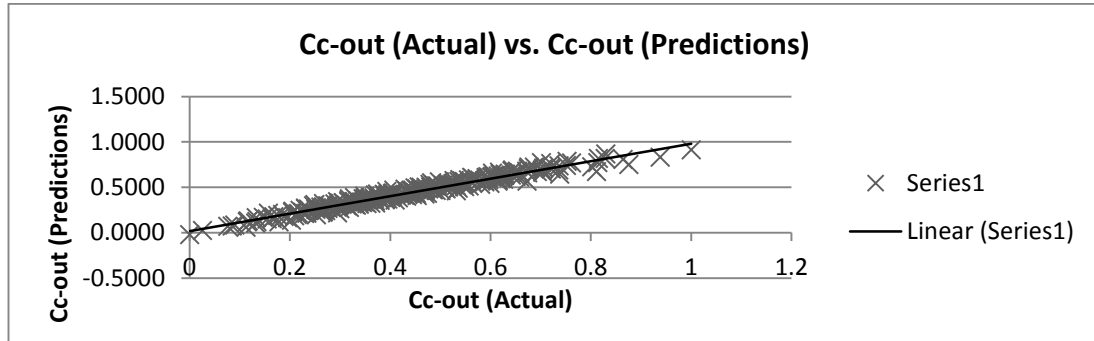


Figure 4 Scatterplot of actual versus predicted concentration of continuous phase outlet for cumeneisobutyric acid with fast rotor speed

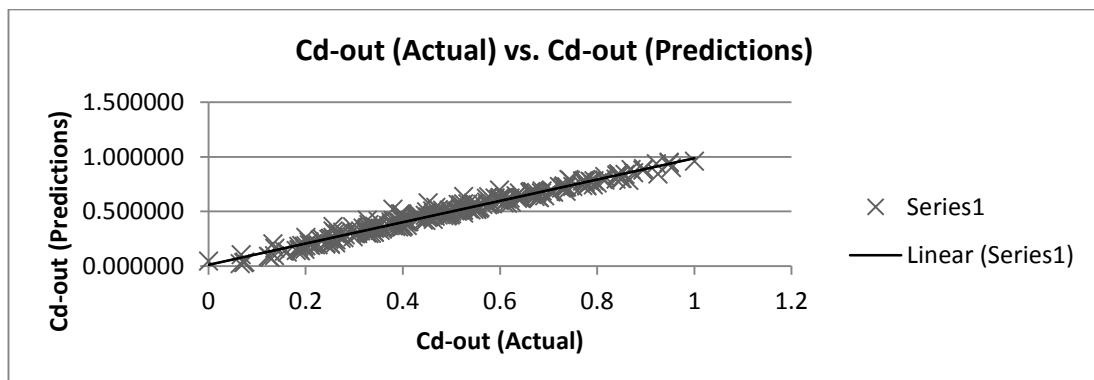


Figure 5 Scatterplot of actual versus predicted concentration of dispersed phase outlet for cumeneisobutyric acid with fast rotor speed

Table 5: MSE and correlation coefficients for predicted outputs of different acids

CumeneIsobutyric Acid with Fast Rotor Speed		
Output Variables	Mean Squared Error (MSE)	Correlation Coefficient (r)
Hold-up ($c - holdup$)	0.009081	0.9403
Sauter mean diameter (d32) ($c - d32$)	0.006434	0.9695
Concentration of continuous phase outlet ($cc - out$)	0.001152	0.9825
Concentration of dispersed phase outlet ($cd - out$)	0.001157	0.9873
CumeneIsobutyric Acid with Slow Rotor Speed		
Output Variables	Mean Squared Error (MSE)	Correlation Coefficient (r)
Hold-up ($c - holdup$)	0.009349	0.9385
Sauter mean diameter (d32) ($c - d32$)	0.009042	0.9569
Concentration of continuous phase outlet ($cc - out$)	0.001322	0.9798
Concentration of dispersed phase outlet ($cd - out$)	0.001399	0.9846
Butanol Acid with Fast Rotor Speed		
Output Variables	Mean Squared Error (MSE)	Correlation Coefficient (r)
Hold-up ($c - holdup$)	0.019015	0.8338
Sauter mean diameter (d32) ($c - d32$)	0.015319	0.9422
Concentration of continuous phase outlet ($cc - out$)	0.005323	0.9292
Concentration of dispersed phase outlet ($cd - out$)	0.001800	0.9788

Comparisons of cumeneisobutyric acid with different rotor speed and between cumeneisobutyric acid and butanol acid with same rotor speed are made based on Table 5. It

is clearly seen that MSE values for all four outputs which consist of hold-up, Sauter mean diameter (d_{32}), concentration of continuous phase outlet and concentration of dispersed phase outlet in cumeneisobutyric acid with fast rotor speed are generally much lower than that in cumeneisobutyric acid with slow rotor speed. Meanwhile, higher correlation coefficients for outputs in cumeneisobutyric acid with fast rotor speed are noticed as well. On the other hand, the same observation is also detected when comparing cumeneisobutyric acid and butanol acid of the same rotor speed. These conditions imply that cumeneisobutyric acid with fast rotor speed has better predicted outputs when compared to that of cumeneisobutyric acid with slow rotor speed and butanol acid. Hence, it can be concluded that PSO prediction shows a better performance in cumeneisobutyric acid with fast rotor speed as compared to that of slow rotor speed and butanol acid with the same rotor speed.

4 Conclusion

All objectives stated have been carried out and fulfilled in this research. Numerous concepts of particle swarm optimization (PSO) have been carefully studied and understood in this research. Inputs and outputs of rotating disc contactor (RDC) column are modelled using the PSO technique in which the fitness function is formed with the dependent and independent variables as inputs and outputs from RDC column respectively. Moreover, the results of this research indicate that PSO gives good performance in predicting outputs of RDC column with reasonably high accuracy. Nevertheless, these findings are only applicable to the prediction of four outputs in the RDC column namely, hold – up, Sauter mean diameter (d_{32}), concentration of continuous phase outlet and concentration of dispersed phase outlet. It is hoped that this research can assist engineers and scientists in improving the performance of RDC column by using PSO so that maximum outputs of RDC column can be obtained.

References

- Attarakih, M., Abu-Khader, M., and Bart, H. (2013). Modeling and dynamic analysis of a rotating disc contactor (RDC) extraction column using one primary and one secondary particle method (OPOSPM). *Chemical Engineering Science*.91, 180 – 196. Elsevier.
- Chong, K. P., and Zak S. H. (2013). *An Introduction to Optimization*. (4thed.) Hoboken, New Jersey: John Wiley & Sons Inc.
- Engelbrecht, A. P. (2005). *Fundamentals of Computational Swarm Intelligence*. West Sussex, England: John Wiley & Sons Ltd.
- Haderer, T., Marr, R., Martens, S., and Siebenhofer, M. (2004). Design of Rotating Disc Contactors; Implementation of CFD Tools. *2004 Annual Meeting*. 7 – 12, November. Austin, Texas: AIChE.
- Ismail, W. N. A., Zakaria, S. A., Mohd Noor, N. F., Sulong, I., Arshad, K. A. (2014). Modeling of Rotating Disc Contactor (RDC) Column. *AIP Conference Proceedings*.1635, 572 – 581. AIP Publishing.
- Kamrani, E. (2010). *Modeling and Forecasting long-term Natural Gas (NG) consumption in Iran, using Particle Swarm Optimization (PSO)*. Master, Dalarna University.
- Kennedy, J., and Mendes, R. (2002). Population Structure and Particle Swarm Performance. *Proceedings of the 2002 Congress*.12 – 17, May. Honolulu, HI: IEEE, 1671 – 1676.

Ritcey, G. M., and Ashbrook, A. W. (1979). *Solvent Extraction: Principles and Applications to Process Metallurgy* (1st ed.). New York: Elsevier Science Publishers B. V.

Van den Bergh, F., and Engelbrecht, A. P. (2005). A Study of Particle Swarm Optimization Particle Trajectories. *Information Sciences*.176, 937 – 971. Elsevier.

Venter, G., and Sobieszczanski-Sobieski, J. (2003). Particle Swarm Optimization. *AIAA Journal*.41(8), 1583 – 1589.

SIMULATION OF A TWO-DIMENSIONAL DIFFUSION ADVECTION EQUATION BY USING MATLAB PDE TOOLBOX

Chan Poh Ching & Assoc. Prof. Dr. Khairil Anuar Bin Arshad

1.1 Introduction

Theoretically, the diffusion occurs when there is an uneven concentration of a dissolved substance in liquid [1]. The higher concentration moves to the area with lower concentration until they reach equilibrium. This is also referred as the movement of substance down a concentration gradient. However, if there is an additional force added into the diffusion process, the diffusion will move faster and takes a shorter time to reach its equilibrium. This additional force is known as advection force. Advection is a one way motion which only moves downstream. Advection is a process that transfers the mass, heat or any other property. Hence, we have diffusion-advection process by adding the advection in the process of diffusion. In nature, transport occurs in fluids through the combination of advection and diffusion. Diffusion advection equation can also be used as a stochastic differential equation to describe the random motion with diffusivity and bias. For example, diffusion advection equation can describe the Brownian motion of a single particle.

In real life, there are a lot of problems involving diffusion advection process. One of the real life examples is fumigation in agriculture. Fumigation is probably the most efficient and economical method for adequate sterilization of seed-bed soils [2]. Fumigation is the action of releasing a toxic chemical in gaseous state into the silo in order to control the pest in a closed space [3]. So, through this research, we are able to solve the general equation of the diffusion advection to predict and find the solution which is the concentration of the chemical in a closed space.

1.2 Literature Review

The diffusion advection process can be represented as a partial differential equation which model the concentration of the substance at certain time, t . In diffusion process, no bulk motion is required to move the substances unlike the other transport mechanisms such as convection and advection. In advection, fluid is the main sources which move the substance from one point to another. A fluid transport some conserved quantity or material via bulk motion. Advection is essentially the effect of the wind blowing the fluid in a given direction without significantly dispersing them. Diffusion takes place when this molecule

will transfer from one place to another place not in a linear form then advection also takes place [4]. The two-dimensional advection diffusion equation is

$$\frac{\partial c}{\partial t} + u \frac{\partial c}{\partial x} + v \frac{\partial c}{\partial y} = D \left(\frac{d^2 c}{dx^2} + \frac{d^2 c}{dy^2} \right) + S \quad (1)$$

where u, v are the horizontal and vertical advection velocities, D is the diffusion coefficient and S is the source or sink term. Peclet number (Pe) is a dimensionless number related to the transport of substance. Peclet number is the ratio of rate of advection by the rate of diffusion. Generally, Peclet number is defined as

$$Pe = \frac{\text{Advective Transport Rate}}{\text{Diffusive Transport Rate}}$$

We know that Peclet number for mass transfer is the product of Reynolds number and the Schmidt number. This will results in:

$$\begin{aligned} Pe &= Re \times Sc \\ &= \frac{vL}{b} \times \frac{b}{D} \\ &= \frac{vL}{D} \end{aligned}$$

where, v is mean velocity of the object relative to the fluid ($\frac{m}{s}$), L is the travelled length of the fluid (m), b represents kinetic viscosity ($\frac{m^2}{s}$), and D denotes mass diffusivity ($\frac{m^2}{s}$).

Practically, if Peclet number less than 1 (i.e. $Pe < 1$), this means that the advection term is significantly smaller than the diffusion term. Physically, diffusion nominates in the diffusion advection process and advection process is negligible. The whole process will only follows diffusion process which results in spreading occurs almost symmetrically despite the directional bias of the weak flow. In the other hand, if Peclet number greater than 1 (i.e. $Pe > 1$), this means that the diffusion term is significantly smaller than the advection term. So, in overall, advection process will dominates and diffusion process can be neglected. These dimensionless groups of fluid properties play a prominent role in dimensionless equations system in which competing transport processes occur [5].

1.3 Methodology

Diffusion advection equation is ready to be examined. The variables are well explained and to be assigned constant to different variables in order to get different results.

We will use MATLAB and PDE Toolbox to solve the diffusion advection equation. The Partial Differential Equation (PDE) Toolbox provides a powerful and flexible environment for the study and solution of partial differential equations in two space dimensions and time. The PDE Toolbox uses finite element method for solution of partial differential equations in two space dimensions [6]. Two-dimensional diffusion advection equation used in this paper is given as below:

$$\frac{\partial c}{\partial t} + u \frac{\partial c}{\partial x} + v \frac{\partial c}{\partial y} = D \left(\frac{\partial^2 c}{\partial x^2} + \frac{\partial^2 c}{\partial y^2} \right) \quad (2)$$

where c is concentration or the mass of the substances, t is timespan, u and v are the velocity in the direction of x and y (ms^{-1}) respectively and D denotes diffusivity coefficient, $\frac{\text{m}^2}{\text{s}}$.

1.3.1 Solving the diffusion advection equation using MATLAB PDE Toolbox

The parameters involved in this thesis are given as below.

$$t = 3600 \text{ seconds}, u = v = 0.01 \text{ ms}^{-1}, D = 0.05 \text{ m}^2\text{s}^{-1}, x = 5\text{m}, y = 4\text{m}$$

Below is the step involved in solving the equation:

Step 1: Define the 2D geometry

Table 1: Functions of plotting the geometry

pdetool	Open PDE app
pdecirc	Draw circle
pdeellip	Draw ellipse
pdepoly	Draw polygon
pdirect	Draw rectangle
csgchk	Check validity of Geometry Description matrix
csgdel	Delete borders between minimal regions
decsg	Decompose Constructive Solid Geometry into minimal regions

pdearcl	Interpolation between parametric representation and arc length
pdegeom	Write custom function for defining geometry
wgeom	Write geometry specification function

Table 1 shows the function that can be used in drawing the geometry of equations. In this paper, we consider the rectangle shape with an inlet which is the entrance of gas or solute. First of all, we need to call out the PDE Toolbox window by typing *pdetool* in MATLAB command windows as shown in Figure 1. After the command read by MATLAB, another new window will appear as shown in Figure 2.

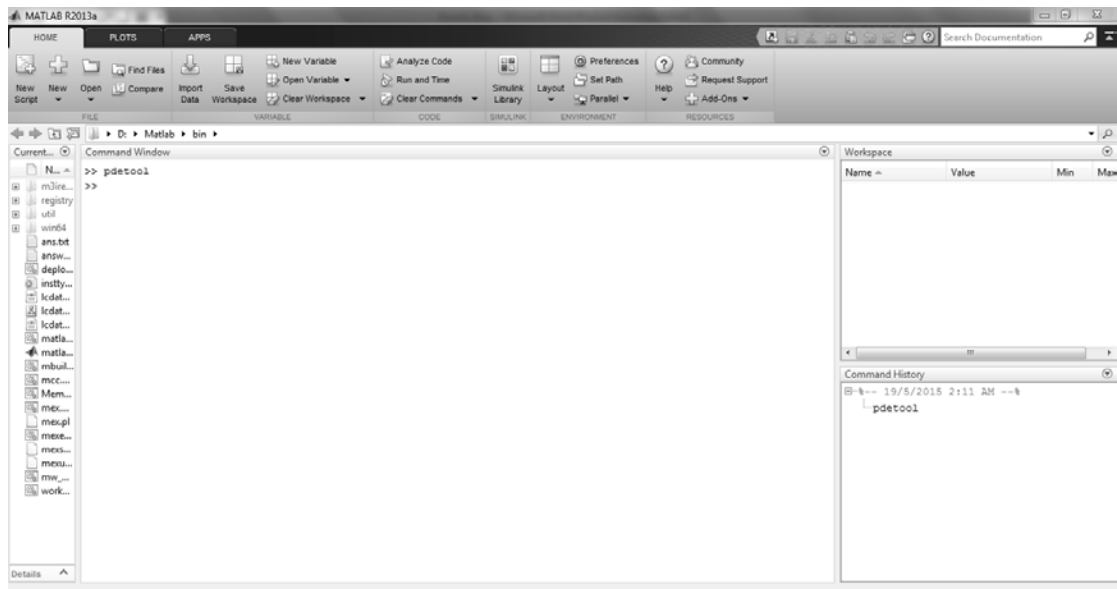


Figure 1: Calling out the PDE Toolbox.

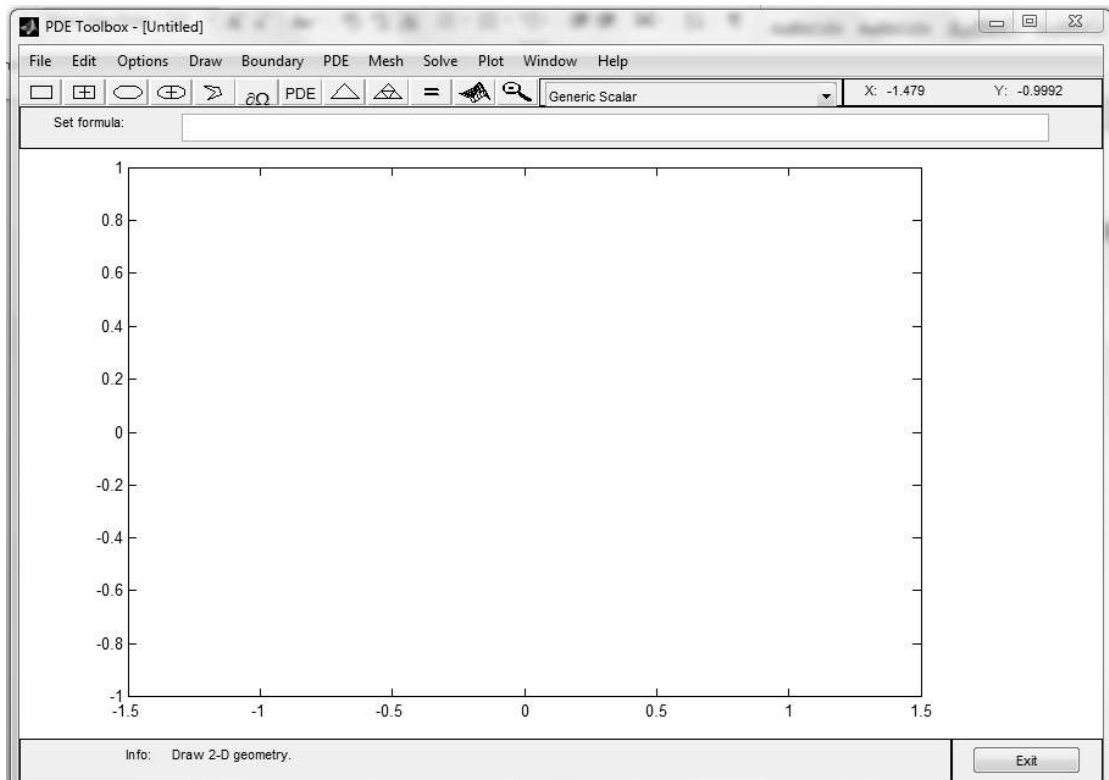


Figure 2: The PDE Toolbox Window.

After the window of PDE Toolbox appeared, we can start planning and solving our equation. In this research, we will solve the equation with confined spaces. So, we draw the rectangle with domain $0 \leq x \leq 5$ and $0 \leq y \leq 4$ while the domain of the inlet of the confined space is set as $x = 0.01675$ and $1.9563 \leq y \leq 2.1563$. After the plotting of geometry in PDE Toolbox window, we get the geometry as shown below.

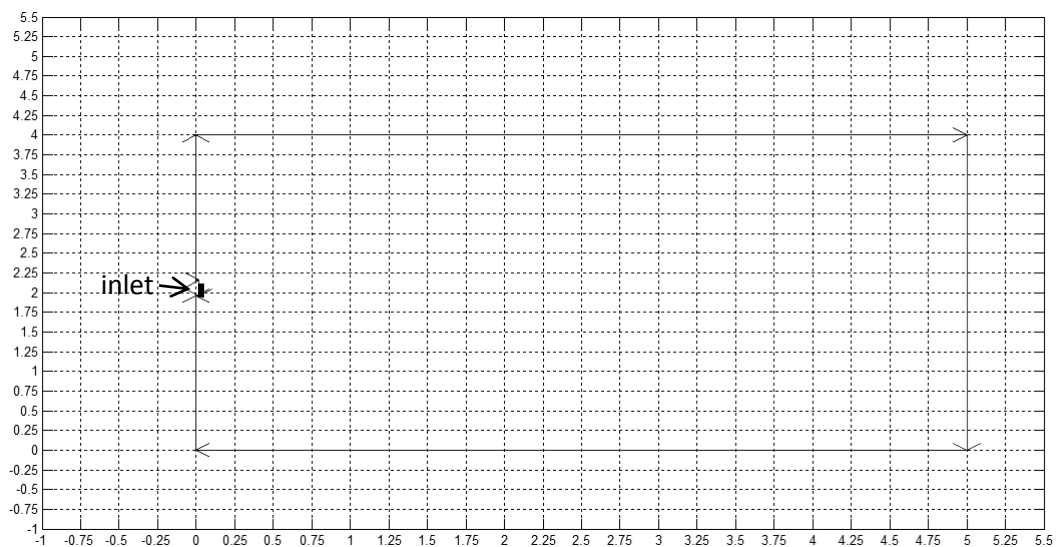


Figure 3: 2D geometry of the equation.

Step 2: Define the boundary conditions

There are two types of boundary conditions in MATLAB PDE Toolbox which are Neumann and Dirichlet.



Figure 4: Dirichlet Boundary Condition.

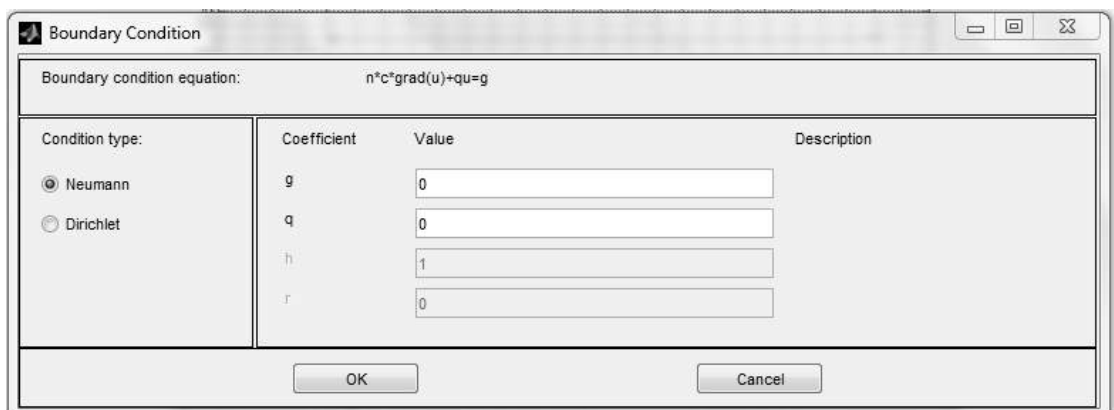


Figure 5: Neumann Boundary Condition.

Figure 4 and Figure 5 are the two types of boundary conditions. We have to assign the boundary condition on every edge. The boundary condition is given as:

Dirichlet boundary condition: $h * u = r$

Neumann boundary condition: $n \cdot (c \nabla u) + qu = g$

In this research, the Dirichlet boundary condition will apply on the inlet and also the most right wall. Our boundary conditions are set as below:

Initial condition: $c(x, y, 0) = 0$;

Boundary conditions: $c(0, y, t) = c(x, 0, t) = c(L, y, t) = c(x, k, t) = 0$

where L and k are the length of x and y respectively.

From the boundary condition, we can easily substitute the constant into the Dirichlet boundary condition and Neumann boundary condition. Initially, the concentration in the closed space geometry is 0 ppm. The concentration of 100 ppm is injected through the inlet thus the concentration at the inlet is 100 ppm. Also, the Dirichlet boundary condition is set at the end of the geometry where the concentration of the chemical at the end of the geometry is 0 ppm. So, $r = 0$ is set at the end of the closed space geometry. Next, the flux of every wall was set to zero i.e. $n \cdot \nabla c = 0$ since there is no any substance can pass through the walls or diffuse through the walls of the confined space.

Step 3: Define the PDE coefficients

Due to the two variables in second order partial differential equation, we use generic system in the PDE Toolbox to compute the graph. Two-dimensional diffusion advection equation indicates $N > 1$ thus we use 2-N elements method to solve it. The advection-diffusion equation belongs to the class of parabolic PDEs [7].

The equation of parabolic PDE is

$$d * u' - \text{div}(c * \text{grad}(u)) + a * u = f. \quad (3)$$

the available coefficients in the PDE specification are a , c , d and f . From previous section, we know that the equation of diffusion advection equation is

$$\frac{\partial c}{\partial t} + u \frac{\partial c}{\partial x} + v \frac{\partial c}{\partial y} = D \left(\frac{\partial^2 c}{\partial x^2} + \frac{\partial^2 c}{\partial y^2} \right)$$

We rearrange and get

$$\frac{\partial c}{\partial t} - D \left(\frac{\partial^2 c}{\partial x^2} + \frac{\partial^2 c}{\partial y^2} \right) = - \left(u \frac{\partial c}{\partial x} + v \frac{\partial c}{\partial y} \right).$$

Then, we rearrange again to get the equation form as Equation (3).

$$1 * c' - \text{div}(D * \text{grad}(c)) + 0 * c = - \left(u \frac{\partial c}{\partial x} + v \frac{\partial c}{\partial y} \right)$$

$$1 * c' - \text{div}(D * \text{grad}(c)) + 0 * c = -V \left(\frac{\partial c}{\partial x} + \frac{\partial c}{\partial y} \right), \quad \text{where } V = u = v.$$

Thus, we have

$$d * u' - \text{div}(c * \text{grad}(u)) + a * u = f.$$

$$1 * c' - \text{div}(D * \text{grad}(c)) + 0 * c = -V \left(\frac{\partial c}{\partial x} + \frac{\partial c}{\partial y} \right)$$

From the above explanation, we are able to substitute the coefficient into the PDE specification now. The PDE specification for diffusion advection equation is shown as below:

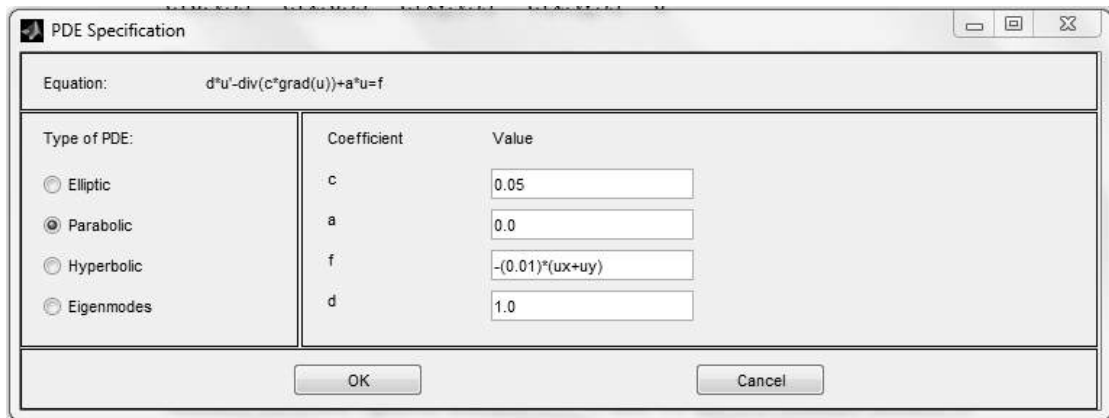


Figure 6: PDE Specification in PDE Toolbox.

Step 4: Mesh generations

In MATLAB, the mesh refinement divides each triangle into four similar triangles by creating new corners at the mid-sides, adjusting for curve boundaries. In order to improve the accuracy of results, the elements are required not to deviate too much. Mesh generation in a complex domain is not easy even with a mesh generations program. However, a simple domain can be meshed using a simple algorithm. For example, a rectangular shape of 2D domain can be broken into a number of rectangular elements easily [8]. Thus, in this thesis, the geometry is broken down into a number of rectangular elements by using the mesh function. Figure 3.7 shows the geometry after mesh refinement is applied.

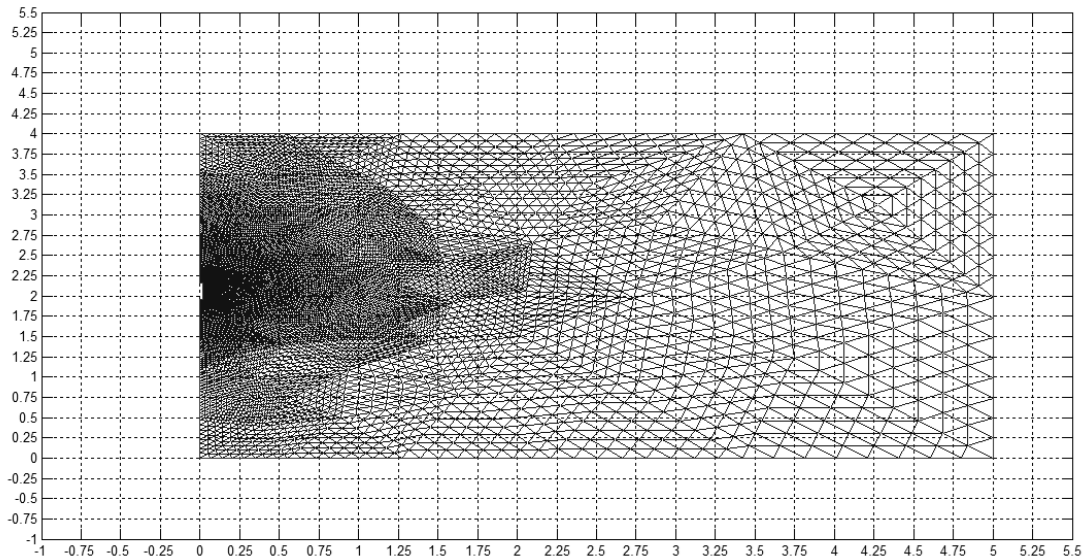


Figure 7: Mesh generations on geometry of the equation.

Step 5: Solve the PDE

Before we solve the PDE, we have to set the timespan for this diffusion advection equation. The unit for the timespan in PDE Toolbox is in seconds. In the drop down menu of PDE, there is an option named Parameters. In Parameters, we can simply adjust the timespan of the process. I had adjusted the timespan from 0 to 3600 seconds which is one hour as shown in Figure 8.

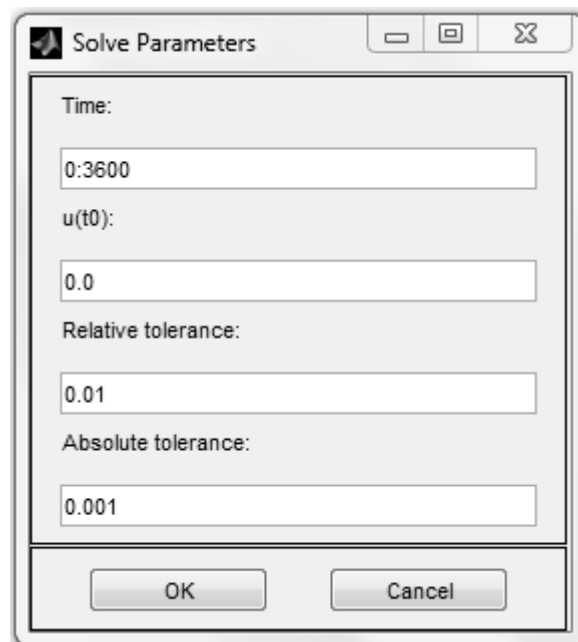


Figure 8: Timespan adjustment.

Step 6: Plot the solution

After the timespan adjustment, we can solve the PDE by clicking the solve PDE. The PDE Toolbox uses finite element method to solve the diffusion equation. There are a few choices in the drop down menu of Plot. Plot menu in PDE Toolbox enables us to add on some graphics in the geometry. I had added the total number of 20 contours in the geometry in order to visualize and understand the flow direction of chemical. The menu is as given as Figure 9.

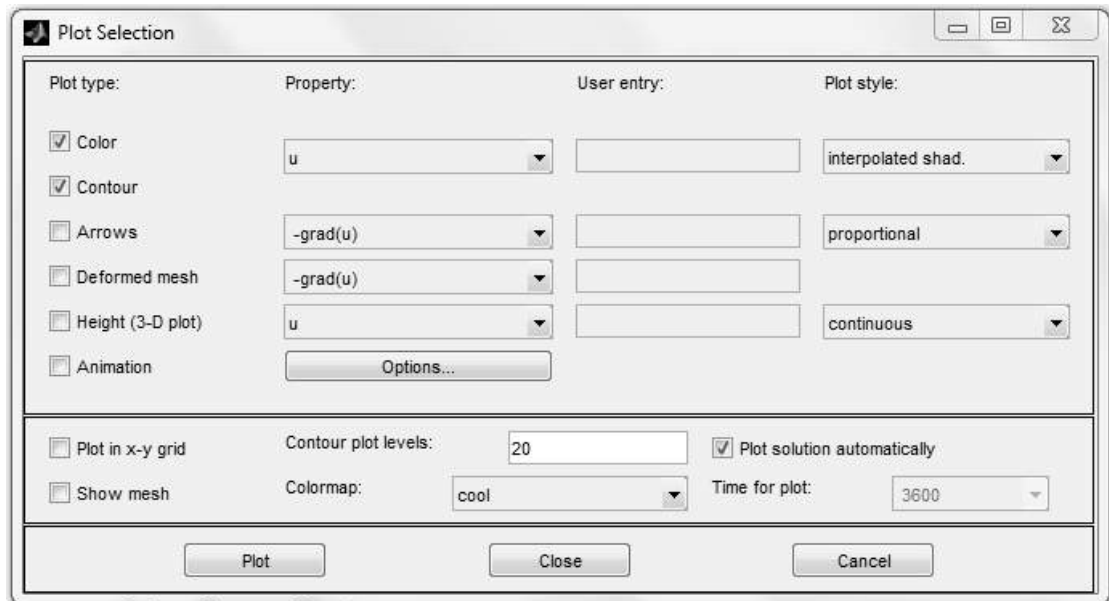


Figure 9: The Plot Selection in PDE Toolbox.

From the above step, we will get a coloured geometry where it shows the distribution of a particular substance let's say, a drop of ink in a solvent. Apart from the coefficient stated above, I had replaced them with different value in order to study the relationship and the pattern of different values.

Step 7: Mesh independent test

After we exported the solution from PDE Toolbox, we then conduct the mesh independent test. The purpose of mesh independent test is to getting accurate results. Therefore, the simulation is repeated for a smaller mesh size which means higher number of elements. Since every refinement of mesh will leads to a smaller triangular-based mesh, the error of the result will reduced if a smaller mesh is created. In order to have a smaller error, we compare the result of every refinement of mesh. If the results are closed enough or identical, we can say that the errors are constant and do not have a large variance. Thus, we can conclude that the previous mesh is accurate enough to compute the result. I have done the mesh independence test and found out that refinement of mesh for three times will

compute an accurate result. The result of mesh independent test applies to every case in this research. The results and graphs are discussed in Chapter 4. Also, further details and analysis will be explained in Chapter 4.

1.3.2 Process Chart

The following chart is how the work is done to solve the diffusion advection equation.

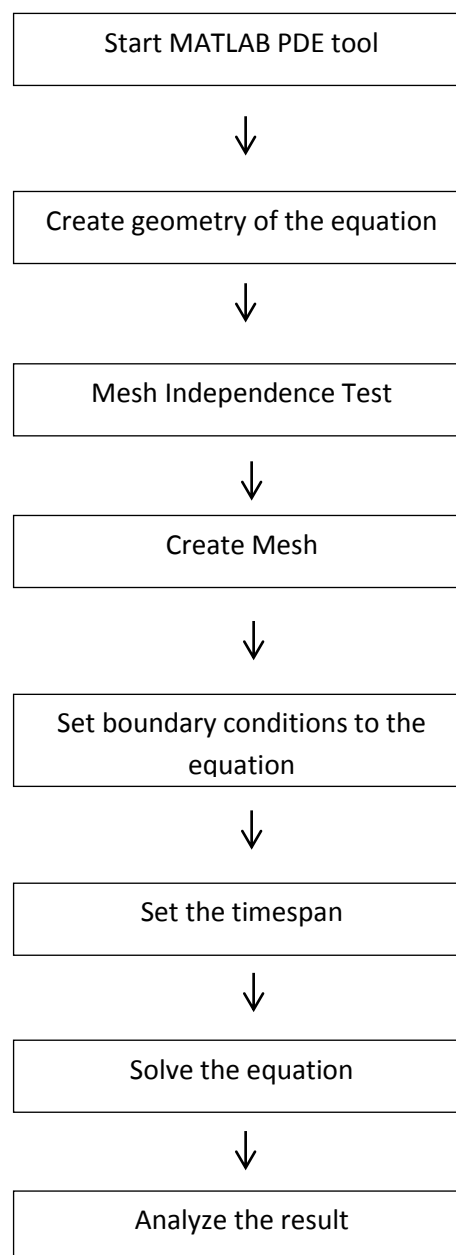


Chart 1: Process Chart

1.4 Results and discussion

The diffusion is the process where the bulk motion is not required. In this section, we discuss about the diffusion with advection in the equation.

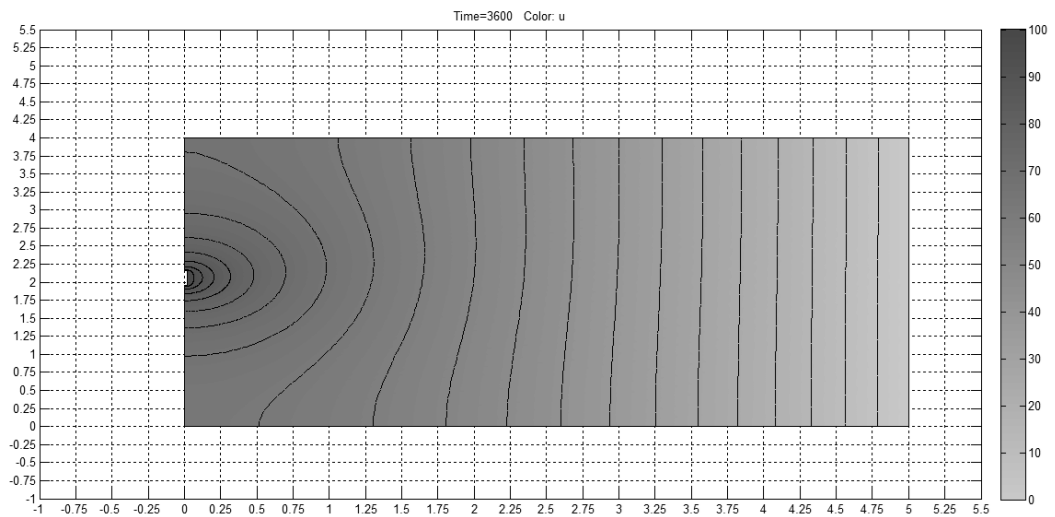


Figure 10: Concentration distribution in a closed space of width 5m for the duration of $t = 3600\text{s}$ (one hour) with velocity, $v = 0.01 \text{ ms}^{-1}$, concentration at the inlet, $c_0 = 100\text{ppm}$ and diffusion coefficient, $D = 0.005 \text{ m}^2\text{s}^{-1}$.

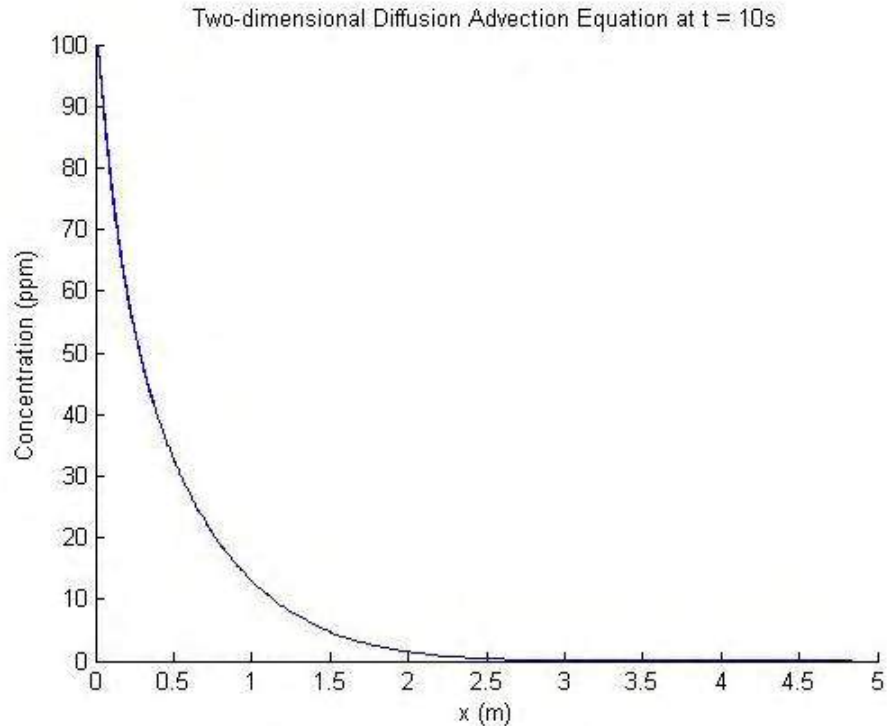


Figure 11: Concentration along the centre in a closed space of width 5 m for the duration of $t = 3600\text{s}$ (one hour) with velocity, $v = 0.01 \text{ ms}^{-1}$, concentration at the inlet, $c_0 = 100\text{ppm}$ and diffusion coefficient, $D = 0.005 \text{ m}^2\text{s}^{-1}$.

Figure 10 shows the concentration contour plot for two-dimensional diffusion advection in a closed space of width 5m for the duration of $t = 3600\text{s}$ (one hour) with velocity, $v = 0.01 \text{ ms}^{-1}$, concentration at the inlet, $c_0 = 100\text{ppm}$ and diffusion coefficient, $D = 0.005 \text{ m}^2\text{s}^{-1}$. And, Figure 11 is the line graph which shows the concentration of substances along the centre at $t = 10\text{s}$.

In the next sub-topic, we conduct a few tests on various diffusion coefficients and Peclet number in order to study and examine the effect of these parameters on the concentration. And, we assumed velocity is constant throughout the research. Thus, we do not examine on the effect of various velocity on concentration distribution. The results and analysis are discussed as below,

1.4.1 Various Diffusion Coefficients

Diffusion coefficient might give impact on the concentration distribution of the substances in a closed space. Below are the results and analysis on the impact of various diffusion coefficients on concentration distribution.

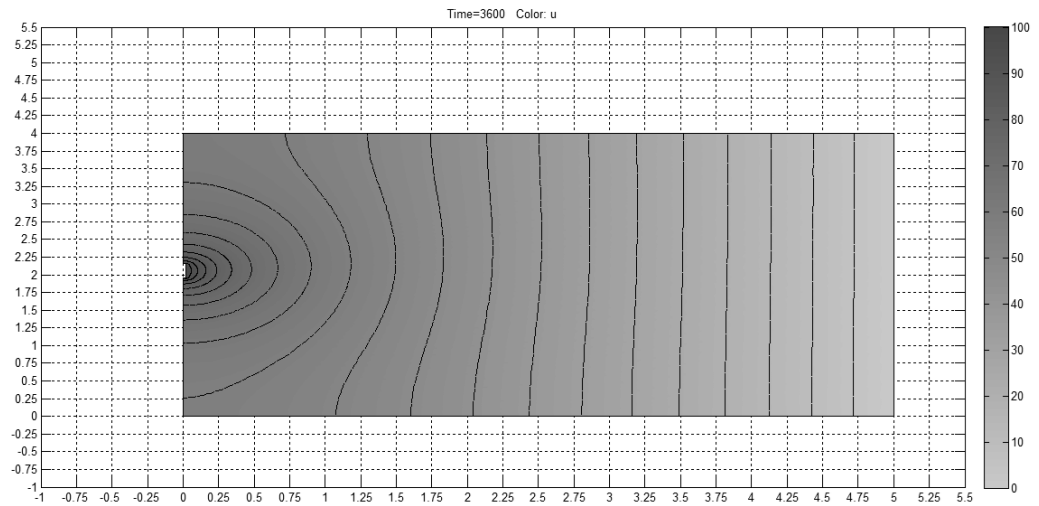


Figure 12: Concentration distribution in a closed space of width 5 m for the duration of $t = 3600\text{s}$ (one hour) with velocity, $v = 0.01 \text{ ms}^{-1}$, concentration at the inlet, $c_0 = 100 \text{ ppm}$ and diffusion coefficient, $D = 0.1 \text{ m}^2\text{s}^{-1}$.

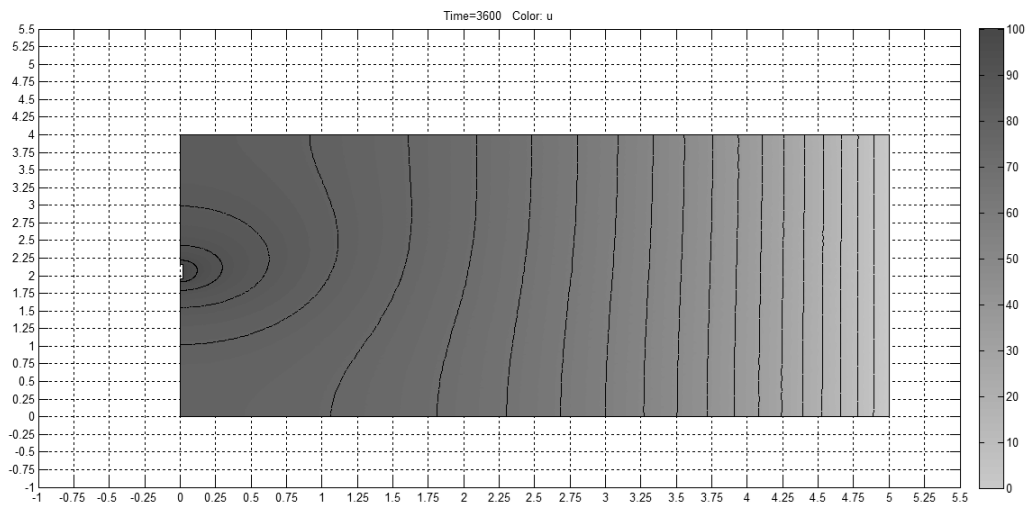


Figure 13: Concentration distribution in a closed space of width 5 m for the duration of $t = 3600\text{s}$ (one hour) with velocity, $v = 0.01 \text{ ms}^{-1}$, concentration at the inlet, $c_0 = 100 \text{ ppm}$ and diffusion coefficient, $D = 0.02 \text{ m}^2\text{s}^{-1}$.

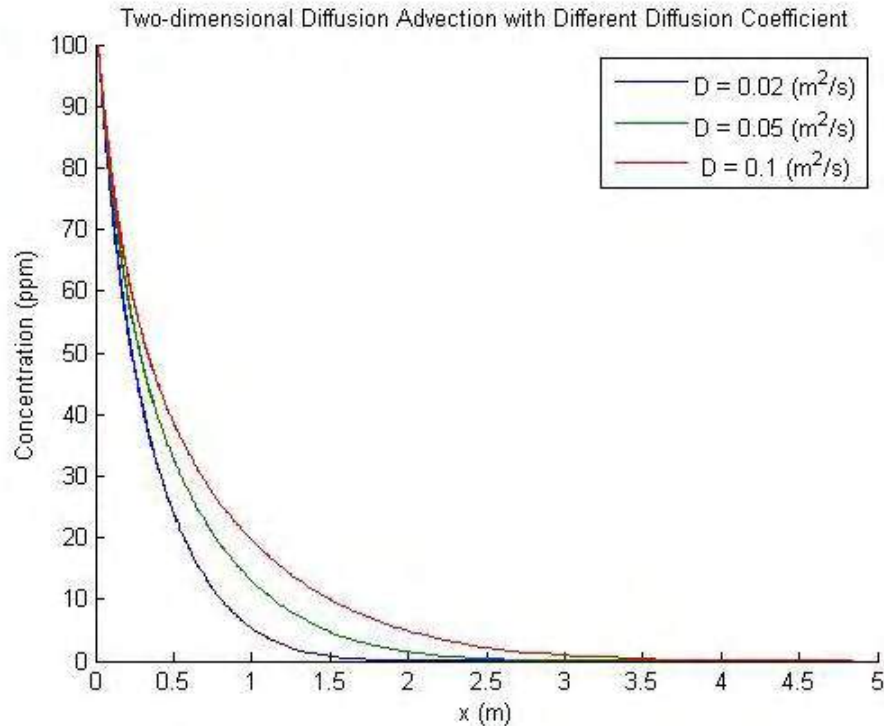


Figure 14: Comparison between the concentration along the centre in a closed space of width 5m with different diffusion coefficient for the duration of $t = 3600\text{s}$ (one hour) with velocity, $v = 0.01 \text{ ms}^{-1}$, concentration at the inlet, $c_0 = 100 \text{ ppm}$.

Figure 12 shows the solution of the two-dimensional diffusion advection equation with diffusion coefficient of $0.1 \text{ m}^2\text{s}^{-1}$. Figure 13 displays the solution by setting the diffusion coefficient as $0.02 \text{ m}^2\text{s}^{-1}$. By observing Figure 12 and Figure 13, we can see that the contours are slightly different from each other.

In Figure 13, the fourth contour line moves unevenly which is towards the direction of upwards. The concentration diffuses slight to the top and causes the shape of the contours turns out differently. The pattern of contour in Figure 13 is expected to be caused by the high number in Peclet number (Pe).

Figure 14 is the comparison of concentration between the three different diffusion coefficients. Generally, the pattern of concentration distribution looks similar to the diffusion model. However, with the additional forces added into the diffusion equation, we have a concentration distribution with faster rate. From Figure 14, we can see that the higher diffusion coefficient yields a faster diffusion advection equation. Thus, by comparing the concentration distribution of three different diffusion coefficients, we know that diffusion advection equation with the highest diffusion coefficient is the fastest.

1.4.2 Various Peclet number

Various Peclet number are assigned and the solutions are computed by PDE Toolbox. The results and analysis are discussed as below.

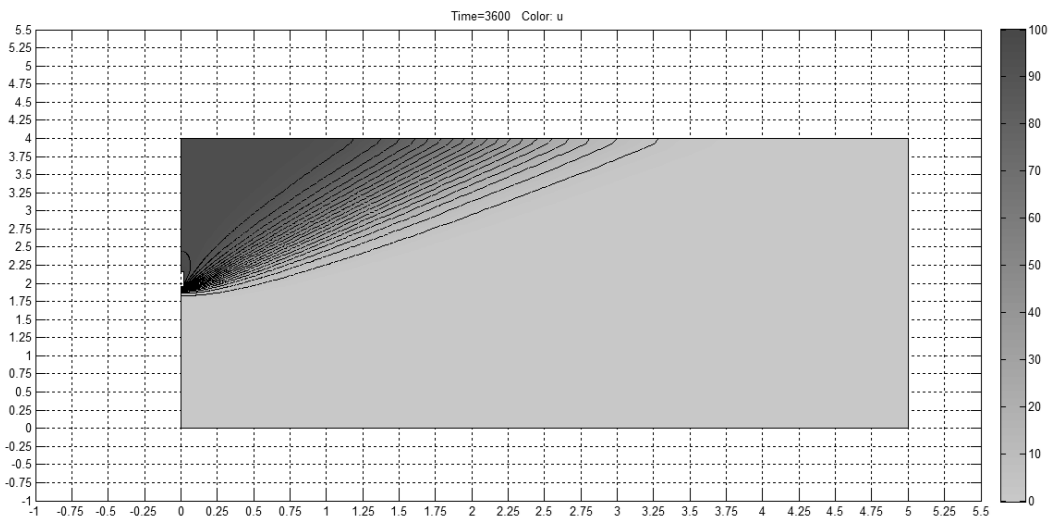


Figure 15: Concentration distribution in a closed space of width 5 m for the duration of $t = 3600\text{s}$ (one hour) with velocity, $v = 0.01 \text{ ms}^{-1}$, concentration at the inlet, $c_0 = 100 \text{ ppm}$ and diffusion coefficient, $D = 0.0005 \text{ m}^2\text{s}^{-1}$ and the Peclet number = 100.

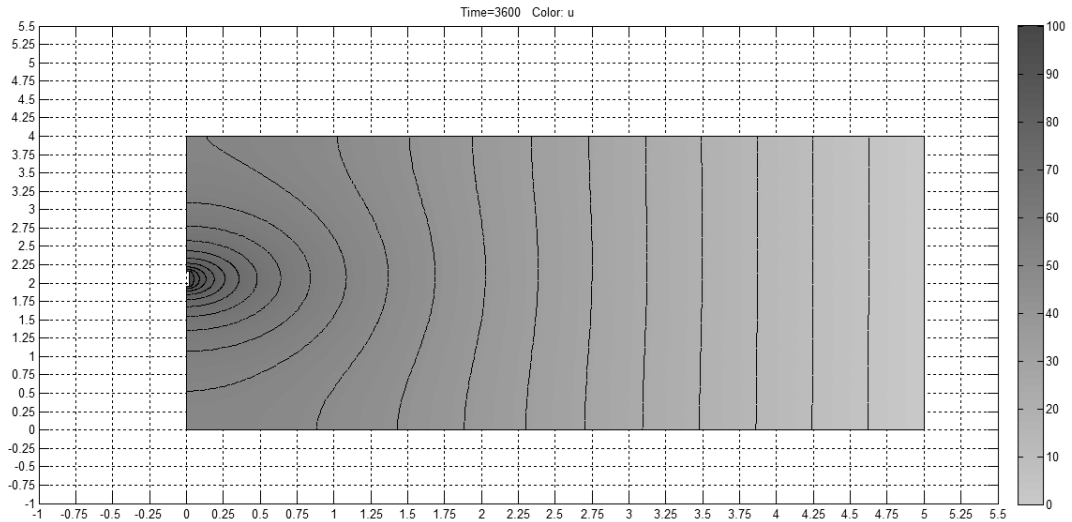


Figure 16: Concentration distribution in a closed space of width 5m for the duration of $t = 3600\text{s}$ (one hour) with velocity, $v = 0.01 \text{ ms}^{-1}$, concentration at the inlet, $c_0 = 100 \text{ ppm}$ and diffusion coefficient $D = 3 \text{ m}^2\text{s}^{-1}$ and the Peclet number = 0.01667.

As discussed in Chapter 3, the Peclet number (Pe) will influence the efficiency of the numerical scheme in solving diffusion-advection equation. Recall back, equation of Pe is

$$Pe = \frac{\mathbf{v}L}{D}.$$

If the Peclet number is smaller than 1 (i.e. $Pe < 1$), the diffusion term will dominates and advection term will be neglected [9]. This means that the concentration of substance diffuses in the solvent without the help of advection force. If the Peclet number is larger than 1 (i.e. $Pe > 1$), the advection term will dominates and diffusion term is negligible. In order to get Peclet number equal to 1 (i.e. $Pe = 1$), we have to determine the range of diffusivity and assumed that the velocity is constant in this thesis.

Figure 15 is the concentration distribution with diffusion coefficient, $D = 0.0005 \text{ m}^2\text{s}^{-1}$. By default, we have $v = 0.01 \text{ ms}^{-1}$ and $L = 5\text{m}$. So, the Peclet number for this case is

$$Pe = \frac{\mathbf{v}L}{D} = \frac{(0.01)*5}{0.0005} = 100.$$

Since the Peclet number equal to 100 which is greater than 1. Thus, in this case, the advection term dominates and diffusion is negligible. The concentration follows the advection term which is moving upwards. Recall back, advection is one way process. Thus,

this yields the positive sign of velocity and hence, the direction of the concentration moves upward.

Figure 16 is the concentration distribution with diffusion coefficient, $D = 3 \text{ m}^2\text{s}^{-1}$. We can see that the concentration distribution in Figure 16 is nearly the same with the concentration distribution in Figure 10. This is because the Peclet number for this situation is smaller than 1 which is $Pe < 1$.

$$Pe = \frac{\mathbf{v}L}{D} = \frac{(0.01) * 5}{3} = 0.01667.$$

The condition of Peclet number smaller than 1 indicates that the diffusion term dominates in this example. Since the diffusion dominates, the concentration spread in two way directions. Hence, there is no advection force to push the movement of concentration. The diffusion occurred slowly in this example.

1.5 Conclusion

Diffusion-advection process is the main mathematical equation in this thesis. We investigate the effect of different values of diffusivity on the concentration distribution. Since PDE Toolbox is the built-in software in MATLAB which can solve the partial differential equation by substituting the related parameters, we then examine the effects by changing the parameters values and study the results computed by PDE Toolbox. Understanding the behaviour of diffusion advection equation and the method to solve it helps in investigating many real applications. Unfortunately, conducting several numbers of experiments is too costly. Thus, mathematical model and computational software are used to overcome the high cost of experiments.

From the significances and objectives of this research, we prove that computational software or developed models can contribute more than the expectation. I believe that the computational tools can be further develop and for future use. So, I hope that not only one-dimensional and two-dimensional problems are illustrated in these computational tools but other higher order of partial differential equation.

1.6 References

- [1] John S. Rigden (2009). Einstein 1905: The Standard of Greatness, Harvard University Press, 49
- [2] [George Harold Godfrey](#), [Paul Allen Young](#) (1943). Soil Fumigation for Plant Disease Control. Texas Agricultural Experiment Station. 33
- [3] Tuan Nurul Atieqah binti Tuan Hassan (2014). One-dimensional fumigant distribution model in grain storage. Universiti Teknologi Malaysia: Bachelor of Science (Mathematics) Project Report.
- [4] Brajesh Kumar Jha, Neeru Adlakha and M. N. Mehta (2012). Analytic Solution of Two Dimensional Advection Diffusion Equation Arising In Cytosolic Calcium Concentration Distribution. International Mathematical Forum. Vol. 7. 135 – 144.
- [5] R. Ryon Bird, Warren E. Stewart and Edwin N. Lightfoot (2007). Transport Phenomena. 2nd Ed. Chemical and Biological Engineering Department University of Wisconsin-Madison. 513-516.
- [6] [Stanley Dunn](#), [Alkis Constantinides](#), [Prabhas V. Moghe](#) (2005). Numerical Methods in Biomedical Engineering. Academic Press. 331.
- [7] [Professor D. M. Causon](#), [Professor C. G. Mingham](#) (2010). Introductory Finite Difference Methods for PDEs. Ventus Publishing ApS. 77-79
- [8] Young W. Kwon, Hyochoong Bang (2000). The Finite Element Method using MATLAB. 2nd Ed. CRC Press. 593-594.
- [9] Marijke Huysmans, Alain Dassargues (2004). Review of the use of Péclet numbers to determine the relative importance of advection and diffusion in low permeability environments. Hydrogeology Journal Official Journal of the International Association of Hydrogeologists. 1-20.

IPHONE 6 SALES FORECASTING BY USING BASS AND LOGISTIC MODELS

Chew Siew Cheng & Prof. Zhuhaimy Ismail

1.0 INTRODUCTION

Sales forecasting is very important for companies especially in industrial fields. The performance of sales forecasting for a new product or service is one of the most difficult part and critical tasks. They need to know that how well the performance of their product is and take action whenever needed. New product forecasting has low accuracy level due to the lack of or no historical data. Yet, it is just based on the certain assumptions, such as compared to the historical data on similar product which is analogous method. The time needed to develop forecast of new product is longer because it required more manual and continuous attention.

In this study, we focus on new product demand forecasting which receives less attention among the researchers as described by Goodwin *et al.* (2011). Due to that, it is a good opportunity for doing a research in sales forecasting of a new product iPhone 6 that will be launched in September 2014. Hence, this study is carried out the sales data of iPhone 6 models and forecast the future sales based on the historical sales data of similar features iPhone 5 from year 2012 to the year 2013. In the case where limited data available of a new product, there are various types of models or mathematical approaches can be used to forecast the sales volume.

Past experiences have shown that the Bass Diffusion Model is more effective and accurate compare to other models even with insufficient previous data on the new products such as smartphone, car, electronic and so on. Other than that, Logistic Growth Model is also widely used nowadays in forecasting and it showed a good performance compare to other models as described by Bonett (1987). Therefore, we will use the Bass Diffusion Model and Logistic Growth Model to model the iPhone 6 sales and use the best model to forecast the future data. The analysis of the data will be conducted using Microsoft Excel 2010 software. Due to that, in this study we are trying to determine the better model between Bass Diffusion Model and Logistic Growth Model to forecast the future unit sales of new product.

1.1 LITERATURE REVIEW

1.1.1 Literature on Bass Diffusion Model

The Bass diffusion model was first developed by Professor Frank M. Bass in 1969 and was widely used for new product forecasting. It consists of a simple differential equation that describes the process of how new products get adopted in a population. The assumption underlying the Bass diffusion model is spread through two types of communication channels, that is mass media (external influence) and word-of-mouth (internal influence) as described by Lee et al. (2013).

This model accounts for two categories of adopters: who are generally interested in new things and the first to adopt the innovation and whose adoption decision depends on other members of the social system. According to Bass (1969), some individuals decide to adopt an innovation independently of the decisions from other individuals in a social system defined as innovators while adopters are influenced in the timing of adoption by the pressure of the social system defined as imitators. The Bass model is the most common diffusion model used in marketing and it is a mixed model capturing both innovative and imitative effects.

Forecasting demand for a mature-stage product is not a problem since enough historical sales data are available. However, forecasting the future sales of a new product that has a short history or no history at all is complicated. We can forecast the sales of iPhone 6 by using the information on similar product iPhone 5. Using financial data for the release of each innovation, the Bass Diffusion Model predicted the magnitude, time and size of peak sales with impressive accuracy as mentioned by Michael (2012). Therefore, the Bass model has significant implications for forecasting, decisions about new product viability, and product launch performance tracking by marketers.

1.1.2 Literature on Logistic Growth Model

The most widely used of the exponential growth model is the Logistic model. It was introduced by Pierre Verhulst in 1838. A Logistic function is a common "S" shape (sigmoid curve). The initial stage of growth is approximately exponential. As saturation begins, the growth will slow and at maturity stage, the growth will stop. Most biological growth follows an "S-shape" curve and decline over time. Since the adoption of technology based products is similar to biological growth, the simple Logistic model is widely used for technology forecasting. Modern literature such as Stoneman (2010) suggested that the Logistic function may be suitable for the forecasts as described by Kanjanatarakul and Suriya (2012).

Although S-curves started from studying natural ecosystems, it soon became apparent that they could be equally successful in modelling non-biological "populations" by using the same basic principles. S-curves can bring into the marketing field such as product sales, competition among products and stock prices could be approximated by using forecasting models based on Logistic Growth Model. According to Bonett (1987), a Logistic growth curve will be defined that can be used to forecast new product sale. Growth curve analysis is the most common used analysis to sales forecasting. Researcher will implement cumulative sales data of a company to the Growth curve analysis to understand the sales pattern of the products, and then only give to the company on when new products should be introduced into the market.

Logistic Growth Model models imitate life cycle of products and follows a common pattern: a period of slow growth just after introduction of new product, a period of rapid growth, slowing growth in a mature phase and decline. Growth model have its own lower and upper limit. According to Ramos (2013), Growth curve usually occurs with bounds or limitations. When the system reaches a saturation point, certain limitations will arise. There are upper limits and a maturity phase occurs in which growth slows and finally ceases. In this study, we will apply the simple Logistic S-curve due to the ease in interpreting the meaning of their parameters and the simplicity in estimating the parameters.

1.2 METHODOLOGY

1.2.1 Bass Diffusion Model

The main point in Bass Diffusion Model is about adoption and diffusion of innovative products. The derivative of $F(t)$ is the probability density function, $f(t)$ which indicates the rate at which the probability of adoption is changing at time, t . To estimate the unknown function $F(t)$, we specify the conditional likelihood $L(t)$ that a customer will adopt the innovation at exactly time t since introduction, given that the customer has not adopted before that time. Using the foregoing definition of $F(t)$ and $f(t)$, we can write $L(t)$ as (via Bayes' rule)

$$L(t) = \frac{f(t)}{1 - F(t)} \quad (1)$$

According to Bass (1969) proposed that $L(t)$ be defined to be equal to

$$L(t) = p + \frac{q}{m} Y(t) \tag{2}$$

In equation 2, $L(t)$ is the likelihood of purchase at time t given that no purchase has yet been made; p is the coefficient of innovation and q is the coefficient of imitation; m is the total number of buyers of the product. Equating the both equations 1 and 2 above, we get

$$\frac{f(t)}{1 - F(t)} = p + \frac{q}{m} Y(t) \tag{3}$$

Then, after some algebraic process, Bass (1969) shows that the number of purchasing at time t as:

$$S(t) = pm + (q - p)Y(t) - \frac{q}{m} [Y(t)]^2 \tag{4}$$

The optimal time at peak sales and the size of peak sales are obtained by taking first derivatives of the Bass model. Time at peak sales, T^* is given by:

$$T^* = \frac{\ln(\frac{q}{p})}{p + q}$$

Size of peak sales, S^* is given by:

$$S^* = \frac{m(p + q)^2}{4q}$$

The following analogues to equation 4 were then used to estimate the parameters q , p and m , which is an OLS multiple regression. In estimating the new parameters, an analogue method for sales forecasting of iPhone 6 is used equation below:

$$S(t) = a + bY(t - 1) + cY(t - 1)^2, t = 2,3,4... \tag{5}$$

We can calculate a , b , and c by using linear regression method. By comparing equation 4 and 5, we can get the formulas as below:

$$m = \frac{-b - \sqrt{b^2 - 4ac}}{2c}$$

$$p = \frac{a}{m}$$

$$q = -mc$$

Therefore, a estimates pm ; b estimates $(q-p)$; and c estimates $-q/m$. The parameters p , q , and m can be identified by using regression and ordinary least square method. We can forecast the sales data of new iPhone 6 by using the equation below:

$$S(t) = [p + \frac{q}{m} Y(t)][m - Y(t)] \tag{6}$$

1.2.2 Logistic Growth Model

Growth usually occurs with bounds or limitations. The logistic equation is an example of bounded growth which is limited by saturation with respect to time. In this study, a logistic growth curve model will be defined that can be used to forecast new product cumulative sales. A logistic growth curve model is defined as follows:

$$Y(t) = \frac{L}{(1 + Ae^{-Bt})} \quad (7)$$

where L is upper bound of $Y(t)$, A is the location of the curve and B is control the shape of the curve. To estimate the parameters for A and B , the equation 7 of the logistic growth curve model is transformed into linear function using natural logarithms.

$$y(t) = \ln\left[\frac{L}{Y(t)} - 1\right] = \ln A - Bt \quad (8)$$

Performing linear regression operation on the patent data in accordance with equation 8 will generate

$$y(t) = \ln\left[\frac{L}{Y(t)} - 1\right] \quad (9)$$

and

$$y(t) = \alpha + \beta t \quad (10)$$

The parameters for α and β are estimated by using simple linear regression. Comparing the equations of 8 and 10, we can get $A = \exp(\alpha)$ and $B = -\beta$.

Note that parameter L is a scale parameter which scales the logistic function “up and down.” Scale parameter L must be specified. If the saturation level itself is to be forecast, for example: the total number of adopters, then L must be found by trial and error. In this case, various values of L are tried in a systematic fashion until a value is found which minimizes Mean Standard Error (MSE) of the estimates. Alternatively, you can use Solver to automatically find the value for L which minimizes MSE.

1.3 MODEL ACCURACY

In this study, after we find the value of parameters in Bass Diffusion Model and Logistic Growth Model, then we calculate Mean Absolute Percentage Error (MAPE) of the out-of-sample test, Mean Absolute Error (MAE) and Mean Square Error (MSE) to evaluate the accuracy of the considered models. The accuracy of forecast values is evaluated based on the estimation of error. Consequently, if the values of measurement are small, then the fit and predicted performance is acceptable.

1.4 RESULT AND DISCUSSION

1.4.1 Comparison between Time Series

For this section, we will discuss the parameters of Bass Diffusion and Logistic Growth models by using the MAPE and R-squared. In order to evaluate the performance between Bass Diffusion Model and Logistic Growth Model, we determine the smallest value of error. This is because the smaller the error, the higher the accuracy of forecasting value. The estimation result of parameters value for iPhone 5 model is shown in Table 1.1 with different time series.

Table 1.1 The estimation of parameters for Bass Diffusion Model

Bass Model	m	p	q	R-squared	MAPE (%)
Sept,12 – Aug,13	84.5846	0.0840	0.3475	0.8857	17.03
Sept,12 – Feb,13	65.2955	0.0872	0.6087	0.8887	45.00

The historical time series data for iPhone 5 and the parameters results in Table 4.9 were used to generate the Bass model. We can see that there are different values of parameters for different time series. For Bass Diffusion Model, we do not choose the parameters for the September 2012 until February 2013 because the Mean Absolute Percentage Error (MAPE) is greater. In order to choose a good model, the range of coefficients p and q must between 0 and 1. Since the values of imitation coefficient q is greater than the value of innovation coefficient p , we choose the September 2012 until August 2013 as the best parameters.

In addition, this time series gives the reasonable parameter estimation as the MAPE is smaller compared to September 2012 until February 2013. Fitting MAPE of Bass model for September 2012 until August 2013 predicted data is 17.03% where the model fitting performance is considered good. Besides that, the market potential, m exceeds first purchase and R-squared value is 89% describe that the growth rate from September 2012 until August 2013 quite well. Therefore, parameter estimation results from September 2012 until August 2013 were used in forecasting of iPhone 6.

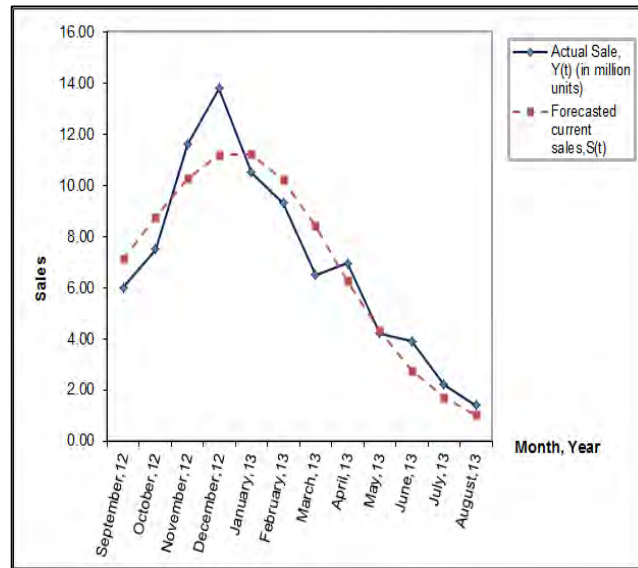


Figure 1.1 Current sales and sales predicted for Bass model

Figure 1.1 shows that the diffusion pattern of iPhone 5 from September 2012 until August 2013 by using Bass Diffusion Model. As we can observe from the figure, the predicted curve describes that the sales data increase dramatically until January 2013 and started gradually as the market gets saturated. Since the inflection point of the Bass Diffusion Model occurs in January 2013, the forecasting peak sale was reached about one month later than the actual sales. This is because when the potential market, m changes, the maximum peak sales of the product will also change.

Table 1.2 The estimation of parameters for Logistic Growth Model

Logistic Model	L	A	B	R-squared	MAPE (%)
Sept,12 – Aug,13	86.2910	11.2970	0.4554	0.9632	34.15
Sept,12 – Feb,13	56.9591	35.3157	1.1230	0.9629	56.44

For Logistic Growth Model, we also choose the best parameters from September 2012 until August 2013. This is because the R-squared value is higher compared to September 2012 until February 2013 which is 96.32%. It means that the growth rate of predicted value is quite good.

In order to choose a suitable model, the MAPE must be small. Fitting MAPE of Logistic model to September 2012 until August 2013 predicted data is 34.15%. This means that the model fitting performance is considered reasonable forecasting. Therefore, the time

series from September 2012 until February 2013 is not suitable due to large value of Mean Absolute Percentage Error (MAPE). Furthermore, the upper bound of Logistic model, L were equivalent to the potential market, m of Bass model exceeds the first purchase. As a result, the parameter estimation result from September 2012 until August 2013 was suitable used in forecasting of iPhone 6.

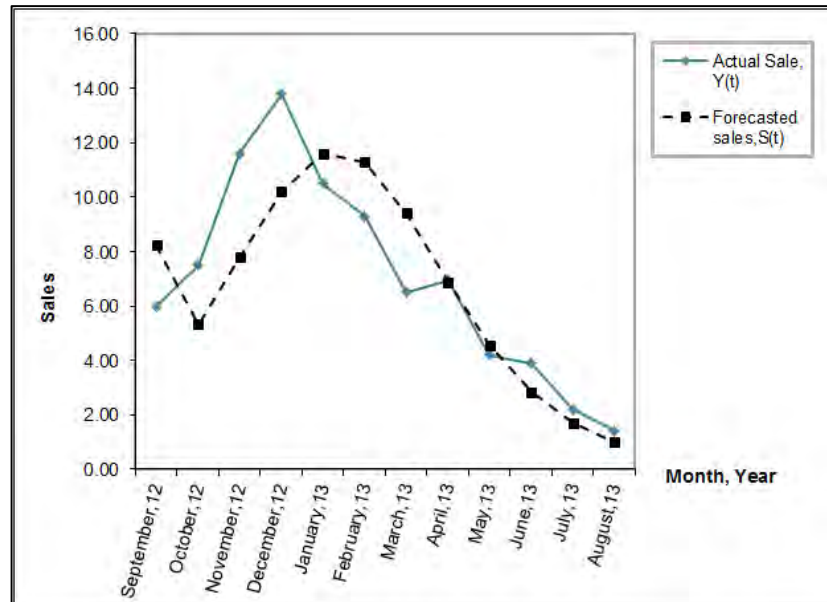


Figure 1.2 Current sales and sales predicted for Logistic model

Figure 1.2 indicate that the diffusion pattern of iPhone 5 from September 2012 until August 2013 by using Logistic Growth Model. As shown in figure above, the predicted curve describes that it will increase until January 2013 and started gradually as the market gets saturated. Since the maximum sale of the Bass Diffusion Model occurs in January 2013, therefore the forecasting peak point is reached about one month later than actual sales. However, the forecasted sales by Logistic model is said to be underestimating from the actual sales of iPhone 5.

1.4.2 Comparison between Bass and Logistic model

Now, we are comparing the predicted value for both of the models with one month sale data of iPhone 6. In this section, we will evaluate the forecast performance by determine the MAE, MSE and MAPE value. Assume that there are only one month data for iPhone 6, then we use the first month sale to calculate the different types of error. As we know that, the smaller the value of error, the better the forecasting model. The actual sales of iPhone 6 and forecasted value for both models are shown in the figure below.

Table 1.3 Forecast error for Bass Diffusion and Logistic Growth model

Type	Bass model	Logistic model
MAE	0.1086	1.2339

MSE 0.0118 1.5226

MAPE (%) 1.55 17.63

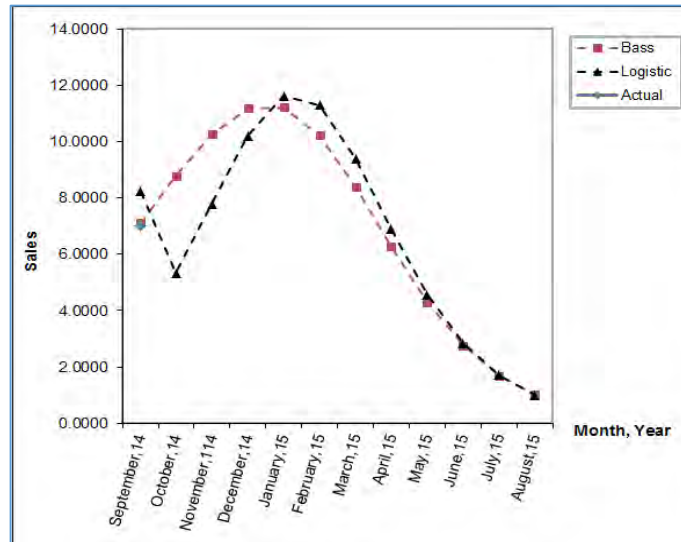


Figure 1.3 Actual sales of iPhone 6, forecasted value for Bass and Logistic model

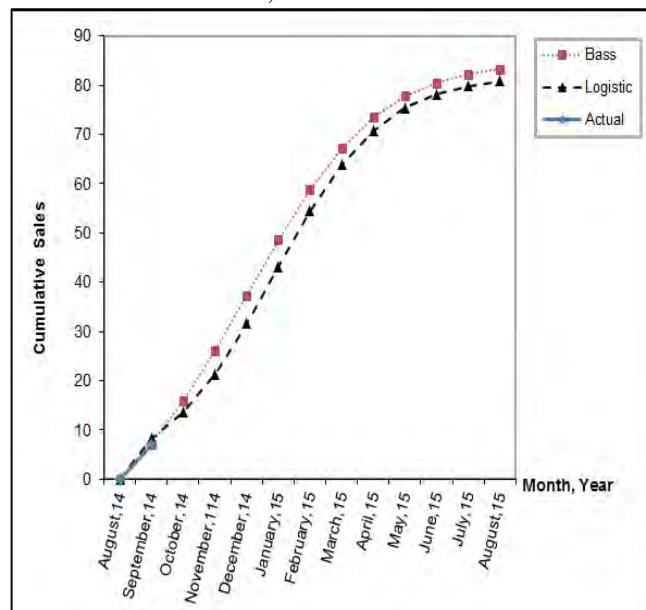


Figure 1.4 Cumulative sales of iPhone 6 and forecasted value for Bass and Logistic model

Figure 1.3 and Figure 1.4 show that forecasting result for iPhone 6 from Bass Diffusion Model are more accurate than Logistic Growth Model. As we can see from the graph, it indicates that actual data and predicted data for iPhone 6 by using Bass Diffusion Model are quite similar, which the product will increase and get saturated as it reached the maximum sales. Furthermore, the cumulative diffusion pattern by using Bass model illustrates S-shape curve in productivity growth is strong fitted compared to Logistic model.

This finding is supported by MAE, MSE and MAPE. It is observed that the value of MAE for Bass model is less than the MAE of Logistic model which is 0.1086 and 1.2339 respectively. Similarly, the values of MSE also give smaller error compared to Logistic model. Other than that, the MAPE indicates that the forecasted value of Bass model is smaller from the actual number approximately 1.55% compared with 17.63%. Therefore, the prediction capability levels of MAPE considered highly forecasting. As a result, the smaller the error, the better the model to be chooses. Finally, we choose the parameters of Bass Diffusion Model to forecast the sales data of iPhone 6.

1.4.3 New Product Forecasting Analysis

As we conclude that the Bass Diffusion Model is the best model for sales forecasting compared to Logistic Growth Model, therefore, the Bass model is chosen to forecast the sales of new iPhone 6 by using the OLS method. Bass model is widely used in forecasting new product. Since there are limited historical data available for iPhone 6, method of analogy was used to forecast the demand of iPhone users. By using the parameters $m = 84.5846$, $p = 0.0840$ and $q = 0.3475$, forecast the sales of iPhone 6 from September 2014 until September 2015. The result of predicted values is shown in the table below.

Based on the parameters value, we can calculate peak sales:

$$S(t)^* = \frac{85.5846(0.0840 + 0.3475)^2}{4(0.3475)}$$

$$= 11.3319 \text{ million}$$

and the time of peak sales:

$$T^* = \frac{\ln\left(\frac{0.3475}{0.0840}\right)}{0.0840 + 0.3475}$$

$$= 3.29$$

$$\square\square\square\square\square \approx 4$$

This shows that the peak sales of the iPhone 6 will reach around 11.33 million, while time of peak sales will occur approximately in the 4th month after the product was launched on September 2014. This result is presented in the form of graph as in Figure 1.5 and Figure 1.6 respectively.

Table 1.4 Sales for parameters in million units

Month	Actual Sales, S(t)	Cumulative Sales, Y(t)	Forecasted current sales, S(t)	Forecasted cumulative sales, S(t-1)
September 2014	7.000	7.000	7.1086	7.1086
October 2014			8.7737	15.8823

	10.2563	26.1386
November 2014	11.1877	37.3263
December 2014	11.2181	48.5443
January 2015	10.2160	58.7603
February 2015	8.4039	67.1643
March 2015	6.2705	73.4347
April 2015	4.3006	77.7353
May 2015	2.7628	80.4982
June 2015	1.6947	82.1929
July 2015	1.0085	83.2014
August 2015	0.5890	83.7904
September 2015		

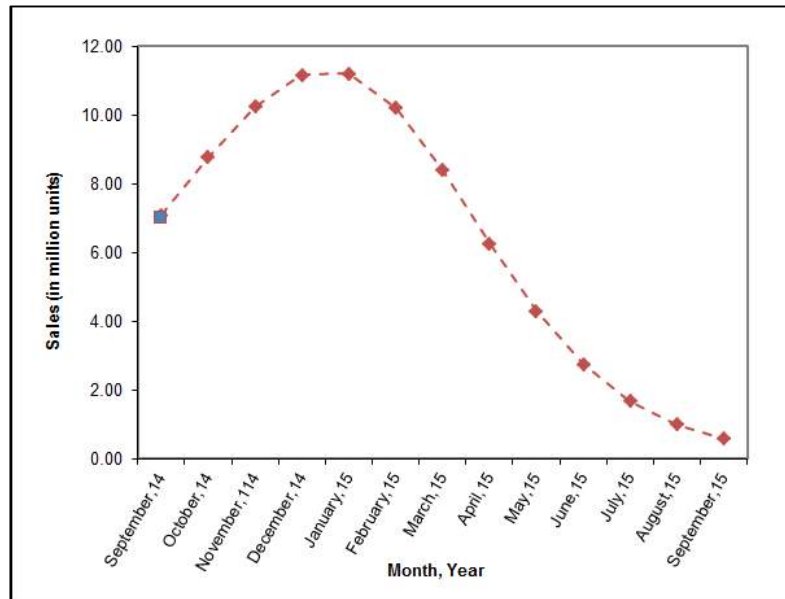


Figure 1.5 Forecasting sales of iPhone 6

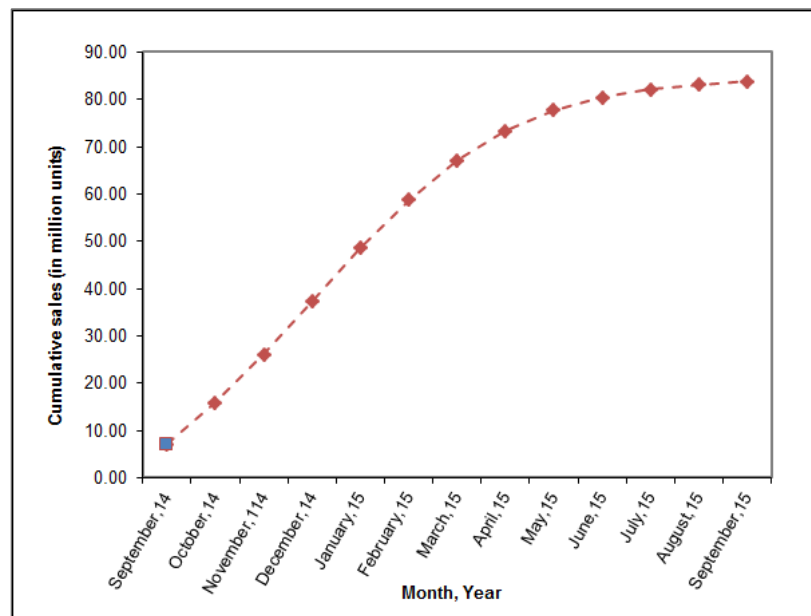


Figure 1.6 Forecasting cumulative sales of iPhone 6

Figure 1.5 and 1.6 give the forecasting results obtained for cumulative sales and current sales of iPhone 6 using Bass Diffusion Model respectively. From the observation, we can see that the predicted sales of iPhone 6 using Bass Diffusion Model will achieve the maximum point at month January 2015 and then drops gradually as the market saturated. This figure indicates that after the iPhone 6 was launched in September 2014, the sales increase every month. Then, the sales will slowly drop until September 2015 because its reach saturated state. While the cumulative sales of maximum point are assumed to be reach around 90 million. In conclusion, both of the graphs show that the pattern of the adoption for forecasting results on new product follows the Bass model diffusion process.

1.4 CONCLUSION

As a conclusion, this study compares the fit and prediction performance of the Bass Diffusion Model and Logistic Growth Model for sales forecasting of a new product. We

discuss the selection of parameter estimation method and selection of different value of potential market. Even though there are no historical data available for iPhone 6, we have to prove that both of the models can be applied in sales forecast. By comparing the accuracy of both models, choose the best model to forecast the sales data of iPhone 6 from September 2014 until September 2015.

Based on Mean Absolute Percentage Error (MAPE), we can conclude that the most suitable model for forecasting new product diffusion with limited historical data is Bass Diffusion Model. In this study, we study the diffusion pattern and estimate the parameters of analogous product by using Ordinary Least Square (OLS) method. From regression analysis, the diffusion of iPhone 5 from September 2012 until August 2013 for Bass Diffusion Model describe growth pattern accurately and successful because of parameters were estimated very well. The result shows that after iPhone 6 was launched, the number of adopters increases every year and reach its maximum sales on 4th month. Then, the sales drop slowly as the market saturated. At this point, the company will take actions to maintain their sales performance as demand go down.

Sales forecasting of a new product plays an important role in a firm. Therefore, the sales forecast is a best tool to get a good estimate of the demand for the new products that sell. This finding can help business companies to manage their strategies on developing some plans when the sales go down. In order to increase the sales volume of product, company have to lower the marketing price, do more advertisement, giving out free samples and so on. It is important to use a solution that is appropriate to the situation the business faces.

1.5 RECOMMENDATIONS

In Bass Diffusion Model, further research can be done by using different parameters of m , p and q . In this study, two main factors were considered namely the innovators, p and the imitators, q . Further works can be done to include other factors such as pricing, advertising, product knowledge and others. In the area of parameter estimations, other methods may able to be used such as maximum likelihood, non-linear regression, genetic algorithm and so on.

There are few limiting factors in this study that could be resolved in further studies. The external factors such as population changes, direct and indirect competition, styles or fashions may affect the sales forecasting. Therefore, the external factors which may influence demand for new product will consider in our future research. At last, more complex model like Grey Model (GM) can be used and compare to the result of this study, so that a better model in forecasting monthly sales data of iPhone 6 in million units can be determined.

REFERENCES

- Bass, F. M. (1969). A new product growth for model consumer durables. *Journal of Management Science*. Vol. 15, No. 5, 215-227.
- Bonett, D. G., (1987). New product sales forecasting using a growth curve model. *Journal of Applied Business Research*.
- Mahajan, V., and Wind, Y. (1988). New product forecasting models. *International Journal of Forecasting*. 4, 341-358.
- Golder, P. N., and Tellis, G. J. (1998). Beyond diffusion: An affordability model of the growth of new consumer durables. *Journal of Forecasting*. 17, 259-280.

- Ismail, Z., and Abu, N. (2013). A study on new product demand forecasting based on Bass diffusion model. *Journal of Mathematics and Statistics*. Vol. 9, No. 2, 84-90.
- Lee, H., Kim, S. G., Park, H., and Kang, P.(2014). Pre-launch new product demand forecasting using the Bass model. *Journal of Science and Technology*. 86, 49-64.
- Michael H. (2012). A Bass Diffusion Model Analysis: Understanding Alternative Fuel Vehicle Sales. CMC Senior Theses. Paper 399.
- Ramos, R. A. (2013). Logistic function as a forecasting model. *Journal of Engineering and Applied Sciences*. Vol. 2, No. 3.
- Kanjanatarakul, O., and Suriya, K. (2012). Comparison of sales forecasting models for an innovative agro-industrial product. *Journal of Economics*. Vol. 1, No. 4, 89-106.
- Kanjanatarakul, O., and Suriya, K. (2013). Forecasting the sales of an innovative agro-industrial product with limited data. *Journal of Intelligent Technologies and Applied Statistics* 6.
- Lin, C. -S. (2013). Forecasting and analyzing the competitive diffusion of mobile cellular broadband and fixed broadband in Taiwan with limited historical data. *Journal of Economic Modelling*. 35, 207-213.
- Satoh, D. (2001). A discrete Bass Model and its parameter estimation. *Journal of the Operations Research*. Vol. 44, No. 1.
- Naseri, M. B., and Elliott, G. (2013). The diffusion of online shopping in Australia: Comparing the Bass, Logistic and Gompertz growth models. *Journal of Marketing Analytics*. Vol. 1, 1, 49-60.
- Liu, C. -Y., and Wang, J. -C. (2010). Forecasting the development of the biped robot walking technique in Japan through S-curve model analysis. No. 82, 21-36.
- Lim, J., Nam, C., Kim, S., Rhee, H., Lee, E., and Lee, H. (2012). Forecasting 3G mobile subscription in China. *Journal of Telecommunications Policy*. 36, 858-871.
- Goodwin, P., Dyussekeneva K., and Meeran S. (2011). The use of analogies in forecasting the annual sales of new electronics products. *Journal of Management Mathematics*. No. 1-16.
- Markovic, D., and Jukic D. (2013). On parameter estimation in the Bass Model by nonlinear least squares fitting the adoption curve. *Journal of Applied Mathematics*. Vol. 23, No. 1, 145-155.

EXACT SOLUTIONS OF THE KORTEWEG de VRIES EQUATION

Assoc. Prof. Dr. Ong Chee Tiong And Chong Juhn Yung

ABSTRACT

Soliton is a solitary wave that maintains its shape when it propagates at a constant speed due to its wave and particle properties. Korteweg-de-Vries (KdV) equation is a non-linear partial differential equation that models the wave propagation in shallow water waves that exhibit solitons solution. In this research, the analytical solution of KdV equation will be focus on one, two and three solitons solutions. Hirota Bilinear method was used to obtain these analytical solutions. Maple 18 was invoked to generate various graphical outputs of 2-D, 3-D and various animations of solitons interactions.

Keywords : Soliton, KdV equation, Hirota Bilinear Method, Maple 18

Panel : Applied Mathematics

Introduction

The first recorded solitary wave was observed in the 1834 when a young engineer named John Scott Russell was hired for a summer job to investigate how to improve the efficiency of designs for barges that were designated to ply canals—particularly the Union Canal near Edinburgh, Scotland. One August day, the tow rope that was connecting the mules to the barge broke and the barge suddenly stopped—but the mass of water in front of its blunt prow "... rolled forward with great velocity, assuming the form of a large solitary elevation, a rounded, smooth and well defined heap of water, which continued its course along the channel without change of form or diminution of speed."

Russell pursued this serendipitous observation and "... followed it on horseback, and overtook it still rolling on at a rate of some eight or nine miles per hour, preserving its original form some thirty feet long and a foot to a foot and a half in height."

He then conducted controlled laboratory experiments using a wave tank and quantified the phenomenon in an 1844 publication. He demonstrated four facts:

1. The solitary waves that he observed had a hyperbolic secant shape.
2. A sufficiently large initial mass of water can produce two or more independent near-solitary waves that separate in time.
3. Solitary waves can cross each other "without change of any kind".
4. In a shallow water channel of height h , a solitary wave of amplitude A travels at a speed of $[g(A+h)]^{1/2}$, where g is the gravitational acceleration. That is, larger-amplitude waves move faster than smaller ones—a nonlinear effect.

A **solitary wave** is a localized "wave of translation" that arises from a balance between nonlinear and dispersive effects. In most types of solitary waves, the pulse width depends on the amplitude. A **soliton** is a solitary wave that behaves like a "particle", in that it satisfies the following conditions:

1. It must maintain its shape when it moves at constant speed.
2. When a soliton interacts with another soliton, it emerges from the "collision" unchanged except possibly for a phase shift.

Literature Review

In fact, soliton theory lay dormant until the appearance of the important paper by Korteweg and deVries in 1895, in which the KdV equation first appeared as a model for shallow water waves in weakly dispersive media, that one have one solution to KdV describes an invariant, hump like wave travelling at constant speed. But it wasn't until Zabusky and Kruskal published a paper in 1965, that the full potential of soliton theory began to emerge. Working numerically on the Fermi-Pasta-Ulam problem, in which a system of $N-1$ identical masses are connected in a 1-dimensional lattice with N connecting springs, Zabusky and Kruskal recovered the KdV equation. They found (numerically) that KdV solitary waves could be shown to remain shape invariant upon interaction, undergoing only a

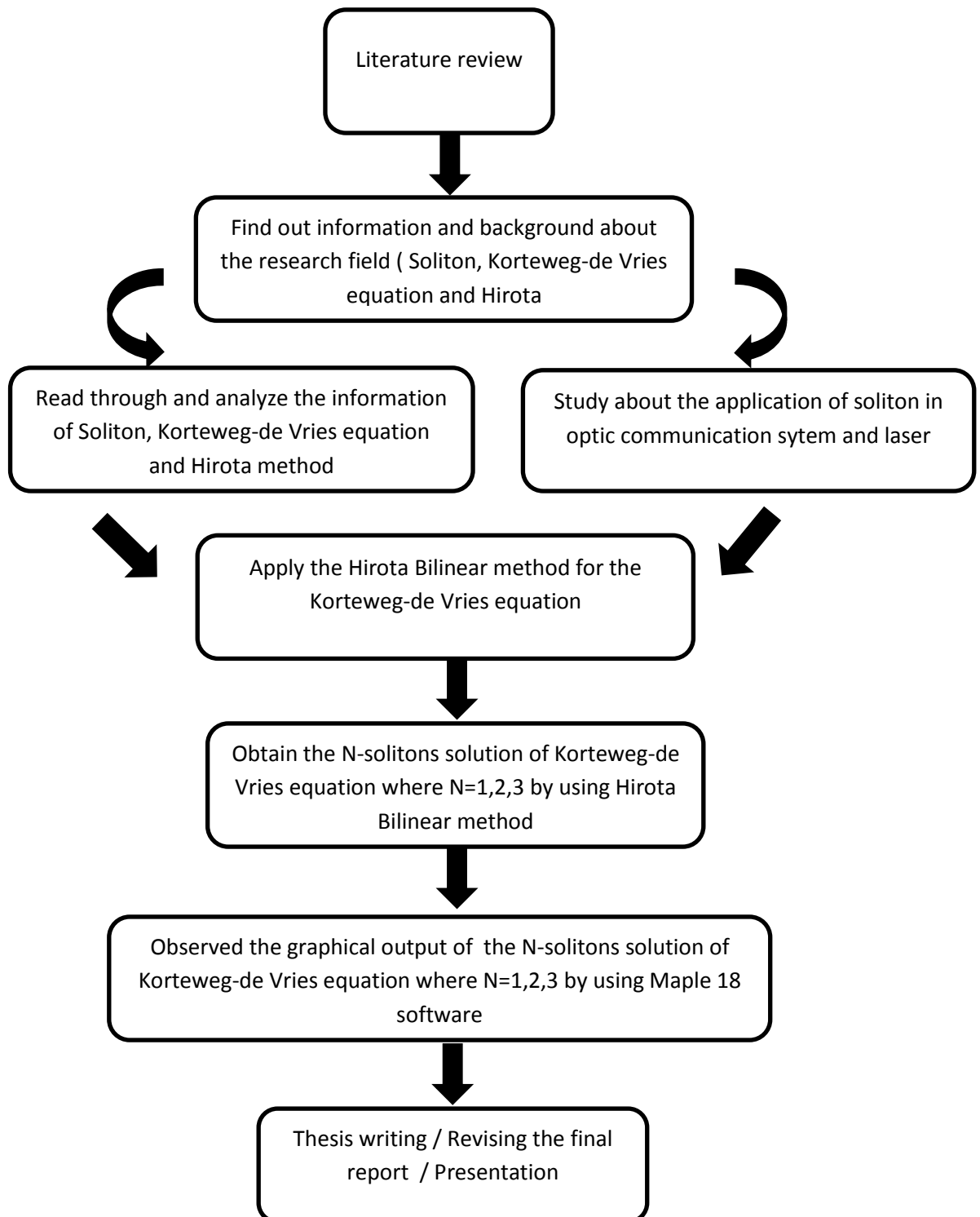
phase shift and interacting elastically. Since this behavior is more reminiscent of particle collisions than of wave interactions, Zabusky and Kruskal coined the word soliton, whose suffix on highlights the particle like nature of a solitary wave.

The Zabusky and Kruskal discovery had revived the study of the solitary wave. A seminal series of papers by Gardiner et al in 1967 paved the way for the inverse scattering transform to be developed. This technique finally showed that an analytical solution was possible for solitons. Zabusky and Kruskal had investigated the invariance properties of solitons numerically, but a slither of doubt had remained, as small oscillations appeared in the results. Without an analytical solution, they had been unable to tell if these oscillations were due to numerical error or instability, or if they were a property inherent in the solution itself. The inverse scattering transform finally put the question of soliton invariance firmly to rest, showing that solitons remain shape invariant as they travel, and interact elastically after a collision. In 1972 soliton theory had its big break, when Zakharov and Shabat showed that inverse scattering could be generalised to other soliton equations, not just the KdV equation.

Today, soliton theory has multiple applications in physics, in areas such as plasma physics and non-linear optics. Due to their invariance properties, solitons are of great potential use in light wave communication technology. Solitons can be observed in the ocean, often in the narrow Strait of Gibraltar. Solitons are also created in the atmosphere, forming cloud rolls called Morning Glory - and also in tidal bores, where they form solitary waves.

In general solitons may propagate in many different media, ranging from infinitesimal, to meteorological and astrophysical. There are certain conditions in space in which quarks may form a soliton. Other theories predict that solitons are related to movements at the center of a massive star, and can even be as large as several light years across. Boojums, compactons, fluxons, kinks, antikinks, and twists are other names for types of solitons predicted in everything from supercooled fluids to empty space.

Methodology



Result And Discussion

Exact Solution to the KdV Equation

$$y = \frac{3\beta}{\alpha} \left[\operatorname{sech}^2 \left(\frac{1}{2} \sqrt{\frac{\beta}{\gamma}} (x - \beta t) \right) \right]$$

Let $\alpha, \beta, \gamma > 0$

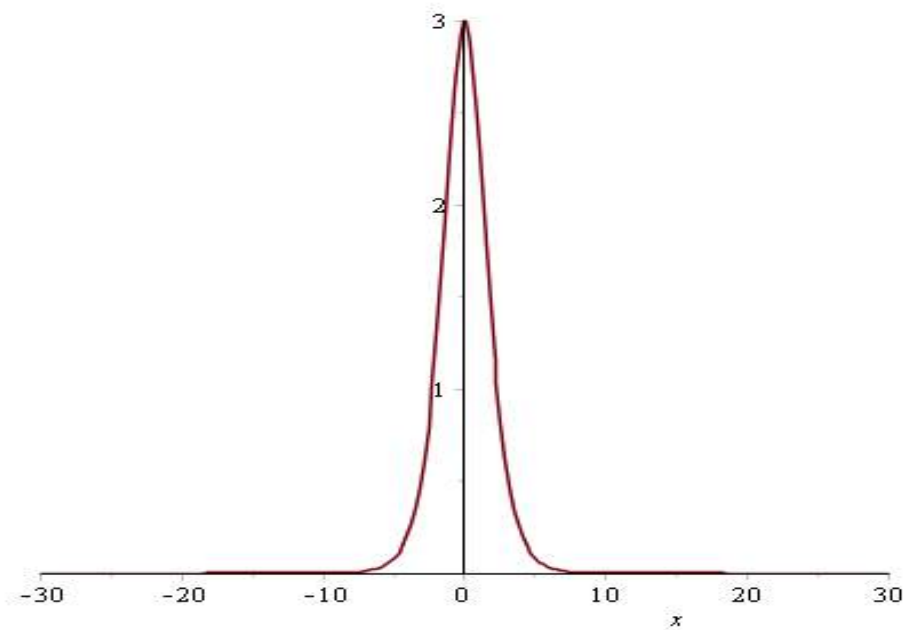


Figure 1 :Graphical output when $\alpha, \beta, \gamma = 10$

a. $\beta_1 \neq \beta_2$

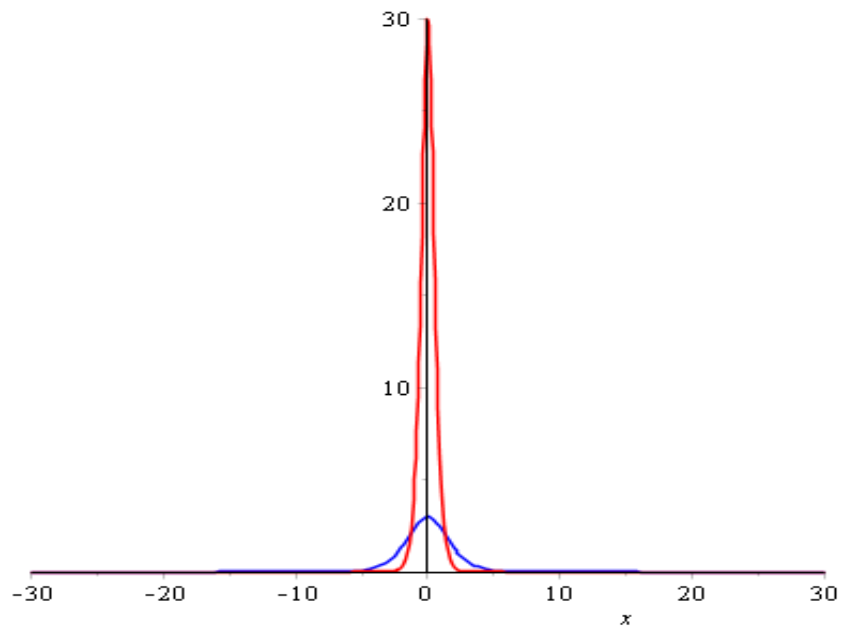


Figure 2 :e) Red represent $\beta_1 = 100$ Blue represent $\beta_2 = 10$

b. $\gamma_1 \neq \gamma_2$

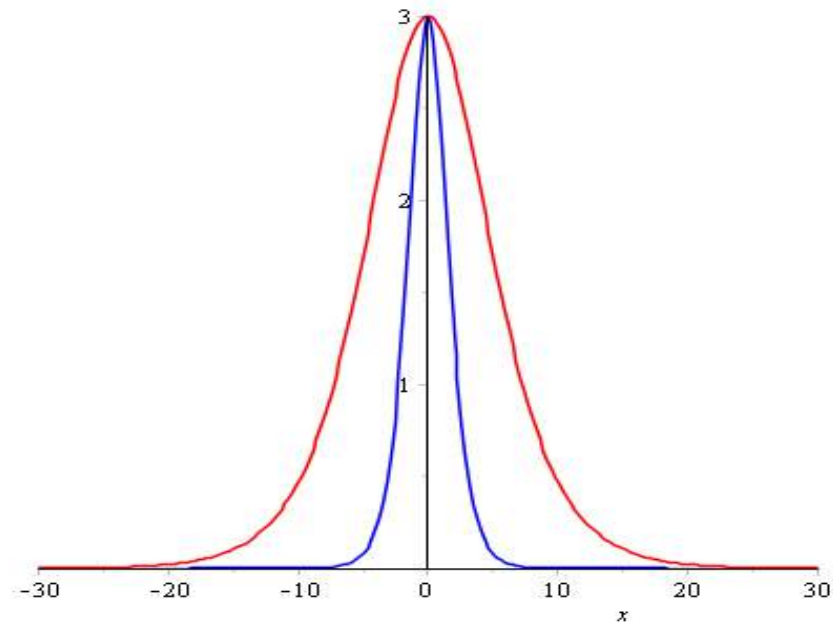


Figure 3 :f) Red represent $\gamma_1 = 100$ Blue represent $\gamma_2 = 10$

From the figure 2, there were two curve with different in colours. The graphical output shows value of $\beta_1 = 100 > \beta_2 = 10$, whereas β_1 in red colour and β_2 in blue colour. In

figure 3, there were two curve in the graphical output with different values of γ . The graphical output shows value of $\gamma_1 = 100 > \gamma_2 = 10$, whereas γ_1 in red colour and γ_2 in blue colour.

Conclusion

Recall the equation,

$$u_t + u u_x = 0.$$

The value of the β is controlling the nonlinearity of the wave which mean the power of the energy of the wave. The larger the value of the β , the larger the amplitude are. This also means that the stronger the energy of the wave are.

Second, the size of the wave is depend of the value of the γ , we can observed from the figure 3.3, 3.6, 3.9 and 3.12. All these figures show two curves with different sizes as $\gamma_1 = \pm 100, \gamma_2 = \pm 10$

Recall the equation

$$u_t + u_{xxx} = 0.$$

The value of the γ is controlling the dispersion of the wave which mean the wave of different wavelengths travel at different phase speed. The larger the value of the γ , the larger the wavelengths and the faster the speed are. This means that the wave will propagate faster

Whereas the value of the α , represent the constant in the equation.

References

- [1] AsliPekean, "THE HIROTA DIRECT METHOD" M.S. in Mathematics, July 2005
- [2] Jose de Jesus Martinez, "An introduction to the Hirota bilinear" Department of Mathematics, Kobe University, Rokko, Kobe 657-8501, Japan
- [3] Klaus Brauer, "The Korteweg de Vries Equation: History, exact solutions and graphical" 25 Feb 2014
- [4] Raphael Cote, Yvan Martel, Frank Merle, "Construction of multi solitons solutions" 4 May 2009
- [5] J. Hietarinta, "Introduction to the Hirota bilinear method" 14 Aug 1997
- [6] Richard S. Palais, "An Introduction to Wave Equations and Solitons" The Morningside Center of Mathematics Chinese Academy of Sciences Beijing Summer 2000

THE n^{th} COMMUTATIVITY DEGREE OF SOME NONABELIAN 2-GROUPS WITH A CYCLIC SUBGROUP OF INDEX FOUR

Fadhilah binti Abu Bakar & Nor Muhainiah Mohd Ali

Abstract

Suppose a and b are elements of a group G . Then by considering the total number of pair (a, b) for which a and b commute and then divide by the total number of pair of (a, b) which is possible. Thus the result will give the commutativity degree of a group G . Then, by considering the total number of pair (a, b) for which a^n and b commute and then divide by the total number of pair of (a, b) which is possible, thus the result is said to be the n^{th} commutativity degree of a group G . The commutativity degree of some nonabelian 2-groups with a cyclic subgroup of index four has been determined in 2015. The aim of this study is to find the n^{th} commutativity degree of the nonabelian 2-groups with a cyclic subgroup of index four of order 16. Method that has been used to calculate the n^{th} commutativity degree of those groups is by using formula involving Cayley Table and 0-1 Table.

Keywords: n^{th} commutativity degree and nonabelian 2-groups

Introduction

Probabilistic theory is the branch of mathematics concerned with probability and the analysis of random phenomena. Recently, probabilistic theory shown up to be useful in the solution of some difficult tasks in group theory.

Previously, the commutativity degree of nonabelian 2-group with a cyclic subgroup of index four of order 16 have been done. Extended to that, in this research study, we are trying to find the n^{th} commutativity degree of nonabelian 2-groups with a cyclic subgroup of index four of order 16. The objectives of this research are to examine the basic properties of some nonabelian 2-groups with a cyclic subgroup of index four and to determine the n^{th} commutativity degree of nonabelian 2-groups with a cyclic subgroup of index four of order 16. The scope of study will consider the n^{th} commutativity degree for nonabelian 2-groups with a cyclic subgroup of index four of order 16.

Literature Review

A group G is called abelian if any two elements in G with binary operation $*$ commute that is, $a*b = a*b$ for all a, b in G . However, not all groups are abelian, in which they are called nonabelian groups.

Erdos and Turan [1] have introduced the idea of computing the commutativity degree of a group, $P(G)$ in 1968, that is

$$P(G) = \frac{\text{Total number of ordered pairs } (a, b) \in G \times G \text{ s.t. } ab = ba}{\text{Total number of ordered pairs } (a, b) \in G \times G}$$

$$= \frac{|\{(a, b) \in G \times G \mid ab = ba\}|}{|G|^2}.$$

Previously, the n^{th} commutativity degree of dihedral groups up to degree 12 has been done by Yahya [2]. The idea of that n^{th} commutativity degree is also being considered in this report.

Mohammed Hussein Salleh [3] in 2014 determined the commutativity degree of some nonabelian 2-groups with a cyclic subgroup of index four. Therefore, by using the results obtained, the n^{th} commutativity degree of a group, $P_n(G)$ for nonabelian 2-groups with a cyclic subgroup of index four of order 16 are determined in this research. The n^{th} commutativity degree of a group, $P_n(G)$ is defined as [4],

$$P_n(G) = \frac{|\{(x, y) \in G \times G \mid x^n y = yx^n\}|}{|G|^2}.$$

Definitions of Terms

Definition 2.1 [5] Cayley Table

Cayley table (or operation table) of a finite group is a table with rows and columns labelled by the elements of the group and the entry ab in the row labelled by a and column labelled by b .

Definition 2.2 [6] 0-1 Table

A 0-1 table is a table containing 0's and 1's only where $\forall x, y \in G$ if $xy = yx$, both corresponding cells are placed with 1 and if $xy \neq yx$, both corresponding cells are placed with 0.

Definition 2.3 [7] Group Presentation

A group can be presented by giving a set of generators for the group and certain equations or relations that the generators satisfy written as follows:

$G = \langle g_1, g_2, \dots, g_n \mid r_1 = r_2 = \dots = r_j = e \rangle$ where g_i are the generators with $i = 1, 2, \dots, n$ and r_j are the relations with $j = 1, 2, \dots, t$.

Definition 2.4 [7] Internal Direct Product

Let H and K be two normal subgroups of a group G . We say that G is the internal direct product of H and K where $G = H \times K$ if

1. $G = HK$,
2. $hk = kh; \forall h \in H, k \in K$,
3. $H \cap K = \{e\}$.

Definition 2.7 [8] Cyclic Subgroup

Let $a \in G$. Then

$$\langle a \rangle = \{a^n \mid n \in \mathbf{Z}\} = \{\dots, a^{-3}, a^{-2}, a^{-1}, e, a, a^2, a^3, \dots\}$$

is called a cyclic subgroup of G generated by a .

Definition 2.8 [8] Center of Group, $Z(G)$

The center, $Z(G)$ of a group is the set of elements in G that commute with every element of G . In symbols,

$$Z(G) = \{a \in G \mid ax = xa \text{ for all } x \text{ in } G\}.$$

Theorem 2.1 [9]

Let $m \geq 4$. The finite nonabelian groups of order 2^m which have a cyclic subgroup of index four, but haven't a cyclic subgroup of index two are categorized in the following types:

I. $m \geq 4$:

$$G_1 = \langle a, b : a^{2^{m-2}} = 1, b^4 = 1, b^{-1}ab = a^{1+2^{m-3}} \rangle; \tag{2.1}$$

$$G_2 = \langle a, b, c : a^{2^{m-2}} = c^2 = 1, a^2 = b^2, b^{-1}ab = a^{-1}, ac = ca, bc = cb \rangle; \tag{2.2}$$

$$G_3 = \langle a, b, c : a^{2^{m-2}} = b^2 = c^2, b^{-1}ab = a^{-1}, ac = ca, bc = cb \rangle; \tag{2.3}$$

$$G_4 = \langle a, b, c : a^{2^{m-2}} = 1, b^2 = 1, c^2 = 1, ab = ba, ac = ca, c^{-1}ac = a^{2^{m-3}} \rangle; \tag{2.4}$$

$$G_5 = \langle a, b, c : a^{2^{m-2}} = 1, b^2 = 1, c^2 = 1, ab = ba, c^{-1}ac = ab, bc = cb \rangle; \tag{2.5}$$

Results and Discussion

In this section, the results of $P_n(G_k)$, that is the n^{th} commutativity degree of some nonabelian 2-group with a cyclic subgroup of index four of order 16 are determined using 0-1 Table.

G_1 is the nonabelian 2-group with a cyclic subgroup of index four of order 16 of Type (2.1) as stated in Theorem 2.1 which is:

$$G_1 = \langle a, b : a^4 = 1, b^4 = 1, b^{-1}ab = a^3 \rangle .$$

Thus, $G_1 = \{e, a, a^2, a^3, b, ab, a^2b, a^3b, b^2, ab^2, a^2b^2, a^3b^2, b^3, ab^3, a^2b^3, a^3b^3\}$.

The Cayley table of G_1 is given in the following:

Table 3.1: Cayley Table for G_1

*	e	a	a^2	a^3	b	ab	a^2b	a^3b	b^2	ab^2	a^2b^2	a^3b^2	b^3	ab^3	a^2b^3	a^3b^3
e	e	a	a^2	a^3	b	ab	a^2b	a^3b	b^2	ab^2	a^2b^2	a^3b^2	b^3	ab^3	a^2b^3	a^3b^3
a	a	a^2	a^3	e	ab	a^2b	a^3b	b	ab^2	a^2b^2	a^3b^2	b^2	ab^3	a^2b^3	a^3b^3	b^3
a^2	a^2	a^3	e	a	a^2b	a^3b	b	ab	a^2b^2	a^3b^2	b^2	ab^2	a^2b^3	a^3b^3	b^3	ab^3
a^3	a^3	e	a	a^2	a^3b	b	ab	a^2b	a^3b^2	b^2	ab^2	a^2b^2	a^3b^3	b^3	ab^3	a^2b^3
b	b	a^3b	a^2b	ab	b^2	a^3b^2	a^2b^2	ab^2	b^3	a^3b^3	a^2b^3	ab^3	e	a^3	a^2	a
ab	ab	b	a^3b	a^2b	ab^2	b^2	a^3b^2	a^2b^2	ab^3	b^3	a^3b^3	a^2b^3	a	e	a^3	a^2
a^2b	a^2b	ab	b	a^3b	a^2b^2	ab^2	b^2	a^3b^2	a^2b^3	ab^3	b^3	a^3b^3	a^2	a	e	a^3
a^3b	a^3b	a^2b	ab	b	a^3b^2	a^2b^2	ab^2	b^2	a^3b^3	a^2b^3	ab^3	b^3	a^3	a^2	a	e
b^2	b^2	ab^2	a^2b^2	a^3b^2	b^3	ab^3	a^2b^3	a^3b^3	e	a	a^2	a^3	b	ab	a^2b	a^3b
ab^2	ab^2	a^2b^2	a^3b^2	b^2	ab^3	a^2b^3	a^3b^3	b^3	a	a^2	a^3	e	ab	a^2b	a^3b	b
a^2b^2	a^2b^2	a^3b^2	b^2	ab^2	a^2b^3	a^3b^3	b^3	ab^3	a^2	a^3	e	a	a^2b	a^3b	b	ab
a^3b^2	a^3b^2	b^2	ab^2	a^2b^2	a^3b^3	b^3	ab^3	a^2b^3	a^3	e	a	a^2	a^3b	b	ab	a^2b
b^3	b^3	a^3b^3	a^2b^3	ab^3	e	a^3	a^2	a	b	a^3b	a^2b	ab	b^2	a^3b^2	a^2b^2	ab^2
ab^3	ab^3	b^3	a^3b^3	ab^3	a	e	a^3	a^2	ab	b	a^3b	a^2b	ab^2	b^2	a^3b^2	a^2b^2
a^2b^3	a^2b^3	ab^3	b^3	a^3b^3	a^2	a	e	a^3	a^2b	ab	b	a^3b	a^2b^2	ab^2	b^2	a^3b^2
a^3b^3	a^3b^3	a^2b^3	ab^3	b^3	a^3	a^2	a	e	a^3b	a^2b	ab	b	a^3b^2	a^2b^2	ab^2	b^2

From Table 3.1, we can produce the 0-1 Table for G_1 as shown in the following.

Table 3.2: 0-1 Table for G_1

*	e	a	a^2	a^3	b	ab	a^2b	a^3b	b^2	ab^2	a^2b^2	a^3b^2	b^3	ab^3	a^2b^3	a^3b^3
e	1	1	1	1	1	1	1	1	1	1	1	1	1	1	1	1
a	1	1	1	1	0	0	0	0	1	1	1	1	0	0	0	0

a^2	1	1	1	1	1	1	1	1	1	1	1	1	1	1	1	1
a^3	1	1	1	1	0	0	0	0	1	1	1	1	0	0	0	0
b	1	0	1	0	1	0	1	0	1	0	1	0	1	0	1	0
ab	1	0	1	0	0	1	0	1	1	0	1	0	0	1	0	1
a^2b	1	0	1	0	1	0	1	0	1	0	1	0	1	0	1	0
a^3b	1	0	1	0	0	1	0	1	1	0	1	0	0	1	0	1
b^2	1	1	1	1	1	1	1	1	1	1	1	1	1	1	1	1
ab^2	1	1	1	1	0	0	0	0	1	1	1	1	0	0	0	0
a^2b^2	1	1	1	1	1	1	1	1	1	1	1	1	1	1	1	1
a^3b^2	1	1	1	1	0	0	0	0	1	1	1	1	0	0	0	0
b^3	1	0	1	0	1	0	1	0	1	0	1	0	1	0	1	0
ab^3	1	0	1	0	0	1	0	1	1	0	1	0	0	1	0	1
a^2b^3	1	0	1	0	1	0	1	0	1	0	1	0	1	0	1	0
a^3b^3	1	0	1	0	0	1	0	1	1	0	1	0	0	1	0	1

From Table 3.2, 160 pairs of elements commute with each other. Therefore,

$$P(G_1) = \frac{160}{256} = \frac{5}{8}.$$

In Table 3.3 and Table 3.4, the power of each element in G_1 , are computed up to a certain value and the value of $P_n(G_1)$ is computed for $n = 1, 2, 3, 4, 5, 6, 7$ and 8.

Table 3.3: The n^{th} power of elements in G_1

Power 1	Power 2	Power 3	Power 4
$(e)^1 = e$	$(e)^2 = e$	$(e)^3 = e$	$(e)^4 = e$

$(a)^1 = a$	$(a)^2 = a^2$	$(a)^3 = a^3$	$(a)^4 = e$
$(a^2)^1 = a^2$	$(a^2)^2 = e$	$(a^2)^3 = a^2$	$(a^2)^4 = e$
$(a^3)^1 = a^3$	$(a^3)^2 = a^2$	$(a^3)^3 = a$	$(a^3)^4 = e$
$(b)^1 = b$	$(b)^2 = b^2$	$(b)^3 = b^3$	$(b)^4 = e$
$(ab)^1 = ab$	$(ab)^2 = b^2$	$(ab)^3 = ab^3$	$(ab)^4 = e$
$(a^2b)^1 = a^2b$	$(a^2b)^2 = b^2$	$(a^2b)^3 = a^2b^3$	$(a^2b)^4 = e$
$(a^3b)^1 = a^3b$	$(a^3b)^2 = b^2$	$(a^3b)^3 = a^3b^3$	$(a^3b)^4 = e$
$(b^2)^1 = b^2$	$(b^2)^2 = e$	$(b^2)^3 = b^2$	$(b^2)^4 = e$
$(ab^2)^1 = ab^2$	$(ab^2)^2 = a^2$	$(ab^2)^3 = a^3b^2$	$(ab^2)^4 = e$
$(a^2b^2)^1 = a^2b^2$	$(a^2b^2)^2 = e$	$(a^2b^2)^3 = a^2b^2$	$(a^2b^2)^4 = e$
$(a^3b^2)^1 = a^3b^2$	$(a^3b^2)^2 = a^2$	$(a^3b^2)^3 = ab^2$	$(a^3b^2)^4 = e$
$(b^3)^1 = b^3$	$(b^3)^2 = b^2$	$(b^3)^3 = b$	$(b^3)^4 = e$
$(ab^3)^1 = ab^3$	$(ab^3)^2 = b^2$	$(ab^3)^3 = ab$	$(ab^3)^4 = e$
$(a^2b^3)^1 = a^2b^3$	$(a^2b^3)^2 = b^2$	$(a^2b^3)^3 = a^2b$	$(a^2b^3)^4 = e$
$(a^3b^3)^1 = a^3b^3$	$(a^3b^3)^2 = b^2$	$(a^3b^3)^3 = a^3b$	$(a^3b^3)^4 = e$
$P_1(G_1) = \frac{5}{8}$	$P_2(G_1) = 1$	$P_3(G_1) = \frac{5}{8}$	$P_4(G_1) = 1$

Table 3.4: The n^{th} power of elements in G_1

Power 5	Power 6	Power 7	Power 8
$(e)^5 = e$	$(e)^6 = e$	$(e)^7 = e$	$(e)^8 = e$
$(a)^5 = a$	$(a)^6 = a^2$	$(a)^7 = a^3$	$(a)^8 = e$
$(a^2)^5 = a^2$	$(a^2)^6 = e$	$(a^2)^7 = a^2$	$(a^2)^8 = e$
$(a^3)^5 = a^3$	$(a^3)^6 = a^2$	$(a^3)^7 = a$	$(a^3)^8 = e$
$(b)^5 = b$	$(b)^6 = b^2$	$(b)^7 = b^3$	$(b)^8 = e$
$(ab)^5 = ab$	$(ab)^6 = b^2$	$(ab)^7 = ab^3$	$(ab)^8 = e$
$(a^2b)^5 = a^2b$	$(a^2b)^6 = b^2$	$(a^2b)^7 = a^2b^3$	$(a^2b)^8 = e$
$(a^3b)^5 = a^3b$	$(a^3b)^6 = b^2$	$(a^3b)^7 = a^3b^3$	$(a^3b)^8 = e$
$(b^2)^5 = b^2$	$(b^2)^6 = e$	$(b^2)^7 = b^2$	$(b^2)^8 = e$
$(ab^2)^5 = ab^2$	$(ab^2)^6 = a^2$	$(ab^2)^7 = a^3b^2$	$(ab^2)^8 = e$
$(a^2b^2)^5 = a^2b^2$	$(a^2b^2)^6 = e$	$(a^2b^2)^7 = a^2b^2$	$(a^2b^2)^8 = e$
$(a^3b^2)^5 = a^3b^2$	$(a^3b^2)^6 = a^2$	$(a^3b^2)^7 = ab^2$	$(a^3b^2)^8 = a^2$
$(b^3)^5 = b^3$	$(b^3)^6 = b^2$	$(b^3)^7 = b$	$(b^3)^8 = e$
$(ab^3)^5 = ab^3$	$(ab^3)^6 = b^2$	$(ab^3)^7 = ab$	$(ab^3)^8 = e$
$(a^2b^3)^5 = a^2b^3$	$(a^2b^3)^6 = b^2$	$(a^2b^3)^7 = a^2b$	$(a^2b^3)^8 = e$
$(a^3b^3)^5 = a^3b^3$	$(a^3b^3)^6 = b^2$	$(a^3b^3)^7 = a^3b$	$(a^3b^3)^8 = e$
$P_5(G_1) = \frac{5}{8}$	$P_6(G_1) = 1$	$P_7(G_1) = \frac{5}{8}$	$P_8(G_1) = 1$

From Table 3.3 and Table 3.4, we can generalize the n^{th} commutativity degree of some nonabelian 2-group with a cyclic subgroup of index four of order 16 as the following theorem:

Teorem3.1:

Let $G_1 = \langle a, b : a^4 = 1, b^4 = 1, b^{-1}ab = a^3 \rangle$ be a nonabelian 2-group with a cyclic subgroup of index four of order 16, then for $n \in \mathbf{Z}^+$, the n^{th} commutativity degree of G_1 , is given as follows:

$$P_n(G_1) = \begin{cases} \frac{5}{8} ; & \text{if } n \text{ is odd,} \\ 1 ; & \text{if } n \text{ is even.} \end{cases}$$

Proof For all elements x in G_1 , the order of x is equal to 1, 2 or 4. Thus for any $x \in G_1$, $x^n = e$ where $n = 4k, k \in \mathbf{Z}^+$.

By Definition 2.5 and 0-1 Table of G_1 , we have

$$\begin{aligned} P_1(G_1) &= \frac{|\{(x, y) \in G_1 \times G_1 \mid xy = yx\}|}{|G_1|^2} \\ &= \frac{160}{256} = \frac{5}{8}. \end{aligned}$$

The number of $(x, y) \in G_1 \times G_1$ such that $xy = yx$ is also equal to the number of (x, y) such that $x^n y = yx^n$ where n is odd number i.e $n = 1 + 4k$ and $n = 4k - 1$ for $k \in \mathbf{Z}^+$.

Thus we just need to show

$$x^{1+4k} y = yx^{1+4k} \text{ and } x^{4k-1} y = yx^{4k-1} \text{ can be reduced to } xy = yx.$$

$$x^{1+4k} y = yx^{1+4k},$$

$$xx^{4k} y = yxx^{4k}.$$

$$\text{Suppose } x^{4k} = e,$$

then,

$$xey = yxe,$$

$$xy = yx,$$

and

$$x^{4k-1} y = yx^{4k-1},$$

$$x^{4k} x^{-1} y = yx^{4k} x^{-1}.$$

$$\text{Suppose } x^{4k} = e,$$

then,

$$\begin{aligned} ex^{-1}y &= yex^{-1}, \\ x^{-1}y &= yx^{-1}. \end{aligned}$$

Then by cancellation law,

$$\begin{aligned} xx^{-1}yx &= xyx^{-1}x, \\ yx &= xy. \end{aligned}$$

Therefore, $P_n(G_1) = P_1(G_1)$ for n is odd.

By Definition 2.8, we have $Z(G_1) = \{e, a^2, b^2\}$.

Let $x \in G_1$, then $x^2 \in Z(G_1)$ and thus $x^2y = yx^2$ for all $x, y \in G_1$.

Therefore, by Definition 2.6, we have

$$P_2(G_1) = 1.$$

The number of $(x, y) \in G_1 \times G_1$ such that $x^2y = yx^2$ is also equal to the number of $(x, y) \in G_1 \times G_1$, such $x^n y = yx^n$ where n is even that is $n = 4k$ and $n = 4k - 2$ for $k \in \mathbf{Z}^+$.

Earlier we have shown that for

$$x^n = e \text{ for } n = 4k, \text{ where } k \in \mathbf{Z}^+, \text{ and hence } x^n y = yx^n.$$

Thus we just need to show that,

$$x^{4k-2}y = yx^{4k-2} \text{ can be reduced to } x^2y = yx^2.$$

$$\begin{aligned} x^{4k-2}y &= yx^{4k-2}, \\ x^{4k}x^{-2}y &= yx^{4k}x^{-2}. \end{aligned}$$

Suppose $x^{4k} = e$,

then,

$$\begin{aligned} ex^{-2}y &= yex^{-2}, \\ x^{-2}y &= yx^{-2}. \end{aligned}$$

Then by cancellation law,

$$\begin{aligned} x^2x^{-2}yx^2 &= x^2yx^{-2}x^2, \\ yx^2 &= x^2y. \end{aligned}$$

Therefore, $P_n(G_1) = P_2(G_1)$ for n is even.

Using similar method, we found the generalization of the n^{th} commutativity degree of some nonabelian 2-group with a cyclic subgroup of index four of order 16 as follows:

$$P_n(G_k) = \begin{cases} \frac{5}{8} & ; \text{ if } n \text{ is odd} \\ 1 & ; \text{ if } n \text{ is even} \end{cases} \quad \text{with } k=1,2,3,4 \text{ and } 5 \text{ with } n \in \mathbf{Z}$$

Conclusion

As a conclusion, the n^{th} commutativity degree of groups G_1, G_2, G_3, G_4 and G_5 have been found. All these five nonabelian 2-groups with a cyclic subgroup of index four of order 16 have the same value of $P_n(G)$: the value of

$$P_n(G) = \frac{5}{8} \text{ for } n \text{ is odd and } P_n(G) = 1 \text{ for } n \text{ is even.}$$

Acknowledgement

In the name of Allah, the Most Gracious and Merciful. He who has given me strength and courage to accomplish this report.

I would like to take this opportunity to express my utmost gratitude to everyone involved in completing this report. High appreciation to my PSM supervisor, Dr. NorMuhainiahMohd Ali for her effort and patience in guiding me to conduct this research. Thanks a lot for all the encouragement, criticisms and suggestions.

I would also like to thank my family especially my parents Abu Bakar bin Mohammad and Zubidahbinti Abu Bakar for their full encouragement, support and inspiration while completing this report. Last but not least, I would like to thank all my friends for their assistance and encouragement throughout the process of completing this report.

References

1. Erdos, P. and Turan, P. (1968). On Some Problems of a Statistical Group Theory. *ActaMath.Acad. Of Sci, Hung*, **19**:413-423
2. Yahya, Z. (2011). *The n-th commutativity degree of dihedral groups up to degree 12*. Undergraduate Project Report, UniversitiTeknologi Malaysia.
3. Mohammed Hussein Saleh, H. (2014). *The Commutativity Degree of Some Nonabelian Two-Groups with a Cyclic Subgroup of Index Four*. Master Degree Project Report, UniversitiTeknologi Malaysia.
4. Abu Sama, N (2010). *The Commutativity Degree of Alternating Groups up to Degree 200*. Undergraduate Project Report, UniversitiTeknologi Malaysia.
5. White, D.L. *Cayley Tables and Isomorphism Lecture note MATH 57091*. Department of Mathematics Sciences, Kent State University.
6. Machale, D. (1974). How commutative can a non-commutative group be? *The Mathematical Gazette*. **58**: 199-202
7. Burnside, W. *The Theory of Groups of Finite Order (2nd ed)*. Cambridge University Press.1911.

8. Sarmin, N. H. (2011). *Modern Algebra Lecture Notes*. (5thed.) Department of Mathematics, Universiti Teknologi Malaysia. Desktop Publisher.
9. Ninomiya, Y. (1994). Finite p -group with Cyclic Subgroup of Index p^2 . *Math. Unvi.* 1994.36:1-21.

MODELLING AND FORECASTING THE PRICE OF KIJANG EMAS USING BOX-JENKINS METHOD AND TIME SERIES REGRESSION

Farah Ahyani Mohamad Puad, Maizah Hura Ahmad

1.0 INTRODUCTION

Forecasting methods can be categorized into two which are qualitative and quantitative method. Qualitative forecasting method is used when historical data needed to predict an event is not available. Usually in this case forecaster will rely on the opinion of experts to predict future event. Meanwhile, quantitative forecasting methods require a manipulation of data in order to predict future events. It includes methods such as Box-Jenkins method, decomposition method, regression analysis methods and so on.

Gold are often known as a symbol of wealth. Therefore, gold coins, bar and high-carat jewellery play a crucial role as a defence against misfortune. This is why gold mining brings a lot of benefits to the poorer nations. Hence, it continues to foster the economic development.

The Malaysian KijangEmas is the official bullion gold coin of Malaysia and minted by the Royal Mint of Malaysia. Investing on KijangEmas offers more profit due to the increase of gold price. However, rumour has it that the price of gold might decrease if the interest rate increase. Therefore, information regarding this matter is very useful to any interested investor

The objectives of this research study comprises of (i) to obtain the best model for KijangEmas prices using Box-Jenkins method and Time Series Regression; (ii) to forecast the KijangEmas prices using Box-Jenkins method and Time Series Regression; and (iii) to compare and choose the best method to model the KijangEmas prices.

1.1 STUDY AREA AND DATA

This study focuses on finding the best model model to forecast the KijangEmas prices. The methods used in this study are Box-Jenkins ARIMA method and Time Series Regression. The data is gathered starting at 1st January 2014 to 31th October 2014 from Bank Negara Malaysia (BNM).

1.2 LITERATURE REVIEW

In recent years, the global gold price trend has attracted a lot of attraction and the price of gold has frightening spike compared to historical trend. In times of uncertainty, investors consider gold as hedge against unforeseen disasters so the forecasted price of gold has been a subject of highest amongst all (M. Massarrat, 2013). In this paper, they attempt to develop a forecasting model for gold price by using Box-Jenkins, Auto Regressive Integrated Moving Average (ARIMA) methodology. They managed to suggest that ARIMA (0, 1, 1) is the most suitable model to be used for prediction of the gold price (in US\$ per ounce) from January 2003 to March 2012.

Most of the valued metals have an economic value apart from being trade good especially gold because it is considered as an alternative investment to the US Dollar and also known as ‘safe heaven’ to some of the investors. An increase in value of the US Dollar will lead, all other things being equal, to fall in the dollar value of gold so both assets exhibit a negative correlation. Although the fundamental analysis could be applied for the long term pricing of these metals, predicting daily returns is very difficult (Baker, 1985). He also highlight that there are a lot of speculative interest in the short run price movement of gold.

The Box-Jenkins methodology is widely used in various field of study. For example, in economics, there has been a study of unemployment rate using Box-Jenkins procedure. The paper aims to model the evolution of unemployment rate using monthly data from 1998-2007. The empirical study relieves that the most adequate model for the unemployment rate is ARIMA (2, 1, 2). The result shows that they forecast the unemployment rate for January 2008 is 4.06% (I. Dobre, 2008).

In agriculture, the added value of agricultural sub sectors is affected by many factors such as quantity production per agricultural sub sectors, selling price of producers, government investment and monetary and financial policies. This paper examines the performance the performance of artificial neural network, Box-Jenkins and Holt-Winters-no-seasonal models in forecasting added value of agriculture sub sectors in Iran. The study shows that Box-Jenkins model gave better results in forecasting of unseen data (E. Kahfroushan, 2010). Moreover, there is another study on agriculture where they examine the best fitted ARIMA model to be used in forecasting boro rice production in Bangladesh from 2008-2009 and 2012-2013. It is found from the study that the ARIMA (0, 1, 0), ARIMA (0, 1, 3) and ARIMA (0, 1, 2) are the best model for local, modern and total boro rice production respectively (N. M. F. Rahman, 2010).

Looking into another field of study such as environment, in keeping up with Malaysia’s rapid economic development and nation’s aspiration for a quality life, clean-air legislation limiting industrial and automobile emissions was adopted in 1978. Yet, to this day, air pollution from both sources still poses a problem for the nation. Therefore in order to predict the status of future air quality in Malaysia, a study is carried out and a Box-Jenkins ARIMA approach was applied to model the time series of monthly maximum 1 h carbon monoxide and nitrogen dioxide concentration in the east coast states of Peninsular Malaysia and make a comparison with the west coast area (M. Z. Rahman, 2009).

According to Thompson (2005), in his journal “An Introduction to Time Series Regression”, he wrote that the key in applying Time Series Regression is whether the series are stationary or not. A stationary series has a long history and usually converges to a steady state. Stationary is weaker than normality but regression with stationary variables typically produce reliable statistics. As the number of observations increases, reliability also increases at an increasing rate.

Ghanbarian (2007) has applied time series regression on load forecasting using Neuro-Fuzzy Technique. It is a study of a medium and long-term energy of a complicated electrical system. The energy data of several years in the past were used to train an Adaptive Network based on Fuzzy Inference System. Several simulation were arranged to examine the efficiency of the method.

1.3 METHODOLOGY

1.3.1 Box-Jenkins Method

In this popular method developed by Box and Jenkins, there are four iterative procedures; identification, estimation, diagnostics and forecasting.

1.3.1.1 Model identification

Tentatively identifying a model is done by using a sample autocorrelation function and a sample partial autocorrelation function. We have to determine whether or not the time series we were to forecast is stationary otherwise we have to transform the time series into a series of stationary time series values.

The most popular method to transform non-stationary data is by differencing. If the series is still not stationary after the first difference, then a second differencing must be done and the process will continue until the data become stationary.

The first difference of the time series values y_1, y_2, \dots, y_n are:

$$z_t = y_t - y_{t-1} \text{ where } t = 2, \dots, n. \quad (3.1)$$

The second difference of the time series values y_1, y_2, \dots, y_n are:

$$\begin{aligned} z_t &= (y_t - y_{t-1}) - (y_{t-1} - y_{t-2}) \\ &= y_t - 2y_{t-1} + y_{t-2} \text{ for } t = 3, 4, \dots, n. \end{aligned} \quad (3.2)$$

Once the stationary data is obtained, the next step is to identify the order of the autoregressive (p) and moving average (q) terms. The primary tool to perform this step is by using the autocorrelation plot (ACF) and the partial autocorrelation plot (PACF). The sample autocorrelation plot and the sample partial autocorrelation plot are compared to the theoretical behaviour of these plots when the order is known.

1. Autoregressive Model, AR (p)

Autoregressive model is a model that relies only on the information of the past. The order of this model can easily be determined by using ACF and PACF. If ACF trails off to zero instantly and PACF cut off to zero after p -lag, this shows the behaviour of AR (p). The regression coefficients are calculated by using non-linear least square method. The general form of autoregressive model:

$$y_t = \delta + \phi_1 y_{t-1} + \phi_2 y_{t-2} + \dots + \phi_p y_{t-p} + e_t \quad (3.4)$$

where

y_t = the observation values at time t .

δ = constant.

ϕ_i = regression operator at step p , where $i = 1, 2, \dots, p$.

e_t = random shock at time t .

2. Moving Average Model, MA (q)

Moving average generate forecast based on linear combination of a finite number of past error. The order of this model can also be determined by using ACF and PACF. If the ACF trails off to zero after first lag and PACF die out rapidly, this shows the behaviour of MA(1). The general form of moving average model:

$$y_t = \mu + e_t - \theta_1 e_{t-1} - \theta_2 e_{t-2} - \dots - \theta_q e_{t-q} \quad (3.5)$$

where

- y_t =the observation values at time t .
 μ =mean of the model.
 θ_i =moving average operator at step q , where $i = 1, \dots, q$.
 e_t =random shock at time t .

3. Autoregressive Moving Average Model (ARMA)

This model is obtained from a stationary set of data where the MA and AR model can be observed from the ACF and PACF. If the both graphs die out gradually, then it shows the behaviour of ARMA model which depends on both current and past values of variables and error. The general form of ARMA model:

$$y_t = \delta + \phi_1 y_{t-1} + \dots + \phi_p y_{t-p} + e_t - \theta_1 e_{t-1} - \dots - \theta_q e_{t-q} \quad (3.6)$$

where

- y_t =the observation values at time t .
 δ =constant.
 ϕ_i =regression operator at step p , where $i = 1, \dots, p$.
 θ_i =moving average operator at step q , where $i = 1, \dots, q$.
 e_t =random shock at time t .

4. Autoregressive Integrated Moving Average (ARIMA)

ARIMA model is an integrated model of ARMA mode when we transform a non-stationary data to a stationary data by differencing. The general form of ARIMA model:

$$y_t = \delta^d + \phi_1 y_{t-1} + \dots + \phi_p y_{t-p} + e_t - \theta_1 e_{t-1} - \dots - \theta_q e_{t-q} \quad (3.7)$$

where

- y_t =the observation values at time t .
 δ^d = d^{th} difference of y .
 ϕ_i =regression operator at step p , where $i = 1, \dots, p$.
 θ_i =moving average operator at step q , where $i = 1, \dots, q$.
 e_t =random shock at time t .

1.3.1.2 Model Estimation

After a tentative Box-Jenkins model has been identified, we estimate the parameter of the model. Although Box and Jenkins favour the maximum likelihood approach to calculating point estimates, this approach can be somewhat difficult and costly to implement and so they suggest using the least squares approach to calculating point estimates.

1.3.1.3 Model Diagnostics

A good way to check the adequacy of an overall Box-Jenkins model is to analyse the residuals obtained from the model in the following manner. Just as we can calculate the sample autocorrelation and partial correlation function of the time series values Z_b, Z_{b+1}, \dots, Z_n , we can calculate such functions for the residuals. We let "RSAC" denote the sample autocorrelation function of the residuals and denote "RSPAC" the sample partial autocorrelation function of the residuals.

One way to use the residuals to check the adequacy of the overall model is to examine a statistic that determines whether the first K sample autocorrelation of the residuals, considered together, indicate the adequacy of the model. Two such statistics have been suggested. These statistics are summarized as follows:

1. The Box-Pierce statistic

$$Q = n' \sum_{l=1}^k r_l^2(\hat{a})$$

2. The Ljung-Box statistic

$$Q^* = n'(n' + 2) \sum_{l=1}^k (n' - 1)^{-1} r_l^2(\hat{a})$$

here $n' = n - (d + LD)$

where

n =number of observations in the original time series.

L =number of season in a year.

d =degree of non-seasonal differencing used to transform the original time series values into

stationary values.

D =degree of seasonal differencing used to transform time series values into stationary values.

the original

However, the theory indicates that Q^* is better of the two statistics. The modelling process is supposed to account for the relationship between the time series observations. If it does account for these relationships, the residuals should be unrelated and hence the autocorrelation of the residuals should be small. Therefore a large value of Q^* indicates that the model is inadequate.

1.3.1.4 Forecasting

After the adequate model has been identified, the last step will be forecasting. Forecasting can be done over any desire period of time.

1.3.2 Time Series Regression Method

Time Series data can be found in many business and economic fields. In time series regression, observations in different time periods are autocorrelated or related since the data collected over time and tend to have trend, seasonal patterns and so forth. The steps in analysing time series regression will be explained in the next section.

1.3.2.1 Trend Model of Time Series y_t

Trend model can be used to describe the time series y_t . Such model is defined as follows:

$$y_t = TR_t + \varepsilon_t \tag{3.8}$$

where

y_t =the value of the time series in period t .

TR_t =the trend in the time period t .

ε_t =the error term in time period t .

In particular, there are three trends that needed to be considered.

1. No Trend

This model indicates that there is no long-run growth or decline in time series over time.

$$TR_t = \beta_0$$

2. Linear Trend

This model implies that there is a straight-line long run growth (if the slope $\beta_1 t$ is greater than zero) or decline (if the slope $\beta_1 t$ is less than zero).

$$TR_t = \beta_0 + \beta_1 t$$

3. Quadratic Trend

This model shows that there is a quadratic (or curvilinear) long-run change over time. This quadratic can be either:

- i. Growth at an increase or decrease rate
- ii. Decline at an increase or decrease rate

However, there is also a complicated trend which can be modelled using the p^{th} –order polynomial function. The p^{th} –order polynomial trend model is:

$$\begin{aligned} y_t &= TR_t + \varepsilon_t \\ &= \beta_0 + \beta_1 t + \beta_2 t^2 + \dots + \beta_p t^p \end{aligned}$$

Third-order ($p = 3$) and higher order ($p > 3$) polynomials model trends with one or more reversals in curvature. It can be noted that regression technique can be used to obtain the least squares point estimates of the parameters in the trend models.

1.3.2.2 Detecting Autocorrelation

Assumption used in the model is that the error terms, ε_t satisfies the content variance independence and normality to reach the validity of the regression methods. But sometimes, this assumption is often violated as the error become autocorrelated. The error terms occurring over time are often called positive autocorrelation or negative autocorrelation.

First order autocorrelation is one type of positive or negative autocorrelation which the error term, ε_t in time period, t is related to ε_{t-1} , the error terms in time period $t - 1$, by the equation:

$$\varepsilon_t = \rho\varepsilon_{t-1} + a_t$$

We assume that, ρ is the correlation coefficient between error terms separately by one time period and a_1, a_2, \dots are values randomly and independently selected from a normal distribution having mean of zero and variance independent of time.

For the residual of forecast model, test for significant autocorrelation is provided by one common portmanteau test which is based on Ljung-Box Q statistic that has chi-square distribution with m minus the number of parameters estimated in the model. The value of Q statistic can be compared with the chi-square table to determine if it is larger than it would be expected to be under null hypothesis that all autocorrelations in the set are zero. The Q statistic is given:

$$Q = n(n+2) \sum_{k=1}^m \frac{r^2(e)}{n-k} \sim \chi_{m-r}^2$$

where

$$r_k^2(e) = \text{the residual autocorrelation at lag } k.$$

n = number of residuals.

m = number of time lags include to be tested.

k = the time lag.

1.3.2.3 Durbin-Watson (DW) Test

In order to test the present of the first-order autocorrelation (positive or negative autocorrelations), we can use the Durbin-Watson (DW) test. The DW statistic is:

$$d = \frac{\sum_{t=2}^n (e_t - e_{t-1})^2}{\sum_{t=1}^n e_t^2}$$

where e_1, e_2, \dots, e_n are time-ordered residuals. The hypotheses to be tested are:

H_0 : The error terms are not correlated.

H_1 : The error terms are positively correlated.

Durbin and Watson have shown that there are three points (denoted as $d_{L,\alpha}$ and $d_{U,\alpha}$) such that with the probability of Type 1 error, then:

1. If $d < d_{L,\alpha}$, we reject H_0 .
2. If $d < d_{U,\alpha}$, we reject H_1 .
3. If $d_{L,\alpha} \leq d < d_{U,\alpha}$, the test is inconclusive.

1.3.2.4 Solving First-Order Autocorrelation

We need to model the autocorrelation when the error terms for the time series regression are autocorrelated. This is because the model is said to be inadequate. Hence, we use the autoregressive model to solve this problem.

The model for first-order autoregressive process is defined by:

$$Y_t = \beta_0 + \beta_1 Y_{t-1} + \varepsilon_t \tag{3.9}$$

where

$$\varepsilon_t = \rho \varepsilon_{t-1} + \alpha_t$$

In this model,

1. ρ is assumed to be an error terms (random shock) with mean zero and satisfies the normality assumptions, constant variance and independent.
2. ρ is defined as the correlation coefficient between error terms separated by one time period, where
 - i. $\rho > 0$ implies that the error terms are positively autocorrelated.
 - ii. $\rho < 0$ implies that the error terms are negatively autocorrelated.

Once this model has been fit to data by least squares, the forecasting equation becomes

$$\hat{Y}_t = b_0 + b_1 Y_{t-1} \tag{3.10}$$

1.3.3 Accuracy Measures

Most of forecasting situations involve some degree of uncertainty. The presence of irregular component, which represents unexplained or unpredictable fluctuations in the data,

means that some error in forecasting must be expected. Denote that the actual and forecasted data in period t as y_t and \hat{y}_t respectively.

1.3.3.1 Mean Squared Error (MSE)

Mean squared error is calculated by:

$$MSE = \frac{\sum_{t=1}^n e_t}{n} = \frac{\sum_{t=1}^n (y_t - \hat{y}_t)^2}{n}$$

3.3.2 Mean Absolute Percentage Error (MAPE)

Mean absolute percentage error is calculated by:

$$MAPE = \frac{100}{n} \sum_{t=1}^n \left| \frac{\hat{y}_t - y_t}{y_t} \right|$$

1.4 RESULTS AND DISCUSSION

1.4.1 Box-Jenkins Method

Data analysis of Box-Jenkins method can be classified into four steps which are model identification, parameter estimation, diagnostic and forecasting.

1.4.1.1 Model Identification

The first step in the model identification process is to plot the trend analysis of the series. We can observe if the data is stationary by looking at the straight line. If the line growth or decline, it means that the mean is not constant. Figure 4.1 shows the trend analysis plot of KijangEmas prices.

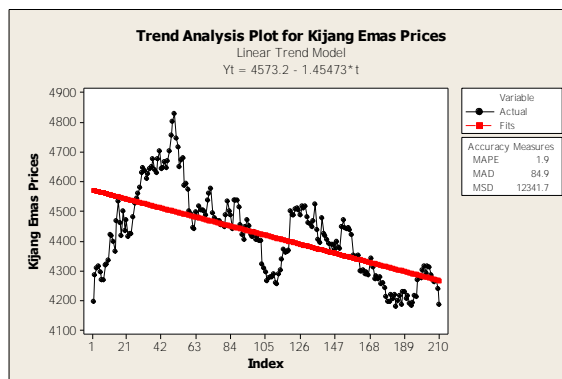


Figure 4.1: Trend Analysis Plot of KijangEmas Prices

From Figure 4.1, it shows the presence of a downward trend. Hence, we can conclude that the time series data is not stationary and non-seasonal. In order to determine the tentative model, the autocorrelation need to be plotted. Figure 4.2 shows the autocorrelation function plot of KijangEmas prices and Figure 4.3 illustrates the partial autocorrelation function plot of KijangEmas prices.

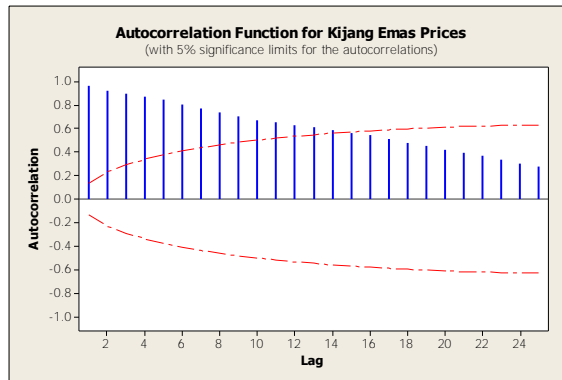


Figure 4.2: Autocorrelation Function Plot for KijangEmas Prices

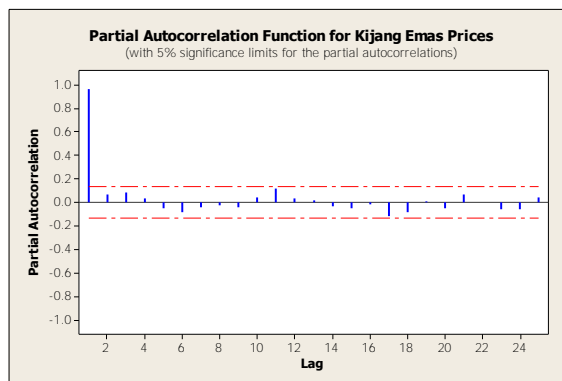


Figure 4.3: Partial Autocorrelation Function Plot for KijangEmas Prices

Figure 4.2 show that the series does not trail off to zero rapidly. Therefore we can conclude that the time series data is not stationary and we need to transform the data into stationary data by using differencing method before we begin to analyse it. Figure 4.4 shows the trend analysis plot for the first difference of KijangEmas prices.

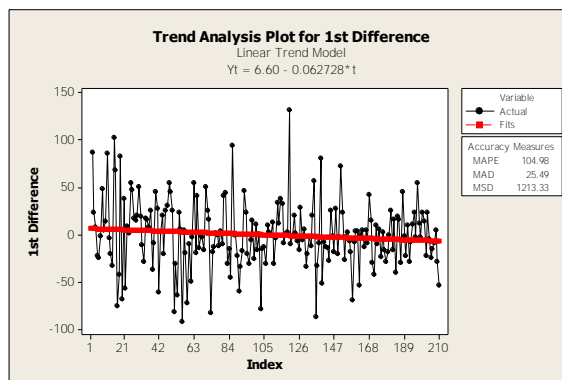


Figure 4.4: Trend Analysis Plot for the First Difference of KijangEmas Prices

Looking at Figure 4.4, we can see that the downward trend is still present. Therefore, we have to continue differencing the data for the second time. Figure 4.5 shows the trend analysis plot of the second difference of KijangEmas prices.

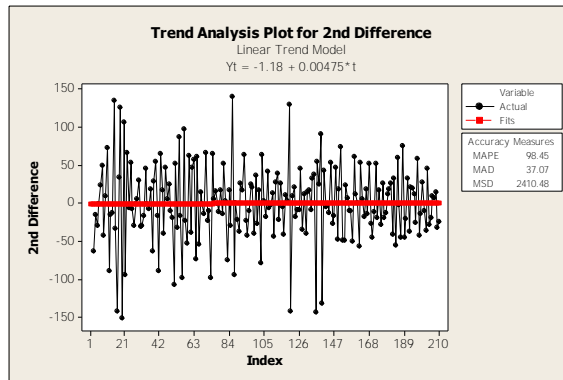


Figure 4.5: Trend Analysis for the Second Difference of KijangEmas Prices

Figure 4.5 shows that there is no more trend detected so, we can conclude that the time series data is already stationary as the series vary about a fixed level or fluctuate around a constant mean. Next we plot the ACF and PACF to ensure that the data is stationary and to determine whether the series is seasonal or non-seasonal. Figure 4.6 and Figure 4.7 are the plots of autocorrelation function and partial autocorrelation function of KijangEmas prices respectively.

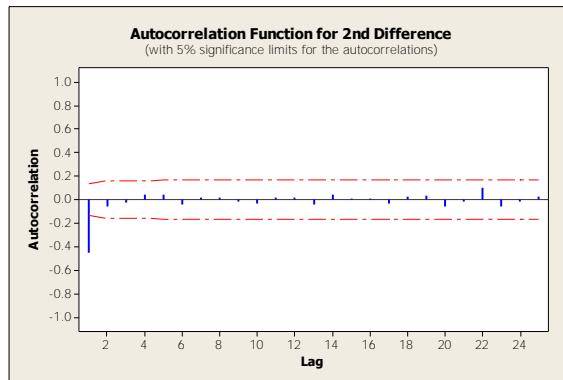


Figure 4.6: Autocorrelation Function Plot of the Second Difference

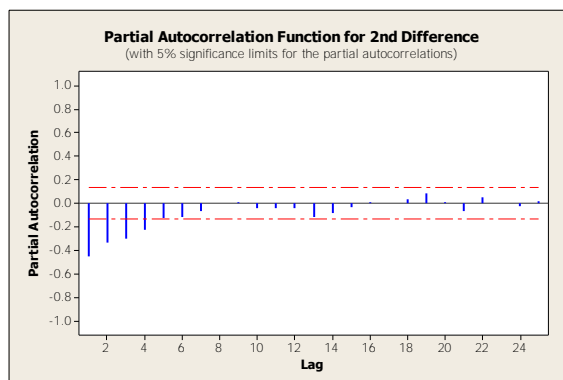


Figure 4.7: Partial Autocorrelation Function Plot of the Second Difference

From Figure 4.6, we can see that the ACF cuts off after lag 1 while in Figure 4.7, PACF plot dies down after lag 4. Hence, the model to be considered are ARIMA (p, d, q) where $p = 0, 1, 2, 3, 4$, $d = 2$ and $q = 0, 1$. The t -ratios of these models obtained using Minitab software is tabulated in Table 4. 1

Table 4 1: t-ratio Value for ARIMA (p, d, q) Model

ARIMA (p,d,q)	t-ratio					MSE
	AR I	AR II	AR III	AR IV	MA I	
0,2,1	-	-	-	-	46521.81	1217
1,2,0	-7.37	-	-	-	-	1927
1,2,1	-0.31	-	-	-	2448.43	1222
2,2,0	-9.42	-5.31	-	-	-	1701
2,2,1	-	-	-	-	-	-
3,2,0	-11.09	-7.44	-4.95	-	-	1524
3,2,1	-	-	-	-	-	-
4,2,0	-12.23	-8.75	-6.58	-4.03	-	1415
4,2,1	0.03	-1.17	-0.53	0.80	1540.27	1225

From Table 4.1, we can conclude four models that are not significant which are ARIMA (1, 2, 1), ARIMA (2, 2, 1), ARIMA (3, 2, 1) and ARIMA (4, 2, 1). Among the rest of the adequate model, we choose the best model with the smallest value of MSE.

Table 4.2: Mean Squared Error of ARIMA Models

ARIMA (p, d, q)	MSE
0,2,1	1217
1,2,0	1927
2,2,0	1701
3,2,0	1524
4,2,0	1415

From Table 4.2, the ARIMA model with the least MSE is ARIMA (0, 2, 1) model. Hence, this model is selected and will be used to forecast the future values.

1.4.1.2 Model Estimation

The next step is to estimate the parameter value. The ARIMA (0, 2, 1) can be written as:

$$y_t = e_t - \theta_1 e_{t-1}$$

The Minitab output shows that:

Table 4.3: Final Estimate of Parameter

Type	Coefficient	SE Coefficient	T	P
MA 1	0.9939	0.000	46521.81	0.000
Constant	-0.06155	0.04045	-2.26	0.025

Therefore the above equation can be written as:

$$y_t = e_t - 0.9939e_{t-1}$$

1.4.1.3 Model Diagnostic

After the parameter has been estimated, the next step is to perform the diagnostic checking. This is to ensure that the tentative model is adequate. The tests run in two hypotheses which are:

H_0 : ARIMA (0, 2, 1) is adequate

H_1 : ARIMA (0, 2, 1) is not adequate

The Box-Pierce Q statistic is compared to the value of χ^2 with $K - p - q$ degree of freedom that is obtained from the statistical table with $\alpha = 0.05$ level of significance and $K = 12, 24, 36, 48$ as the time lag. The results are shown in Table 4.4.

Table 4.4: Test Statistic for ARIMA (0, 2, 1)

Time Lag	χ_{test}^2	χ_{K-p-q}^2
12	8.8	18.3
24	14.3	33.9
36	24.0	48.6
48	36.5	62.8

The H_0 will be rejected if the value of $\chi_{test}^2 > \chi_{K-p-q}^2$. From Table 4.4, we can see that for all K , the value of $\chi_{test}^2 < \chi_{K-p-q}^2$. Hence, we accept the H_0 and we can conclude that ARIMA (0, 2, 1) is the suitable model for forecasting.

1.4.1.4 Forecasting

The last step is forecasting by using the ARIMA (0, 2, 1) model. The KijangEmas prices are forecasted from 1st November 2014 to 30th November 2014 and are tabulated in Table 4.5.

Table 4.5: Forecast of KijangEmas Prices Using ARIMA (0,2,1)

Period (Day)	Forecast Value, \hat{Y}_t
1/11/2014	4176.428
2/11/2014	4165.765

3/11/2014	4155.011
4/11/2014	4144.165
5/11/2014	4133.228
6/11/2014	4122.199
7/11/2014	4111.079
8/11/2014	4099.868
9/11/2014	4088.565
10/11/2014	4077.171
11/11/2014	4065.685
12/11/2014	4054.108
13/11/2014	4042.440
14/11/2014	4030.680
15/11/2014	4018.829
16/11/2014	4006.887
17/11/2014	3994.853
18/11/2014	3982.727
19/11/2014	3970.511
20/11/2014	3958.203
21/11/2014	3945.803
22/11/2014	3933.312
23/11/2014	3920.730
24/11/2014	3908.056
25/11/2014	3895.291
26/11/2014	3882.435
27/11/2014	3869.487
28/11/2014	3856.448
29/11/2014	3843.318
30/11/2014	3830.096

1.4.2 Time Series Regression

This analysis is carried out using Minitab software and Microsoft Excel. Durbin-Waston test will be used to determine the autocorrelation. Other than that, autoregressive model will be utilized to eliminate the presence of autocorrelations.

1.4.2.1 Data Analysis

The independent variable for this analysis is time, (X_1) and the dependent variable is the Kijang Emas Prices, (Y). Time series plots of Kijang Emas Prices and time are in Figure 4.8.

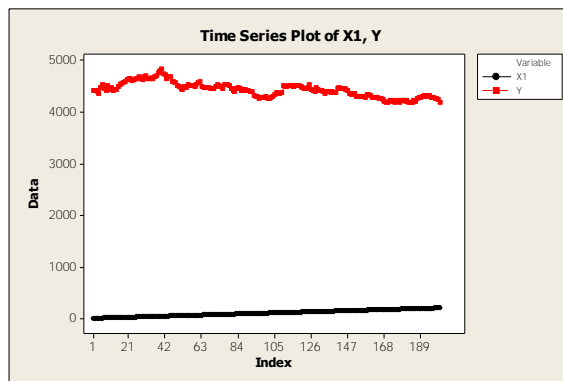


Figure 4.8: Time Series Plot of KijangEmas Prices and Time

Figure 4.8 shows that the dependent and independent variable appear to be moving together. So it is possible that the two variables are related. This relationship can be determined using simple linear regression model. The scatter plot of dependent variable against the independent variable is shown in Figure 4.9.

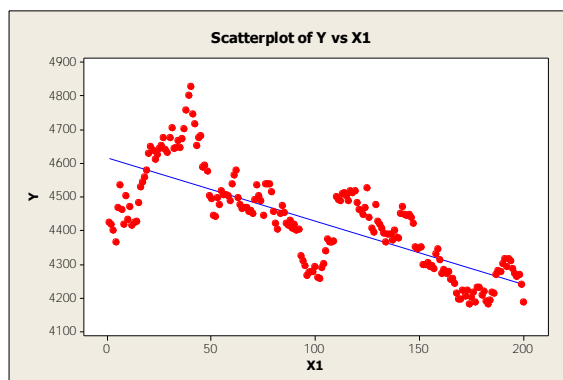
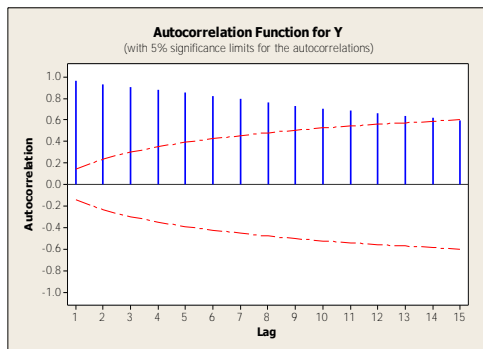


Figure 4.9: Scatter Plot of KijangEmas Prices versus Time

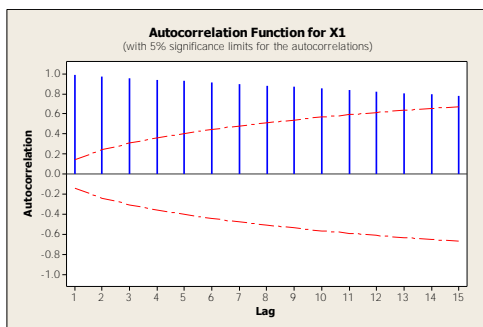
The graphical and numerical autocorrelation for the dependent variable (Y) and independent variable (X_1) are plotted in Figure 4.10 and Figure 4.11 respectively.



Autocorrelation Function: $Y(t)$

Lag	ACF	T	LBQ
1	0.963543	13.63	188.48
2	0.930995	7.79	365.33
3	0.904955	5.97	533.28
4	0.880192	4.99	692.97
5	0.853394	4.33	843.86

Figure 4.10: Autocorrelation Function Plot for KijangEmas Prices



Autocorrelation Function: $X1$

Lag	ACF	T	LBQ
1	0.985000	13.93	196.97
2	0.970002	8.00	388.95
3	0.955006	6.15	575.99
4	0.940015	5.16	758.13
5	0.925030	4.51	935.40

Figure 4.11: Autocorrelation Function Plot for Time

Figure 4.10 and Figure 4.11 shows that sequence of the observations are highly correlated. We can see at the LBQ column for both figures at 5 time lags are 843.86 and 935.40 respectively. These values are greater than the chi-square value for 4 degree of freedom at $\alpha = 0.01$ level of significance which is 13.277. The Durbin-Watson test is also conducted to determine the autocorrelation.

4.3.2 Durbin-Watson Test for Serial Correlation

The autocorrelation can be detected by using the Durbin-Watson test. Equation below is the model with t representing time:

$$Y_t = \beta_0 + \sum_{i=1}^k \beta_i X_{it} + \varepsilon_t$$

and

$$\varepsilon_t = \rho\varepsilon_{t-1} + Z_t$$

The hypotheses tested are:

$$H_0 : \rho = 0$$

$$H_1 : \rho > 0$$

The results obtained by using Minitab software are shown in Figure. 4.12.

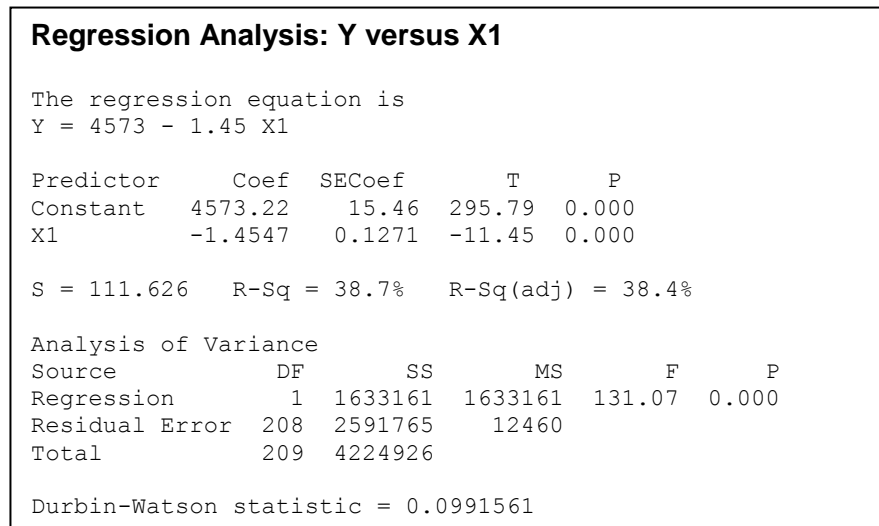


Figure 4.12: Minitab Output for KijangEmas Prices (Y) versus Time X_1

From Figure 4.12, we can see that the Durbin-Watson statistics is 0.0991561 and using level of significance of 0.01 and $n = 210, k = 1$, we will have:

$$d_L = 1.66 \quad , \quad d_U = 1.68$$

Since $DW = 0.0991561 < d_L = 1.66$, we reject the null hypothesis. Hence we can say that there exist a positive autocorrelation between Y and X_1 .

1.4.2.4 Solving the Autocorrelation

The autocorrelation is solved by using the autoregressive model method. The first autoregressive model can be written as:

$$Y_t = \beta_0 + \beta_1 Y_{t-1} + \varepsilon_t$$

The model is fitted by using least squares method. The equation becomes:

$$\hat{Y}_t = b_0 + b_1 Y_{t-1}$$

A first order autoregressive model is developed with KijangEmas prices lagged one day (Y-lagged) as the predictor variable. Figure 4.13 shows the Minitab output for the autoregressive model fitted.

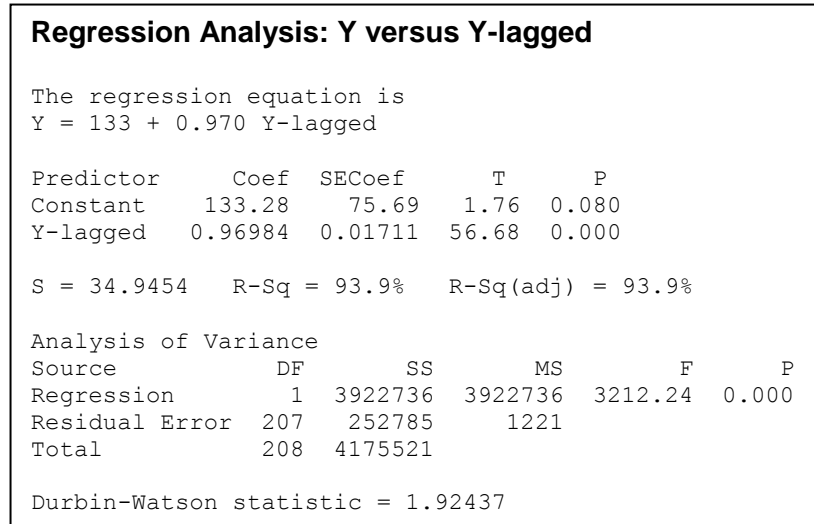


Figure 4.13: Minitab Output for Autoregressive Model Fitted

Based on Figure 4.13, the equation for fitted model is

$$\hat{Y}_t = 133 + 0.97Y_{t-1}$$

Thus, this equation can be used to forecast the KijangEmas prices.

1.4.2.5 Forecasting

The KijangEmas Prices forecasted by using the fitted model from 1st November 2014 to 30th November 2014 are tabulated in Table 4.6.

Table 4.6: Forecast Values for Kiang Emas Prices Using Time Series Regression

Period (Day)	Forecast Value, \hat{Y}_t
1/11/2014	4176.428
2/11/2014	4165.765
3/11/2014	4155.011
4/11/2014	4144.165
5/11/2014	4133.228
6/11/2014	4122.199
7/11/2014	4111.079
8/11/2014	4099.868
9/11/2014	4088.565
10/11/2014	4077.171
11/11/2014	4065.685
12/11/2014	4054.108
13/11/2014	4042.44
14/11/2014	4030.68
15/11/2014	4018.829
16/11/2014	4006.887
17/11/2014	3994.853
18/11/2014	3982.727

19/11/2014	3970.511
20/11/2014	3958.203
21/11/2014	3945.803
22/11/2014	3933.312
23/11/2014	3920.73
24/11/2014	3908.056
25/11/2014	3895.291
26/11/2014	3882.435
27/11/2014	3869.487
28/11/2014	3856.448
29/11/2014	3843.318
30/11/2014	3830.096

1.4.3 Comparison between Box-Jenkins and Time Series Regression.

In order to make a comparison between these two models, the errors of both models are tabulated in Table 4.7 and Table 4.8.

Table 4.7: Absolute Error and MAPE Value for Box-Jenkins ARIMA Model

Period (Day)	Actual Price	Forecasted Value	Mean Absolute Error
1/11/2014	4,091	4176.428	0.0209
2/11/2014	4,116	4165.765	0.0121
3/11/2014	4,140	4155.011	0.0036
4/11/2014	4,059	4144.165	0.0210
5/11/2014	4,053	4133.228	0.0198
6/11/2014	4,098	4122.199	0.0059
7/11/2014	4,126	4111.079	0.0036
8/11/2014	4,107	4099.868	0.0017
9/11/2014	4,117	4088.565	0.0069
10/11/2014	4,211	4077.171	0.0318
11/11/2014	4,219	4065.685	0.0363
12/11/2014	4,260	4054.108	0.0483
13/11/2014	4,229	4042.44	0.0441
14/11/2014	4,256	4030.68	0.0529
15/11/2014	4,272	4018.829	0.0593
16/11/2014	4,260	4006.887	0.0594
17/11/2014	4,256	3994.853	0.0614
18/11/2014	4,244	3982.727	0.0616
19/11/2014	4,166	3970.511	0.0469
20/11/2014	4,388	3958.203	0.0979
21/11/2014	4,375	3945.803	0.0981
22/11/2014	4,422	3933.312	0.1105
23/11/2014	4,414	3920.73	0.1118
24/11/2014	4,451	3908.056	0.1220
25/11/2014	4,545	3895.291	0.1430
26/11/2014	4,560	3882.435	0.1486

27/11/2014	4,550	3869.487	0.1496
28/11/2014	4,544	3856.448	0.1513
29/11/2014	4,447	3843.318	0.1358
30/11/2014	4,435	3830.096	0.1364
Total			2.0024
MAPE (%)			6.6748

Table 4.8: Absolute Error and MAPE Value for Time Series Regression Model

Period (Days)	Actual Price	Forecasted Value	Mean Absolute Error
1/11/2014	4,091	4194.39	0.0253
2/11/2014	4,116	4201.558	0.0208
3/11/2014	4,140	4208.512	0.0165
4/11/2014	4,059	4215.256	0.0385
5/11/2014	4,053	4221.799	0.0416
6/11/2014	4,098	4228.145	0.0318
7/11/2014	4,126	4234.3	0.0262
8/11/2014	4,107	4240.271	0.0324
9/11/2014	4,117	4246.063	0.0313
10/11/2014	4,211	4251.681	0.0097
11/11/2014	4,219	4257.131	0.0090
12/11/2014	4,260	4262.417	0.0006
13/11/2014	4,229	4267.544	0.0091
14/11/2014	4,256	4272.518	0.0039
15/11/2014	4,272	4277.342	0.0013
16/11/2014	4,260	4282.022	0.0052
17/11/2014	4,256	4286.562	0.0072
18/11/2014	4,244	4290.965	0.0111
19/11/2014	4,166	4295.236	0.0310
20/11/2014	4,388	4299.379	0.0202
21/11/2014	4,375	4303.397	0.0164
22/11/2014	4,422	4307.295	0.0259
23/11/2014	4,414	4311.077	0.0233
24/11/2014	4,451	4314.744	0.0306
25/11/2014	4,545	4318.302	0.0499
26/11/2014	4,560	4321.753	0.0522
27/11/2014	4,550	4325.1	0.0494
28/11/2014	4,544	4328.347	0.0475
29/11/2014	4,447	4331.497	0.0260
30/11/2014	4,435	4334.552	0.0226
Total			0.7166
MAPE (%)			2.3886

From Table 4.7 and Table 4.8, we can look at the value of MAPE respectively and see that the time series regression model has the smaller value of MAPE which is 2.3886% compared to Box-Jenkins ARIMA model with 6.6748%.

1.5 CONCLUSION

In this study, a univariate model from Box-Jenkins and Time Series Regression method were used to forecast the KijangEmas prices. Data from 1st January 2014 to 31st October 2014 were analysed.

By using Box-Jenkins method, the model selected was ARIMA (0, 2, 1) which has the smallest value of MSE and was used to forecast the KijangEmas prices. The model ARIMA (0, 2, 1) is as follows:

$$y_t = e_t - 0.9939e_{t-1}$$

Next, the data were analysed using Time Series Regression. The model obtained that fitted the data is:

$$\hat{Y}_t = 133 + 0.97Y_{t-1}$$

This model is then used to forecast the KijangEmas Prices.

Forecast performance was evaluated for both methods by comparing the value of mean absolute percentage error (MAPE). The MAPE of Box-Jenkins and Time Series Regression are 6.6748% and 2.3886% respectively. Hence, we can conclude that the Time Series Regression method is more suitable to model and forecast the KijangEmas prices as compared to Box-Jenkins method.

ACKNOWLEDGEMENT

Firstly, all praises to Allah the Almighty for giving me health and strength in completing this thesis. Also, I want to express my deepest gratitude to my supervisor, Assoc. Prof. Dr. Maizah Hura Ahmad for her continuous support and guidance. Not forgotten to my family, friends and classmates who have been giving me support and encouragement in completing this project.

Lastly, I would like to thank everyone who has directly or indirectly help me throughout the process of completing this project. My thesis would not have been completed in time without your support. Thank you.

REFERENCES

- Baker, S.A., and Van Tassel, R.C. (1985). *Forecasting the Price of Gold: A Fundamental Approach*. Atlantic Economic Journal, 13, 43-51.
- Bowerman B.L., and O'Connell R.T. (1993). *Forecasting and Time Series: An Applied Approach*. (3rded.) Wadsworth.
- Dobre, I., and Alexandru, A.A. (2008). *Modelling unemployment rate using Box-Jenkins procedure*. Journal of applied quantitative methods, 3(2), 156-165.

- Ghanbarian, M., Kavehnia, F., Askari, M.R., Mohammadi, A., and Keivani, A. (2007). *Applying Time-Series Regression to Load Forecasting Using Neuro-Fuzzy Techniques*. Powereng, Setubal, Portugal.
- Madsen, H. (2007). *Time Series Analysis*. Boca Raton. Chapman & Hall/CRC
- Hepsen, A., and Vatansever, M. (2011). *Forecasting future trends in Dubai housing market by using Box-Jenkins autoregressive integrated moving average*. International Journal of Housing Market and Analysis. 4(3), 210-223.
- Ibrahim, M.Z., Zailan, R., Ismail, M., and Lola, M.S. (2009). *Forecasting and time series analysis of air pollutants in several area of Malaysia*. American Journal of Environment Sciences. 5(5), 625-632.
- Ismail, Z., Yahya, A. and Shabri, A. (2009). *Forecasting Gold Prices Using Multiple Linear Regression Method*. American Journal of Applied Sciences. 6(8): 1509-1514.
- Kahforoushan, E., Zarif, M., and Mashahir, E.B. (2010). *Prediction of added value of agricultural subsections using artificial neural network: Box-Jenkins and Holt-Winter methods*. Journal of Development and Agricultural Economics. 2(4), 115-121.
- Levin, E.J. and Wright, R.E. (2006). *Short-run and Long-run Determinants of the Price of Gold*. World Gold Council Report, Research study No. 32, Cass Business School, London.
- M., and Massarrat, A.K. (2013). *Forecasting of gold prices (Box Jenkins Approach)*. International Journal of Emerging Technology and Advanced Engineering. 3(3), 662-670.
- Makridakis, S. (1995). *Forecasting: Its roles and value for planning and strategy*. Decision Science and Information Systems. 54, 1-34.
- Nanda, S. (1988). *Forecasting: Does the Box-Jenkins method work better than regression?*. Whitmore School of Business and Economics, University of New Hampshire, Durham.
- Rahman, N.M.F. (2010). *Forecasting of boro rice production in Bangladesh: an ARIMA approach*. Journal of Bangladesh Agriculture. 8(1), 103-112.
- Thompson, H. (2005). *An Introduction to Time Series Regression*. Auburn University.

One Way Cluster Analysis in Grouping Types of Beverages

Farah Hani Abdul Ghani and En. Muhammad Fauzee Hamdan

ABSTRACT

Malaysia is a country that is known for its unique cuisine, and that includes beverages. It is important to learn how different beverages fit into your lifestyle. There are many types of beverages such as juice, carbonate drink, milk and dairy based drink, coffee and tea. However, many people are not aware that some of the beverages might be similar in their compositions. Therefore, one way to identify the similarity of different types of beverages is using the hierarchical one way cluster analysis. In this study, the compositions of beverages dataset consists of calories, carbohydrates, sugars and proteins were analysed. Three different clustering methods which are single linkage, average linkage and complete linkage were applied to the dataset. From the raw dataset, the Euclidean distance was used to measure the closeness between different types of beverages as well as their compositions. Consequently, groups of similar beverages based on their composition were obtained. The results are shown in tree diagrams also known as dendograms. The similarities between types of beverages that high in each of the nutrient compositions can be identify from the clusters that were obtained from the dendograms.

Keywords: *Hierarchical cluster analysis, single linkage, average linkage, complete linkage, Euclidean distance*

Introduction

Malaysia is a country that is known for its unique cuisine, and that includes beverages. It is important to learn how different beverages fit into your lifestyle. While all beverages hydrate, some also provide important nutrients for body needs. Beverages also can energize body, manage health concerns, and satisfy people natural taste for sweetness. Some of the beverages can be a part of a weight-maintenance diet.

However, the varieties of beverages available in local food outlet can sometimes be difficult for people to make their decisions. People might not be aware that some of the beverages might be similar in their compositions in term of calories, carbohydrates, sugar and protein.

One way of identifying the similarity of different types of beverages is by using cluster analysis. Cluster analysis is a method in multivariate statistics to create group of related samples according to their high similarity which are then clustered. In this study, the compositions of Malaysian beverages dataset consists of calories, carbohydrates, sugars and proteins were analysed.

The method used is cluster analysis. Cluster analysis is the task of grouping a set of objects in such a way that objects in the same group are more similar to each other than to those in other groups or clusters. Whether for understanding or utility, cluster analysis has long played an important role in a wide variety of fields such as psychology, biology, statistics, pattern recognition, information retrieval, machine learning and data mining [3].

According to Sharma (1995) [13], this cluster must obey the rules that:

- Data objects in the same cluster should be similar to each other where all of the objects must be homogeneous according to the selected criteria
- Characteristics of data objects in different clusters should be dissimilar or heterogeneous from the objects of other groups.

The objective of clustering is to assign new observations to a known number of groups. It is possible to begin with no assumptions about the number of groups that will be formed. It is just done by accessing similarities or distances [10]. It is easier for people to predict behaviour or properties based on the group membership because they are similar.

One of the most important parts in cluster analysis is distance and similarities. The similarity of two data points can be determined by finding their similarity coefficient, the greater the similarity coefficient, the more similar. The joining or tree clustering method uses the dissimilarities and similarities or distances between objects when forming the clusters. Similarities are a set of rules that serve as criteria for grouping or separating items. The most straightforward way of computing distances is by compute the Euclidean distance. However, there are many types of distances that can be used to measure the similarity and dissimilarity such as Minkowski distance, Manhattan distance and Chebyshev distance. In this study, we will use Euclidean distance.

There are many methods towards clustering, such as hierarchical clustering, partitioning method, rank-invariant method and many more. However, there are two main types of clustering, which are non-hierarchical clustering and hierarchical clustering. Hierarchical

clustering consists of a series of partitions which may run from a single cluster containing all individuals, to n clusters each containing a single individual [1]. Whereas, non-hierarchical technique identify homogeneous groups of cases based on selected characteristics using an algorithm that can handle large number of cases [2]. Nonetheless, in this thesis, we only focus on one way hierarchical cluster analysis.

One way hierarchical cluster analysis is a general approach to cluster analysis in which the objects from a sample of data is been grouped together because they are close to each other on measured characteristics. Hierarchical procedures involve the construction of a hierarch or tree-like structure. One way hierarchical cluster analysis is subdivided into two subgroups which are agglomerative and divisive.

The divisive hierarchical method proceeds in the opposite way of the agglomerative hierarchical method. It separates n objects successively into finer groupings. Divisive hierarchical starts at the top with all data in one cluster. The cluster is split using a flat clustering algorithm [15]. This procedure is applied repeatedly until each data is in its own singleton cluster.

Divisive hierarchical cluster is conceptually more complex than agglomerative hierarchical cluster since it needs a second, flat clustering algorithm as a subroutine. It has the advantage of being more efficient in generate cluster in simple dataset. However, divisive hierarchical technique is less commonly used rather than agglomerative hierarchical technique [16].

In this study we have focused on agglomerative hierarchical cluster analysis to cluster the types of beverages. In the agglomerative methods, each object or observation starts out as its own cluster. Agglomerative hierarchical clustering is a bottom-up clustering method where clusters have sub-clusters, which in turn have sub-clusters. Thus, it reducing the number of clusters by one in each step and it will make all individuals are grouped into one large cluster. For this reason, agglomerative procedures are sometimes referred to as build-up methods [17]. The difference between agglomerative hierarchical cluster and divisive hierarchical cluster are shown by Figure 1.

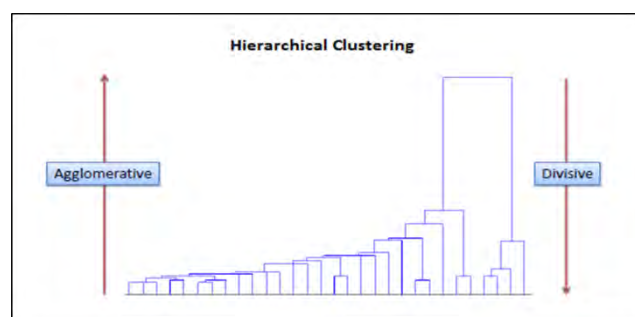


Figure 1: Sample of a dendrogram that differentiate between agglomerative hierarchical cluster and divisive hierarchical cluster.

An agglomerative hierarchical clustering procedure produces a series of partitions of the data, P_n, P_{n-1}, \dots, P_1 . The first P_n consists of n single object 'clusters', the last P_1 , consists of single group containing all n cases [16].

At each particular stage the method joins together the two clusters which are closest together which also indicates the most similar. Differences between methods arise because of the different ways of defining distance or similarity between clusters. Five popular agglomerative procedures used to develop clusters are single linkage, complete linkage, average linkage, Ward's method and centroid. These rules differ in how the distance between clusters is computed. In this study there are only three agglomerative procedures that will be used which is single linkage clustering, complete linkage clustering and average linkage clustering.

There are three main objectives of this study. The first objective is to determine groups of Malaysian beverages compositions which are similar using one way hierarchical cluster analysis. The second objectives is to compare the result between the different clustering methods in one way hierarchical cluster analysis which are single linkage method, complete linkage method and average linkage method. The last objective is to solve the one way hierarchical cluster analysis by using R-software and S-Plus software.

This study may provide information on analysing Malaysian beverages and their compositions which are similar according to calories, carbohydrate, sugar and protein. In addition, this research is important in comparing the results obtained by using different methods of hierarchical cluster analysis. Other than that, it also can help Malaysian people to have an idea when choosing their beverages that fit their lifestyle.

1. Methodology

The data used in this research is a beverages database. Malaysia is well known for the variety of foods and beverages. Thus, there are many beverages that are being served such as Teh Tarik, Neslo, juices and many more.

The data used in this study was obtained from a free Malaysian food and beverages calorie guide website. This website has been created by Kevin Zahri, a Malaysian fitness speaker. He is very active in many fitness consultations and has been a moderator for various health forums and seminars. Besides this, he had appeared and hosted many television shows about fitness, health and lifestyle such as *Gaya HidupSihat* and *Get Set Go*.

The website can be viewed at <http://www.cekodok.com>. The website is created as a free reference for Malaysian about health, fitness tips and nutrition. It includes many useful items such as Malaysian food database, meal planning tools and health tips. Apart from that, we can choose the serving size that we want based on the measure units available there.

Other than that, the data was also taken from www.caloriecount.about.com. The website includes many useful items such as meal planning tools, health tips and food database. This website shows the appropriate serving size for the food nutrition facts per serve. It gives user the option to set the serving size in gram (g), cup, ounce (oz), kilogram (kg), pounds (lbs), millilitre (ml) and litre (l). We have used millilitre (ml) for the measurement in this study and it is strictly taken at 250ml per serve. It also shows the grade for each drink which is easier for user to know whether the drinks are healthy or not.

2.1 Distance Measure

The distance between two objects is used to measure the similarity. Distance can be measured in a variety of ways. For example, there are Euclidean distance, Manhattan distance and Chebyshev distance [12]. However, we are using Euclidean distance for this study.

Euclidean distance is the most common use of distance. Euclidean distance examines the root of square differences between coordinates of a pair of objects [10]. The formula for computing Euclidean distance for n variables is given by

$$d_{ij} = \sqrt{\sum_{k=1}^n (x_{ik} - x_{jk})^2}$$

d_{ij} is root of square distance between object i and j

x_{ik} is the value of the k th variable for i th object

x_{jk} is the value of the k th variable for j th object

n is the number of variables

The more similar the objects, the smaller the distance between them and vice versa.

2.2 Single Linkage Clustering

One of the simplest agglomerative hierarchical clustering methods is single linkage, also known as the nearest neighbour technique. In single linkage, we define the distance between two clusters to be the minimum distance between any single data point in the first cluster and any single data point in the second cluster [11]. On the basis of this definition of distance between clusters, at each stage of the process we combine the two clusters that have the smallest single linkage distance. The formula is as follows.

$$d_{AB} = \min_{i \in B}^{i \in A} (d_{ij})$$

Where d_{AB} is the distance between two clusters A and B , d_{ij} is the distance between individuals i and j .

2.3 Average Linkage Clustering

In the average linkage clustering, the distance between two clusters is defined as the average of distances between all pairs of objects [11], where each pair is made up of one object from each group. The formula is as follow.

$$d_{AB} = \frac{1}{kl} \sum_{i=1}^k \sum_{j=1}^l d_{ij}$$

Where d_{AB} is the distance between two clusters A and B , d_{ij} is the distance between individuals i and j .

2.4 Complete Linkage Clustering

The complete linkage, also called farthest neighbor, clustering method is the opposite of single linkage. Distance between groups is now defined as the distance between the most distant pair of objects, one from each group [11]. This method is the actual opposite of the nearest-neighbor method which is the single linkage. The formula is as follow.

$$d_{AB} = \max_{i \in B}^{i \in A} (d_{ij})$$

Where d_{AB} is the distance between two clusters A and B , d_{ij} is the distance between individuals i and j .

2. Data Analysis

2.1 Calories

Throughout this study, we used three different linkages in agglomerative hierarchical clustering in defining the distance of calories composition data using Euclidean distance. Those methods are single linkage, average linkage and complete linkage method. Based on their respective dissimilarities distance, the groupings of calories composition are shown in the figure below.

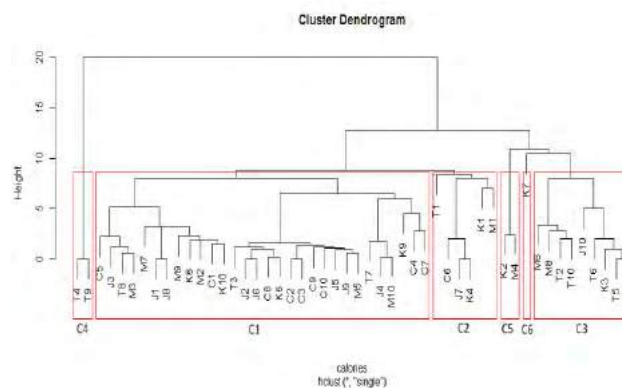


Figure 2: Dendrogram of calories composition clusters using Single Linkage clustering method.

The cluster presented in the Figure 2 was obtained by using the method of nearest neighbour method which is Single Linkage clustering. From this dendrogram, we get seven clusters. Cluster 1 has more members compared to the other cluster. All types of juices were grouping in Cluster 1 except for Mango Juice and Coconut drink. The members of carbonated drinks are also in Cluster 1 except for Red Bull. There were three types of tea in this cluster which are Ice Lemon Tea, Green Tea with sugar and The Tarik. Other than that, four types of coffee also are members in Cluster 1 which are Neslo, Nescafe Mocha, Coffee Bean Vanilla Latte and Nescafe 3 in 1. All types of milk and based also become a member in Cluster 1 except for Goat Milk, Yakult Ace, Low fat yoghurt drink and Vitagen.

Besides, Cluster 2 consist only six members which are Mango juice, Red Bull, White coffee, Ice mocha drink coffee, green tea apple flavour and Goat Milk. For Cluster 3, four out of nine members are come from tea which are Black tea with sugar, Nestea iced tea, Nestea red tea and Yeo’s ice green tea. The other member in Cluster 3 are Coconut drink, Caramel coffee, Cappuccino decaffeinated, low fat yoghurt drink and Vitagen.

Both Cluster 4 and Cluster 5 have two members. Lipton tea and Green tea were in Cluster 4 while Dark roast coffee and Yakult ace in Cluster 5. Cluster 6 also consist one member which is Nescafe Cappuccino.

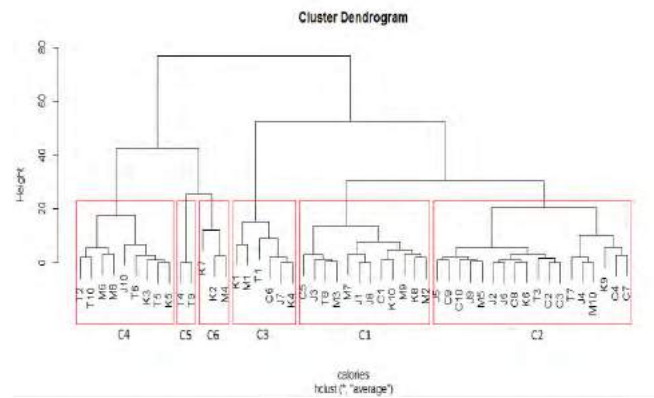


Figure 3: Dendrogram of calories composition clusters using Average Linkage clustering method.

Figure 3 demonstrates the result of calories composition based on the Average Linkage clustering method. From the figure, we have noticed that the dendrogram of clusters grouping are slightly different compared to dendrogram in Figure 2. We obtained six clusters from this dendrogram. Cluster 1 consist twelve members which come from all different groups and the most members in this cluster are milk and dairy based drinks. There is only one member from tea group which is Teh Tarik.

For Cluster 2, five types of juices and seven types of carbonated drinks are the members in this cluster. Green tea with sugar is the only one from the tea group in this cluster and there are addition of two coffee and two milk and dairy based. Cluster 3 has seven members. There are three types of beverages that have only one member in the cluster which are Mango juice, Red Bull and Goat Milk.

Besides, four out of nine members in Cluster 4 are come from tea group which make it the most members in the cluster. There is only one juice in this cluster which is coconut drink. Cluster 5 consists only two members and both are from tea group which are Lipton tea and Green tea. There are three members in Cluster 6 which are Dark roast coffee, Nescafe Cappuccino and Yakult Ace.

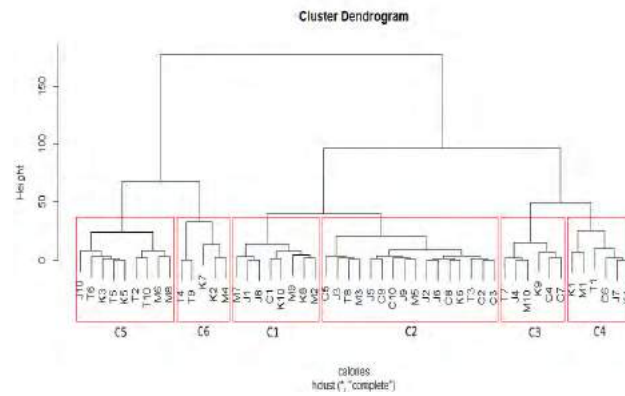


Figure 4: Dendrogram of calories composition clusters using Complete Linkage clustering method.

Figure 4 illustrated the result of calories composition clusters by using Complete Linkage clustering method. From this figure, we obtained six clusters. Cluster 1 has eight members and three of it comes from milk and dairy based group. 100 Plus is the only member from carbonated drink in the cluster. Next, Cluster 2 consist the highest number of members from juices and carbonated drinks and there is only one member from coffee group which is Neslo.

Besides, both Cluster 3 and Cluster 4 have six members. In Cluster 3 and Cluster 4, there are four members that is the only one member come from its group. The four members in Cluster 3 are Pineapple juice, Green tea with sugar, Coffee bean vanilla latte and Nestle Milo while in Cluster 4 the four members are Mango juice, Red bull, Green tea apple flavour and Goat Milk.

Apart from that, teas are the most members in Cluster 5. There is also one member from juice group which is coconut drink. Cluster 6 consist only five members which are Lipton tea, Green tea, Dark roast coffee, Nescafe Cappuccino and Yakult Ace.

From the figure, we can see the cluster membership of each beverage's calories for each of the three methods used. As we can see, the single linkage, average linkage and complete linkage methods formed the same number of clusters which is six clusters. Thus, the numbers of clusters being suggested by these three methods are the same which is six.

Cluster 5 results the same member of cluster for single linkage and average linkage methods. Cluster 7 from single linkage method consist only one member. There are also slight differences in other cluster by comparing the members on each cluster from the three methods used.

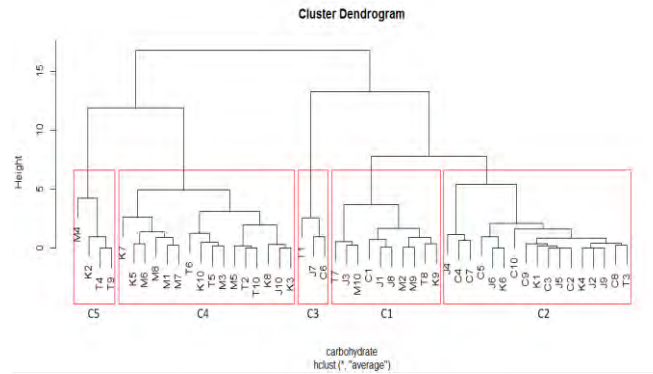


Figure 6: Dendrogram of carbohydrate composition clusters using Average Linkage clustering method.

The clusters presented in Figure 6 were obtained by using Average Linkage clustering method. We have found that the cluster obtained is slightly different from Figure 5. From the dendrogram, we can observe that there are five clusters. The most members of Cluster 1 come from juices and milk and dairy based. There is only one member from carbonated which is 100 Plus and one member from coffee which is Coffee bean vanilla latte. For Cluster 2, all carbonated drinks are included except 100 Plus and Red Bull while ice lemon tea is the only one tea in the cluster.

Besides, there are only three members in Cluster 3 which are Mango juice, Red Bull and Green tea apple flavour. In Cluster 4, the most members are from coffee and milk and dairy based drink while there is one juice in the cluster which is coconut drink. Next, Cluster 5 consist four members and two from it are tea. The members are Lipton tea, Green tea, Dark roast coffee and Yakult Ace.

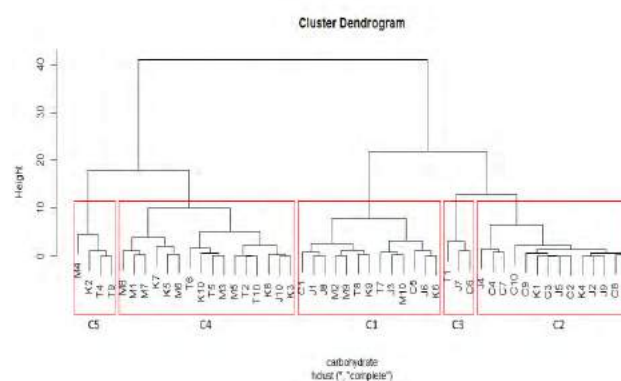


Figure 7: Dendrogram of carbohydrate composition clusters using Complete Linkage clustering method.

The cluster presented in the Figure 7 was obtained by using Complete Linkage clustering method. From this figure, we get five clusters. Juices are the most members in

Cluster 1. There are two members from each group which are carbonated drinks, tea and coffee in this cluster. For Cluster 2, all the members from carbonated drinks are included except 100 Plus, 7up and Red Bull. There is only one tea in Cluster 2 which is Ice lemon tea.

From the cluster obtained, Cluster 3 has only three members which are Mango juice, Red Bull and Green tea apple flavour. Other than that, milk and dairy based drinks are the most members in the Cluster 4. Coconut drink is the only juices in that cluster. Lastly, Cluster 5 consists of four members which are Lipton tea, Green tea, Dark roast coffee and Yakult Ace.

From the comparison, we can analyse the cluster membership of each beverage's carbohydrate for each of the three methods used. As we can see, the average linkage and complete linkage formed the same number of clusters which is five clusters whereas single linkage method formed seven clusters. However, the numbers of clusters being suggested by these three methods are quite the same which is between five and seven.

Cluster 1 for single linkage has more members than average linkage and complete linkage. There are slight differences in cluster 2 for all the three methods. Cluster 3, 4 and 5 results the same member for average linkage method and complete linkage method. Cluster 5 of average linkage and complete linkage merged four beverages from cluster 6 and 7 of single linkage which are Lipton tea, green tea, dark roast coffee and Yakult Ace. Single linkage method formed single member in cluster 7 which is Yakult Ace.

2.3 Sugar

In this section, we want to analyse the clusters formed for sugar composition in beverages in three different methods of hierarchical cluster. The three different methods are single linkage, average linkage and complete linkage clustering method.

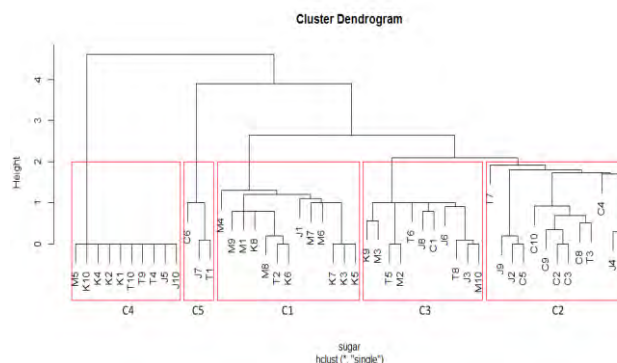


Figure 8: Dendrogram of sugar composition clusters using Single Linkage clustering method.

Figure 8 demonstrates the results sugar composition cluster by using Single Linkage clustering method. From this figure, five clusters were obtained. Cluster 1 has thirteen members and most of it are from milk and dairy based. There are one element from each group of juice and tea which are Lemon juice and Black tea with sugar. For Cluster 2, all members of carbonated drinks are included except 100 Plus and Red Bull. Cluster 2 also consist of two members from tea which are Ice lemon tea and Green tea with sugar.

Besides, there are three members from each group that listed in Cluster 3 which come from juices, tea and milk and dairy based drinks. 100 Plus is the only carbonated drink in Cluster 3. The most members in Cluster 4 are come from coffee group and low fat milk is the only member from milk and dairy based drinks. Next, there are three elements in Cluster 5 which are Mango juice, Red Bull and Green tea apple flavour.

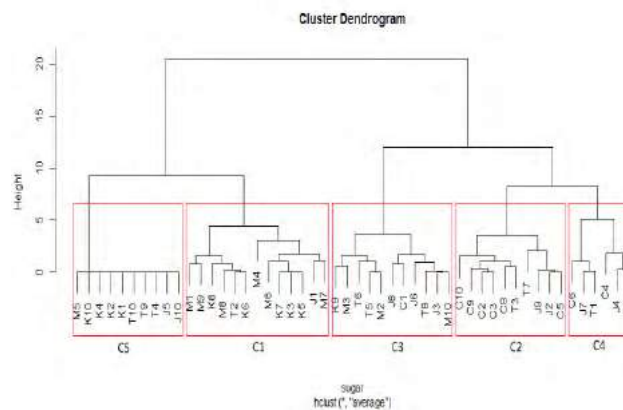


Figure 9: Dendrogram of sugar composition clusters using Average Linkage clustering method.

Figure 9 illustrated the result of sugar composition clusters by using Average Linkage clustering method. From this figure, we obtained five clusters. Cluster 1 grouped milk and dairy based as the most members and followed by coffee. The only members from their group are Lemon juice from juices group and Black tea with sugar from tea group. Carbonated drinks are the most members in Cluster 2 and it has two members from each group of juices and tea.

Other than that, we can see that tea and milk and dairy based are the most members in Cluster 3. There is only one element from carbonated drinks and coffee which are 100 Plus and Coffee bean vanilla latte. Cluster 4 has six members and carbonated drinks are most of it. The other members in that cluster are Pineapple juice, Mango juice and Green tea apple flavour. Besides, coffee has become the most members in Cluster 5 and low fat milk is the only member from milk and dairy based drinks.

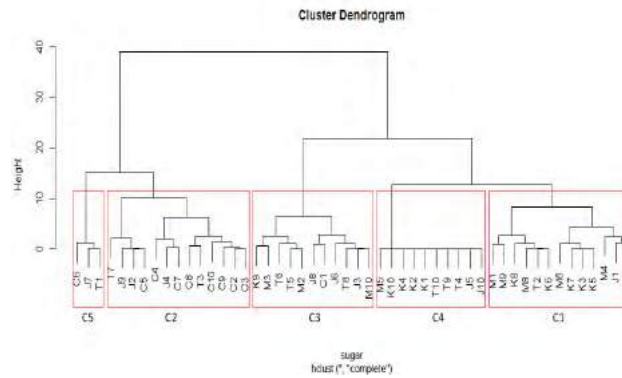


Figure 10: Dendrogram of sugar composition clusters using Complete Linkage clustering method.

The clusters illustrated in dendrogram of Figure 10 were obtained after applying Complete Linkage clustering method to the sugar composition in beverages. From this figure, five clusters were obtained. As we can see, milk and dairy based are the most members in Cluster 1 and followed by coffee. Lemon juice and Black tea with sugar are the only members come from its own group which is juices and tea. All members of carbonated drinks are included in Cluster 2 except 100 Plus and Red Bull and there are three members from juice and two members from tea.

Next, in Cluster 3, three members from three groups were in these clusters which are from juices, tea and milk and dairy based drinks. 100 Plus and coffee bean vanilla latte are the only one from its group. Coffee has the most members in Cluster 4 and low fat milk is the only one from milk and dairy based drinks. There are only three members in Cluster 5 which are Mango juice, Red Bull and Green tea apple flavour.

From the three different figures, we can analyse the cluster membership of each sugar composition in beverages for each of the three methods used. As we can see, all the three methods formed the same number of clusters which is five clusters.

Cluster 1 result the same members of cluster for all three methods. Cluster 2, 4 and 5 from single linkage and complete linkage also has the same member. Cluster 3 from all three methods method consists of same membership except the absence of Nestle Milo at single linkage method.

2.4 Protein

In this section, we want to analyse the clusters formed for protein composition in beverages in three different methods of hierarchical cluster. The three different methods are single linkage, average linkage and complete linkage clustering method.

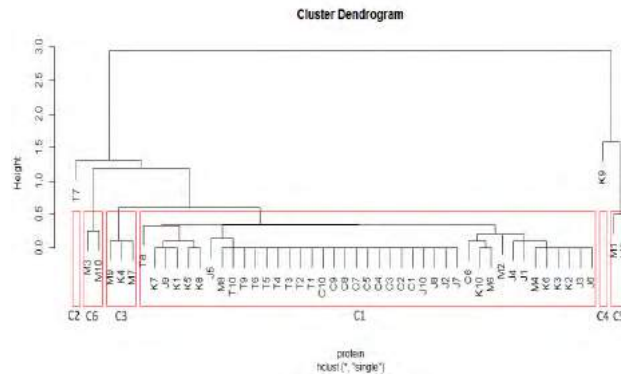


Figure 11: Dendrogram of protein composition clusters using Single Linkage clustering method.

Figure 11 showed the result obtained by applying Single Linkage clustering method to the protein composition in beverages. From the figure, we obtained six clusters. Cluster 1 has the most members in it compared to the other clusters. All types of juices and carbonated drinks were grouped in this cluster. Tea also has all the members included except Green tea with sugar. The only elements that were not listed in Cluster 1 from coffee are Ice mocha drink coffee and Coffee bean vanilla latte.

Cluster 2 and Cluster 4 have only one member which is Green tea with sugar in Cluster 2 and Coffee bean vanilla latte in Cluster 4. There are only three members in Cluster 3 which are Ice mocha drink coffee, Mango milkshake and Horlicks. Besides, both Cluster 5 and Cluster 6 have two members each. The members in Cluster 5 are Goat milk and low fat milk while the members in Cluster 6 are Soya milk and Nestle Milo.

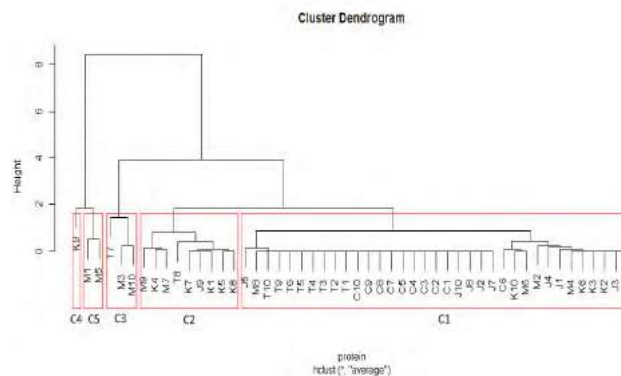


Figure 12: Dendrogram of protein composition clusters using Average Linkage clustering method.

Figure 12 demonstrates the results of protein composition clusters by using Average Linkage clustering method. Five clusters were obtained from the dendrogram. All carbonated drinks were grouped in Cluster 1. Juices and tea also included all their members

in Cluster 1 except fruit cocktail, green tea with sugar and tehtarik. In Cluster 2, the most members are from coffee and there exist single members from juice and tea group which are fruit cocktail and tehtarik.

Cluster 3 consist three members which are green tea with sugar, soya milk and Nestle milo while Cluster 4 consist only one member which is coffee bean vanilla latte. Besides, the number of members in Cluster 5 is two. The two members are goat milk and low fat milk.

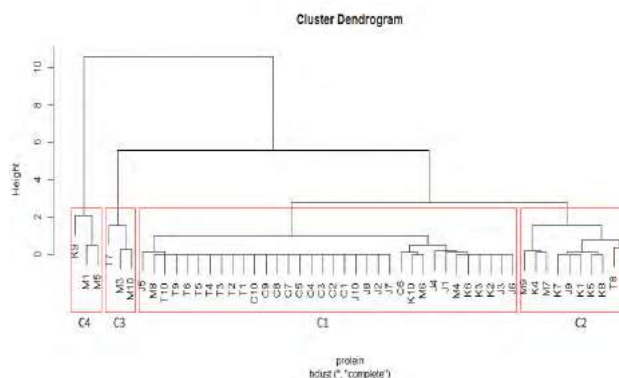


Figure 13: Dendrogram of protein composition clusters using Complete Linkage clustering method.

The cluster presented in the Figure 13 was obtained by using Complete Linkage clustering method to the protein composition of beverages. From this dendrogram, we get four clusters. As we can see from Cluster 1, carbonated drinks members were all grouped in this cluster. Juices and tea also included all its members except fruit cocktail, green tea with sugar and tehtarik. There are also four members from coffee and three members from milk and dairy based in Cluster 1.

Apart from that, Cluster 2 has the most members come from coffee and there are single members from juice and tea which are fruit cocktail and tehtarik. Next, both Cluster 3 and Cluster 4 have three members grouped in it. The members of Cluster 3 are green tea with sugar, soya milk and Nestle milo. The members of Cluster 4 are coffee bean vanilla latte, goat milk and low fat milk.

From the comparison, we can see the cluster membership of each protein composition in beverages for each of the three methods used. As we can see all three methods formed different number of clusters. Single linkage formed six clusters, average linkage formed five clusters and complete linkage formed four clusters. However the numbers of clusters being suggested by these three methods are quite the same which is between range four to six.

Cluster 1 from average linkage method and complete linkage method consist the same members except there is absence of Nestle Bliss in average linkage method. Cluster 2 has the same members for average linkage method and complete linkage method except the

addition of Nestle Bliss in complete linkage method. Cluster 3 also contains the same members for average linkage method and complete linkage method. Single linkage and average linkage methods formed same membership in Cluster 4 and 5. Single linkage formed two members in cluster 6 which are soya milk and Nestle Milo.

3. Results

We use complete linkage method because it is the most suitable method to this data. Complete linkage method also grouped the data according to its range. Table 1 is the range amount of calories in cluster by using complete linkage method.

Table 1:Range amount of calories (kcal)

Cluster	Range
Cluster 1	70.1 – 90
Cluster 2	100.1 – 130
Cluster 3	130.1 – 150
Cluster 4	150.1 – 170
Cluster 5	40.1 – 70
Cluster 6	0 – 40

Based on Table 1, we can see that cluster 4 is the highest range amount of calories. We can say that cluster 4 is a ‘high calories-beverages’. Most of the high calories beverages are come from juices and carbonated drinks. It then follows by cluster 3, 2, 1, 5 and 6. Members in cluster 6 have the lowest amount of calories. Tea and coffee have the most members listed in lowest amount of calories.

Table 2 is the range amount of carbohydrates in cluster by using complete linkage method.

Table 2: Range amount of carbohydrates (grams)

Cluster	Range
Cluster 1	20.1 - 27.0
Cluster 2	27.1 - 35.0
Cluster 3	35.1 - 45.0
Cluster 4	5.1 - 20.0
Cluster 5	0 - 5.0

From Table 2, we can see that the range amount of carbohydrates of cluster 3 is the highest among all clusters. Thus, we can say that cluster 3 is a 'high carbohydrates-beverages'. The beverages include in this cluster are mostly come from juices and carbonated drinks. It then follows by cluster 2, 1, 4 and 5 from high amount of carbohydrates to the lowest. Cluster 5 has the members with lower amount of carbohydrates. Most of the members are from milk and dairy based tea and coffee.

Table 3 is the range amount of sugars in cluster by using complete linkage method.

Table 3: Range amount of sugars (grams)

Cluster	Range
Cluster 1	1.1 – 15.0
Cluster 2	22.1 – 35.0
Cluster 3	15.1 – 22.0
Cluster 4	0 – 1.0
Cluster 5	35.1 – 40.0

Table 3 shows the range amount of sugars in cluster. From the table we can see that members in cluster 5 and cluster 2 have the highest amount of sugars. Thus, they can be classified as 'high sugar-beverages'. Most of the members of these clusters are come from juices and carbonated drinks. It then follows by cluster 3, 1 and 4. Cluster 4 has the lowest range amount of sugar. Most of the members listed in this cluster are from tea and coffee.

Table 4 is the range amount of proteins in cluster by using complete linkage method.

Table 4: Range amount of proteins (grams)

Cluster	Range
Cluster 1	0 – 1.0
Cluster 2	1.1 – 3.0
Cluster 3	3.1 – 6.0
Cluster 4	6.1 – 12.0

From Table 4 we can see that cluster 4 has the highest range amount of proteins. Thus, we categorized it as ‘high protein-beverages’. Members in this cluster are mostly from milk and dairy based. It then follows by cluster 3, 2 and 1 from highest to lowest amount of proteins. Cluster 1 has the lowest range amount of proteins. Most of juices, carbonated drinks, tea and coffee are listed in the cluster 1.

4. Conclusions

Based on the overall study, the numbers of clusters obtained by different methods are quite similar for each of the selected nutrient compositions.

From the cluster of the beverages, based on the result obtained, we got that most of the high calories beverages are come from juices and carbonated drinks. Beverages that high in carbohydrates and sugars are also mostly from juices and carbonated drinks. Besides, milk and dairy based are the most members that listed in a cluster which have the highest amount of protein. Thus, we categorized milk and dairy based as ‘high protein-beverages’. Finally, all the results were obtained by using R-software.

For future research, there are some recommendations that can be suggested from this study. Further studies should be conducted using larger number of variables (i.e more nutrient compositions) so that there are more information about the nutrients in beverages. Besides, there are more beverages that had been consumed by Malaysian. Therefore, the number of data set should be increased. This will make the results more accurate if the sample size is increased.

References

- [1] Everitt, B. S. (1993). Cluster Analysis. (3rd ed.). John Wiley & Sons Inc. Publication.
- [2] Cluster Analysis. Available at :
http://en.wikipedia.org/wiki/Cluster_analysis accessed: 20/10/2014
- [3] Cluster Analysis Tool. Available at :

<http://edndoc.esri.com/> accessed: 25/10/2014

- [4] Adams, I. (2012). Making Healthy Beverage Choices: What You Don't Know Can Hurt You. *Making Healthy Lifestyle Choices*. 120(9). 102-104
- [5] Valsta, L., Borg, P., Heiskanen, S., Keskinen, H., Mannisto, S., Rautio, T., Sarlio-Lahteenkorva, S., and Kara, R. (2008), *Beverages in Nutrition*, 2-3
- [6] Nielsen, S. J. and Popkin, B. M. (2004). Changes in Beverage Intake Between 1977 and 2001. 205-210
- [7] Langfelder, P., Zhang, B., and Horvath, S. (2007). Defining Clusters from a Hierarchical Cluster Tree: The Dynamic Tree Cut Package for R. 719-720
- [8] Xu, R. and Wunsch, D. C. (2009). *Clustering*. 1-33
- [9] Castro, V. E. (2002). Why So Many Clustering Algorithms – A Position Paper. 65-75
- [10] Wilkinson, L., Engelman, L., Corter, J., and Coward, M. (2003). *Cluster Analysis*. 11-13
- [11] Sharma, S.C. (1995), *Applied Multivariate Techniques*, John Wiley & Sons Publication
- [12] Iyigun, C. (2008). Probabilistic Distance Clustering. *Journal of Classification*. 25, 5-26
- [13] Halkidi, M., Batistakis, Y., and Vazirgiannis, M. (2005). Clustering Validity Checking Method: Part 2. 31(3), 19-27
- [14] Rujasiri, P. and Chomtee, B. (2009). Comparison of Clustering Techniques for Cluster Analysis. 43(2), 378-388
- [15] Hair, J. F., Anderson, R. E., Black, W.C. and Babin, B.J. (2009). *Multivariate Data Analysis*. (7th ed.). Prentice Hall.
- [16] Walthouwer, M. J. L., Oenema, A., Soetens, K., Lechner, L. and Vries, H. D. (2014). Are clusters of dietary patterns and cluster membership stable over time? Result of a longitudinal cluster analysis study. *Appetite*. 82, 154-159
- [17] Bsoul, Q., Salim, J. and Zakaria, L. Q. (2013). An intelligent Document Clustering Approach to Detect Crime Patterns. *Procedia Technology*. Vol. 11, 1181-1187
- [18] Yu, S. (2014). Studying the health care systems in seven East Asian countries by the cluster analysis. *Development and Society*. 43(1), 81-107
- [19] Adam, J. M., Hart, W., Gilmer, L., Lloyd-Richardson, E. E. and Burton, K. A. (2014). Concrete images of the sugar content in sugar-sweetened beverages reduce attraction to and selection of these beverages. *Appetite*. 83, 8-10
- [20] Zheng, M., Rangan, A., Olsen, N. J., Andersen, L. B., Wedderkopp, N., Kristensen, P., Grontved, A., Larsen, M. R., Lempert, S. M. and Farnelli, M. A. (2013), Substituting sugar-sweetened beverages with water or milk is inversely associated with body fatness development from childhood to adolescence. *Nutrition*. 31(1), 38-44

GLOBAL DYNAMICS OF A LOTKA-VOLTERRA MODEL WITH TWO PREDATORS COMPETING FOR ONE PREY

Farzana Izzah Binti Adnan & Dr. Faridah Mustapha

Abstract

In the Lotka-Volterra predator-prey model, it is assumed all predators are able to attack prey and reproduce. In this research, the global dynamics of a class 3-dimensional Lotka-Volterra system with eight parameters is studied. This system describes two predators competing for the same food and they share the same prey. This study only focuses on the global dynamics of a system with limited resources of prey. Thus, the sufficient and necessary conditions for the principle of competitive exclusion to hold and give the global dynamical behavior of three species in the first octant will be determined. The model with two predators competing for one prey is formulated from the Lotka-Volterra model with constant and uniform environment. Plus, it is assumed that the two predator species compete purely exploitatively with no interference between rivals and the growth rate of the prey species is logistic in the absence of predation. Basically, there are mathematical modelling consists of ordinary differential equation need to be analyzed. The stability of the equilibrium points in this system is determined by using the Routh-Hurwitz Criteria. Some of the outcomes are shown in the numerical simulation. The result of this research may be implied in ecological studies and provide a new approach to the problem.

Keywords: predator-prey, Lotka-Volterra model, global dynamics, extinction, coexistence, ordinary differential equations, Routh-HurwitzCriteria.

Introduction

Applied math also can be define as a group of methods aimed for solution of problems in sciences, engineering, economics, medicine and etc. study of applied math requires expertise in many areas of mathematics and science, physical intuition and common sense, as well as collaboration skills. Applied math allows for many approaches to the problem and the majority of applied problems need to build mathematical model of a phenomenon, solve the model, and make a development and recommendations for improvement of the performance. Predator-prey system is one of the examples of mathematical modeling that is applied on the ecology system. Lotka –Volterra (Arneodo, A. et al, 1980) was proposed independently the model of a system with two equations to study the predator-prey interaction. The model is the simplest model of predator-prey interactions. They are among the first to study this interaction by making a number of simplifying assumptions that led to nontrivial but tractable mathematical problem.

Literature Review

Predator-prey system problem are introduced by Italian Mathematician Volterra where he developed his ideas about predation from watching the rise and fall of Adriatic fishing fleets. Moreover, the number of fisherman increased when fishing is good, drawn by the success of others. After a time, the fish decrease, may due to over-harvested, and then the number of fisherman also decrease. Then after some tie, the cycle repeated (Trophic Links, 2005). The Lotka-Volterra model is composed of a pair of differential equations that describes predator-prey dynamics in the simplest case which involves only one predator population and also one prey population. It was developed independently by Alfred Lotka and Vito Volterra in 1920's, and is characterized by oscillations in the population size of both predator and prey, with the peak of the predator's oscillation lagging slightly behind the peak of the prey's oscillation.

Huang, Chen and Zhong (2006) found that the stability of ecological systems and the persistence of species within them are fundamental concerns in ecology. Mathematical models of ecological systems, reflecting these concerns, have been used to investigate the stability of a variety of systems. The dynamic relationship between predator and their prey has long been and will continue to be one of the dominant themes in both ecology and mathematical ecology due to its universal existence and importance (Berryman, 1992). Many excellent works have been done for the Lotka–Volterra type predator–prey system.

According to Hardin (1960), “complete cannot coexist”. Hardin’s principle states that two distinct but ecologically, behaviorally, and biologically identical species will not be able presence at the same time and use the same resources indefinitely. One species must eventually outcompete the other. If the principle of competitive exclusion holds, then either predator or prey goes to extinction and the other coexist at steady state. If the principle of competitive exclusion does not hold, both species will coexist at a positive equilibrium.

Mathematical modeling with two predators competing for one prey can be described that the system consist of two predators competing for the same food and share for one prey. By theoretical analysis on this system, we will obtain sufficient and necessary conditions for principle of competitive exclusion to hold and give the global dynamical behavior of the three species in the first octant.

Methodology

Routh-Hurtwitz criteria are a technique of linear stability theory. The methods for gaining insight into models for k species interacting in a community, where $k > 2$. A system comprised of k species with populations N_1, N_2, \dots, N_k would be governed by k equations:

$$\begin{aligned} \frac{dN_1}{dt} &= f_1(N_1, N_2, \dots, N_k) \\ &\vdots \\ \frac{dN_k}{dt} &= f_k(N_1, N_2, \dots, N_k) \end{aligned}$$

This version in fact can be modified to

$$\frac{dN_i}{dt} = f_i(N_1, N_2, \dots, N_k) (i = 1, 2, 3, \dots, k)$$

Or, better still the vector notation

$$\frac{dN}{dt} = F(N)$$

For $N = (N_1, N_2, \dots, N_k)$, $F = (f_1, f_2, \dots, f_k)$ where each of the functions f_1, f_2, \dots, f_k may depend on all some of the species populations N_1, N_2, \dots, N_k .

We shall now suppose that it is possible to solve the equation

$$F(N) = 0$$

as to identify one equilibrium point, $\bar{N} = (N_1, N_2, \dots, N_k)$, satisfying $F(\bar{N}) = 0$

In linearizing equation, we find Jacobian of $F(N)$. This is often symbolized

$$J = \frac{\partial F}{\partial N}(\bar{N})$$

Means that,

$$J = \begin{pmatrix} \frac{\partial f_1}{\partial N_1} & \frac{\partial f_1}{\partial N_2} & \dots & \frac{\partial f_1}{\partial N_k} \\ \vdots & \vdots & \ddots & \vdots \\ \frac{\partial f_k}{\partial N_1} & \frac{\partial f_k}{\partial N_2} & \dots & \frac{\partial f_k}{\partial N_k} \end{pmatrix}_{\bar{N}}$$

So that J is now is $k \times k$ matrix. Eigenvalues J of this matrix now satisfy:

$$\det(J - \lambda I) = 0.$$

Therefore, λ must satisfy a characteristic equation of the form

$$\lambda^k + a_1 \lambda^{k-1} + a_2 \lambda^{k-2} + \dots + a_k = 0.$$

The characteristic equation is a polynomial whose degree k is equal to the number of species interacting. Although for $k = 2$ the quadratic characteristic equation is easily solved, for $k > 2$ this is no longer true.

While we are unable in principle to find all the eigenvalues, we can still obtain information about their magnitudes. Suppose $\lambda_1, \lambda_2, \dots, \lambda_k$ are all known eigenvalues of the linearized system.

The eigenvalues can be obtained in formation of the magnitudes. This known as

$$\frac{dN}{dt} = J \cdot N$$

Recall that all the eigenvalues must all have negative real part since close to the steady states each of species populations can be presented by a sum of exponentials in $\lambda_1 t$ as follows:

$$N_i = \bar{N}_1 + \alpha_1 e^{\lambda_1 t} + \alpha_2 e^{\lambda_2 t} + \dots + \alpha_k e^{\lambda_k t}$$

If one or more eigenvalues have positive real parts, $N_i - \bar{N}_i$ will be an increasing function of t , meaning that N_i will not return to its equilibrium value \bar{N}_i . thus the question of stability of a steady state can be settled if it can be determined whether or not all eigenvalues $\lambda_1, \dots, \lambda_k$ have negative real parts.

Table 1: Ruth-Hurwitz Criteria

Theorem 1 : Ruth-Hurwitz Criteria

Given the characteristics equation for k species

$$\lambda^k + a_1\lambda^{k-1} + a_2\lambda^{k-2} + \dots + a_k = 0$$

Define k matrices as follows:

$$H_1 = (a_1), \quad H_2 = \begin{pmatrix} a_1 & 1 \\ a_3 & a_2 \end{pmatrix}, \quad H_3 = \begin{pmatrix} a_1 & 1 & 0 \\ a_3 & a_2 & a_1 \\ a_5 & a_4 & a_3 \end{pmatrix},$$

$$H_j = \begin{pmatrix} a_1 & 1 & 0 & 0 & \dots & 0 \\ a_3 & a_2 & a_1 & 1 & \dots & 0 \\ a_5 & a_4 & a_3 & a_2 & \dots & 0 \\ \dots & \dots & \dots & \dots & \dots & \dots \\ a_{2j-1} & a_{2j-2} & a_{2j-3} & a_{2j-4} & \dots & a_j \end{pmatrix}, \dots \quad H_k = \begin{pmatrix} a_1 & 1 & 0 & \dots & 0 \\ a_3 & a_2 & a_1 & \dots & 0 \\ \vdots & \vdots & \vdots & \dots & \vdots \\ 0 & 0 & \dots & \dots & a_k \end{pmatrix}$$

Where the (l, m) term in the matrix H_j is

$$a_{2l-m} \quad \text{for } 0 < 2l - m < k,$$

$$1 \quad \text{for } 2l - m,$$

$$0 \quad \text{for } 2l < m \text{ or } 2l > k + m.$$

Then all eigenvalues have negative real part that is, the steady states \bar{N} is stable if and only if the determinants of all Hurwitz matrices are positive:

$$\det H_j > 0 \quad (j = 1, 2, \dots, k)$$

Table 2: Ruth-Hurwitz Criteria for $k = 2, 3, 4$

Ruth-Hurwitz Criteria for $k = 2, 3, 4$

$$k = 2: \quad a_1 > 0 \quad a_2 > 0$$

$$k = 3: \quad a_1 > 0 \quad a_2 > 0 \quad a_1 a_2 > 0$$

$$k = 4: \quad a_1 > 0 \quad a_3 > 0 \quad a_4 > 0 \quad a_1 a_2 a_4 > a_3^2 + a_1^2 a_4$$

For eigenvalues equation, $\lambda^k + a_1\lambda^{k-1} + a_2\lambda^{k-2} + \dots + a_k = 0$.

If all conditions for every k are satisfied, then the steady state for the system will be stable.

Results and Discussion

The model which is assumed that the two predator species compete purely exploitatively with no interference between rivals, the growth rate of the prey species is logistic or linear in the absence of predation, respectively, and the predator's functional response is linear. The model can be written as a system of ordinary differential equations as follows

$$f_1 = \frac{dS(t)}{dt} = S(t) \left(r_3 - \frac{1}{K}S(t) - b_1x(t) - b_2y(t) \right),$$

$$f_2 = \frac{dx(t)}{dt} = x(t)(-r_1 + a_1S(t)),$$

$$f_3 = \frac{dy(t)}{dt} = y(t)(-r_2 + a_2S(t)),$$

Where $x(t)$ represents the population density of the first predator at time t ,
 $y(t)$ represents the population density of the second predator at time t ,

$S(t)$ represents the population density of the prey at time t ,

$r_3 > 0$ is the intrinsic rate of growth of the prey,

$r_i > 0$ is the natural death rate of the i th predator in the absence of prey

$b_i > 0$ is the effect of the i th predation on the prey

a_i is the efficiency and propagation rate of the i th predator in the presence of prey

$K > 0$ is the carrying capacity of the prey.

There are five cases of equilibrium points. There are conditions for each point to be stable.

Case 1: Equilibrium point at the origin: $O = (S, x, y) = (0,0,0)$

At this point of equilibrium, the population density of prey and population density for both predators become extinct. This point is unstable. This can be concluded that it is not possible for population density for both predators and the population density of prey goes to extinction.

Case 2: Equilibrium point at the absence of predators: $E_0 = (S, x, y) = (r_3K, 0,0)$

At this point of equilibrium, there is no predator exist. Point E_0 can be concluded as a degenerated equilibrium if either $r_3K = \frac{r_1}{a_1}$ or $r_3K = \frac{r_2}{a_2}$. This implies that if $r_3K < \min \left\{ \frac{r_1}{a_1}, \frac{r_2}{a_2} \right\}$ then the point of equilibrium $E_0(r_3K, 0,0)$ is stable.

Case 3: Boundary equilibrium point at: $E_1 = (S, x, y) = \left(\frac{r_3}{a_2}, 0, \frac{Ka_2r_3-r_2}{Ka_2b_2} \right)$

At this point of equilibrium, there are the existence of population density of prey and population density of predator 1.

Case 4: Additional boundary equilibrium point at: $E_2 = (S, x, y) = \left(\frac{r_1}{a_1}, \frac{Ka_1r_3-r_1}{Ka_1b_1}, 0 \right)$

At this point of equilibrium, there are the existence of population density of prey and population density of predator 2.

Case 5: Additional boundary equilibrium point at: $E_3 = (S^*, x^*, y^*)$

At this point of equilibrium, there are the existence of population density of prey and population density of both predators.

Interaction of Predator Prey System by Runge-Kutta and Differential Transformation Methods

Fasihah Zulkiflee & Assoc. Prof Dr Normah Bt Maan

1.1 INTRODUCTION

Ordinary differential equations (ODEs) arise in many branches of science such that in physics, astronomy, geology, chemistry, biology, ecology and also in population. They are used in mathematical biology such as in population dynamics and genetics, modelling infectious diseases, biochemical and many more [1]. One of the examples of nonlinear ODEs is predator prey model [2]. Predator prey model which is also denoted as Lotka-Volterra equation is a first order nonlinear differential equations that describe the dynamics of biological systems in which two species interact with each other. Lotka-Volterra equations are the earliest model developed for analysis in population dynamics and have been used as a basis for many models [3]. Ordinary differential equations can be solved by using many methods such that Euler's method, Improved Euler method, Runge-Kutta second and fourth order, Adomian Decomposition Method, differential transformation method, finite difference method and also finite element method. In this research, two types of method which are differential transformation method and Runge-Kutta fourth-order methods will be used for solving the nonlinear ODEs.

1.2 BACKGROUND OF STUDY

1.2.1 Predator prey system

In 1920s, a mathematical model for the population dynamics of predator prey was proposed by Lotka and Volterra and was called Lotka-Volterra predator prey model. The Lotka-Volterra predator prey model describes two species in an ecosystem, which is predator and prey. The model is one of the nonlinear ODEs. This model is also have been used worldwide by many researchers. Many researchers have developed different prey predator model based on Lotka-Volterra model [1]. They used the Lotka-Volterra model and developed into other model with different parameter and boundary conditions [2].

Parra et al. [2] used differential transformation method for solving predator prey model while Manaa et al. [4] used Galerkin method to solve the model and compare it with RungeKutta method. Batiha [10] also solved predator prey problem using the same method as Parra et al. [2] which is differential transformation method but compare the solutions with Adomian decomposition method and power series method. Beck [5] used Euler method while Stefanescu et al. [6] used Newton Rhapsion method. Differential transformation method and Runge-Kutta fourth-order were used to solve the systems

1.2.2 Differential Transformation Method

Differential transformation method was proposed by Zhou, he applied the method to solve linear and non-linear initial value problem in circuit analysis and other differential equations. Many researchers used Differential transformation method to solve ODEs. Batiha [10] uses Differential transformation method to solve predator prey problem while Mirzaee [11] in other hand used Differential Transform Method in solving nonlinear ODEs.

1.2.3 Basic definitions and properties of differential transformation

method. [9]

Definition 1

If $u(t)$ is analytic in the domain T , then it will be differentiated continuously with respect to time t ,

$$\frac{d^k u(t)}{dt^k} = \phi(t, k), \text{ for all } t \in T \quad (1.1)$$

for $t = t_i$, then $\phi(t, k) = \phi(t_i, k)$, where k belongs to the set of non-negative integers, denoted as the K -domain. Therefore, Eq (2.1) can be rewritten as

$$U(k) = \phi(t_i, k) = \left[\frac{d^k u(t)}{dt^k} \right] \Big|_{t=t_i}, \quad (1.2)$$

where $U(k)$ is called the spectrum of $u(t)$ at $t = t_i$

Definition 2

If $u(t)$ can be expressed by Taylor's series, then $u(t)$ can be represented as

$$u(t) = \sum_{k=0}^{\infty} \left[\frac{(t-t_i)^k}{k!} \right] U(k) \quad (1.3)$$

Eq (2.4) is called the inverse of $U(k)$. Using the symbol "D" denoting the differential transformation process and combining (2.2) and (2.3), it is obtained that

$$u(t) = \sum_{k=0}^{\infty} \left[\frac{(t-t_i)^k}{k!} \right] U(k) \equiv D^{-1}U(k) \quad (1.4)$$

Using the differential transformation, a differential equation in the domain of interest can be transformed to an algebraic equation in the K-domain and the $u(t)$ can be obtained by a finite-term of Taylor's series plus a remainder. Thus

$$u(t) = \sum_{k=0}^{\infty} \left[\frac{(t-t_i)^k}{k!} \right] U(k) + R_{n+1}(t) \quad (1.5)$$

1.2.4 The operation properties of differential transformation. [9]

If $u(t)$ and $v(t)$ are two uncorrelated functions with time t where $U(k)$ and $V(k)$ are the transformed functions corresponding to $u(t)$ and $v(t)$ then we can easily proof the fundamental mathematics operations performed by differential transformation and listed as follows

1. If $z(t) = u(t) \pm v(t)$ then,

$$Z(k) = U(k) \pm V(k)$$

2. If $z(t) = \alpha u(t)$ then,

$$Z(k) = \alpha U(k)$$

3. If $z(t) = \frac{du(t)}{dt}$ then,

$$Z(k) = (k+1)U(k+1)$$

4. If $z(t) = \frac{d^2u(t)}{dt^2}$ then,

$$Z(k) = (k+1)(k+2)U(k+2)$$

5. If $z(t) = \frac{d^m u(t)}{dt^m}$ then,

$$Z(k) = (k + 1)(k + 2) \dots (k + m)U(k + m)$$

6. If $z(t) = u(t)v(t)$ then,

$$Z(k) = \sum_{l=0}^k V(l)U(k - l)$$

7. If $z(t) = t^m$ then,

$$Z(k) = \delta(k - m), \delta(k - m) = \begin{cases} 1, & \text{if } k = m \\ 0, & \text{if } k \neq m \end{cases}$$

8. If $z(t) = e^{\lambda t}$ then,

$$Z(k) = \frac{\lambda^k}{k!}$$

9. If $z(t) = (1 + t)^m$ then,

$$Z(k) = \frac{m(m - 1) \dots (m - k + 1)}{k!}$$

10. If $z(t) = \sin(\omega t + \alpha)$ then,

$$Z(k) = \frac{\omega^k}{k!} \sin\left(\frac{\pi k}{2} + \alpha\right)$$

11. If $z(t) = \cos(\omega t + \alpha)$ then,

$$Z(k) = \frac{\omega^k}{k!} \cos\left(\frac{\pi k}{2} + \alpha\right)$$

12. If $U(k) = D[u(t)], V(k) = D[v(t)]$, and c_1 and c_2 are independent of t and k then,

$$D[c_1 u(t) + c_2 v(t)] = c_1 U(k) + c_2 V(k)$$

13. If $z(t) = u(t)v(t), u(t) = D^{-1}[U(k)], v(t) = D^{-1}[V(k)]$,

$$D[z(t)] = D[u(t)v(t)] = U(k) \otimes V(k) = \sum_{l=0}^k V(l)U(k - l), \quad (1.6)$$

where \otimes denotes the convolution.

Therefore, the transform of $u^m(t)$, where m is a positive integer, can be obtained as follows:

$$D[u^m(t)] = U^m(k) = U^{m-1}(k) \otimes U(k) = \sum_{l=0}^k U^{m-1}(l)U(k-l) \quad (1.7)$$

1.2.5 Runge-Kutta fourth order.

The RungeKutta methods are an important family of implicit and explicit iterative methods for the approximation of solution of initial value problems. These techniques were developed around 1900 by the mathematicians C.Runge and M.W.Kutta. Parra et al. [2] usesRungeKutta method to solve predator prey models and the error were compared with exact solutions.

RungeKutta order 4th is one of the explicit RungeKutta methods and this method is called the classic fourth order method. This method is the most common form of the RungeKutta method.

Formula of RungeKutta order 4th

$$\frac{dy}{dx} = f(x, y(x)), y(x_0) = y_0$$

$$K_1 = h f(x_i, y_i)$$

$$K_2 = h f(x_i + \frac{h}{2}, y_i + \frac{K_1}{2})$$

$$K_3 = h f(x_i + \frac{h}{2}, y_i + \frac{K_2}{2},)$$

$$K_4 = h f(x_i + h, y_i + K_3)$$

$$y_{i+1} = y_i + \frac{1}{6} (K_1 + 2K_2 + 2K_3 + K_4) \quad (1.8)$$

1.3 METHODS OF SOLUTIONS FOR PREDATOR PREY SYSTEMS.

There are many methods that can be used to solve the predator prey systems. Some methods were introduced which are Adomian Decomposition Method, Differential Transformation Method, Variational Iteration Method, Euler's method, Taylor's method, Runge-kutta method, Finite Element Method, Galerkin Method and many more. But in this research the

main focus is to find solutions using differential transformation method and Runge-Kutta fourth-order. Details for each method will be discussed in the next sections.

1.3.1 Differential Transformation Method.

The differential transformation method is one of the methods for solving predator prey systems which uses the form of polynomials as the approximation to the exact solution. This method is an iterative procedure for obtaining Taylor series solutions of differential equations. These are the general procedure for finding the solution of predator prey system using differential transformation method:

Step 1: Transform the Predator prey system using basic definition and Transformed function in table 3.3.1, the predator prey transformation is shown in below equation.

$$X(k + 1) = \frac{1}{k+1} [aX(k) - b \sum_{m=0}^k X(m)Y(k - m)] \quad (1.9)$$

$$Y(k + 1) = \frac{1}{k+1} [-cY(k) + d \sum_{m=0}^k X(m)Y(k - m)] \quad (1.10)$$

Step 2 :Start with $k = 0, 1, 2, \dots, n$, the higher the n values, the higher the rate of convergence.

Step 3: Then, use the calculated $X(k+1)$ and $Y(k+1)$ and express it into polynomials function $x(t)$ and $y(t)$.

Step 4 :After getting the solution in polynomials form, insert the value of t and plot the graph to see the interaction between species.

1.3.2 Runge-Kutta order fourth Method.

Runge-Kutta fourth-order is one of the methods that commonly used in solving many ODEs. Runge-Kutta fourth-order method is similar with Euler's and others Runge-Kutta method. This method is an iterative method to reduce the approximation error. Runge-Kutta fourth-order was choose because it is more accurate to exact solution than Euler's method or Runge-kutta second-order. Before we start to discuss the Runge-Kutta fourth-order method, the formula for solving Predator prey systems is given first.

RungeKutta order fourth in Predator Prey systems

Hence the general procedure for finding the solution of Predator Prey Method is:

Step 1 :Use the formula RK-4 given for solving predator prey systems.

$$\frac{dx}{dt} = f(t, x(t), y(t)) \quad x(t_0) = x_0$$

$$\frac{dy}{dt} = g(t, x(t), y(t)) \quad y(t_0) = y_0$$

$$K1 = h f(t_i, x_i, y_i)$$

$$L1 = h g(t_i, x_i, y_i)$$

$$K2 = h f\left(t_i + \frac{h}{2}, x_i + \frac{K1}{2}, y_i + \frac{L1}{2}\right)$$

$$L2 = h g\left(t_i + \frac{h}{2}, x_i + \frac{K1}{2}, y_i + \frac{L1}{2}\right)$$

$$K3 = h f\left(t_i + \frac{h}{2}, x_i + \frac{K2}{2}, y_i + \frac{L2}{2}\right)$$

$$L3 = h g\left(t_i + \frac{h}{2}, x_i + \frac{K2}{2}, y_i + \frac{L2}{2}\right)$$

$$K4 = h f(t_i + h, x_i + K3, y_i + L3)$$

$$L4 = h g(t_i + h, x_i + K3, y_i + L3) \quad (1.11)$$

$$x_{i+1} = x_i + \frac{1}{6}(K_1 + 2K_2 + 2K_3 + K_4) \quad (1.12)$$

$$y_{i+1} = y_i + \frac{1}{6}(L_1 + 2L_2 + 2L_3 + L_4) \quad (1.13)$$

Step 2 :Find stopping point, $i = 0,1,2 \dots n$. Stopping point are to estimate until what iteration needed.

Step 3 :Do the iteration until the stopping point.

Step 4 : Plot the graph to see the relation between species.

1.4 DATA ANALYSIS

The predator prey equations below were solved using differential transformation method and Runge-Kutta fourth order to see the interaction between species. To see the interaction between species, need to considered two cases where prey population $x(t)$ is greater than predator $y(t)$ and prey population $x(t)$ is lesser than predator population $y(t)$.

Prey population is greater than predator population

$$\begin{aligned}x'(t) &= 0.5471x(t) - 0.0281x(t)y(t) \\y'(t) &= -0.8439y(t) + 0.0266x(t)y(t)\end{aligned}\tag{1.14}$$

$$x_0 = 30, y_0 = 4$$

Prey population is lesser than predator population

$$\begin{aligned}x'(t) &= 0.5471x(t) - 0.0281x(t)y(t) \\y'(t) &= -0.8439y(t) + 0.0266x(t)y(t)\end{aligned}\tag{1.15}$$

$$x_0 = 4, y_0 = 30$$

The equations were solved using Mathematica Software. The solutions obtained are listed in table 1.1 and table 1.2 and plotted in Figure 1.1 and Figure 1.2. From the figure, when population of prey is larger than predator, the population for predator is increasing as the source of food for predator is increases while when prey population is smaller, the predator population will decrease as their source of food is decreasing. It shows that predator depends on prey for its source of food.

1.5 CONCLUSION

The initial task of the work was to study Lotka-Volterra predator prey model. Lotka-Volterra predator prey model consists of two species, which are predator and prey. After understanding the system, the system was solved using differential transformation method and Runge-Kutta fourth-order method. Simple predator prey model were given to illustrate the interaction between predator and prey. From the solutions, it shows that predator depends on prey to survive.

Table 1.1: Table of predator prey solution when $x(t)$ larger than $y(t)$

Time	Prey RK-4	Predator RK-4	Prey DTM	Predator DTM
t	x(t)	y(t)	x(t)	y(t)
0	30	4	30	4
0.1	31.3335	3.9887	31.3335	3.9887
0.2	32.7266	3.9920	32.7266	3.99192
0.3	34.1806	4.0103	34.1806	4.01052
0.4	35.6965	4.0447	35.6965	4.04587
0.5	37.2753	4.0963	37.2749	4.10002
0.6	38.9172	4.1663	38.9161	4.17589
0.7	40.6223	4.2563	40.6192	4.27756
0.8	42.3901	4.3685	42.3827	4.41043
0.9	44.2194	4.5051	44.2029	4.58161
1.0	46.1082	4.6691	46.0742	4.8002

Table 1.2: Table of predator prey solution when $x(t)$ smaller than $y(t)$

Time	Prey DTM	Predator DTM	Prey RK-4	Predator RK-4
t	x(t)	y(t)	x(t)	y(t)
0	4	30	4	30
0.1	3.89519	27.8631	3.8952	27.8633
0.2	3.81518	25.872	3.8152	25.8725
0.3	3.75704	24.0188	3.757	24.0196
0.4	3.71842	22.2955	3.7184	22.2964
0.5	3.69743	20.6943	3.6974	20.6953
0.6	3.69253	19.2073	3.6925	19.2085
0.7	3.70251	17.8273	3.7025	17.8286
0.8	3.72642	16.5473	3.7264	16.5486
0.9	3.7635	15.3604	3.7634	15.3617
1	3.81316	14.2602	3.8131	14.2616

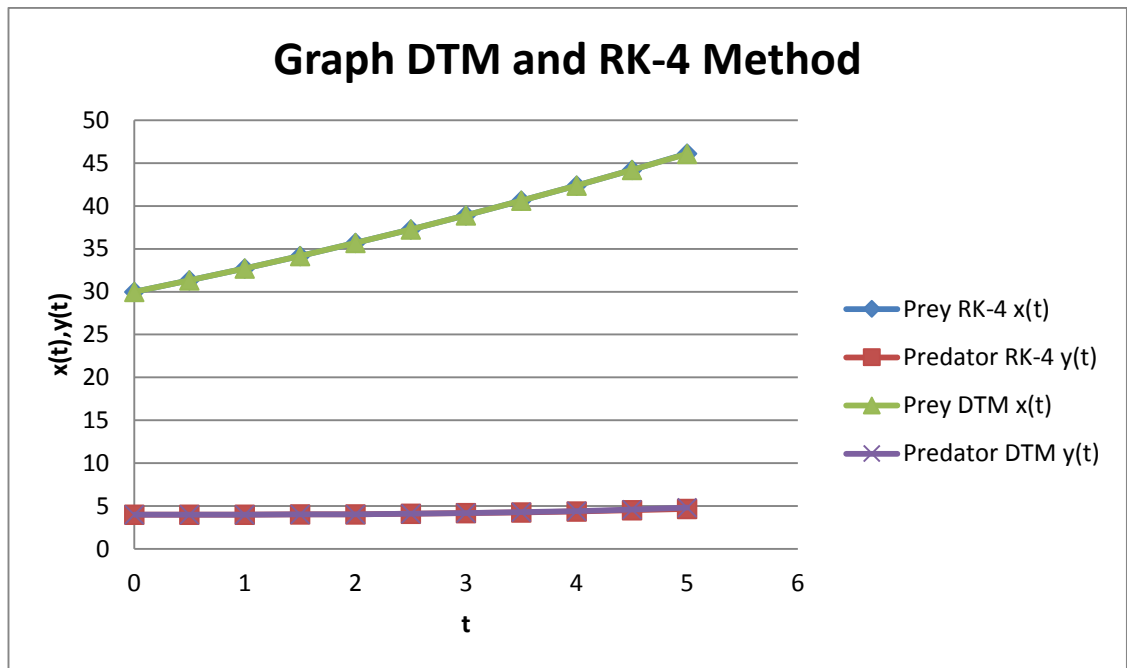


Figure 1.1 Solution graph of predator prey system when $x(t)$ is larger than $y(t)$

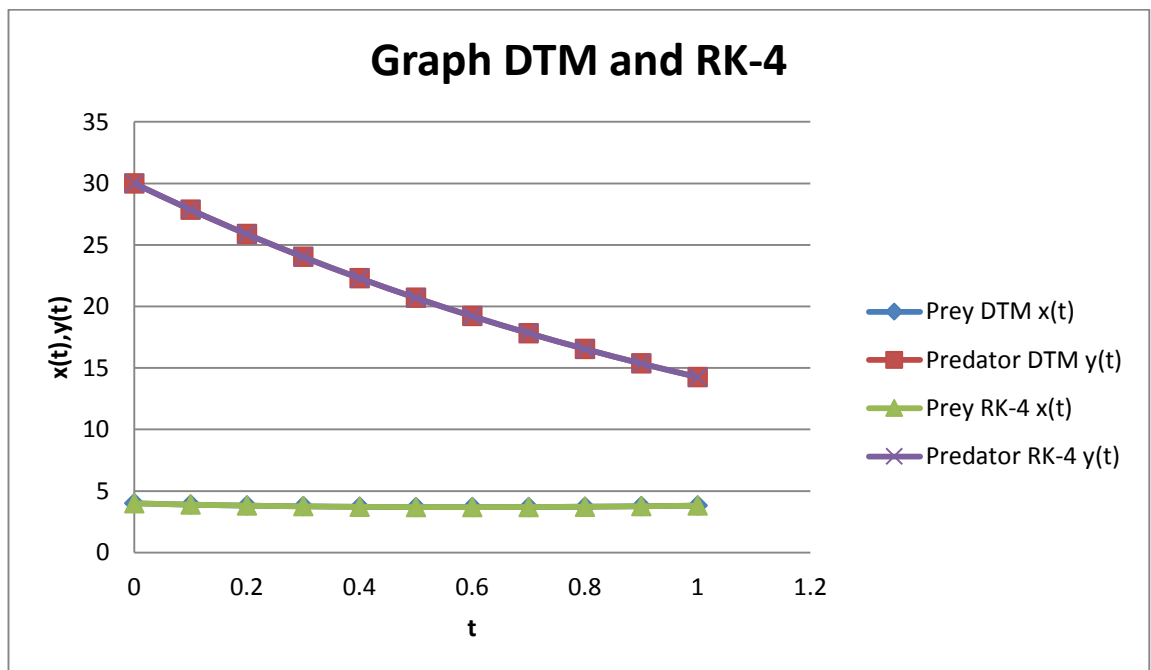


Figure 1.2 Solution graph of predator prey system when $x(t)$ is smaller than $y(t)$

REFERENCES

- [1] Chasnov, J. (2009). *Modelling in Biology*. Hong Kong: The Hong Kong University of Science and Technology.
- [2] Gilberto Gonzalez-Parra, A. J., & Cogollo, M. R. (2013). Numerical-analytical solutions of predator prey models. *Wseas Transactions on Biology and Biomedicine*, 79-86.
- [3] Obaid, T. A. (2013). The Predator-Prey Model Simulation. *Basrah Journal of Science*, 31(2): 103-109.
- [4] Saad A. Manaa, A. F. (2007). Numerical solution of non-linear prey predator system using finite element method. *Raf. J. of comp. & Math's, Vol 4*, 113-128.
- [5] Beck, M. (2003). *Symplectic Methods Applied to the Lotka-Volterra System*. Canada: McGill University, Montreal Quebec.
- [6] Razvan Stefanescu, Gabriel Dimitriu. (2009). Numerical Approximation of a Free Boundary Problem for a Predator-Prey Model. *Free Boundary Problem for a Predator Prey Model*, 548-555.
- [7] Hussein, S. (2010). Predator-Prey Modelling. *Undergraduate Journal of Mathematical Modelling: One+Two*, Article 32.
- [8] Gonze, D. (2013). *Numerical methods for Ordinary Differential Equations*.
- [9] Hassan, I.A.H (2008). Application to differential transformation method for solving systems of differential equations. *Applied Mathematical Modelling*. 32,2552-2559
- [10] Batiha, B. (2015). The solution of the prey and predator problem by differential transformation method. *International Journal of Basic and Applied Sciences*, 36-43.
- [11] Mirzaee, F. (2011). Differential Transform Method for Solving Linear and Nonlinear Systems of Ordinary Differential Equations. *Applied Mathematical Science, Vol. 5*, 3456-3472.
- [12] El-Shahed, M. (2008). Application of differential transform method to nonlinear oscillating systems. *Communication in Nonlinear Science and Numerical Simulation* 13, 1714-1720.
- [13] M.S.H. Chowdhury, I. Hashim, S. Mawa. (2009). Solution of prey-predator problem by numeric-analytic technique. *Communication in Nonlinear Science and Numerical Simulation* 14, 1008-1012.

Conclusion

Thus the results of the research will lead to a new insight into the mechanism of natural selection and provide a new approach to the problem of biological pest control. Usually biological pest control requires the introduction of a harmless or less harmful predator decreasing the pest predator population to an acceptable level which implies that the introduced predator species must have higher survival capacity than the pest predator expected. The expected results will show that the intuition is not always true if the resources for prey are limited. This is because there exist some parameter values such that the two predator species can eventually become extinct and only the prey species survive.

References

- Arneodo, A., Couillet, P., and Tresser, C., *Occurrence of strange attractors in three-dimensional Volterra equations*, Phys. Lett., 79A (1980), pp. 259-263
- Bascompte J, Solé RV (1996) *Habitat Fragmentation and Extinction Thresholds In Spatially Explicit Models*. Journal of Animal Ecology 65: 465-473.
- Berryman, A. A. (1992). *The Origins and Evolutions Of Predator-Prey Theory*. Ecology 73. 1530-1535
- G. Hardin, *The competitive exclusion principle*, Science, 131 (1960), pp 1292-1297.
- Huang Y., Chen, F And Zhong L. (2006). *Stability Analsis Of Predator Prey Model With Holling Type 3 Response Function Incorporating A Prey Refuge*.
- Tilman D, May RM, Lehman CL, Nowak MA (1994) *Habitat destruction and the extinction debt*. Nature 371: 65-66

MATHEMATICAL MODELING OF ANIMAL DISEASE BY USING ARTIFICIAL NEURAL NETWORK

Fatin Naemah Mohd Farid & Norma Alias

Abstract

This paper studies the implementation of Artificial Neural Network (ANN) where it well-known recently in veterinary disease research field in Malaysia. The parameter identification under consideration is types of animal disease, types of species and locations of disease based on the Geographical Information System (GIS) data set. There are many types of animal diseases that affect farm animals in Malaysia. In this research, the method of multilayer perceptron neural network is used as main model since it is an effective solving method in predicting the future of veterinary disease. ANN has ability to visual animal diseases involving the computational model. The model is to present the relationship between cause of the species and location and consequence of animal disease without emphasizing the process, considering the initial and boundary condition and considering the nature of the relations. The data collection of animal disease is considered as a large sparse data set. Therefore method of ANN is well suited for optimizing of the data, to train the data operational and to predict the parameter identification of animal disease. The output layers of ANN are plotted in SPSS software for statistical solution and MATLAB programming for sequential ANN implemented. The ANN will be compare to genetic algorithm for the performance and effectiveness of the method. The numerical simulation of ANN helps in future prediction of animal disease based on the species and location parameters.

Keywords: mathematical modeling, artificial neural network, genetic algorithm, GIS, VRI, SPSS, MATLAB

Introduction

Farm animal is a living animal which easily infected by diseases if there is no intensive care. These infected diseases are mainly caused by unnatural pollution, weather and habitat. Thus, it leads bacteria to grow. Therefore, the bacteria spread either to human or animal hence, the bacteria is then called as disease since it gives negative effect to human and animal. The common disease that attack animal's farm mostly is Brucellosis based on the data given by Veterinary Research Institute (VRI) 2011. This type of disease will cause retention of placenta, abortion, calf loss in animals, still birth and infertility, and it is also can result in an economic loss in industries (Blackburn *et. al.*, 2007).

Brucella organism is a small aerobic intracellular coccobacilli, it is located in the reproductive organs of host animals and also causing abortions and sterility. They are tears in large numbers in animal's urine, milk, placental fluid, and other fluids. There are 8 species of Brucella organism that have been identified, named primarily for the source animal or features of infection. The following four have moderate-to-significant human pathogenicity; sheep is infected by *Brucella melitensis* with highest pathogenicity, pig is infected by *Brucella suis* with high pathogenicity, cattle is infected by *Brucella abortus* with moderate pathogenicity and dog is infected by *Brucella canis* with moderate pathogenicity.

In present days, farmed animals are easily infected by disease such as BACFT, BMCFT, JOCFT, LMAT, CLA, and MCFT. These are suspected disease identified by a group of research where JOCFT which it is a species of Johnes. While, BMCFT and BACFT are the species of Brucellosis, MCFT and LMAT are the species of Meliodosis and

Leptospirosis, respectively. This research is conducted by using the data of the veterinary disease that is generated by the Geographical Information System (GIS) Malaysia. The data obtained is lack of future prediction on what is the dominant and disease that is infected at specific location and species.

Literature Review

In machine learning and related fields, artificial neural network (ANN) is a computational model inspired by a central nervous system (neuron(s) in brain), and are used to estimate functions that can depend on a large number of inputs and are generally unknown (Neha *et al.*, 2014). The development of neurobiology study enables researchers to create mathematical models of neurons to stimulate neural behavior. Neural network consist a number of simple neuron like processing elements and a number of weighted connections between the elements. Those weights are on connections encode the network (Volna, 2010). In this research, ANN is used to give an output to predict animal disease, hence, it will help to predict the disease based on location and species happen for future study.

The basic definition or concept can be seen through paper as written by Khashei *et al.* in 2010 says that Artificial neural network is a computational model that tries to account for the parallel nature of human brain. Besides ANN is one of the most accurate and widely used forecasting model applied in forecasting social, economic and etc (Al-Shayea *et al.*, 2010). The characteristics of ANN are fault tolerance, distributed memory, learning ability, collective solution, weighted parameter and network structures (Vidushi, 2012).

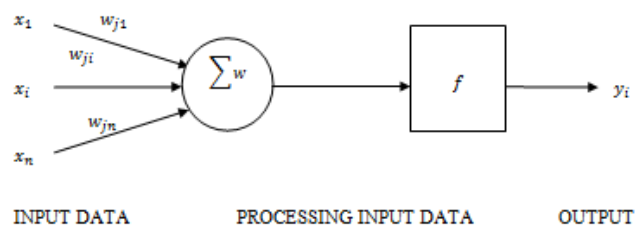


Figure 1 Basic Elements of ANN

For multilayer perceptron, it contains several single layer perceptron. Those single layer perceptron as in Figure 1 were arranged according some hierarchy. The hierarchy should follow the characteristics. Some of the characteristics were inputs of first layer is taking with the number of perceptron same the number of vectors X of the problem. Then, the output layer generate outputs with the number of neuron equal to the desired number of quantities computed from the inputs as well as there is one layer between single perceptron with another (Husna, 2013).

From (Karlik *et al.*, 2011), the function of activation ANN is to transfer the activation level of a neuron to an output signal. The most important unit in Neural Network structure is their net inputs by using a scalar-to-scalar function called as activation function or threshold function or transfer function and the output of result value called as unit's activation. During the training process, the weights are adjusted in order to make the actual outputs (predicted) close to the target (measured) outputs of the network. The transfer function or also known as activation function used to solve non-linear problems include Unipolar Sigmoid function, Bipolar Sigmoid function, Hyperbolic Tangent function, Radial Basis function, Conic Section function and etc. This is because it is convenient to differentiate, and this can minimize the calculation contents for training

Methodology

The mathematical modeling of ANN is started with acquiring GIS data which contains mapping system information about farm mapping department for resource management of livestock and farm infrastructure, mapping animal disease index in Malaysia and, mapping information and the location of the premises registered under Veterinary Services Department, Malaysia. The input data consists of species and location. The output signal consists in a single number representing the animal disease.

By Safi, 2011 stated that, to train the network, we used the well-back propagation algorithm (BP) of MLP, which consists of an optimization procedure aimed at minimizing the RMSE error observed at the output layer. This algorithm uses a supervised learning mode, meaning that the output corresponding to each input is a priori known, which makes it possible to compute signal errors and try to reduce them through epochs. The iteration of BP consists of two main steps. The first step consists in presenting a training example at the input layer of the network and propagating forward the corresponding signal in order to produce a response at the output layer. The second step consists in computing error gradients and propagating them backward in order to update the synaptic weights of all by updating the nodes in hidden layer(s), activation function, transfer function and training function in order to obtain the small RMSE. MATLAB was used to carry out this step. After getting the results, classification and identification for data can be done. In addition, this chapter also discussed about the definition of prediction performance measurement that had been used in this study.

The study has 3 main parts. First is process understanding of overall of ANN. While this process of understanding, the data are manually extracted from VRI data into excel and SPSS software by selected parameters as input and output variables. Second is developing model and code for ANN to show the architecture of ANN, and to train the data by using the of MATLAB software. The process can be proceeding to mathematical modeling. Otherwise, the process needs to adapt with ANN. If satisfy with convergence criterion, visualization and prediction, the numerical analysis and performance evaluations can be performed based on the objectives.

Performance measurement is aim to measure the performance of the method and checks the error. This part shows the analyses that have been done for ANN result. There were mean square error and root mean square error. The result of these MSE and RMSE will then be compare to the MSE and RMSE of genetic algorithm and compare the RMSE between the softwares. MSE is the average of the square of the difference between each output processing element and the desired output. It is used to determine how well the network output fits the desired output, but it doesn't reflect whether two sets of the data move in the same direction. (Rohit, 2012)

$$MSE = \left[\sum_1^N \left(\frac{Q_{ob} - Q_{pr}}{n} \right)^2 \right]$$

RMSE is actually the root of MSE presents information on the short term efficiency, which is the benchmark of the difference of predicted values about observed values. The lower RMSE, the more accurate is the evaluation and the coefficient of determination (also called R square) measures the variance that is interpreted by the model, which is the reduction of variance when using the model.

$$RMSE = \sqrt{\frac{1}{n} \left[\sum_1^N \left(\frac{Q_{ob} - Q_{pr}}{Q_{ob}} \right)^2 \right]}$$

Results and Discussion

The data of veterinary disease were collected based on selected input and output variables that generated by the geographical information system (GIS). The data were sorted using SPSS from VRI Excel data. The data were sorted in different disease, species and location. The total data used in this research are 698 data. From this data, 465 data have been used to train the network while another 233 data are used to test the network

Table 1 The Number of Suspected Disease Reported in each area

Disease State	BACFT	BMCFT	CLA	JOCFT	LMAT	MCFT	Grand Total
Johor	4	17	4	5	2	9	41
Kedah	-	6	-	-	-	-	6
Kelantan	-	4	1	-	-	1	6
Melaka	26	17	4	30	3	4	84
Negeri Sembilan	5	28	11	15	14	25	98
Pahang	2	18	15	33	26	15	109
Perak	33	37	19	32	3	22	146
Perlis	-	1	-	-	-	1	2
Pulau Pinang	-	9	-	-	-	-	9
Sabah	4	28	8	32	-	36	108
Sarawak	1	1		1	1	1	5
Selangor	-	13	9	6	-	-	28
Terengganu	-	28	25	-	-	3	56
Grand Total	75	207	96	154	49	117	698

The Table 4.1 shows the number of suspected diseases reported in each location. The highest number of cases reported is in Perak. The second highest is in Sabah and Pahang. There are 108 and 109 cases reported in each location, respectively. Perlis has the lowest number of suspected diseases attacked to species in this area which is 2. On the other hand, the most infected disease was observed in Perak is BMCFT. We also found out that BMCFT is the highest disease that infected in all locations with grand totals of 207 cases reported following by JOCFT, MCFT, CLA, BACFT and LMAT by each reported 154, 117, 96, 75 and LMAT cases respectively. LMAT is a suspected disease that less happen in all locations which is 49 cases reported.

Table 2 The Number of Species and Suspected Disease cases reported

Disease Species	BACFT	BMCFT	CLA	JOCFT	LMAT	MCFT	Grand Total
Buffalo	5	-	-	4	2	-	11
Cow	65	3	-	97	23	5	193
Goat	5	180	93	50	21	104	453
Sheep	-	22	3	3	3	8	39
#NULL!	-	2	-	-	-	-	2
Grand Total	75	207	96	154	49	117	698

Table 2 shows the number of species attacked by suspected disease in all locations. Goat has the highest number of infected by BMCFT which is 180 cases of infection. The second highest is 97 of cow which is infected by JOCFT. Buffalo is a species has less infected by suspected disease name LMAT. The goat is a species that have most infected by all the suspected disease with the grand total of 453 cases infected by suspected disease. Also, it was highlighted that BMCFT is the most disease attacked to goat as it stated 180 cases. Buffalo has least number of species to be infected by the suspected disease which it only has three types of disease infected; BACFT, LMAT and JOCFT.

Based on this study, the selection of number of nodes in the hidden layer was used by using the implementation of MATLAB. For each number of nodes, it undergoes 20 times of network running in order to approach the smallest value of RMSE. The optimal selection of neurons is 16 neurons in hidden layer as shown in Table 3. From the hidden nodes 4 to 18, the RMSE decrease gradually, this might be due to too many hidden nodes are used, hence, the network may lose its ability to generalize over trained or over forced and inspection of the cross validation set is crucial for the detection of this effect. In addition, the transfer function had been used in this network is hyperbolic tangent function in hidden layer and linear function in output layer.

Table 3 RMSE for every numbers of nodes

No. of Nodes in Hidden layer	RMSE
4	0.289259
5	0.277413
8	0.279916
9	0.290749
10	0.277169
12	0.276905
16	0.275055
18	0.276369

The behavior of an ANN depends on both weights and the input-output function or we call it as a transfer function. In every node of network model, we need a transfer function.

Every feedforward neural network model often has one or more hidden layers. However we only use one hidden layer in this case. The combination of transfer function allows the network to learn the relationships between input and output vectors.

Table 4 RMSE Value for Combination of Activation Functions

Activation-Transfer Function	RMSE
Logsig- Purelin	0.276191
Logsig-Logsig	0.279868
Tansig-Purelin	0.275055
Tansig-Tansig	0.279378
Logsig-Tansig	0.277455
Tansig-Logsig	0.279266

Based on the Table 4, the selection transfer functions in hidden and output layer were considered based on the smallest RMSE value that we have got by using implementation of MATLAB. We were using 16 nodes for every combination since we already got the smallest value of RMSE for tansig-purelin. Although, we had undergo about 20 times trials for each combination of transfer functions with different nodes in order to obtain the smallest value of RMSE. However, only a combination of transfer functions with a specific number of nodes got the smaller value of RMSE compare to any trials of other the final result. Thus, we obtain the best transfer function is *tansig* (hyperbolic tangent) in hidden layer and *purelin* (linear function) in output layer with 16 nodes in hidden layer.

The Geographical Information system provides the map to locate the infected veterinary disease all over Peninsular Malaysia. The Figure 2 shows the dominant veterinary disease that is infected at specific location. The yellow dots represent as predicted BMCFT disease. Perak will have the most infected disease of BMCFT. While, the less infected disease by BMCFT is predicted in Perlis



Figure 2 The Mapping predicted Disease in Malaysia

The current map that is abstracted by the Geographical Information System shows that types of veterinary disease all over the states in Malaysia. It shows that Perak has the highest number of infected disease which is Brucellosis also known as BMCFT. According

to the visualization of the map by previous paper (Lydia,2014) in Figure 3, it also shows that Perak has the highest number of infected disease which is Brucellosis. Thus, according to this research, we obtain the similarity of the highest disease. Hence, we can predict in the future that Perak has the highest number of Brucellosis disease.



Figure 3 Veterinary disease located in Peninsular Malaysia

For prediction of disease in both condition which is location and species, we obtain the classification of predicted disease by using SPSS Neural Network. The data was divided by two parts which is 70% of data is observed as training sample and 30% of data is observed as testing sample. The prediction of disease is observed by both training and testing sample

Table 5 Prediction of Disease for both Location and Species

Classification								
Sample	Observed	Predicted						% Correct
		JOCFT	LMAT	CLA	BMCFT	MCFT	BACFT	
Training	JOCFT	57	0	0	18	19	12	53.8%
	LMAT	12	0	0	12	0	2	.0%
	CLA	0	0	0	61	7	0	.0%
	BMCFT	2	0	0	109	20	0	83.2%
	MCFT	5	0	0	54	21	0	26.2%
	BACFT	33	0	0	5	0	18	32.1%
	Overall Percent	23.3%	.0%	.0%	55.5%	14.3%	6.9%	43.9%
Testing	JOCFT	24	0	0	7	9	8	50.0%
	LMAT	11	0	0	12	0	0	.0%
	CLA	0	0	0	27	1	0	.0%
	BMCFT	1	0	0	65	8	0	87.8%
	MCFT	0	0	0	22	15	0	40.5%
	BACFT	14	0	0	0	0	5	26.3%
	Overall Percent	21.8%	.0%	.0%	58.1%	14.4%	5.7%	47.6%

Table 6 shows the prediction of disease for both training sample and testing sample. It shows the comparison of percentage value of disease prediction with the percentage value for the actual of disease. From the table, we can observed that the highest percentage of

correct disease is BMCFT for both training and testing sample which are 83.2% and 87.8% . The second highest for correct percentage is JOCFT for both sample 53.8% and 50.0% . Other than that, The third highest of correct percentage for training sample is BACFT, 32.1%, while for testing sample is MCFT 40.5%

For the predicted classification of disease, we observe that BMCFT for both sample has the highest percentage of predicted disease. The second highest predicted is JOCFT for both sample. The third highest predicted is MCFT for both sample and the least percentage for predicted disease is BACFT. Hence for both observation of predicted percentage and correct percentage, we can conclude that, BMCFT has the highest percentage for both percentage compare to other disease. Thus, we can predict that BMCFT has the highest cases compare to other diseases.

The Table 6 is about the comparison of ANN result with the previous study of Genetic Algorithm (Rusli N.L., 2014) based on the same problem of animal disease.

Table 6 Comparison of Performance Analysis between ANN and Genetic Algorithm

Measurement	ANN	Genetic Algorithm
Mean Square Error (MSE)	0.0756	0.325
Root Mean Square (RMSE)	0.275	0.570

Based on Table 7 above, the comparison MSE between ANN and genetic algorithm show the difference values of error. ANN has less value of error than the genetic algorithm means we can conclude that ANN is a superior method compare to method of genetic algorithm.

Table 7 Comparison of Performance Analysis between Software

Measurement	ANN MATLAB	ANN SPSS
Mean Square Error (MSE)	0.0756	0.05133
Root Mean Square (RMSE)	0.275	0.2266

Table 7 shows the comparison of ANN by using MATLAB and SPSS software. The MSE and RMSE show the differences of values for both MATLAB and SPSS where the SPSS has a smallest value of error compare to MATLAB means SPSS is the best software to use of neural network.

Conclusion & Recommendation

The RMSE of ANN with the smallest value is obtained by using the implementation of programming of MATLAB. The best result of RMSE is obtained when we used 16 nodes in the hidden layer with a combination of transfer functions which is a tangent hyperbolic function in the hidden layer and linear function in the output layer. It is done after

undergoing 20 times of trials for different nodes and different combination of transfer functions.

The implementation of ANN by using SPSS and programming of MATLAB is successfully built with the obtaining results that have been discussed in chapter 4. From the analysis obtained, goat is the species that has a lot of infected disease reported. While Johor is the location has most infected disease area. The main focuses of this research is to predict the animal disease based on locations and species. Hence, the results obtained show the Brucellosis species which are BMCFT, it is the most infected disease detected at almost all locations and species.

Last but not least, the result is comparing the RMSE of ANN method with RMSE of genetic algorithm with the same parameters of animal disease. The result shows that the RMSE of ANN has less value of the error which is 0.275 compare to the genetic algorithm which is 0.570. Hence, we can conclude that the ANN method is a superior method compare to genetic algorithm.

Lastly, with the same parameter, 16 nodes in only one hidden layer, same transfer functions and other component, we can compare the RMSE value of ANN that implemented by using MATLAB with the RMSE of SPSS Neural Network. From the result obtain shows that SPSS Neural Network is the best software compare to ANN MATLAB with obtaining less value of MSE 0.05133 and RMSE 0.2266.

The neural network technique is used to model non-linear problems and predict the output values for giving input parameters. Most of the infected diseases and the related veterinary cases are non-linear in nature and hence, neural network is finding application in veterinary. Since neural networks are known to be good at solving classification problems, it is not surprising if this research has been done in identification and classification.

The recommendation for further study of this animal disease, we suggest to add more parameter to get a more accurate result, such as the parameter of time and temperature, which is we can predict the future time of disease will occur and to predict a better temperature for habitat, hence to maintain the population of the species. Then, from the previous study of genetic algorithm, it is better if we use a huge data to obtain the optimal solution and it is desirable to maintain the population size as large as possible not only use a slight number of cases and parameter. Besides, the weakness GA method is using the limited data set in the previous study.

References

- Al Shamisi, M. H., Assi, A. H., and Hejase, H. A. (2011). Using MATLAB to Develop Artificial Neural Network Models for Predicting Global Solar Radiation in Al Ain City-UAE. *INTECH Open Access Publisher*
- Areerachakul, S., Junsawang, P., & Pomsathit, A. (2011). Prediction of dissolved oxygen using Artificial Neural Network. In *Int Conf Comput Commun Manage* .5: 524-528.
- Krenker, A., Kos, A., & Bešter, J. (2011). Introduction to the Artificial Neural Networks. *INTECH Open Access Publisher*.
- Krenker, A., Kos, A., and Bešter, J. (2011). Introduction to the artificial neural networks. *INTECH Open Access Publisher*.
- Leow, B. L., Shajarutulwardah, M. Y., and Ramlan, M. (2011). Newcastle disease in Malaysia: diagnostic cases in Veterinary Research Institute (VRI) Ipoh from 2004–2009. *Malaysian Journal of Veterinary Research*. 2(1): 45-51.

- Martínez-Morales, J. D., Palacios-Hernández, E. R., and Velázquez-Carrillo, G. A. (2014). Artificial neural network based on genetic algorithm for emissions prediction of a SI gasoline engine. *Journal of Mechanical Science and Technology*, 28(6): 2417-2427.
- Mihajlović, I., Nikolić, Đ., Štrbac, N., and Živković, Ž. (2010). Statistical modeling in ecological management using the artificial neural networks (ANNs). *Serbian Journal of Management*. 5(1):39-50.
- Nanda, S. K., Tripathy, D. P., Nayak, S. K., and Mohapatra, S. (2013). Prediction of Rainfall in India using Artificial Neural Network (ANN) Models. *International Journal of Intelligent Systems and Applications (IJISA)*. 5(12):1.
- Nandy, S., Sarkar, P. P., and Das, A. (2012). Training a feed-forward neural network with artificial bee colony based backpropagation method. *arXiv preprint arXiv:1209-2548*.
- Pintér, J. D. (2012). Calibrating Artificial Neural Networks by Global optimization. *Expert Systems with Applications*. 39(1):25-32.
- Ramli N.A. (2014), Modeling Corrosion Rate in Gas Pipelines using Artificial Neural Network, *Bachelor of Science (Mathematics)*.
- Rusli N.L. (2014), Mathematical Modeling of Veterinary Disease by using Genetic Algorithm, *Bachelor of Science (Industrial Mathematics)*.
- Safi, Y., & Bouroumi, A. (2011). A neural network approach for predicting forest fires. In *Multimedia Computing and Systems (ICMCS), 2011 International Conference on 1-5. IEEE*.
- Seyam, M., and Mogheir, Y. (2011). Application of artificial neural networks model as analytical tool for groundwater salinity. *Journal of Environmental Protection*. 2(1):56.
- Volna, E., Kotyrba, M., Kocian, V., and Janosek, M. (2012,). Cryptography Based On Neural Network. In *ECMS*. 386-391.

Mathematical Modelling of Input and Output In Rotating Disc Contactor Column Using Genetic Algorithm

Ham Mei Hwee & Prof. Madya. Dr. Khairil Anuar Arshad

Abstract

Genetic Algorithm is one of the useful approximation methods in solving a wide range of problems in mathematics, physics and engineering. This study using GA to concern the modelling of inputs and outputs of rotating disc contactor (RDC) column. In this research, the Genetic Algorithm is used to predict outputs of rotating disc contactor (RDC) column. From this study, it was found that the Genetic Algorithm show good performances by giving the lowest value of MSE, the value of r close to 1 and the percentage of error is less than 10%. Hence, this shows that the Genetic Algorithm is effective for predicting output variables.

1 Introduction

1.1 Background of the Study

Liquid-liquid extraction is a method for separating components of a solution. Utilizing an unequal distribution of the components between two immiscible liquid phases. The process of separating is carried out by intimately mixing the two immiscible phases where transfer of one of the solution to other phase, then allowing two liquid phases to separate. Normally, one of the liquid phases will be an aqueous solution and the other phase will be an organic solvent. In this research, the column extractor type used is called Rotating Disc Contactor (RDC) column. RDC column was developed during the period 1948-1952 by the Royal Dutch / shell group at Amsterdam [1]. The RDC column is the best apparatus if compared with other equipments of liquid-liquid extraction due to its high performance and more efficient. The objectives of this research study comprises of (i) to study and understand genetic algorithm, (ii) to apply Genetic Algorithm for prediction of the outputs in rotating disc contactor column and (iii) to compare the actual output and predicted output derived from the Genetic Algorithm. This study will focus on developing Genetic Algorithm in the prediction of the outputs in rotating disc contactor column. Matlab version R2013a software is used to analyze the data by using Genetic Algorithm.

1.2 Literature Review

Mathematical model is using mathematical concepts and language to describe a system. Mathematical models are used not only in the natural sciences and engineering disciplines, but also in the social sciences. Aims of the mathematical modelling are to describe the different aspects of the real world problem [2].

Genetic Algorithm (GA) was in essence invented by John Holland in the 1960's. Genetic Algorithm (GA) is a numerical optimization algorithm inspired by both natural genetics and natural selection [3]. Many GA applied to real world problems endure only a passing

resemblance to the canonical GA. The most common type of genetic algorithm works such as a population is created with a group of individuals created randomly. The control parameters of the genetic algorithm may be fixed at a specific value or can be made vary as the genetic algorithm progresses. The control parameters that have to be initially specified are the population size, mutation and crossover probabilities, maximum number of generations and termination criterion.

The 'better' chromosomes are identified and will be likely to be selected to reproduce [4]. Genetic Algorithm is known as a powerful technique. Crossover happens according to a crossover probability p_c , which is an adjustable parameter [5]. The purpose of the mutation operator is to prevent the genetic population from converging to a local minimum of solved problem [6]. Without crossover and mutation, will be found that the solution less optimal [4]. First advantage of the genetic algorithm is the solution space is wider. GA can solve problem with more complex and finite number of parameter, it uses fitness function.

Rotating disc contactor (RDC) column is developed in Europe by Reman in 1951 [7]. The rotating disc contactor column is one of the agitated columns equipment, especially in the petroleum and petrochemical industrial. RDC is preferable compared to other extractor columns since the through-puts is high and the capacity range is large. Performance of RDC is affected by its column diameter, rotor disc diameter, stator ring opening, compartment height, number of compartments and disc rotational speed. Besides, there are two phases in RDC column which comprise light phase and heavy phase as well as dispersed phase and continuous phase. The common characteristics of RDC column are suitable for viscous and fouling materials, sensitive to emulsions due to shear mixing and limited efficiency due to axial backmixing.

2 Methodology

2.1 Mathematical Modelling Process of RDC Column Using GA

The mathematical modeling process has seven stages. In the first stage, the real world problem is to enhance the performance of liquid-liquid extraction process in RDC column by using GA. In the second stage, making assumptions on the formulated problem. There is an assumption of RDC column that is low solute concentration in both phases. In addition, the third stage is formulated mathematical problem. The fitness function may be based on the data obtained or on the position of the member in the population. Next, applying the mathematical software to solve mathematical problem, Matlab version R2013a. A code is build in based on the GA algorithm to run in the Matlab software. In the fifth stage, the solution will be analysed and interpreted after getting result from the Matlab software. The solution obtained is analysed for accuracy. If inaccuracy in the solution means has errors in the previous stage. If the solution is accurate, the sixth stage can be continued. The name of sixth stage is to verify the model. A valid model should show small differences in errors between the actual values and predicted values. The process of modelling will be stopped if the model is not valid. That means we need to review the second stage which is the stage of making assumptions for the problem. Assumptions may have to be redo or adjusted and continue with the next step. However, if the model is valid, the results and solutions obtained from the model will be further explained and discussed in details.

2.2 Collection of Data

The experimental data is gained from the researchers at the University of Bradford under contract to Separation Processes Service, AEA Technology, Harwell. There are two sets of data with 256 sets of data available and 1 set with 243 sets of data available, each sets of data attaches four columns of independent variables which are rotor speed (Nr), dispersed phase flow rate (Fd), concentration of continuous phase inlet ($ccin$) and concentration of dispersed phase inlet ($cdin$). There are also four dependent variables which are hold-up ($c\text{-holdup}$), souter mean diameter ($d32$) ($c\text{-}d32$), concentration of continuous phase outlet ($Cc\text{-out}$) and concentration of dispersed phase outlet ($Cd\text{-out}$). It is important to make reasonable of how much data we will need to develop the genetic algorithm properly.

2.3 Data Preparation

In the process of preparing the data sets for GA, the data have to be normalized. In this GA, a simple normalization formula can be used to normalize the data by using Microsoft Excel. The formula of simple normalization is given by

$$x_{new} = \frac{x - x_{min}}{x_{max} - x_{min}}$$

where

- x = Actual value,
- x_{new} = New value after normalized,
- x_{min} = Minimum value of x in sample data,
- x_{max} = Maximum value of x in sample data.

2.4 Model for Linear Regression

In this study, we are using Linear Regression as our fitness function to predict the output of rotating disc contactor column. Linear regression is the input data and output data fit. The regression equation will be used for predicting output. Linear regression can be expressed using the equation:

$$y = \beta_0 + \beta_1 x_1 + \beta_2 x_2 + \dots + \beta_m x_m + \varepsilon$$

where

- y = The response / dependent variables
- x_1, \dots, x_m = The several independent variables,
- β_0, \dots, β_m = The coefficient of variables,
- ε = The random error.

2.5 Analysis and Comparison of the Data

The performance of prediction can be measured by computing the accuracy. Mean Square Error (MSE) will be used as a performance measure for the efficiency of the prediction model. The smallest MSE value, the more accuracy prediction data to the actual data. The formula of MSE is defined by

$$MSE = \frac{1}{n} \sum_{i=1}^n (y_t - \hat{y}_t)^2$$

where

$$\begin{aligned}
 y_t &= \text{The actual value,} \\
 \hat{y}_t &= \text{The predicted value,} \\
 n &= \text{The number of observations.}
 \end{aligned}$$

In addition to determine the MSE value, another method to check for accuracy in results obtained is Pearson correlation coefficient (r), or correlation coefficient for short is a measure of the strength of the linear relationship between actual values and predicted values obtained after applying the GA. The correlation coefficient, r , has a specific range of values from -1 to 1 which illustrates a strong relationship between predicted and actual values. Other than that, we also use another method to measure for accuracy in results obtained which is percentage of error. If the percentage of error is lower than 10%, it implies that the predicted value is accurate to the actual value. The formula of percentage of error is defined by

$$\%_{error} = \frac{|Accepted - Measured|}{Accepted} * 100$$

where

$$\begin{aligned}
 \%_{error} &= \text{Percentage of error,} \\
 Accepted &= \text{Actual value,} \\
 Measured &= \text{Predicted value,} \\
 |Accepted - Measured| &= \text{Absolute error.}
 \end{aligned}$$

3 Result and Analysis

Our objectives are to predict outputs of rotating disc contactor (RDC) column by applying Genetic Algorithm. In this research, we are using Matlab software to predict the outputs. In this analysis, for cumene isobutyric acid with fast rotor speed, we take 10 data from the actual output and predicted output of hold-up, sauter mean diameter (d_{32}), concentration of continuous phase outlet and concentration of dispersed phase outlet to do analysis and determine whether predicted data is accurate. For here, we are using percentage error formula for determining the precision of prediction of the outputs. The predicted data is accurate to the actual data if the percentage of error is less than 10%.

Actual output	Predicted output	Error between predicted value and actual value	Percentage of error, (%)
0.58224	0.57889	0.003346	0.5747
0.58174	0.57878	0.002954	0.5079
0.58224	0.57883	0.003403	0.5845
0.58174	0.57888	0.002852	0.4903
0.58224	0.57894	0.003301	0.5669
0.033688	0.033404	0.000284	0.8420
0.033688	0.033359	0.000329	0.9762
0.033688	0.03341	0.000278	0.8249
0.033688	0.033461	0.000227	0.6736
0.033688	0.033353	0.000335	0.9933

Table 3.1: GA result for prediction of the hold-up in RDC column for cumene isobutyric acid with fast rotor speed

Actual output	Predicted output	Error between predicted value and actual value	Percentage of error, (%)
0.87173	0.8465	0.025225	2.8937
0.87173	0.84639	0.025337	2.9065
0.87173	0.84661	0.025118	2.8814
0.87173	0.8465	0.02523	2.8942
0.87173	0.84639	0.025342	2.9071
0.87173	0.84627	0.025454	2.9199
0.87173	0.84649	0.025235	2.8948
0.87173	0.84638	0.025347	2.9077
0.87173	0.84627	0.025459	2.9205
0.87173	0.84616	0.02557	2.9332

Table 3.2: GA result for prediction of the sauter mean diameter (d₃₂) in RDC column for cumene isobutyric acid with fast rotor speed

Actual output	Predicted output	Error between predicted value and actual value	Percentage of error, (%)
0.51386	0.5263	0.012439	2.4207
0.59122	0.60628	0.015054	2.5463
0.46948	0.4718	0.0023187	0.4938
0.54894	0.55178	0.0028369	0.5168
0.62782	0.63175	0.0039352	0.6268
0.70586	0.71173	0.0058723	0.8319
0.57902	0.57725	0.0017649	0.3048
0.65786	0.65723	0.00062667	0.0953
0.73651	0.73721	0.00070612	0.0956
0.81476	0.81719	0.0024272	0.2979

Table 3.3: GA result for prediction of the concentration of continuous phase outlet in RDC column for cumene isobutyric acid with fast rotor speed

Actual output	Predicted output	Error between predicted value and actual value	Percentage of error, (%)
0.37043	0.3736	0.0031639	0.8541
0.34426	0.35619	0.01194	3.4683
0.40117	0.41465	0.013475	3.3589
0.46491	0.4731	0.0081869	1.7610
0.536	0.53155	0.0044554	0.8312
0.5254	0.51415	0.011251	2.1414
0.58452	0.5726	0.011924	2.0400
0.64436	0.63105	0.013306	2.0650
0.70372	0.6895	0.014222	2.0210
0.68525	0.6721	0.013145	1.9183

Table 3.4: GA result for prediction of the concentration of dispersed phase outlet in RDC column for cumene isobutyric acid with fast rotor speed

From Table 3.1, 3.2, 3.3 and 3.4 we can conclude that predicted data is accurate to the actual data since all the percentages of error are smaller than 10%. Hence, predicted data is closer to the actual data.

In addition, we also conclude that for cumene isobutyric acid with slow rotor speed and butanol acid with fast rotor speed that predicted data also accurate to the actual data since all the percentages of error are smaller than 10%. Hence, predicted data is closer to the actual data.

From all the analyse above, we can conclude that the predicted data is accurate to the actual data since all the percentages of error are smaller than 10%. The MSE and correlation coefficient values of four output variables are summarized in Table 3.5.

Output variables	cumene isobutyric acid with fast rotor speed		cumene isobutyric acid with slow rotor speed		butanol acid with fast rotor speed	
	Mean Square Error (MSE)	Correlation coefficient, r	Mean Square Error (MSE)	Correlation coefficient, r	Mean Square Error (MSE)	Correlation coefficient, r
Hold-up (<i>c-holup</i>)	0.009081	0.940319	0.0093493	0.938497	0.019015	0.833779
Sauter mean diameter (<i>c-d32</i>)	0.0064341	0.969532	0.0090423	0.956906	0.015319	0.942176
Concentration of continuous phase outlet (<i>Cc-out</i>)	0.00115162	0.982456	0.0013219	0.979834	0.0053228	0.929167
Concentration of dispersed phase outlet (<i>Cd-out</i>)	0.0011565	0.987265	0.0013987	0.984578	0.0018004	0.97884

Table 3.5: GA result for prediction of the four output variables in RDC column for cumene isobutyric acid with fast rotor speed, cumene idobutyric acid with slow rotor speed and butanol acid with fast rotor speed

As shown in Table 3.5, we can be concluded that cumene isobutyric acid with fast rotor speed has the best prediction value than cumene idobutyric acid with slow rotor speed and butanol acid with fast rotor speed. It is because the MSE and correlation coefficient for cumene isobutyric acid with fast rotor speed are the best. It is said that the MSE value for cumene isobutyric acid with fast rotor speed is smaller than the MSE value for cumene idobutyric acid with slow rotor speed and butanol acid with fast rotor speed. For cumene isobutyric acid with fast rotor speed, the MSE values of *c-holup*, *c-d32*, *Cc-out* and *Cd-out* output variables are 0.009081, 0.0064341, 0.00115162 and 0.0011565 which are smaller than the MSE values for cumene isobutyric acid with slow rotor speed and butanol acid with fast rotor speed, those MSE values are 0.0093493, 0.0090423, 0.0013219, 0.0013987, 0.019015, 0.015319, 0.0053228 and 0.0018004 respectively. For cumene isobutyric acid with fast rotor speed, it has smallest MSE value means the deviation between predicted values and actual values is smallest.

Moreover, the correlation coefficient for cumene isobutyric acid with fast rotor speed is higher than the correlation coefficient for cumene idobutyric acid with slow rotor speed and butanol acid with fast rotor speed. For cumene isobutyric acid with fast rotor speed, the correlation coefficient of *c-holup*, *c-d32*, *Cc-out* and *Cd-out* output variables are 0.940319, 0.969532, 0.982456 and 0.987265 which are larger than the correlation coefficient for cumene idobutyric acid with slow rotor speed and butanol acid with fast rotor speed, those correlation coefficients are 0.938497, 0.956906, 0.979834, 0.984578, 0.833779, 0.942176, 0.929167 and 0.97884 respectively. For cumene isobutyric acid with fast rotor speed, the predicted values is closer to the actual values and near to the line.

In conclusion, it can be said that GA can be a good prediction method in cumene isobutyric acid with fast rotor speed if compared to cumene idobutyric acid with slow rotor speed and butanol acid with fast rotor speed based on the graph and data.

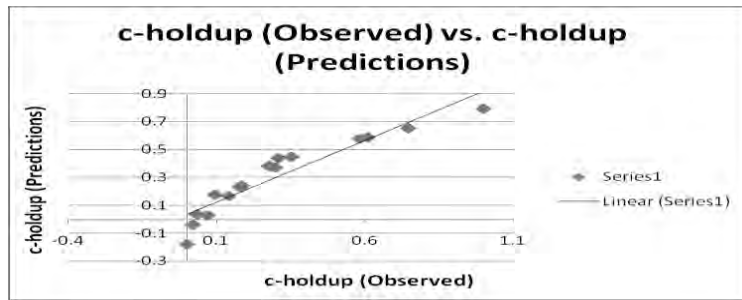


Figure 3.1: Graph of hold-up (*c-holdup*) for the correlation coefficient for cumene isobutyric acid with fast rotor speed

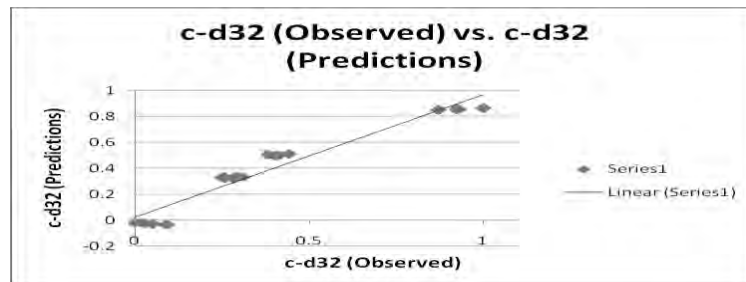


Figure 3.2: Graph of sauter mean diameter (*c-d32*) for the correlation coefficient for cumene isobutyric acid with fast rotor speed

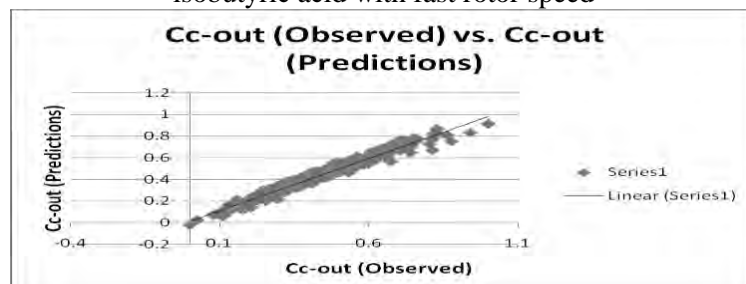


Figure 3.3: Graph of concentration of continuous phase outlet (*Cc-out*) for the correlation coefficient for cumene isobutyric acid with fast rotor speed

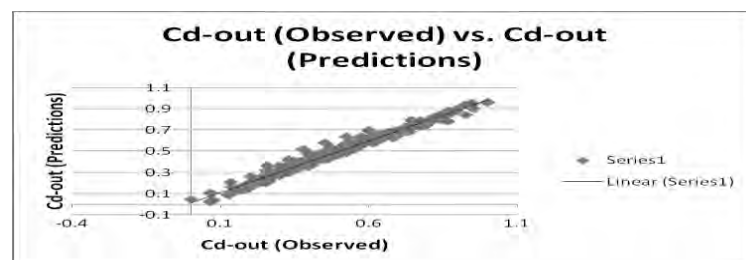


Figure 3.4: Graph of concentration of dispersed phase outlet (*Cd-out*) for the correlation coefficient for cumene isobutyric acid with fast rotor speed

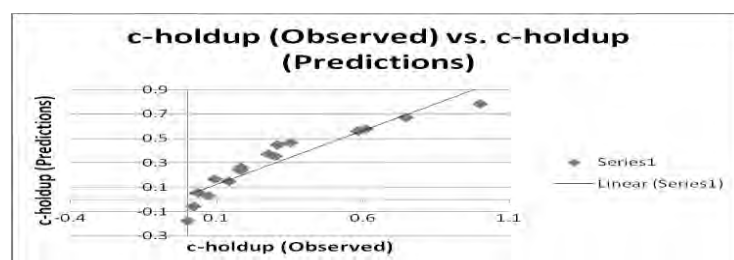


Figure 3.5: Graph of hold-up (*c-holdup*) for the correlation coefficient for cumene isobutyric acid with slow rotor speed

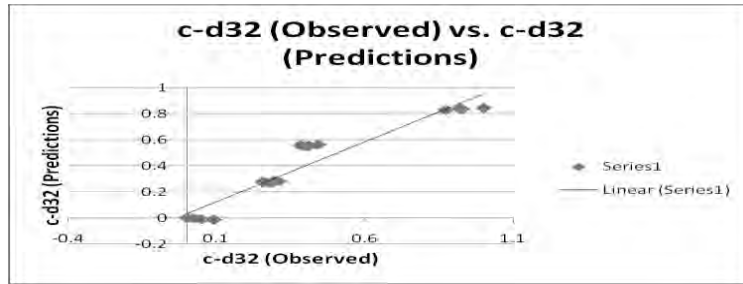


Figure 3.6: Graph of sauter mean diameter ($c-d32$) for the correlation coefficient for cumene isobutyric acid with slow rotor speed

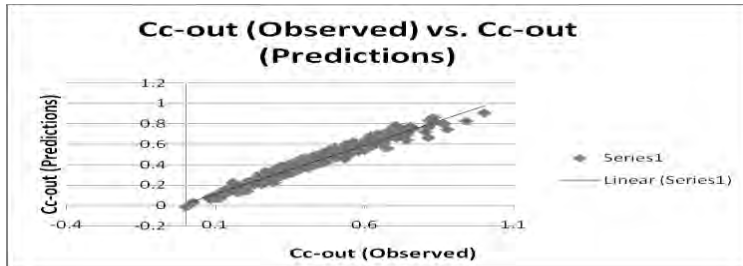


Figure 3.7: Graph of concentration of continuous phase outlet ($Cc-out$) for the correlation coefficient for cumene isobutyric acid with slow rotor speed

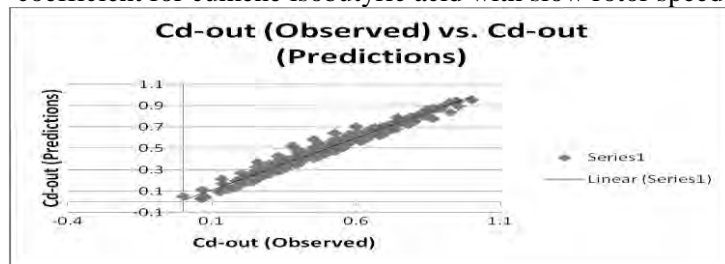


Figure 3.8: Graph of concentration of dispersed phase outlet ($Cd-out$) for the correlation coefficient for cumene isobutyric acid with slow rotor speed

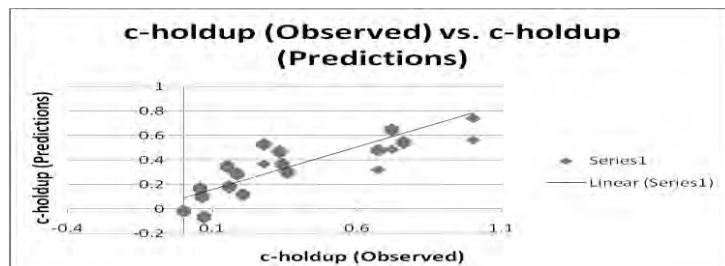


Figure 3.9: Graph of hold-up ($c-holdup$) for the correlation coefficient for butanol acid with fast rotor speed

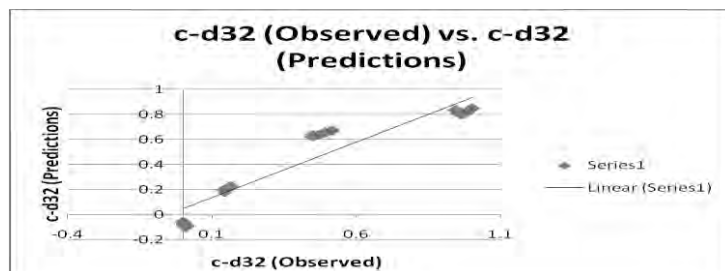


Figure 3.10: Graph of sauter mean diameter ($c-d32$) for the correlation coefficient for butanol acid with fast rotor speed

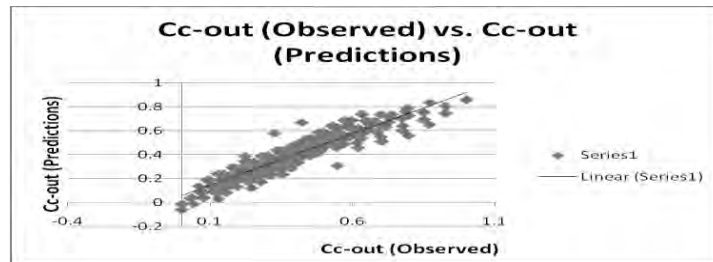


Figure 3.11: Graph of concentration of continuous phase outlet ($Cc\text{-out}$) for the correlation coefficient for butanol acid with fast rotor speed

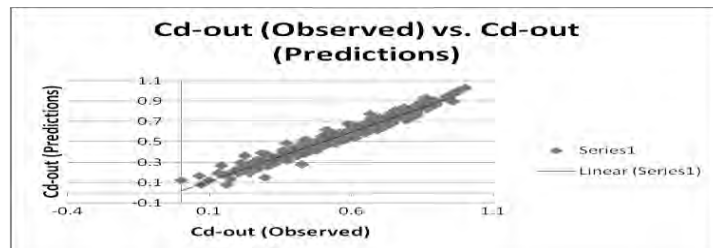


Figure 3.12: Graph of concentration of dispersed phase outlet ($Cd\text{-out}$) for the correlation coefficient for butanol acid with fast rotor speed

4 Conclusion

In this research, the Genetic Algorithm (GA) is applied in the prediction of the output variables in rotating disc contactor (RDC) column. From the results and analysis, predicted data of $Cd\text{-out}$ is more accurate to actual data of $Cd\text{-out}$. It can be conclude that GA can be a good prediction method in cumene isobutyric acid with fast rotor speed since the predicted data is closer to the actual data. Its mean square error (MSE) value is smaller than others. The correlation coefficient value also give the nearest to 1 and its percentage of error is smaller than 10%.

Nevertheless, these findings could only be concerned with the prediction of hold-up, sauter mean diameter (d_{32}), concentration of continuous phase outlet and concentration of dispersed phase outlet in RDC column. This analysis only true for these RDC data. Hence, the same research has to be carried out to other fields and problems look over if any resemblance to the prediction results with the best model. By using GA, hopefully it can help engineers and scientists to build a better RDC in the future to maximize its outputs.

References

- [1] Talib, J. (1994). *Mathematical Modelling of A Rotating Disc Contactor*. Ph.D. Thesis. Bradford University, Bradford, U.K.
- [2] Quarteroni, A. (2009). Mathematical Models in Science and Engineering. *Notices of the AMS*. 56(1), 10-19.
- [3] Coley, D. A. (1999). *An Introduction to Genetic Algorithms for Scientists and Engineers*. University of Exeter: World Scientific.

- [4] Tabassum, M. and Mathew, K. (2014). A Genetic Algorithm Towards Optimization Solutions. *International Journal of Digital Information and Wireless Communications (IJDIWC)*. 4(1), 124-142.
- [5] Srivastava, P. R. and Tai, H. K. (2009). Application of Genetic Algorithm in Software Testing. *International Journal of Software Engineering and Its Applications*. 3(4), 87-96.
- [6] Heidari, E. and Movaghar, A. (2011). An Efficient Method Based on Genetic Algorithm to Solve Sensor Network Optimization Problem. *International Journal on Applications of Graph Theory in Wireless Ad Hoc Networks and Sensor Networks*. 3(1), 18-33.
- [7] Swirbutowicz, K. (2012). *Hydrodynamics and Mass Transfer Performance of Rotating Disc Contactor*. Master of Philosophy. Thesis. University of Manchester, United Kingdom.

MODELING THE SPREAD OF DENGUE FEVER BY USING SIR MODEL

Hor Ming An, PM. Dr. Yudariah Mohammad Yusof

Abstract

The establishment and spread of dengue fever is a complex phenomenon with many factors that interact with each other. This report present a study on a mathematical model, the SIR (Susceptible, Infected and Recovered) that serve as a framework for understanding the spread of the infectious dengue fever. We begin with a brief discussion of the origin and historical development of the disease. This is followed by a review on the relation between the three compartments, susceptible, infected and recovered. The modeling steps that lead to the SIR model using ordinary differential equation is explained in detail. The solution gives the basic reproduction number R_0 , and this basic reproduction number is use to determine whether the dengue fever will dies out or persists in human population in the long run. The disease-free equilibrium point is determined and R_0 is used to determine whether the disease free equilibrium is stable or unstable. Establishing the endemic equilibrium point determines when the dengue fever will become calm.

Keywords: SIR model, Basic reproduction number, disease free equilibrium, endemic equilibrium

Introduction

Dengue fever is a dangerous disease having huge social, economic and health burden. It is predominantly present in the tropical countries. Even though the disease has been checked out for long time ago, it still remains a major public health issue. Many researchers had model the dengue fever to investigate the spread of the disease. There are a lot of model that described the dengue fever, such as SIR model, SEIR model, MSIR model, and MSEIR model. The most important thing to build a model is identify the variable involve in the model. So, the variable must be determined correctly. In order to investigate the spread of disease, the most important aspect that we need to find out is basic reproduction number. Basic reproduction number is to determine whether the disease will die out or not. Moreover, basic reproduction number can use to find the disease free equilibrium point and endemic equilibrium point.

In this report, we study how a system of differential equation is used to model the spread of dengue fever. The main purpose of this study are, identify a deterministic dynamics model to represent the transmission of the disease in different compartments, study the dynamics of dengue fever in a deterministic model involving ordinary differential equations, explore the relation of basic reproduction number (R_0), disease free equilibrium (E_0), and endemic equilibrium (E_1).

Literature Review

We will review the studies of the researchers related to the dengue fever. The researches that were presented are SIA model, SEIR model, MSEIR model, SIS model, and statistically presented method. In modeling a model for spread of dengue fever, it is necessary to determine the variables involve in the system and understand the basic reproduction number. The variables are determined base on the situation of the system. Basic reproduction number

is to determine whether the disease is stable or not stable. Both the variables and basic reproduction number are important to study the spread of dengue fever.

A study about SIS model was carried out by Helmersson, Jing (2012) on Mathematical Modeling of Dengue -Temperature Effect on Vectorial Capacity. This research is aims at finding the best way to incorporate temperature effect on dengue transmission. Another research is carried out by Kiyeny, Silas Kipchirchir (2014) on SIA model. A 5-dimensional system of ordinary differential equations (ODEs) is use to model the malaria disease. This is because the model contained of 5 different variables. The model was analyzed for the disease free equilibrium and endemic equilibrium. A research about modeling the spread of dengue in Singapore was done by K.C.Ang and Z.Li. In this research, they developed a model that describes the spread of dengue in Singapore. They considered S-E-I-R (susceptible→exposed→infectious→recovered) model for human population, while S-E-I (susceptible→exposed→infectious) model for mosquito population. Besides that, a model of dengue fever has been published by M Derouich, A Boutayeb, and EH Twizell. In this paper, they consider an S-I-R model. It is about medical research in terms of vaccination and antibiotics of dengue fever.

Methodology

In this report, we will emphasize on the SIR model, which the model is the easiest to understand. First, we need to identify the variables and parameters that need to take into consideration. Such as the birth rate, death rate, recovery rate, and so on. After that, we need to analyse the model to check whether it is adequate or not. If the dimension of the model is too large, then model order reduction is to be applied. Basic reproduction number is a must to find out for every modelling of infectious disease. With the basic reproduction number, we can determine the seriousness of the disease. The basic reproduction number can be use to find the disease free equilibrium point and endemic equilibrium point.

Generally, modelling consists of four steps. First of all, a flow diagram that describes the whole process is a must in order to do the modelling. Flow diagram represents the natural history and transmission of infection. After that, move to second step. Second step is to write a set of mathematical equations to express the transmission process based on the flow diagram that construct in first step. Then, the third step is to find proper values for the parameters used in the equations and make sure that the variable use is appropriate. Finally, we need to solve the equations algebraically or numerically with help of computer simulation programs since some of the equations are very complicated and need the help of computer programming.

The population can be classified into three compartments:

- Susceptible to the disease (Susceptible) – S,
- Currently Infectious (Infectious or Infective) – I,
- Recovered and immune (Recovered or Removals) – R.

Susceptible state means a person is under identify likely or liable to be influenced or harmed by dengue fever but not yet confirm that person is infected. Infectious state means a person is confirmed infected by dengue fever. Recovered state means a person is recovered from infectious. As stated above, every process needs a flow diagram to represent and describe the particular situation. Therefore, at here S, I, R, represent the number of individuals in each compartment. The total host population is $N = S + I + R$.

Each arrow in the flow diagram represents the flow rate at which individuals enter or leave a compartment per unit time, which is called the incidence rate.

Model order reduction is a technique for reducing the complexity of mathematical models in numerical simulation. In the real life process, many modern mathematical models are complicated when process in numerical simulation. This is due to the large size of the mathematical model's dimension. The purpose of reduce the order of the model is to lower down the computational complexity of that model.

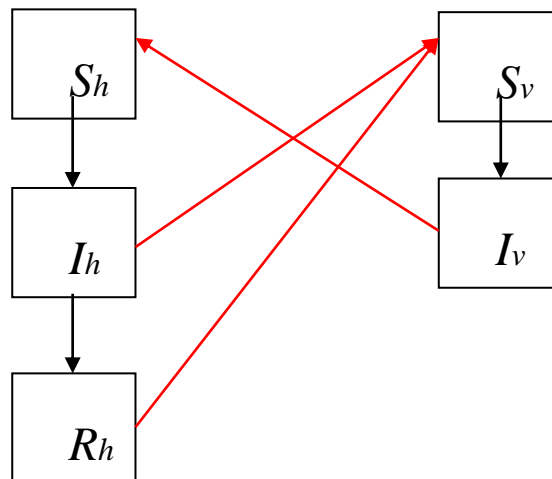
The basic reproduction number is useful because it helps determine whether or not an infectious disease can spread through a population. When $R_0 < 1$, the infection will slowly die out in the long time. When $R_0 > 1$, the infection will be able to spread in a population. Therefore, in generally, the larger the value of R_0 , the harder it is to control the epidemic.

Disease free equilibrium is to see whether the epidemic is stable or unstable when there is no more diseases presence. Disease free equilibrium point is a point where there is no more disease appears. The disease free equilibrium point is depends on the basic reproduction number, R_0 . When $R_0 < 1$, then the disease free equilibrium point is stable. It is, however if the basic reproduction number, $R_0 > 1$, then the disease free equilibrium point is unstable. Thus, R_0 is a threshold parameter for the model.

Endemic equilibrium point is a point where the disease is at the steady state. The endemic equilibrium is to determine whether the epidemic is stable or unstable when the disease is at the steady state. Similarly, endemic equilibrium is also depending on the basic reproduction number, R_0 . When $R_0 < 1$, the endemic equilibrium point is unstable, whereas the endemic equilibrium point is stable if $R_0 > 1$.

Findings and Discussion

Our model is a mathematical simulation of transmission of dengue virus between host and vector (human and mosquito) where humans and mosquitoes interact and infect each other. Basically, the model is considered only on the susceptible, infectious and recovered or immune (SIR model). In the model, we let the notation of total population sizes of human and mosquito as N_h and N_v respectively. In the model of human population, it is divided into three classes; the Susceptible (S_h), the Infectious (I_h), and Recovered (R_h). In the model of mosquito population, it is divided into two classes; the Susceptible (S_v), the Infectious (I_v).



The equations representing the relationship between the population of host and vector are given as:

$$\begin{aligned} \frac{dS_h}{dt} &= \lambda_h - ab_1 I_v \frac{S_h}{N_h} - \mu_h S_h + \gamma(I_h + R_h) \\ \frac{dI_h}{dt} &= ab_1 I_v \frac{S_h}{N_h} - (\mu_h + \alpha + \delta + \gamma) I_h \\ \frac{dR_h}{dt} &= \delta I_h - (\mu_h + \gamma) R_h \\ \frac{dS_v}{dt} &= \lambda_v - ab_2 S_v \frac{I_h}{N_h} - ab_3 S_v \frac{R_h}{N_h} - \mu_v S_v \\ \frac{dI_v}{dt} &= ab_2 S_v \frac{I_h}{N_h} + ab_3 S_v \frac{R_h}{N_h} - \mu_v I_v \end{aligned}$$

After that we analyse the model to test whether the equation is adequate or not.

For human population;

$$N_h(t) = \frac{\lambda_h}{\mu_h} + C e^{-\mu_h t}$$

When t is equal to 0, $N_h(0) = \frac{\lambda_h}{\mu_h} + C$

When t are approaches to infinity, $N_h(\infty) = \frac{\lambda_h}{\mu_h}$

From the above, it implies that the human population is constant in the absence of the disease. Also implies that in the long time, the human's population will become constant.

For mosquito population;

$$N_v(t) = \frac{\lambda_v}{\mu_v} + D e^{-\mu_v t}$$

When t is equal to 0, $N_v(0) = \frac{\lambda_v}{\mu_v} + D$

When t are approaches to infinity, $N_v(\infty) = \frac{\lambda_v}{\mu_v}$

From the above, it implies that the population of mosquito is a constant and would not go to infinity.

Since there are 5 differential equations, then we reduce the model to 4 equations. From the equation $\frac{dN_v}{dt} = \lambda_v - \mu_v N_v$, we can see that the N_v is only the one variable. That is mean the equation only depends on N_v . Hence, by using Vidyasagar theorem, we can reduce the system to four equations.

$$\frac{dI_h}{dt} = ab_1 I_v \frac{S_h}{N_h} - (\mu_h + \alpha + \delta + \gamma) I_h \tag{1}$$

$$\frac{dR_h}{dt} = \delta I_h - (\mu_h + \gamma) R_h \tag{2}$$

$$\frac{dI_v}{dt} = ab_2 S_v \frac{I_h}{N_h} + ab_3 S_v \frac{R_h}{N_h} - \mu_v I_v \tag{3}$$

$$\frac{dN_h}{dt} = \lambda_h - \mu_h N_h - \alpha I_h \tag{4}$$

After reduce the model order, now we can find the basic reproduction number by transform the differential equation to matrix form.

$$\begin{bmatrix} \frac{dI_h}{dt} \\ \frac{dR_h}{dt} \\ \frac{dI_v}{dt} \\ \frac{dN_h}{dt} \end{bmatrix} = \begin{bmatrix} -(\mu_h + \alpha + \delta + \gamma) & 0 & ab_1 \frac{S_h}{N_h} & 0 \\ \delta & -(\mu_h + \gamma) & 0 & 0 \\ ab_2 \frac{S_v}{N_h} & ab_3 \frac{S_v}{N_h} & -\mu_v & 0 \\ -\alpha & 0 & 0 & -\mu_h \end{bmatrix} \begin{bmatrix} I_h \\ R_h \\ I_v \\ N_h \end{bmatrix}$$

$$\begin{bmatrix} \frac{dI_h}{dt} \\ \frac{dR_h}{dt} \\ \frac{dI_v}{dt} \\ \frac{dN_h}{dt} \end{bmatrix} = \begin{bmatrix} 0 & 0 & ab_1 \frac{S_h}{N_h} & 0 \\ 0 & 0 & 0 & 0 \\ ab_2 \frac{S_v}{N_h} & ab_3 \frac{S_v}{N_h} & 0 & 0 \\ 0 & 0 & 0 & 0 \end{bmatrix} - \begin{bmatrix} (\mu_h + \alpha + \delta + \gamma) & 0 & 0 & 0 \\ -\delta & (\mu_h + \gamma) & 0 & 0 \\ 0 & 0 & \mu_v & 0 \\ \alpha & 0 & 0 & \mu_h \end{bmatrix} \begin{bmatrix} I_h \\ R_h \\ I_v \\ N_h \end{bmatrix}$$

$$\begin{bmatrix} \frac{dI_h}{dt} \\ \frac{dR_h}{dt} \\ \frac{dI_v}{dt} \\ \frac{dN_h}{dt} \end{bmatrix} = [F - V] \begin{bmatrix} I_h \\ R_h \\ I_v \\ N_h \end{bmatrix}$$

With the matrices F and V at above, we can use this matrices to find the reproduction number, R_0 . The reproduction number, $R_0 = \lambda^2$, where λ is the eigenvalue of FV^{-1} .

$$R_0 = \lambda^2 = \frac{a^2 b_1 N_v [b_2 (\mu_h + \gamma) + \delta b_3]}{(\mu_v N_h) (\mu_h + \gamma) (\mu_h + \alpha + \delta + \gamma)}$$

The disease free equilibrium point is $E_0 = (0,0,0, \frac{\lambda_h}{\mu_h})$. The purpose of doing this analysis is to determine if the disease free equilibrium point is stable. First of all, we analyze the stability of the disease free equilibrium by linearize the above differential equations (1), (2), (3), and (4) to a Jacobian matrix.

$$J_{DFE} = \begin{bmatrix} -A & 0 & ab_1 & 0 \\ \delta & -(\mu_h + \gamma) & 0 & 0 \\ \frac{ab_2 \lambda_v \mu_h}{\mu_v \lambda_h} & \frac{ab_3 \lambda_v \mu_h}{\mu_v \lambda_h} & -\mu_v & 0 \\ -\alpha & 0 & 0 & -\mu_h \end{bmatrix}$$

Next, we want to determine the eigenvalues of this Jacobian matrix. The eigenvalues of this Jacobian matrix can determine whether the disease free equilibrium point, E_0 is stable.

$$P(\lambda) = |J_{DFE} - \lambda I| = \begin{vmatrix} -(A + \lambda) & 0 & ab_1 & 0 \\ \delta & -(\mu_h + \gamma + \lambda) & 0 & 0 \\ \frac{ab_2 \lambda_v \mu_h}{\mu_v \lambda_h} & \frac{ab_3 \lambda_v \mu_h}{\mu_v \lambda_h} & -(\mu_v + \lambda) & 0 \\ -\alpha & 0 & 0 & -(\mu_h + \lambda) \end{vmatrix} = 0$$

$$\lambda^3 + \lambda^2 [2(\mu_h + \gamma) + \alpha + \delta + \mu_v] + \lambda \left[A(\mu_h + \gamma + \mu_v) + (\mu_h + \gamma)\mu_v - \frac{a^2 b_1 b_2 \lambda_v \mu_h}{\mu_v \lambda_h} \right] + \left[(\mu_h + \gamma)\mu_v A - \frac{a^2 b_1 \lambda_v \mu_h [(\mu_h + \gamma)b_2 + b_3 \delta]}{\mu_v \lambda_h} \right] = 0$$

We can write the equation into third order polynomial, which is equivalent to the above equation.

$$C_1 \lambda^3 + C_2 \lambda^2 + C_3 \lambda + C_4 = 0$$

$$C_1 = 1 > 0$$

$$C_2 = 2(\mu_h + \gamma) + \alpha + \delta + \mu_v > 0$$

$$C_3 = A(\mu_h + \gamma + \mu_v) + (\mu_h + \gamma)\mu_v - \frac{a^2 b_1 b_2 \lambda_v \mu_h}{\mu_v \lambda_h}$$

$$= A(\mu_h + \gamma) + (\mu_h + \gamma)\mu_v + A\mu_v - \frac{a^2 b_1 b_2 \lambda_v \mu_h (\mu_h + \gamma)}{\mu_v \lambda_h (\mu_h + \gamma)} - \frac{a^2 b_1 b_3 \delta \lambda_v \mu_h}{\mu_v \lambda_h (\mu_h + \gamma)}$$

$$+ \frac{a^2 b_1 b_3 \delta \lambda_v \mu_h}{\mu_v \lambda_h (\mu_h + \gamma)}$$

$$\begin{aligned}
 &= (\mu_h + \gamma)(A + \mu_v) + \frac{a^2 b_1 b_3 \delta \lambda_v \mu_h}{\mu_v \lambda_h (\mu_h + \gamma)} + A \mu_v \left[1 - \frac{a^2 b_1 \lambda_v \mu_h [b_2 (\mu_h + \gamma) + \delta b_3]}{(\mu_v^2 \lambda_h) (\mu_h + \gamma) A} \right] \\
 &= (\mu_h + \gamma)(A + \mu_v) + \frac{a^2 b_1 b_3 \delta \lambda_v \mu_h}{\mu_v \lambda_h (\mu_h + \gamma)} + A \mu_v [1 - R_0]
 \end{aligned}$$

C_3 is always greater than zero when R_0 is less than 1.

$$\begin{aligned}
 C_4 &= (\mu_h + \gamma) \mu_v A - \frac{a^2 b_1 \lambda_v \mu_h [(\mu_h + \gamma) b_2 + b_3 \delta]}{\mu_v \lambda_h} \\
 &= (\mu_h + \gamma) \mu_v A \left[1 - \frac{a^2 b_1 \lambda_v \mu_h [(\mu_h + \gamma) b_2 + b_3 \delta]}{(\mu_v^2 \lambda_h) (\mu_h + \gamma) A} \right] \\
 &= (\mu_h + \gamma) \mu_v A [1 - R_0]
 \end{aligned}$$

C_4 is always greater than zero when R_0 is less than 1.

Therefore, the disease free equilibrium point E_0 is stable if $R_0 < 1$. If $R_0 > 1$, then the disease free equilibrium point E_0 is unstable.

The endemic equilibrium point is $E_1 = (\bar{I}_h, \bar{R}_h, \bar{I}_v, \bar{N}_h)$. When the disease has reached its equilibrium point, then the differential equations are equal to zero. Therefore, we can write the differential equation into;

$$\begin{aligned}
 ab_1 \bar{I}_v (\bar{N}_h - \bar{I}_h - \bar{R}_h) - (\mu_h + \alpha + \delta + \gamma) \bar{I}_h \bar{N}_h \\
 = 0
 \end{aligned} \tag{5}$$

$$\begin{aligned}
 \delta \bar{I}_h - (\mu_h + \gamma) \bar{R}_h \\
 = 0
 \end{aligned} \tag{6}$$

$$\begin{aligned}
 ab_2 (N_v - \bar{I}_v) \bar{I}_h + ab_3 (N_v - \bar{I}_v) \bar{R}_h - \mu_v \bar{I}_v \bar{N}_h \\
 = 0
 \end{aligned} \tag{7}$$

$$\begin{aligned}
 \lambda_h - \mu_h \bar{N}_h - \alpha \bar{I}_h \\
 = 0
 \end{aligned} \tag{8}$$

Solve \bar{I}_h , \bar{R}_h , \bar{I}_v , and \bar{N}_h in terms of \bar{I}_h by using the above equations, equation (5), (6), (7), and (8). Hence we get:

$$\bar{I}_h = \frac{-B \pm \sqrt{B^2 - 4AC}}{2A}$$

$$\bar{R}_h = \frac{\delta}{(\mu_h + \gamma)} \bar{I}_h$$

$$\bar{I}_v = \frac{(\mu_h + \alpha + \delta + \gamma)(\lambda_h - \alpha \bar{I}_h)(\mu_h + \gamma) \bar{I}_h}{ab_1 [\lambda_h (\mu_h + \gamma) - [(\mu_h + \gamma)(\alpha + \mu_h) + \mu_h \delta] \bar{I}_h]}$$

$$\bar{N}_h = \frac{\lambda_h - \alpha \bar{I}_h}{\mu_h}$$

Conclusion and Recommendation

We have studied the modeling of dengue disease in a 5-dimensional system of ordinary differential equations. We analyzed the differential equations, and showed that the model that we use is adequate because the population of human and mosquito are both converge to

a constant. The system was then reduced to 4-dimensional system of ordinary differential equation. This is due to by solving the 5-dimensional system of ordinary differential equation has a very tedious computation.

After that, we have defined the basic reproduction number, R_0 in terms of parameters. R_0 must be find correctly because it is greatly use in finding the disease free equilibrium and endemic equilibrium. We also established that if the basic reproduction number $R_0 < 1$, the disease free equilibrium point is stable and the disease will dies out after some period of time. However, if the $R_0 > 1$, the disease free equilibrium point is unstable and the disease will become more serious and continuously spread. We also establish the endemic equilibrium point.

From the results above, the basic reproduction number we obtained is $R_0 = 1.9689$, which the $R_0 > 1$. This number is quite high because it is greater than one. This meaning that in the long run, the dengue fever will not dies out, but it will continuously spread. Such number is not ideal in the future. We can describe the situation from the graph (figure 4.2). It is clearly showed that in the long period of time, the population of human will keep decreasing. Therefore, we need to do change the parameters to reduce the R_0 . For example we can reduce the mosquito birth rate by killing the mosquito, and create a better vaccine to increase the recovery rate.

References

WHO, (World Health Organization), 2002. *Dengue Prevention and Control*.

Shanti Narayan, 1975. *Differential Calculus*. Shyam Lal Charitable Trust, Ran Nagar, New Delhi-110055.

Abubakar, Sazaly, and Norazizah Shafee, 2002. Outlook of dengue in Malaysia: a century later. *Malaysian Journal of Pathology*, 24(1): 23-28.

Clare Rewcastle Brown, Dengue Fever Outbreak. URL:<http://www.sarawakreport.org/2012/06/dont-mention-dengue-fever-outbreak-it-might-spoil-my-party-exclusive/>. 12 January 2015.

Cobra, Claudine, et al, 1995. Symptoms of Dengue Fever in Relation to Host Immunologic Response and Virus Serotype, Puerto Rico, 1990–1991. *American Journal of Epidemiology*, 142(11): 1204-1211.

Helmersson, Jing, 2012. Mathematical Modeling of Dengue-Temperature Effect on Vectorial Capacity. *phmed.umu.se*.

URL: <http://www.denguevirusnet.com/history-of-dengue.html>. 20 January 2015

Kiyeny, Silas Kipchirchir, 2014. Using mathematical model to illustrate the spread of malaria.

Ang, K. C., and Z. Li, 2002. Modeling the Spread of Dengue in Singapore.

Astacio, Jaime, et al, 1996. Mathematical Models to Study the Outbreaks of Ebola. *cms.unipune.ac.in*.

Garba, Salisu Mohammed, Abba B. Gumel, and Mohd Rizam Abu Bakar, (2008). Backward Bifurcations in Dengue Transmission Dynamics. *Mathematical Biosciences*, 215(1): 11-25.

Pinho, Suani Tavares Rubim de, et al, 2010. Modelling the dynamics of dengue real epidemics. *Philosophical Transactions of the Royal Society A: Mathematical, Physical and Engineering Sciences*, 368.1933: 5679-5693.

Derouich, M., A. Boutayeb, and E. H. Twizell, 2003. A model of dengue fever. *BioMedical Engineering OnLine* 2(1): 4.

Anderson, Roy M., and Robert McCredie May, 1991. *Infectious Diseases of Humans. Oxford: Oxford University Press*, Vol. 1.

Keeling, Matt J, 2005. Models of Foot-and-Mouth Disease. *Proceedings of the Royal Society B: Biological Sciences*, 272.1569: 1195-1202.

Schichl, Hermann, 2004. Models and the History of Modeling. *Modeling Languages in Mathematical Optimization. Springer US*, 25-36.

Goel B.S & Sunil Kuman, 1977. *Differential Calculus. Pragati Prakasham, Begum Bridge, Meerut.*

Schilders, Wilhelmus HA, Henk A. Van der Vorst, and Joost Rommes, 2008. *Model Order Reduction: Theory, Research Aspects and Applications. Berlin, Germany: Springer*, Vol. 13.

Diekmann, Odo, J. A. P. Heesterbeek, and Johan AJ Metz, 1990. On the Definition and the Computation of the Basic Reproduction Ratio R_0 in Models for Infectious Diseases in Heterogeneous Populations. *Journal of Mathematical Biology*, 28(4): 365-382.

URL: http://en.wikipedia.org/wiki/Basic_reproduction_number. 15 April 2015.

Van den Driessche, Pauline, and James Watmough, 2002. Reproduction Numbers and Sub-threshold Endemic Equilibria for Compartmental Models of Disease Transmission. *Mathematical Biosciences*, 180(1): 29-48.

A THE BEST ESTIMATED EQUATION TO BE USED IN PREDICTING THE MATERIAL CONSTANTS OF BIOLOGICAL SOFT TISSUE

Lau Mun Hing, B.A. Mahad¹, Mukheta Isa¹

Abstract – The biological soft tissues are made of collagen, elastin, muscle and others ground substances. The chemical composite and structural detail can be used to describe the mechanical properties of the soft tissues. In the past, the invariant based model requires fewer calculations than the structurally based and thus will be more computationally efficient. An invariant based approach describes transverse isotropy by use of directional pseudoinvariants. A number of similar Finite Element Method (FEM) implementations have been published for incompressible, transversely isotropic materials (Holzapfel[25]; Almeida and Spiker[26]; Ruter and Stein[27];) [9]. In this research, I proposed that constitutive model which is based on B.A Mahad[1-5] 's model with physical interpretation(PI) and experimental friendly. We can easily get the constitutive constant. Our model is easy model to analyze the constitutive equation.

Keywords:Finite Element Method;physical interpretation

1.0 INTRODUCTION

Biomechanics is often defined as ‘mechanics applied to biology’ according to Fung [18]. Protein, cells, tissues, organs and organisms reveal an incredible spectrum of material structures and properties. There are lots of researches which are carried out the find out the relationship between Mathematical modelling and biology. Some application can be described and applied by Mathematical modelling. Computer is essential to carry out some analytic processes. All the scientists want to find out the constitutive equations to model set of transversely isotropic materials such as soft biological tissues.

It is known as a change in shape due to applied forces such as compress or pull. In the consideration of transversely isotropic biological tissues, tissues could be damaged due to some forces. It is elastic and it could stand for a certain limit of force. This certain limit of the force is known as elastic constant of the certain material.

Ligaments and tendons are dense connective tissues consisting primarily of parallel fibred collagenous tissues embedded in solid matrix.[20] These tissues are composed by a large amount of collagen and fibrous protein. Ligaments are subjected to uniaxial tensile loads but can undergo mechanical actions while tendon are subjected to high unidirectional tensile loads and their collagen fibers are assigned in parallel arrangement. Material can be classified into three main classes such as isotropic, transversely isotropic and anisotropic. Therefore, in this research, I would like to consider the transversely isotropic biological tissues.

Ogden [10] consider an elastic material for which the material properties are characterized in terms of a strain energy function denoted $W=W(U)$ which is defined on the space of deformation gradients. There are lots of principals which are consider in the strain energy function such as principal Biot , principal Cauchy stress and others. There are lots of restriction and consideration to design the constitutive equation to forecast the value of elastic constant, k of biological tissues. Biological tissue can be divided into two main categories such as soft and hard tissues.

Constitutive equations can be designed by using all the programs which are available nowadays such as MATLAB, Mathematica, Microsoft Excel and others. Constitutive equations can be modified if there is a proof shown in the data given.

2.0 Continuum Mechanics

According to Ogden[10] and Holzapfel[26], we summarized the relevant elasticity theory. Consider the soft tissues regarded as a continuous body. Let points of the body are labelled by their position vectors \mathbf{X} in the initial (unstressed) configuration relative to an arbitrarily chosen origin. Suppose that when the body is deformed the point \mathbf{X} has the new position $\mathbf{x}(\mathbf{X},t)$ in the resulting deformed configuration of the body.

Let \mathbf{X} denote the original position vector of a material point, $\mathbf{x}(\mathbf{X},t)$ denote the new point of deformed position and β is the current configuration which varies with the time, t .

$$\mathbf{x} = \mathbf{x}(\mathbf{X}, t)$$

$\mathbf{x}(\mathbf{X},t)$ is the function of describing the motion. For each t , $\mathbf{x}(\mathbf{X},t)$ is invertible and satisfies appropriate regularity conditions. The deformation gradient tensor, denoted \mathbf{F} is given by $\mathbf{F} = \text{Grad } \mathbf{x}$ and it has Cartesian components $F_{i\alpha} = \frac{\partial x_i}{\partial X_\alpha}$

Local invertibility of the deformation required that \mathbf{F} be non-singular and the usual convention that $J = \det \mathbf{F} > 0$, where the notation J is defined.

$$\mathbf{v} = \frac{\partial \mathbf{x}}{\partial t}(\mathbf{X}, t), \mathbf{a} = \frac{\partial^2 \mathbf{x}}{\partial t^2}(\mathbf{X}, t)$$

$$\mathbf{F} = \mathbf{R}\mathbf{U} = \mathbf{V}\mathbf{R}$$

where \mathbf{R} being a proper orthogonal tensor, \mathbf{U} and \mathbf{V} are positive definite.

$$\mathbf{U} = \sum_{i=1}^3 \lambda_i \mathbf{u}^{(i)} \otimes \mathbf{u}^{(i)}, \mathbf{V} = \sum_{i=1}^3 \lambda_i \mathbf{v}^{(i)} \otimes \mathbf{v}^{(i)}$$

where \mathbf{U} called the Lagrangian principal axes and eigenvectors of \mathbf{V} called the Eulerian principal axes.

$$\mathbf{B} = \mathbf{F}\mathbf{F}^T \equiv \mathbf{V}^2, \mathbf{C} = \mathbf{F}^T \mathbf{F} \equiv \mathbf{U}^2$$

$$I_1 = \text{tr}(\mathbf{B}), I_2 = \frac{1}{2}(I_1^2 - \text{tr}(\mathbf{B}^2)), I_3 = \det(\mathbf{B}) \equiv (\det(\mathbf{F}))^2$$

$$\mathbf{E} = \frac{1}{2}(\mathbf{C} - \mathbf{I})$$

where \mathbf{B} and \mathbf{C} are left and right Cauchy-Green deformation tensors and \mathbf{I} denote identity tensor.

3.0 Stress

Stress is defined as the nature of internal force which is needed to derive field equations expressing the balance of linear and angular momenta. In 1822, the general concept of stress

is first put forward by Cauchy. The nature of internal forces is determined by the assumed structural model of material. In 1821, the equation is described as below.

$$\text{The incompressible Cauchy stress is given by the relation } \sigma = 2F \frac{\partial W_e}{\partial C} F^T - pI$$

where p is the Lagrange multiplier associated with the incompressibility constraints. The proposed alternative formulation requires the symmetric components $(\frac{\partial W_e}{\partial C})_{ij}$ of $\frac{\partial W_e}{\partial C}$ relative to the basis $\{ e_i \}$

$$(\frac{\partial W_e}{\partial C})_{ij} = \frac{1}{2\lambda_i} \frac{\partial W_e}{\partial \lambda_i}$$

$$\text{and the shear components } (\frac{\partial W_e}{\partial C})_{ij} = \frac{\frac{\partial W}{\partial \zeta_1} - \frac{\partial W}{\partial \zeta_2}}{\lambda_i^2 - \lambda_j^2} e_i \bullet A e_j, i \neq j, i, j = 1, 2$$

The strain invariants

$$I_1 = trC, I_2 = \frac{1}{2} ((trC)^2 - trC^2), I_3 = \det C,$$

$$I_4 = a \bullet C \bullet a = \alpha^2, I_5 = a \bullet C^2 \bullet a$$

where C is the right Cauchy Green deformation tensor, tr denotes the trace of a second order tensor and a is the preferred direction.

4.0 Mathematical Modelling

For an incompressible material,

$$\sigma_{11} = \lambda_1 \frac{\partial W}{\partial \lambda_1} ; \sigma_{22} = \lambda_2 \frac{\partial W}{\partial \lambda_2}$$

$$\sigma_{12} = 2(\frac{\partial W}{\partial \zeta_1} - \frac{\partial W}{\partial \zeta_2}) \frac{\lambda_1 \lambda_2 e_1 \bullet A e_2}{\lambda_1^2 - \lambda_2^2}$$

$$\sigma_{13} = 2(\frac{\partial W}{\partial \zeta_1} - \frac{\partial W}{\partial \zeta_3}) \frac{\lambda_1 \lambda_3 e_1 \bullet A e_3}{\lambda_1^2 - \lambda_3^2}$$

$$\sigma_{23} = 2(\frac{\partial W}{\partial \zeta_2} - \frac{\partial W}{\partial \zeta_3}) \frac{\lambda_2 \lambda_3 e_2 \bullet A e_3}{\lambda_2^2 - \lambda_3^2}$$

$$A = a \otimes a$$

$$\sigma_{12} = \sigma_{13} = \sigma_{23} = 0$$

$$w(\lambda_1, \lambda_2, \zeta_1, \zeta_2) = f(\lambda_1)\{\mu_T + 2(\mu_L - \mu_T)\zeta_1 + \frac{B}{2}\zeta_1^2\} + f(\lambda_2)\{\mu_T + 2(\mu_L - \mu_T)\zeta_2 + \frac{B}{2}\zeta_2^2\} \\ + f(\lambda_3)\{\mu_T + 2(\mu_L - \mu_T)\zeta_3 + \frac{B}{2}\zeta_3^2\} + \frac{B}{2}\{2\zeta_1\zeta_2s(\zeta_1)s(\zeta_2) + 2\zeta_1\zeta_3s(\zeta_1)s(\zeta_3) + 2\zeta_2\zeta_3s(\zeta_2)s(\zeta_3)\}$$

$$\lambda_1\lambda_2\lambda_3 = 1$$

$$\lambda_3 = \frac{1}{\lambda_1\lambda_2}$$

The strain energy function can be expressed as

For σ_{11}

$$\frac{\partial w}{\partial \lambda_1} = f'(\lambda_1)\{\mu_T + 2(\mu_L - \mu_T)\zeta_1 + \frac{B}{2}\zeta_1^2\} + f'(\lambda_3)\left(-\frac{1}{\lambda_1\lambda_2}\right)\{\mu_T + 2(\mu_L - \mu_T)\zeta_3 + \frac{B}{2}\zeta_3^2\} \\ + B\{\zeta_1\zeta_2s'(\zeta_1)s(\zeta_2) + \zeta_1\zeta_3[s'(\zeta_1)s(\zeta_3) + s(\zeta_1)s'(\zeta_3)\left(-\frac{1}{\lambda_1\lambda_2}\right)] + \zeta_2\zeta_3s(\zeta_2)s'(\zeta_3)\left(-\frac{1}{\lambda_1\lambda_2}\right)\}$$

$$\sigma_{11} = \lambda_1 \frac{\partial w}{\partial \lambda_1}$$

$$\sigma_{11} = \lambda_1 f'(\lambda_1)\{\mu_T + 2(\mu_L - \mu_T)\zeta_1 + \frac{B}{2}\zeta_1^2\} + f'(\lambda_3)\left(-\frac{1}{\lambda_1\lambda_2}\right)\{\mu_T + 2(\mu_L - \mu_T)\zeta_3 + \frac{B}{2}\zeta_3^2\} \\ + B\{\zeta_1\zeta_2s'(\zeta_1)s(\zeta_2) + \zeta_1\zeta_3[s'(\zeta_1)s(\zeta_3) + s(\zeta_1)s'(\zeta_3)\left(-\frac{1}{\lambda_1\lambda_2}\right)] + \zeta_2\zeta_3s(\zeta_2)s'(\zeta_3)\left(-\frac{1}{\lambda_1\lambda_2}\right)\}$$

$$\lambda_3 = \frac{1}{\lambda_1\lambda_2}$$

$$\sigma_{11} = \lambda_1 f'(\lambda_1)\{\mu_T + 2(\mu_L - \mu_T)\zeta_1 + \frac{B}{2}\zeta_1^2\} - f'(\lambda_3)(\lambda_3)\{\mu_T + 2(\mu_L - \mu_T)\zeta_3 + \frac{B}{2}\zeta_3^2\} \\ + B\{\zeta_1\zeta_2s'(\zeta_1)s(\zeta_2) + \zeta_1\zeta_3[s'(\zeta_1)s(\zeta_3) - s(\zeta_1)s'(\zeta_3)(\lambda_3)] - \zeta_2\zeta_3s(\zeta_2)s'(\zeta_3)(\lambda_3)\}$$

For preferred direction a parallel to e_1 (direction of fiber) and perpendicular to e_2

For σ_{22}

$$w(\lambda_1, \lambda_2, \zeta_1, \zeta_2) = f(\lambda_1)\{\mu_T + 2(\mu_L - \mu_T)\zeta_1 + \frac{B}{2}\zeta_1^2\} + f(\lambda_2)\{\mu_T + 2(\mu_L - \mu_T)\zeta_2 + \frac{B}{2}\zeta_2^2\} \\ + f(\lambda_3)\{\mu_T + 2(\mu_L - \mu_T)\zeta_3 + \frac{B}{2}\zeta_3^2\} + \frac{B}{2}\{2\zeta_1\zeta_2s(\zeta_1)s(\zeta_2) + 2\zeta_1\zeta_3s(\zeta_1)s(\zeta_3) + 2\zeta_2\zeta_3s(\zeta_2)s(\zeta_3)\}$$

$$\frac{\partial w}{\partial \lambda_2} = f'(\lambda_2)\{\mu_T + 2(\mu_L - \mu_T)\zeta_2 + \frac{B}{2}\zeta_2^2\} + f'(\lambda_3)\left(-\frac{1}{\lambda_1\lambda_2}\right)\{\mu_T + 2(\mu_L - \mu_T)\zeta_3 + \frac{B}{2}\zeta_3^2\} \\ + B\{\zeta_1\zeta_2s(\zeta_1)s'(\zeta_2) + \zeta_1\zeta_3s(\zeta_1)s'(\zeta_3)\left(-\frac{1}{\lambda_1\lambda_2}\right) + \zeta_2\zeta_3[s'(\zeta_2)s(\zeta_3)] + s(\zeta_2)s'(\zeta_3)\left(-\frac{1}{\lambda_1\lambda_2}\right)\}$$

$$\sigma_{22} = \lambda_2 \frac{\partial w}{\partial \lambda_2}$$

$$\begin{aligned} \sigma_{22} = & \lambda_2 f'(\lambda_2) \{ \mu_T + 2(\mu_L - \mu_T) \zeta_2 + \frac{B}{2} \zeta_2^2 \} + \lambda_2 f'(\lambda_3) \left(-\frac{1}{\lambda_1 \lambda_2} \right) \{ \mu_T + 2(\mu_L - \mu_T) \zeta_3 + \frac{B}{2} \zeta_3^2 \} \\ & + B \{ \zeta_1 \zeta_2 s(\zeta_1) s'(\zeta_2) + \zeta_1 \zeta_3 s(\zeta_1) s'(\zeta_3) \left(-\frac{1}{\lambda_1 \lambda_2} \right) + \zeta_2 \zeta_3 [\lambda_2 s'(\lambda_2) s(\lambda_3)] + \lambda_2 s(\lambda_2) s'(\lambda_3) \left(-\frac{1}{\lambda_1 \lambda_2} \right) \} \end{aligned}$$

$$\begin{aligned} \sigma_{22} = & \lambda_2 f'(\lambda_2) \{ \mu_T + 2(\mu_L - \mu_T) \zeta_2 + \frac{B}{2} \zeta_2^2 \} + \lambda_2 f'(\lambda_3) \{ \mu_T + 2(\mu_L - \mu_T) \zeta_3 + \frac{B}{2} \zeta_3^2 \} \\ & + B \{ \zeta_1 \zeta_2 s(\zeta_1) s'(\zeta_2) + \zeta_1 \zeta_3 s(\zeta_1) s'(\zeta_3) + \zeta_2 \zeta_3 [\lambda_2 s'(\lambda_2) s(\lambda_3)] + \lambda_2 s(\lambda_2) s'(\lambda_3) \} \\ \lambda_1 = & \lambda_2 = \lambda \end{aligned}$$

$$\begin{aligned} \sigma_{11} = & \lambda f'(\lambda) \{ \mu_T + 2(\mu_L - \mu_T) \zeta_1 + \frac{B}{2} \zeta_1^2 \} - f'(\lambda) \left(\frac{1}{\lambda^2} \right) \{ \mu_T + 2(\mu_L - \mu_T) \zeta_3 + \frac{B}{2} \zeta_3^2 \} \\ & + B \{ \zeta_1 \zeta_2 s'(\zeta_1) s(\zeta_2) + \zeta_1 \zeta_3 [s'(\zeta_1) s(\zeta_3) - s(\zeta_1) s'(\zeta_3) \left(\frac{1}{\lambda^2} \right)] - \zeta_2 \zeta_3 s(\zeta_2) s'(\zeta_3) \left(\frac{1}{\lambda^2} \right) \} \end{aligned}$$

When $\zeta_1 = 1; \zeta_2 = 0; \zeta_3 = 0$

$$\sigma_{11} = \lambda f'(\lambda) \{ \mu_T + 2(\mu_L - \mu_T) + \frac{B}{2} \} - f'(\lambda) \left(\frac{1}{\lambda^2} \right) \{ \mu_T \}$$

$$\sigma_{11} = \mu_T [\lambda f'(\lambda) - f'(\lambda) \left(\frac{1}{\lambda^2} \right)] + \lambda f'(\lambda) \{ 2(\mu_L - \mu_T) + \frac{B}{2} \}$$

Parallel to fiber direction

$$\begin{aligned} \sigma_{22} = & \lambda_2 f'(\lambda_2) \{ \mu_T + 2(\mu_L - \mu_T) \zeta_2 + \frac{B}{2} \zeta_2^2 \} + \lambda_2 f'(\lambda_3) \{ \mu_T + 2(\mu_L - \mu_T) \zeta_3 + \frac{B}{2} \zeta_3^2 \} \\ & + B \{ \zeta_1 \zeta_2 s(\zeta_1) s'(\zeta_2) + \zeta_1 \zeta_3 s(\zeta_1) s'(\zeta_3) + \zeta_2 \zeta_3 [\lambda_2 s'(\lambda_2) s(\lambda_3)] + \lambda_2 s(\lambda_2) s'(\lambda_3) \} \end{aligned}$$

$$\sigma_{22} = \lambda f'(\lambda) \mu_T - \left(\frac{1}{\lambda^2} \right) f' \left(\frac{1}{\lambda^2} \right) \mu_T \tag{4}$$

$$\sigma_{22} = \mu_T \{ \lambda f'(\lambda) - \left(\frac{1}{\lambda^2} \right) f' \left(\frac{1}{\lambda^2} \right) \} \tag{5}$$

$$\sigma_{11} - \sigma_{22} = \lambda f'(\lambda) \{ 2(\mu_L - \mu_T) + \frac{B}{2} \} \tag{6}$$

5.0 Application

Graph 1

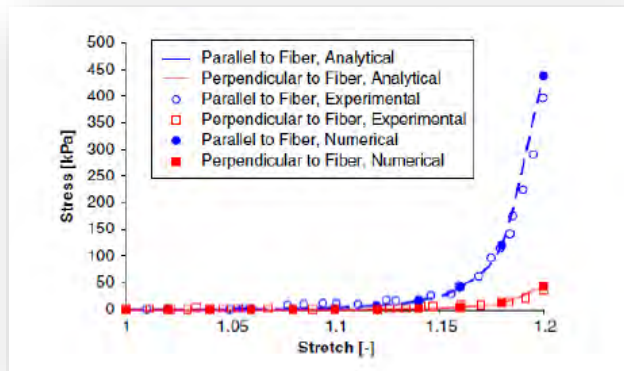


Figure 4.4.1: Equibiaxial strain applied to anterior leaflet (Experimental 1)

x	λ	σ_{11} (parallel)	σ_{22} (perpendicular)	$\sigma_{11}-\sigma_{22}$
15.211	1.0287	0	0	0
33.335	1.0629	0	0	0
37.039	1.0699	5.7541	4.1311	1.6229
70.443	1.1329	20.9344	5.7541	15.1803
72.626	1.137	19.3114	5.7541	13.5573
80.431	1.1518	27.9835	12.2623	15.7213
86.864	1.1639	48.7212	13.4836	35.2376
91.494	1.1726	62.8195	10.2295	52.59
95.86	1.1809	112.6964	18.9016	93.7948
98.373	1.1856	143.0652	17.8196	125.2456
101.747	1.192	229.2699	24.8688	204.4011
105.649	1.1994	401.6793	38.4179	363.2614

Table 4.4.1

Graph 2

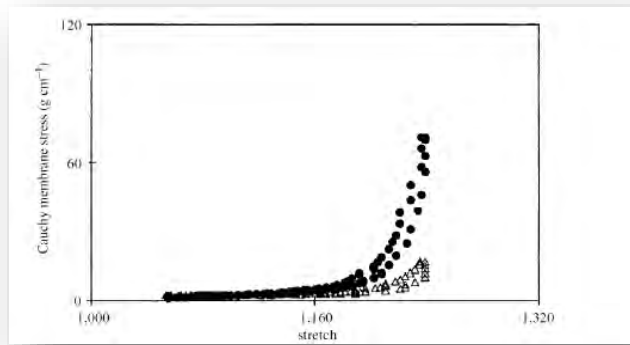


Figure 4.4.2: Typical stress- stretch data for soft tissues. Shown is the nonlinear, anisotropic response of excised epicardium, a collagenous membrane that covers the heart

λ	σ_{11}	σ_{22}	$\sigma_{11}-\sigma_{22}$
1.0537	3.2007	0.6014	2.5993
1.0832	3.6653	0.694	2.9713
1.1048	3.6653	1.0653	2.6
1.1359	4.6554	1.6842	2.9712
1.1602	6.2646	2.4274	3.8372
1.174	7.626	2.6744	4.9516
1.1838	9.854	3.4175	6.4365
1.2016	15.0526	5.1502	9.9024
1.2149	25.327	7.626	17.701
1.221	33.2491	8.6161	24.633
1.229	43.2751	11.4632	31.8119
1.2362	71.2625	17.0463	54.2162

Table 4.4.2

Graph 3

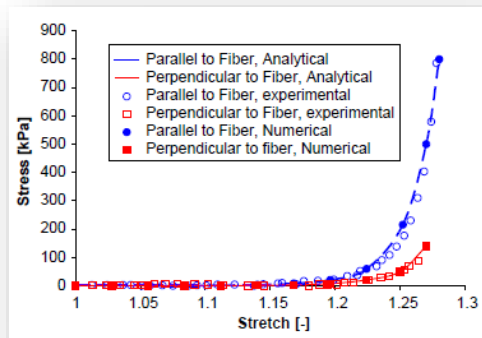


Figure 4.4.3: Equibiaxial strain applied to psterior leaflet

λ	σ_{11}	σ_{22}	$\sigma_{11}-\sigma_{22}$
1.022874	9.073452	0	9.073452
1.039912	9.93759	0	9.93759
1.059492	10.80173	9.073452	1.728277
1.123502	12.09794	9.93759	2.160346
1.15946	18.1469	10.80173	7.345175
1.19476	26.78829	12.09794	14.69035
1.222906	63.08209	15.12242	47.95967
1.252275	213.0101	20.73932	192.2708
1.2615	327.0763	29.3807	297.6956
1.269972	489.1023	44.93519	444.1671
1.281079	801.0562	143.879	657.1771

Table 4.4.3

5.1 Steps of the programming

For Mathematica 9.0

1. FindFit[data, $x^{d(x-1)}$, d, x]
2. F1[x_]:= (x - 1)x^28
3. FindFit[data, a1(F1[x] - F1[1/x^2]), {a1}, x]
4. w[x_]:= 1.02234(F1[x] - F1[1/x^2])
5. G4 = Plot[w[x], {x, 1, 1.21}, PlotRange -> {-0.25, 100}, PlotStyle -> Directive[Red, Thick];

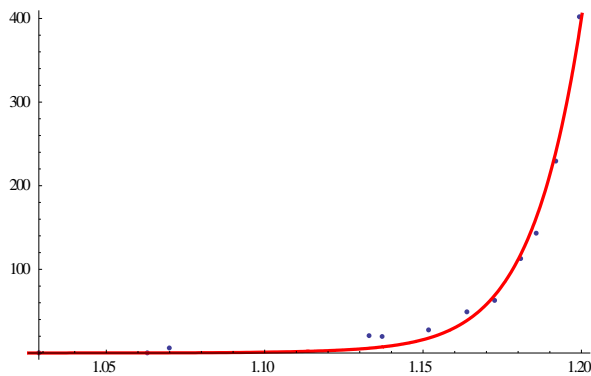
6. Show[G3,G4]

For Maple 15

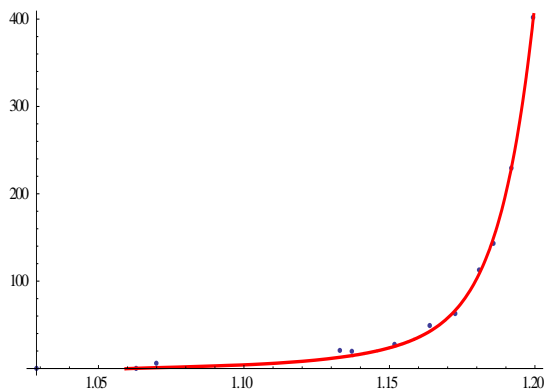
1. restart;
2. with(CurveFitting); with(plots);
3. datax := [1.0287, 1.0629, 1.0699, 1.1329, 1.1370, 1.1518, 1.1639, 1.1726, 1.1809, 1.1856, 1.1920, 1.1994]
4. datay := [0, 0, 1.6229, 15.1803, 13.5573, 15.7213, 35.2376, 52.59, 93.7948, 125.2456, 204.4011, 363.2614]
5. points := [seq([datax[i], datay[i]], i = 1 .. m)]
6. pointplot(points)
7. pp := LeastSquares(points, x, curve = a*Y1(x))
8. display({graph1, graph2}, labels = [lambda, sigma11], axes = boxed)

5.2 First Graph By Using Mathematica

For the analysis of σ_{11}

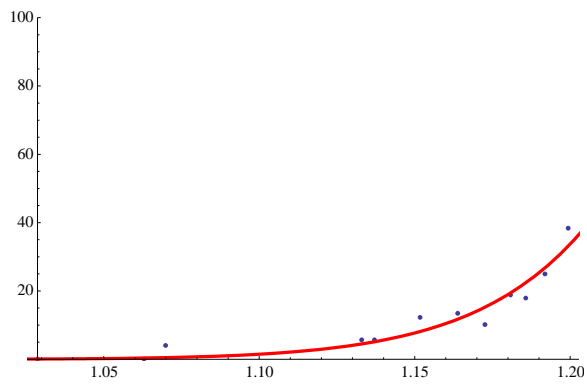


$$Y1 := x \rightarrow x \cdot (x - 1)^9 \cdot \exp(18 \cdot x);$$

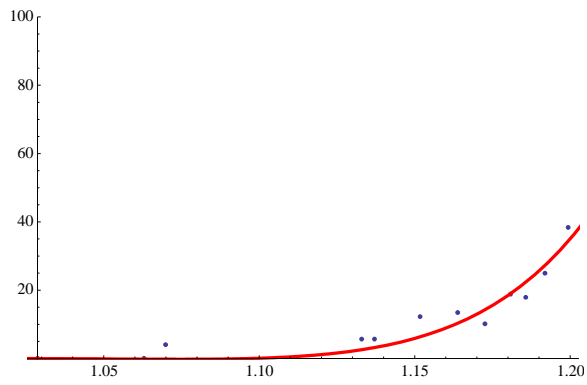


$$Y1 := x \rightarrow x^{23} + (x - 1)^{13} \cdot \exp(23 \cdot x);$$

]For the analysis of σ_{22}

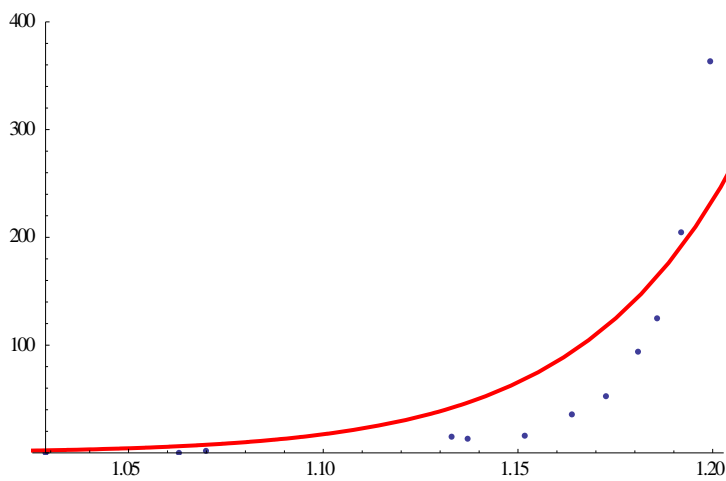


$$YI := x \rightarrow x^{28} \cdot (x - 1);$$

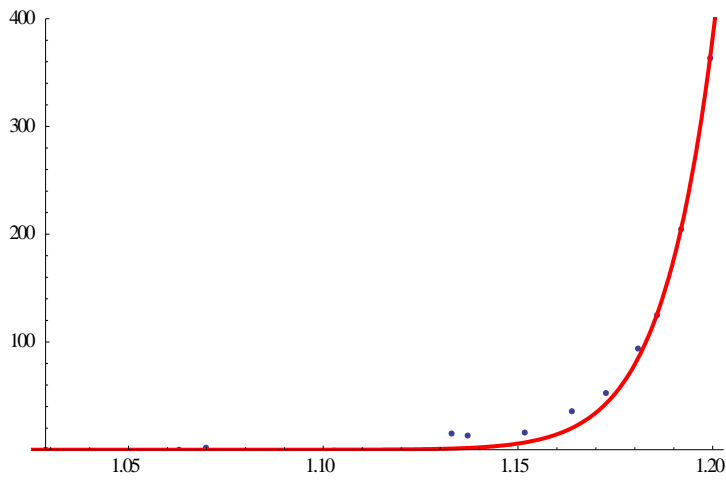


$$YI := x \rightarrow x \cdot (x - 1)^4 \cdot \exp(8.1 \cdot x);$$

For the analysis of σ_{11} - σ_{22}



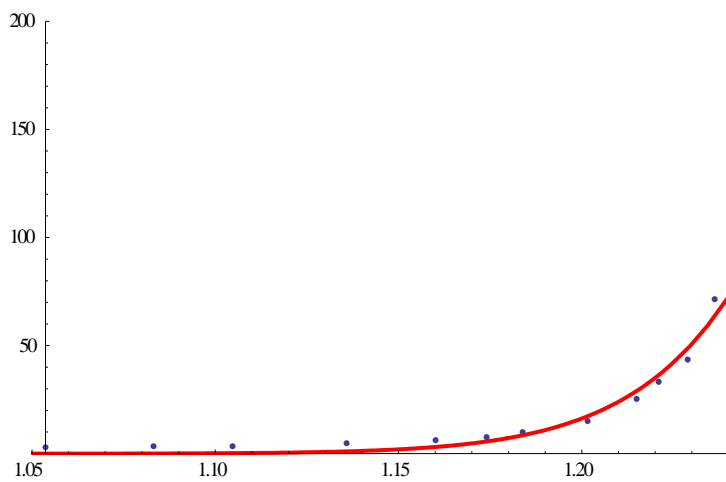
$$YI := x \cdot (x - 1)^{10} \cdot \exp(18 \cdot x);$$



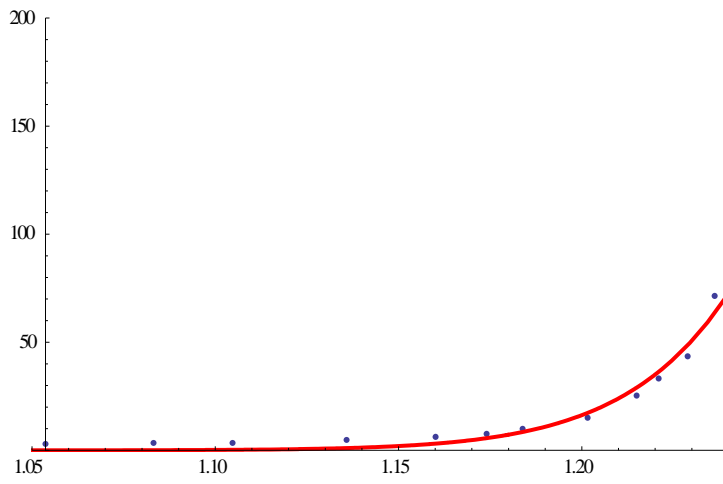
$$YI := x \rightarrow x^{30} + (x - 1)^6 \cdot \exp(x);$$

5.3 Second Graph By Using Mathematica

For the analysis of σ_{11}

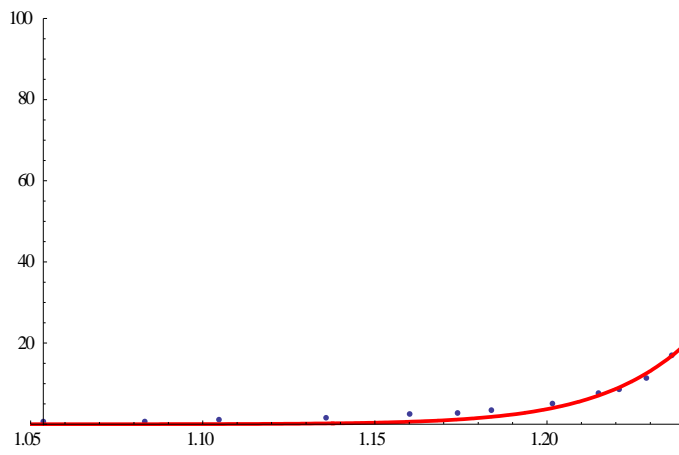


$$YI := x \rightarrow x \cdot (x - 1)^9 \cdot \exp(18 \cdot x);$$

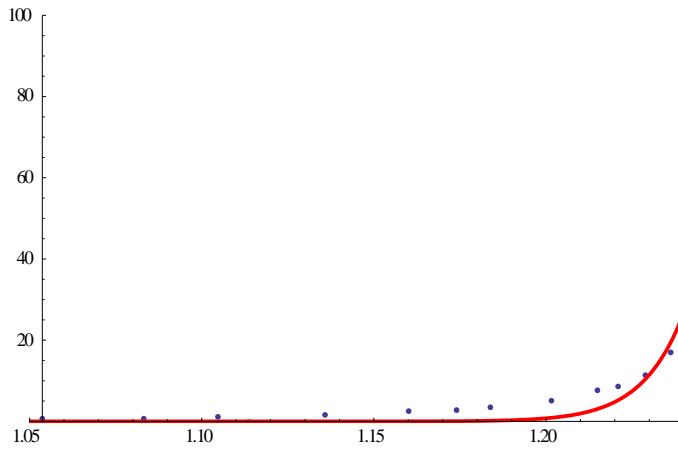


$$YI := x \rightarrow x^{23} + (x - 1)^{13} \cdot \exp(23 \cdot x);$$

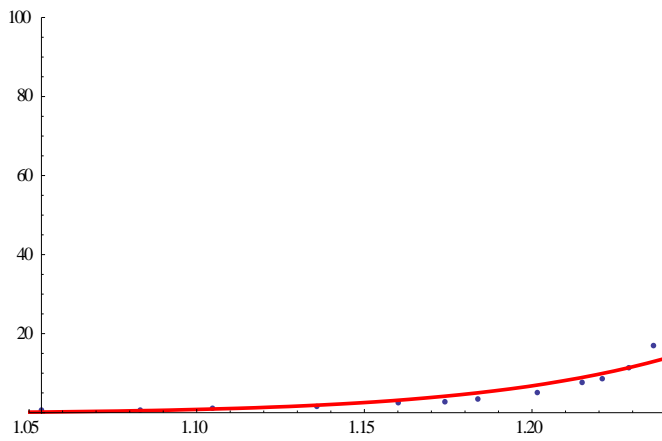
For the analysis of σ22



$$YI := x \rightarrow x^{28} \cdot (x - 1);$$

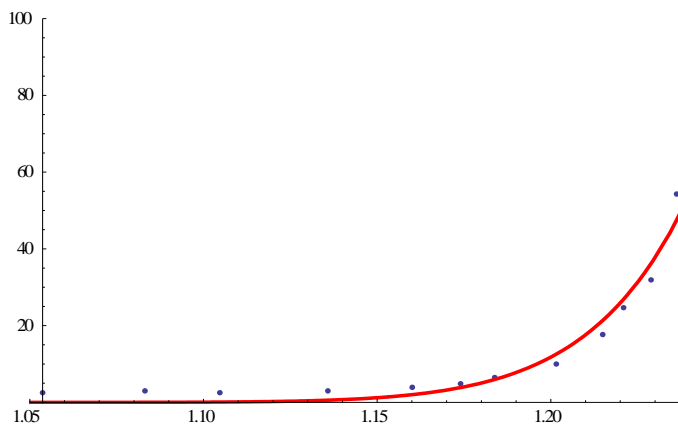


$$YI := x \rightarrow (x - 1)^4 \cdot \exp(8.4 \cdot x);$$

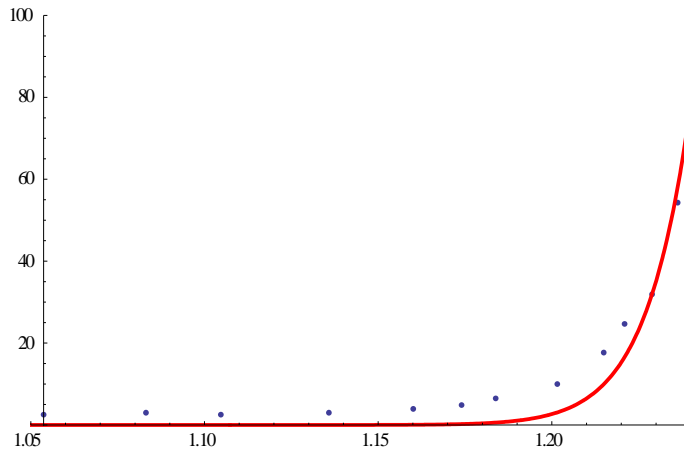


$$YI := x \rightarrow x \cdot (x - 1)^4 \cdot \exp(8.1 \cdot x);$$

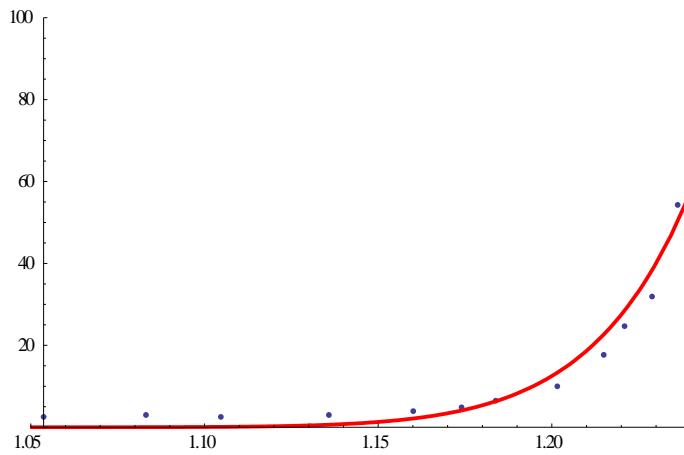
For the analysis of σ_{11} - σ_{22}



$$YI := x \rightarrow x^{30} + (x - 1)^6 \cdot \exp(x);$$



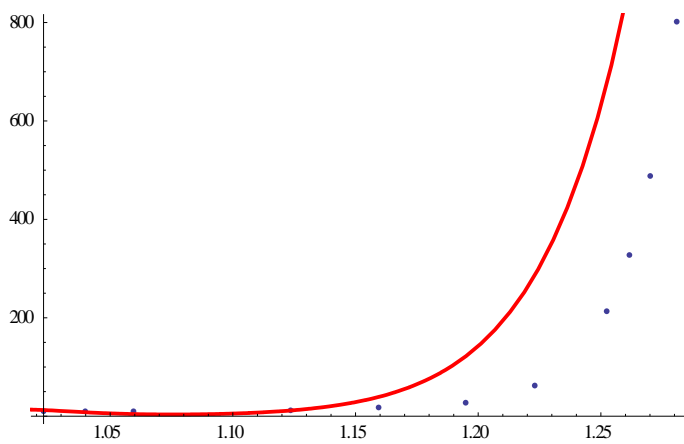
$$YI := x \rightarrow (x - 1)^4 \cdot \exp(10 \cdot x);$$



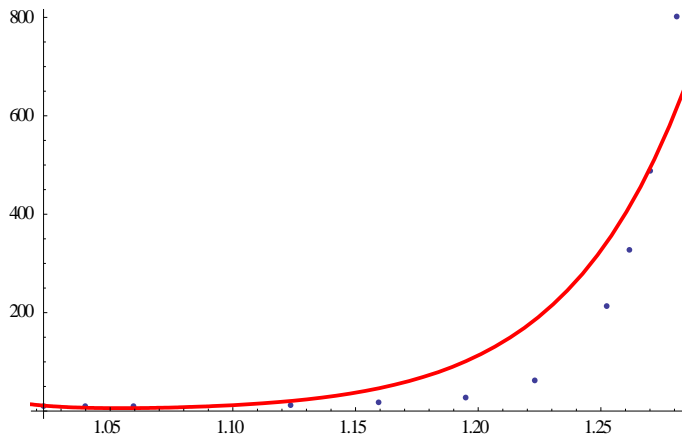
$$YI := x \rightarrow x(x - 1)^2 \cdot \exp(5 \cdot x);$$

5.4 Third Graph By Using Mathematica

For the analysis of σ_{11}

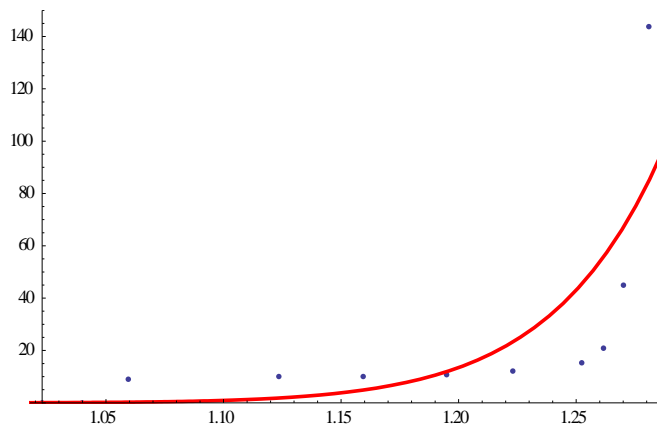


$$Y1[x_] := (x^31)(x-1)$$

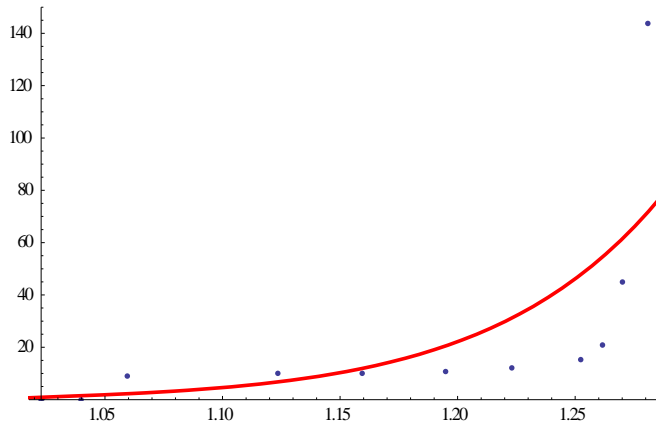


$$YI := x \rightarrow x^{26};$$

For the analysis of σ_{22}

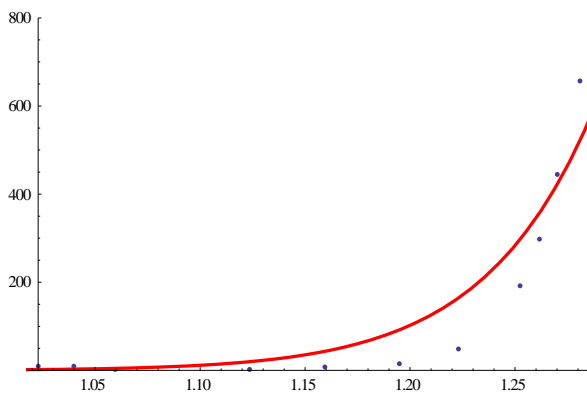


$$YI := x \rightarrow x(x - 1)^{15} \cdot \exp(20 \cdot x);$$

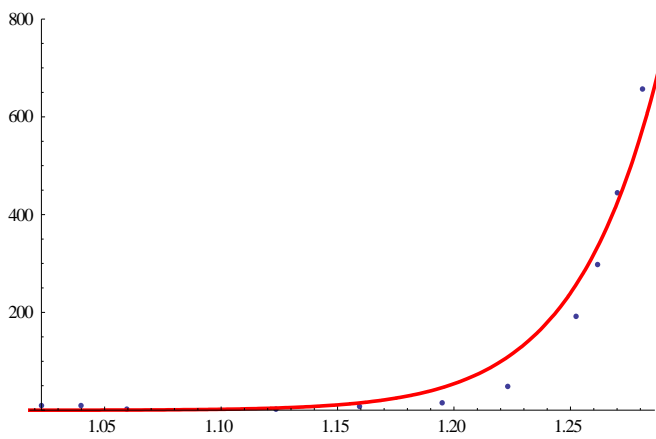


$$YI := x \rightarrow x(x - 1)^3 \cdot \exp(5 \cdot x);$$

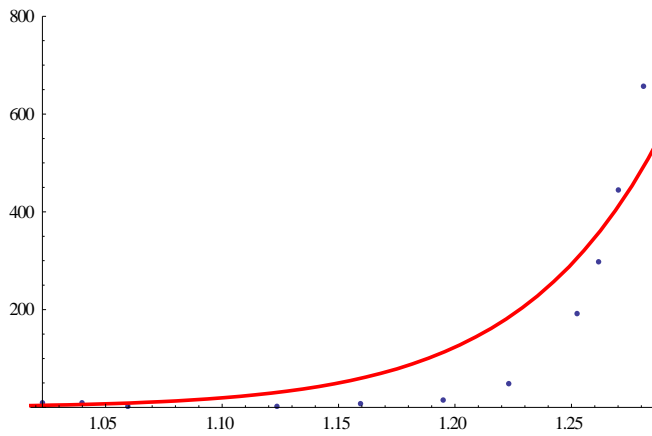
For the analysis of σ_{11} - σ_{22}



$$YI := x \rightarrow x^{25}$$



$$YI := x \rightarrow x^{31}(x - 1)$$



$$YI := x \rightarrow x^{20} \exp(x)$$

6.0 Results

Graph 1(Maple) - Equibiaxial strain applied to anterior leaflet (Experimental 1)

	Equation	$\frac{2(U_L - U_T)}{\beta/2}$	U_T
σ_{11}	$YI := x \rightarrow x \cdot (x - 1)^9 \cdot \exp(18 \cdot x);$	0.26427	2.3848
	$YI := x \rightarrow x^{23} + (x - 1)^{13} \cdot \exp(23 \cdot x);$	0.43244	26.77257
σ_{22}	$YI := x \rightarrow x^{28} \cdot (x - 1);$		1.0223
	$YI := x \rightarrow x \cdot (x - 1)^4 \cdot \exp(8.1 \cdot x);$		1.15374
$\sigma_{11} - \sigma_{22}$	$YI := x \cdot (x - 1)^{10} \cdot \exp(18 \cdot x);$	1.2572	
	$YI := x \rightarrow x^{30} + (x - 1)^6 \cdot \exp(x);$	0.9874	

Table 6.1

Graph 1(Mathematica) -Equibiaxial strain applied to anterior leaflet (Experimental 1)

	Equation	U_T	U_L	β	$\frac{2U_L - U_T}{\beta/2}$
σ_{11}	$YI := x \rightarrow x \cdot (x - 1)^9 \cdot \exp(18 \cdot x);$	2.3965	0.6652	2.6608	5.4582

	$YI := x \rightarrow x^{23} + (x - 1)^{13} \cdot \exp(23 \cdot x);$	26.8326	6.8162	27.265	60.4815
σ_{22}	$YI := x \rightarrow x^{28} \cdot (x - 1);$	1.02234			
	$YI := x \rightarrow (x - 1)^4 \cdot \exp(8.4 \cdot x);$	0.9944			
	$YI := x \rightarrow x \cdot (x - 1)^4 \cdot \exp(8.1 \cdot x);$	1.15374			
$\sigma_{11} - \sigma_{22}$	$YI := x \rightarrow x^{30} + (x - 1)^6 \cdot \exp(x);$	-0.1646	0.1646	0.6582	-0.1647
	$YI := x \rightarrow (x - 1)^4 \cdot \exp(10 \cdot x);$	-0.1409	0.1409	-0.5637	
	$YI := x \rightarrow (x - 1)^{18} \cdot \exp(30 \cdot x);$	-0.05256	0.05256	0.2102	
	$YI := x \rightarrow (x - 1)^{11} \cdot \exp(20 \cdot x);$	-0.0981	0.0981	0.3924	

Table 6.2

Graph 2(Mathematica)- Figure 2: Typical stress- stretch data for soft tissues. Shown is the nonlinear, anisotropic response of excised epicardium, a collagenous membrane that covers the heart

	Equation	U_T	U_L	β	$2U_L - U_T + \beta/2$
σ_{11}	$YI := x \rightarrow x(x - 1)^6 \cdot \exp(10 \cdot x);$	-1.2212	0.0059	0.02379	
	$YI := x \rightarrow x(x - 1)^{-1}$	5.09256	1.3799	5.5198	
	$YI := x \rightarrow x^{18}$	5.7248	1.6800	6.7201	
σ_{22}	$YI := x \rightarrow x(x - 1)^7 \cdot \exp(10 \cdot x);$	1.3881			
	$YI := x \rightarrow x(x - 1)^{15} \cdot \exp(20 \cdot x);$	0.7225			

	$YI := x \rightarrow x(x-1)^3 \cdot \exp(5 \cdot x);$	1.5056			
$\sigma_{11} - \sigma_{22}$	$YI := x \rightarrow x(x-1)^7 \cdot \exp(10 \cdot x);$	-0.1572	0.1572	0.6288	
	$YI := x \rightarrow x(x-1)^{14} \cdot \exp(20 \cdot x);$	-0.0850	0.0850	0.3401	
	$YI := x \rightarrow x(x-1)^2 \cdot \exp(5 \cdot x);$	-0.1667	0.1667	0.6668	

Table 6.3

Graph 3(Maple)-Equibiaxial strain applied to psterior leaflet

	Equation	$2U_L - U_T + \beta/2$	U_T
σ_{11}	$YI := x \rightarrow x^{26};$	0.98657	30.0991
	$YI := x \rightarrow (x^{31} \cdot (x-1));$	1.1374	1136.465
σ_{22}	$YI := x \rightarrow x^{23} \cdot (x-1);$		1.0644
	$YI := x \rightarrow x^{18} - 7.766;$		0.876
$\sigma_{11} - \sigma_{22}$	$YI := x \rightarrow x^{25}$	1.0706	
	$YI := x \rightarrow x^{20} \exp(x)$	0.9673	

Table 6.4

Graph 3 (Mathematica)-Equibiaxial strain applied to psterior leaflet

	Equation	U_T	U_L	β	$2U_L - U_T + \beta/2$
σ_{11}	$YI := x \rightarrow x^{26};$	-30.2067	-7.30517	-29.2207	
	$YI := x \rightarrow (x^{31} \cdot (x-1));$	1137.77	284.728	1138.91	

σ_{22}	$YI := x \rightarrow x^{23} \cdot (x - 1);$	1.01615			
	$YI := x \rightarrow x^{18} - 7.766;$	0.8314			
$\sigma_{11} - \sigma_{22}$	$YI := x \rightarrow x^{25}$	-0.1784	0.1784	0.7136	
	$YI := x \rightarrow x^{31}(x - 1)$	-0.1625	0.1625	0.6512	
	$YI := x \rightarrow x^{20} \exp(x)$	-0.1612	0.1612	0.6448	

Table 6.5

7.0 Discussion

After all the findings, I tend to conclude this research since the results are found even the result show us a small conclusion. It is not easy to conclude this research because there are lots of uncertainties. The conclusions I can draw are as follow.

First and foremost, the result show us graph 1 and graph 2 can use the exponential constitutive law. The main parts of the equation are exponential part and the variable (x-1). After that, I tended to find the best equation among lots of equation such as , , and others. Graph 3 has to eliminate the exponential part and its main parts of the designed equation are x and (x-1).

Besides that, there are the small graphs need to be analysis which are known as , and . In the graph , it can be done by finding all the positive constants. In the graph , U(t) are around 1 in all the extracted data. In the graph , the value of U(t) must be equal to -U(l). This result cannot be accepted because the material constant should be positive value.

Finally, the graph fitting are good by using the NonLinearFit in th Maple and LeastSquare Method in Mathematica but the good graph fitting does not provide us the good reading of the material constants.

8.0 Reference

1. B.A. Mahad, M.H.B.M Shariff, Mukheta Isa, Zainal Abdul Aziz, Physical Interpretation Constitutive Model for Biological Tissues with Application to Mitral Valve Leaflet Tissues (2013). *Proceedings of the International Conference on Applied Analysis and Mathematical Modeling (ICAAMM2013)*, Istanbul, Turkey, 2nd – 5th June 2013. UTM Skudai: Conference Paper, <http://eprints.utm.my/38577/>.
2. B.A. Mahad, M.H.B.M Shariff, Mukheta Isa, Zainal Abdul Aziz, Constitutive Equations of Mitral Valve Leaflet in Terms of Principal Stretches (2014). *Proceedings*

of *Global Academic Network International Dubai Conference 2014*, Dubai, 12th – 15th February 2014.

3. B.A. Mahad , M.H.B.M Shariff, Mukheta Isa, Zainal Abdul Aziz, The Constitutive Model of Incompressible Soft Tissues with Physical Invariants and the Correlation Theory and Experiment (2012). A Book Chapter 2 in “*Research in Applied Mathematics*”. B. A. Mahad (Editor). Mathematics Department, Faculty of Science, UTM Skudai: Publisher UTM Skudai.
4. B.A. Mahad, M.H.B.M Shariff, Mukheta Isa, Zainal Abdul Aziz, YusofYaacob, Theory and Experiment for Transversely Isotropic Nonlinear Incompressible Solids (2008). A Book Chapter in *Research in Applied Mathematics*. Mathematics Department, UTM Skudai: UTM Skudai, 89-101. ISBN: 978-983-52-06-6-1.
5. B.A. Mahad, M.H.B.M Shariff, Mukheta Isa, Zainal Abdul Aziz, Constitutive Equations of Mitral Valve Leaflet in Terms of Principal Stretches (2014). *World Virtual Conference On Applied Sciences And Engineering Applications*, 27-29 March 2015
6. M.H.B.M Shariff, B.A. Mahad ,Zainal Abdul Aziz, On the Correlation of Theory and Experiment for Transversely Isotropic Nonlinear Incompressible Solids (2008). *Proceedings of the 9th International Conference on Computational Structures Technology*, Athens, Greece, 2nd – 5th September 2008. B.H.V. Toppings and M. Papadrakakis (Editors). Stirlingshire, Scotland, UK: Civil-Comp Press. Paper 258, doi: 10.4203/ccp.88.258.
7. Salvatore Federico, walter Herzog, 2008, Towards an analytical model for soft biological tissues
8. Walter Jaunzemis, 1967, *Continuum Mechanics*
9. Eli and Mohammad, 26 April 2005, A large strain finite element formulation for biological tissue application to mitral valve leaflet tissue mechanics
10. R.W.Ogden, *Nonlinear Elastic Deformation* (Ellis Horwood, Chichester 1984)
11. M.H.B.M Shariff, *Nonlinear Transversely Isotropic Elastic Solid: An Representation*
12. Jose Daniel D.MeloAndR.W.Radford, 2001, Determination of the Elastic Constants of a Transversely Isotropic Lamina Using Laminate Coefficients of Thermal Expansion.
13. R.W.Ogden, Elastic deformations of rubberlike solids, *Mechanics of Solid*, The Rodney Hill 60th Anniversary Volume (499-537)
14. , *J.Appl.Phys.*38(1967) 2997-3002.
15. M.H.B.M Shariff, An anisotropic model of the Mullins effect, *J.Engng.Math.*56(2006) 415-435.
16. M.H.B.M Shariff, *Nonlinear Transversely Isotropic Elastic Solid: An alternative Representation*

17. Fung, Y C, 1967 Elasticity of soft tissues in simple elongation, *America Journal of Physiology* 213, 1532-1544
18. Jeffrey A.Weiss, Bradley N.Maker, Sanjay Govindjee ,1995 Finite element implementation of incompressible, transversely isotropic hyperelasticity.
19. Georges Limbert, Mark Taylor , 2001 , On the constitutive modeling biological soft connective tissues- A general theoretical framework and explicit forms of the tensors of elasticity for strongly anisotropic continuum fiber-reinforced composites at finite strain.
20. NgaShu Juan, 2014, Constitutive equation for biological tissues.
21. Georges Limbert and John Middleton, 2004, A transversely isotropic viscohyperelastic material- Application to the modelling of biological soft connective tissues.
22. Fulin Lei , A.Z Szeri, 2006 , Inverse analysis of constitutive models: Biological soft tissues
23. Holzapfel, G.A., 2001. *Nonlinear Solid Mechanics: A Continuum Approach for Engineering*. Wiley, New York
24. Almeida, E.S., Spilker, R.L., 1998. Finite element formulations for hyperelastic transversely isotropic biphasic soft tissues. *Computer Methods in Applied Mechanics and Engineering*. 151, 513–538.
25. Ruter, M., Stein, E., 2000. Analysis, finite element computation and error estimation in transversely isotropic nearly incompressible finite elasticity. *Computer Methods in Applied Mechanics and Engineering* 190, 519–541.

MATHEMATICAL MODELLING OF DIFFERENT TYPES OF BUNGEE

Mayamin Syafini binti Mohamed Azlan & PM Hazimah Abdul Hamid

Abstract

'Bungee' is a sport that involves particle motion problems. Classically, the bungee problems can be solved using differential equations in Mathematical Modelling. Most of the modelled equations are solved using the first order and second order ordinary differential equations (ODE) method. The most important components in bungee sport to be determined are the jumpers' motions that involve their displacement, velocity and acceleration at different conditions. Basically, the variables involved in bungee sport are the mass of the jumper, air resistance and spring constant, as well as the time interval of a jump. This research focuses on the basic model of bungee sport of different types of jump and the relationships between variables involved as well as the effects on the displacement, velocity and the acceleration of the jumper when the values of the variables differ.

Keywords: (Bungee Jumping, Mathematical Modelling of Bungee)

Introduction

Recently, there are many discussions relating Mathematical Modelling with physical activities. One of them is bungee, which today is mostly sought by those who are craving for adrenaline rush booster. As it becomes famous day by day throughout the world, the basic problem of bungee jumping is finally formulated and resolved.

The relation between Mathematics and Physics involved in this sport is illustrated to determine the motion of the bungee jumpers. Some of basic laws of Physics such as Newton's Second Law and Hooke's Law as well as Differential Equations are used to formulate the jumper's motion but there are different forces acting in different systems of jump. This study will basically discuss about three types of jump which is a straightforward bungee, bungee run and bungee trampoline. The three types of bungee problem involve both first order and second order Ordinary Differential Equation (ODE) that has specific method to be used. Specific variables and assumptions must be recognized before we can derive the equations for the three types of bungee.

This study will be discussing about the basic mathematical models for different types of bungee. We will be investigating the effects of changing the value of air resistance constant, mass of jumper and time of jump towards the jumpers' displacement, velocities and acceleration for different types of jump. Finally we will plot graphs to relate the affecting factors towards the jumper's motion.

Literature Review

The origin of bungee sport is quite recent, but the activity is related to the centuries-old ritualistic practices of "land divers" of Pentecost Island in the Pacific Archipelago of Vanuatu who demonstrate their courage and offer their injuries to the gods for a plentiful harvest of yams. Menz (1993) stated that the sport sprang up all over the US after it flourished in New Zealand and France in 1990s. In his study he stated that the principle components in the physics of this sport are the gravitational potential energy of the jumper and the elastic potential of the stretched cord. At the bottom of the jump the kinetic energy is

zero since the jumper’s velocity is zero. He also assumed the bungee cord to be massless. Nicole Kelly (2013) stated in her study that if a jumper wants to just barely touch the water under the bridge, the difference between the height of the bridge and how far the rope needs to stretch must be determined.

Ramachandran (2013) has studied about bungee trampoline, he stated that the bungee cords are attached to poles at the sides of the trampoline and the whole process is governed by “energy conversions” from one form to another where the jumper transfers some of the original potential energy into kinetic energy. Newton's Second Law of motion is needed to model the bungee motion as mentioned by Moon and Thompson (2014) in their study and physics are needed to derive differential equation that model the motions is Newton’s Second Law.

Methodology

Both first and second order ODE is involved in this bungee problem. We will be using linear equation to solve first order ODE while we will be using undetermined coefficient method to solve second order non-homogeneous equation.

FIRST ORDER ODE <small>(LINEAR EQUATION)</small>	SECOND ORDER ODE <small>(NON-HOMOGENEOUS EQUATION-use Undetermined coefficient method)</small>
$\frac{dy}{dx} + P(x)y = Q(x)$	$P(x)y'' + Q(x)y' + R(x)y = G(x)$
$y(x) = \frac{\int \mu(x)Q(x)dx + C}{\mu(x)}$	$y(x) = y_h(x) + y_p(x)$

For straightforward bungee we will be using Newton’s Second Law to derive the equation.

$$F = ma$$

$$v = x'$$

$$a = v'$$

$$v' = x''$$

$$mx'' = -(mg + K_r x')$$

We reduce the order and will be getting first order linear ODE,

$$v' + \frac{K_r}{m}v = -g$$

$$v(t) = \frac{mg}{K_r} \left(e^{-\frac{K_r t}{m}} - 1 \right)$$

Freedman (2012) stated that acceleration is the rate of change of velocity; so we have to differentiate the equation of velocity w.r.t t,

$$a(t) = \frac{d}{dt} \left(\frac{mg}{K_r} \left(e^{-\frac{K_r t}{m}} - 1 \right) \right)$$

$$a(t) = -g e^{-\frac{K_r t}{m}}$$

$$x' = \frac{mg}{K_r} \left(e^{-\frac{K_r t}{m}} - 1 \right)$$

As velocity is the rate of change of displacement, to get displacement we have to integrate velocity equation w.r.t t ,

$$x(t) = \int \frac{mg}{K_r} \left(e^{-\frac{K_r t}{m}} - 1 \right) dt$$

$$x(t) = x_0 - \frac{mg}{K_r} t + \frac{m^2 g}{K_r^2} \left(1 - e^{-\frac{K_r t}{m}} \right)$$

While for bungee run and bungee trampoline, Newton's Second Law and Hooke's law are governed in order to derive the equation.

a) For bungee run

$$F = ma$$

$$F = F_s + W$$

$$ma = mg - kx$$

$$a = g - \frac{k}{m} x$$

$$x'' + \frac{k}{m} x = g$$

We used undetermined coefficient method to solve second order non-homogeneous ODE

$$x(t) = x_0 + \frac{mg}{k} \left(1 - \cos \sqrt{\frac{k}{m}} t \right)$$

We have to differentiate the displacement equation w.r.t t once to get velocity equation and once again to get the acceleration equation.

$$v(t) = \sqrt{\frac{k}{m}} \frac{mg}{k} \sin \sqrt{\frac{k}{m}} t$$

$$a(t) = g \cos \sqrt{\frac{k}{m}} t$$

b) For bungee trampoline we will be using the same method as in bungee run and will be getting

$$x(t) = x_0 + \frac{mg}{2k} \left(1 - \cos \sqrt{2 \frac{k}{m}} t \right)$$

$$v(t) = \sqrt{2 \frac{k}{m} \frac{mg}{k}} \sin \sqrt{2 \frac{k}{m}} t$$

$$a(t) = 2g \cos \sqrt{2 \frac{k}{m}} t$$

Case Studies and Discussion

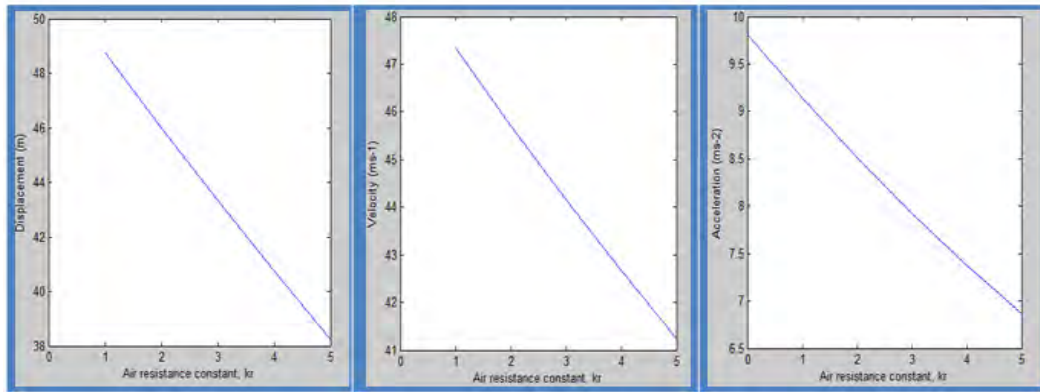
DIFFERENT AIR RESISTANCE IN STRAIGHTFORWARD BUNGEE

- A man of mass 70kg plan to bungee jump from a bridge which is 71m above the river .Assuming the air resistance is constant, K_r is 1.0. If he can make sure that his velocity going down is less than 60 ms^{-1} for the first 5 seconds, he will then take the jump. In the same time, he wants to know within that velocity how far he has jumped as well as his acceleration. A constant $g = 9.81 \text{ ms}^{-2}$ is used. Will he take the jump?
- As the jumper moves downwards, the air resistance K_r decreases constantly and when he reaches maximum displacement, there is no air resistance acted on him. We are interested to know his new $x(t)$, $v(t)$ and $a(t)$ within 5seconds?

Table 1: Comparison between Displacement, Velocity and Acceleration at Different Value of Air Resistance constant

K_r	$x(5)/m$	$v(5)/\text{ms}^{-1}$	$a(5)/\text{ms}^{-2}$
0	0	0	9.81
1	- 48.76	- 47.34	9.14
2	- 45.99	- 45.71	8.80
3	- 43.32	- 44.15	7.92
4	- 40.73	- 42.67	7.37
5	- 38.24	- 41.25	6.86

Figure 1: Graph of Air Resistance Constant versus Displacement, Velocity and Acceleration



From the table as the velocity within 5 seconds going down is less than 60 ms^{-1} , then the man will take the jump. We can see that as the air resistance decreases, the displacement, velocity and acceleration of jumper's increases. This shows that air resistance constant is inversely proportional to the motions of jumper.

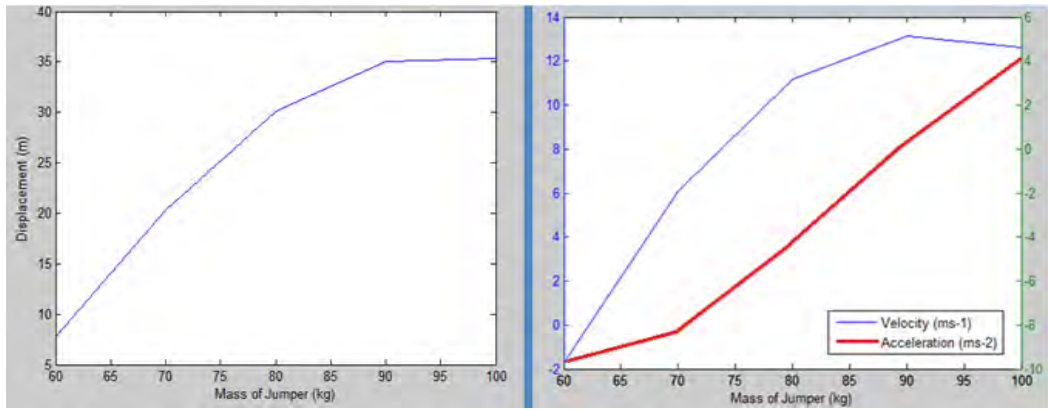
DIFFERENT MASS OF JUMPER IN BUNGEE RUN

- Assuming that the spring constant, k for the bungee run is 50 N/m . There are two runners of mass 60 kg and 90 kg who compete to get the farthest distance on the inflatable run. Below shows the different result for both of the runners within 10.5 seconds. Assuming the anchor point is at 0 meter. We are interested to know which runner will go across the finishing line first.

Table 2: Comparison between Displacement, Velocity and Acceleration of Different Mass of Jumpers.

Runner	Mass (kg)	$x(10.5)/m$	$v(10.5)/\text{ms}^{-1}$	$a(10.5)/\text{ms}^{-2}$
A	60	7.78	-1.72	-9.68
B	70	20.27	6.07	-8.36
C	60	30.17	11.19	-4.24
D	90	35.08	13.16	0.27
E	100	35.36	12.61	4.08

Figure 2: Graph of Mass of Jumpers versus Displacement, Velocity and Acceleration



Runner D with mass 90 kg will go in further displacement compared to Runner A with mass 60 kg. So, Runner D will win the competition. From the graph we can see that as mass of jumpers increase, the displacement and velocity increases while acceleration decrease. This shows that displacement and velocity is directly proportional to the mass of jumpers while acceleration is inversely proportional to the mass of jumpers.

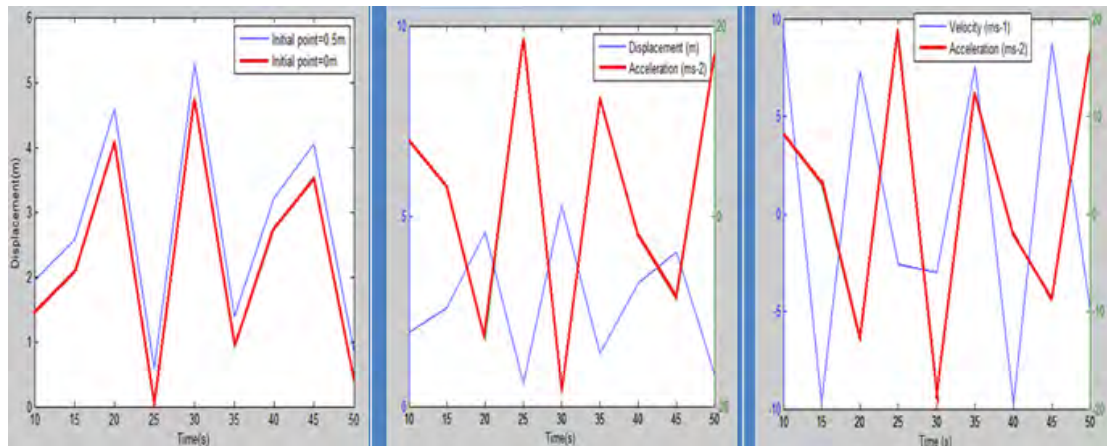
DIFFERENT TIME IN BUNGEE TRAMPOLINE

- A boy who weighs 35 kg is jumping on a bungee trampoline and is connected to two springs with a constant 70 N/m. Assuming that the boy then jumps from a chair on the trampoline making the anchor point is 0.5 m height. What is his new $x(t)$, $v(t)$ and $a(t)$ within the same time interval?

Table 3: Comparison between Displacement, Velocity and Acceleration at Different time of Jump and Different Initial Point

Time(s)	$x_0 = 0.0m$	$x_0 = 0.5m$	$v(t)/ms^{-1}$	$a(t)/ms^{-2}$
10	1.45	1.95	8.96	8.007
15	2.07	2.57	-9.69	3.03
20	4.09	4.59	7.31	-13.09
25	0.086	0.586	-2.57	18.93
30	4.79	5.29	-2.99	-18.69
35	0.89	1.39	7.59	12.43
40	2.72	3.22	-9.75	-2.17
45	3.55	4.05	8.77	-8.79
50	0.34	0.84	-4.97	16.92

Figure 3: Graph of Time of Jump versus Displacement, Velocity and Acceleration



From the graphs we can see that only displacement is affected by the changing of initial anchor point but not velocity and acceleration. The second graph shows that as time of jump increases, when displacement increases the acceleration decreases and this shows that displacement is inversely proportional to acceleration. The third graph does not show any obvious relationship between velocity and acceleration as time of jump increases because it fluctuates over time.

Conclusion

Newton's Second Law of motion and Hooke's Law are mostly governed in most of the three cases in order to get the basic model of displacement, velocity and acceleration in all the three jumps. From the plotted graphs, we can see that different cases will contribute to different relationship between the affecting factors. To get a better result in the future studies, we should not put so many conditions to be neglected because it might give big impacts in real life cases.

References

- Menz. P. G., (1993). The Physics of Bungee Jumping, *The Physics Teacher*, 31.
- Nicole Kelly.,(2013). *Modelling a Bungee Jump*, Fvcc.edu.FlatheaValleyCommunity College
- Ramachandran A.,(2013). Modeling and Understanding the Physics of Bungee Trampoline Jumping, *International Journal of Mechanical Engineering and Research*, 3, 589-596.
- Moon E. and Thompson J., (2014). *Modelling a Bungee Jump Using Differential Equations*.
- Freedman. Y., (2012). *University Physics with Modern Physics*. California: Pearson

SOLUTION OF DUSTY FLOW PAST A VERTICAL PLATE

Mohammad Asqalani Bin Fakarudin & Dr. Anati Ali

Abstract

The presence of contaminating dust particles in fluids can occur naturally or deliberately. These problems associated with the flow characteristics and their properties are of fundamental interest in the field of fluid. From this research, we use the fundamental physical principles to illustrate and derive the governing equation of fluid flow. Continuity equation is derived from the first fundamental physical principle, followed by momentum equation from Newton second law and lastly energy equation. The different model of the flow will produce different mathematical formulation of the governing equation for the fluid and the particles, and the equation obtained is solved by using Laplace transform. The graph of the solution obtained is to observed the effect of temperature against y with the different value of parameter such as time t , angle ω , limit b .

Keyword: Dusty flow, boundary layer.

Introduction

Boundary layer flow is the condition where the fluid or gases are moving near the boundary. The study of the boundary layer flow is general and quite important due to its application in industries such as the process in the automotive, chemical and coating industries, environmental application, gas cooling system to improve heat transfer process. In other words, the studies of these systems are physically useful for various reasons.

In this paper, we are focusing on the two-phase boundary layer flow with the presence of dust particle along the flow. The mechanical behaviour of dusty fluids has been a subject of study receiving greater attention during recent year. The presences of dust particle are everywhere and can occur accidentally or deliberately. So, the presence of dust particle in a fluid makes the study of flow problems quite complicated and encounter in a wide variety of engineering problems.

In this two-phase boundary layer flow, we used the governing equations containing momentum equation for the flow of dusty fluid, the equation of energy and continuity for the fluid phase and particle phase. We will use these governing equations to solve the problem analytically, not numerically. It is because analytic solutions are valid on the whole domain of definition but numerical solutions are only valid at chosen point in the domain of definition. The main objectives of this study are (i) to derive the governing equations that are related in this study such as continuity equation, conservation of momentum and conservation of energy equation, (ii) to find the solution of the equation using Laplace transform technique. The scope of the research will cover two phase boundary layer problem. This research is conducted to derive and solve the equations to see the velocity and the temperature of fluid and dust particles that moving or flowing past a vertical plate. No experiment will be conducted. The importance of the study of two-phase flows has led to the development of several multiphase theories. There have been many developments in the study of two-phase flows due to their wide applications in the field of Engineering, Technology, Nature, Medicine, Chemical Processing.

Literature Review

The boundary layer concept is proposed by Professor Ludwig Prandtl in 1904 (Tulapurkara 2005). This theory states that due to the no-slip condition, the velocity on the surface of a stationary body is zero, but the velocity given by inviscid flow theory would be reached within a thin layer which is called the boundary layer. Since the layer is thin, the velocity gradients are large and the shear stresses are negligible even when viscosity is small. The boundary layer concept grows rapidly and is now applied in almost all branches of engineering. The example of the research is boundary-layer behavior on continuous cylindrical solid surfaces made by B.C. Sakiadis (1961). Governing equation consist the dependent variables of a fluid that is moving. The dependent variables are the fluid-velocity components, pressure, density, temperature, and internal energy or some similar set of variables. The equations governing these variables will be derived from the principles of mass, momentum, and energy conservation and from equations of state. in the better design of airplanes, engine components and many other equipment involving fluid flow. The two-phase fluid systems is the motion of a liquid or gas which containing dust or immiscible inert identical particles. The motion of fluid is governed by Navier-Stokes' equation of motion, while the particle motion is described by a separate set of Euler's equation for change of mass and momentum. There have been many developments in the study of two-phase flows due to their wide applications in the field of engineering, technology, nature, medicine, chemical processing etc. The example of the research about fluid phase is the investigation of gas-liquid flow in inclined pipes to determine the effect of pipe inclination angle on liquid holdup and pressure loss made by H.D. Beggs, J. P. Brill .

The Laplace transform is named after [Pierre-Simon Laplace](#). Laplace transform is a method frequently employed by researcher in solving differential equation. By applying the Laplace transform, we can reduce a differential equation to an algebra problem. Below is the technique to transformed from partial differential equation to Laplace.

$$\mathcal{L}\{w(x,t)\} = \bar{w}(x,s) = \int_0^{\infty} e^{-st} w(x,t) dt$$

(1)

$$\mathcal{L}\{w_t(x,t)\} = s\mathcal{L}\{w(x,t)\} - w(x,0) = s\bar{w}(x,s) - w(x,0)$$

(2)

$$\mathcal{L}\{w_{tt}(x,t)\} = s^2\mathcal{L}\{w(x,t)\} - sw(x,0) - w_t(x,0)$$

(3)

$$\mathcal{L}\{w_x(x,t)\} = \frac{\partial}{\partial x} \mathcal{L}\{w(x,t)\}$$

(4)

$$\mathcal{L}\{w_{xx}(x,t)\} = \frac{\partial^2}{\partial x^2} \mathcal{L}\{w(x,t)\}.$$

(5)

Methodology

In deriving the governing equations from the fundamental physical principles, we need some illustration to help and make it easier to derive.

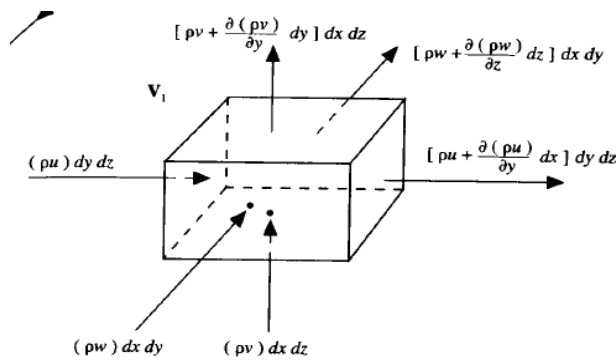


Figure 1: Infinitesimal small element fixed in space.

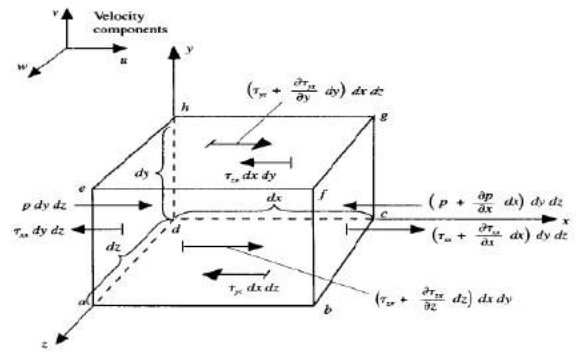


Figure 2: Infinitesimally small, moving fluid element in x direction.

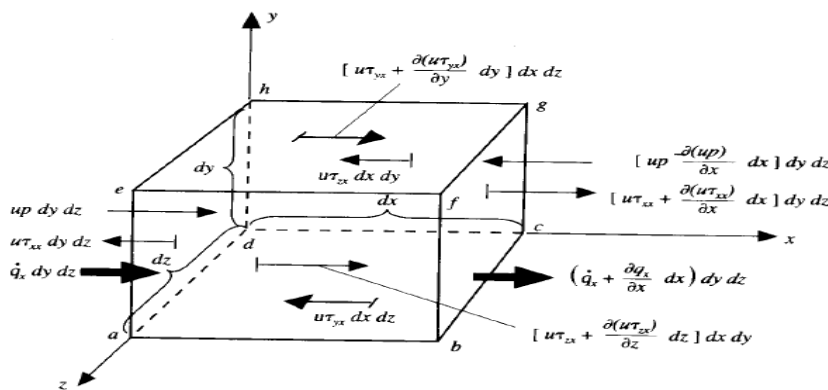


Figure 3: Energy fluxes associated with an infinitesimally small, moving fluid element.

Figure 1 shows the moving mass flow through the infinitesimal small element fixed in space, Since the physical principle of that mass is conserved, the net mass flow out of the element must equal the rate of decrease of mass inside the element. Therefore,

$$\frac{\partial \rho}{\partial t} + \nabla \cdot (\rho \mathbf{V}) = 0. \tag{6}$$

Before deriving momentum equation we should know there are two forces involve in the moving fluid element such as body force and surface forces. The surface forces consist of pressure and shear stress as shown in figure 2 and the body forces can be anything depend on the type of element. Therefore, the momentum equation is

$$\rho \left(\frac{\partial \mathbf{V}}{\partial t} + (\mathbf{V} \cdot \nabla) \mathbf{V} \right) = -\nabla p + \mu (\nabla^2 \mathbf{V}) + \rho f_i \tag{7}$$

The first law of thermodynamics states that the rate of change of energy inside fluid element is equal to the summation of net flux of heat into element and rate of work done on element due to body and surface forces as shown in the figure 3. So the energy equation can be expressed as

$$\rho c_v \left(\frac{\partial T}{\partial t} + u \frac{\partial T}{\partial x} + v \frac{\partial T}{\partial y} + w \frac{\partial T}{\partial z} \right) = \rho q + \frac{\partial}{\partial x} \left(k \frac{\partial T}{\partial x} \right) + \frac{\partial}{\partial y} \left(k \frac{\partial T}{\partial y} \right) + \frac{\partial}{\partial z} \left(k \frac{\partial T}{\partial z} \right) + \left(u \frac{\partial p}{\partial x} + v \frac{\partial p}{\partial y} + w \frac{\partial p}{\partial z} \right) + \phi$$

(8)

where

$$\phi = 2 \left\{ \left(\frac{\partial u}{\partial x} \right)^2 + \left(\frac{\partial v}{\partial y} \right)^2 + \left(\frac{\partial w}{\partial z} \right)^2 \right\} + \left(\frac{\partial v}{\partial x} + \frac{\partial u}{\partial y} \right)^2 + \left(\frac{\partial w}{\partial y} + \frac{\partial v}{\partial z} \right)^2 + \left(\frac{\partial u}{\partial z} + \frac{\partial w}{\partial x} \right)^2$$

We should consider some basic assumptions of fluid flows before the mathematical formulation. First, the fluid that are consider in this study is an incompressible Newtonian fluid, the particle of dust are in the same shape and non-deformable, the net effect of dust is the same to the force $KN(\mathbf{u}_p - \mathbf{u})$ per unit volume, where $\mathbf{u}_p(x, t)$ is the velocity vector of the dust particles, $\mathbf{u}(x, t)$ is the velocity vector of the fluid particles, K , the Stoke's drag constant which is ' $6\pi\mu a$ ' for spherical particles of radius a , and μ is the coefficient of viscosity. The temperature of the particle is different compare to the surrounding fluid, therefore the temperature will be defected, it means there will be heat transfer between fluid and particle. According to P.G Safman 1962, the heat transfer from a particle to fluid has the form $\frac{\rho_p C_s (T_p - T)}{\tau_T}$ where $\rho_p = Nm$, N is the number density, m is the mass of every

particle, ρ_p is the density of the density of the dust particle, C_s is the specific heat of particle, C_p is the specific heat at constant pressure of fluid, $\tau_T = \frac{3PrC_s \tau}{2C_p}$ is thermal

equilibrium time, $Pr = \frac{\mu C_p}{\kappa}$ is the Prandtl Number, κ is the thermal conductivity of the

fluid, T is the temperature of the fluid, T_p the temperature of the dust and $\tau = \frac{2\rho_p a^2}{9\mu}$

(Saffmann 1962).

The continuity equation for the fluid

$$\nabla \cdot \mathbf{u} = 0.$$

(9)

The conservation of momentum equation for the fluid

$$\rho \left[\frac{\partial \mathbf{u}}{\partial t} + (\mathbf{u} \cdot \nabla) \mathbf{u} \right] = -\nabla p + \mu \nabla^2 \mathbf{u} + KN(\mathbf{u}_p - \mathbf{u}). \tag{10}$$

The conservation of energy equation for the fluid

$$\rho C_p \left(\frac{\partial T}{\partial t} + u \frac{\partial T}{\partial x} + v \frac{\partial T}{\partial y} + w \frac{\partial T}{\partial z} \right) = \frac{\partial}{\partial x} \left(\kappa \frac{\partial T}{\partial x} \right) + \frac{\partial}{\partial y} \left(\kappa \frac{\partial T}{\partial y} \right) + \frac{\partial}{\partial z} \left(\kappa \frac{\partial T}{\partial z} \right) + \frac{\partial p}{\partial t} + u \frac{\partial p}{\partial x} + v \frac{\partial p}{\partial y} + w \frac{\partial p}{\partial z} + \phi + \frac{\rho_p C_s (T_p - T)}{\tau_T} \quad (11)$$

Continuity equation for the particle

$$\frac{\partial N}{\partial t} + \nabla \cdot (N \mathbf{u}_p) = 0. \quad (12)$$

Momentum equation for the particle

$$Nm \left[\frac{\partial \mathbf{u}_p}{\partial t} + (\mathbf{u}_p \cdot \nabla) \mathbf{u}_p \right] = KN (\mathbf{u} - \mathbf{u}_p). \quad (13)$$

Conservation of energy equation for the particle

$$\rho_p C_s \left(\frac{\partial T_p}{\partial t} + u_p \frac{\partial T}{\partial x} + v_p \frac{\partial T}{\partial y} + w_p \frac{\partial T}{\partial z} \right) = \frac{-\rho_p C_s (T_p - T)}{\tau_T}. \quad (14)$$

We only consider the fluid flow for unsteady two dimensional flow of a dusty fluid flow. So x and y directions only

$$\frac{\partial u}{\partial x} + \frac{\partial v}{\partial y} = 0. \quad (15)$$

$$\frac{\partial u}{\partial t} + u \frac{\partial u}{\partial x} + v \frac{\partial u}{\partial y} = -\frac{1}{\rho} \frac{\partial p}{\partial x} + \nu \left(\frac{\partial^2 u}{\partial y^2} \right) + \frac{KN}{\rho} (\mathbf{u} - \mathbf{u}_p). \quad (16)$$

$$\rho C_p \left(\frac{\partial T}{\partial t} + u \frac{\partial T}{\partial x} + v \frac{\partial T}{\partial y} \right) = \kappa \frac{\partial^2 T}{\partial y^2} + \frac{\rho_p C_s (T_p - T)}{\tau_T}. \quad (17)$$

$$\frac{\partial}{\partial x} (N u_p) + \frac{\partial}{\partial y} (N v_p) = 0. \quad (18)$$

$$\frac{\partial u_p}{\partial t} + u_p \frac{\partial u_p}{\partial x} + v_p \frac{\partial u_p}{\partial y} = \frac{K}{m} (\mathbf{u} - \mathbf{u}_p). \quad (19)$$

$$\rho_p C_p \left(\frac{\partial T_p}{\partial t} + u_p \frac{\partial T_p}{\partial x} + v_p \frac{\partial T_p}{\partial y} \right) = -\frac{\rho_p C_s (T_p - T)}{\tau_T}. \quad (20)$$

Non-dimensional equation will be used in the equation of motion for the fluid and particle phase. It is because non dimensional equation can eliminate the unit from the different variables in the equation and simplify it. Since the study is about the dusty flow across vertical plate, the x variable can be simply ignored. These are the non-dimensional quantities:

$$y = \frac{U_0 y'}{\nu}, \quad t = \frac{t' U_0}{\nu}, \quad \theta = \frac{T' - T'_\infty}{T'_w - T'_\infty}, \quad u = \frac{u'}{U_0}, \quad \nu = \frac{\mu}{\rho}$$

$$u_p = \frac{u'_p}{U_0}, \quad \theta_p = \frac{T'_p - T'_\infty}{T'_w - T'_\infty}, \quad \lambda = \frac{\tau U_0^2}{\nu}, \quad \text{Pr} = \frac{\nu \rho C_p}{\kappa},$$

From equation (16), we substitute the dimensional quantities with non dimensional quantities to get velocity equation for the fluid phase, we get:

$$\frac{\partial u}{\partial t} = \frac{\partial^2 u}{\partial y^2} + \alpha(u_p - u).$$

(21)

From equation (17), we substitute the dimensional quantities with non dimensional quantities to get model of heat equation for the fluid phase, we get:

$$\frac{\partial \theta}{\partial t} = \frac{1}{\text{Pr}} \frac{\partial^2 \theta}{\partial y^2} + \beta(\theta_p - \theta).$$

(22)

From equation (19), we substitute the dimensional quantities with non dimensional quantities to get velocity equation for the particle phase, we get

$$\frac{\partial u_p}{\partial t} = -\gamma(u_p - u).$$

(23)

From equation (20), we substitute the dimensional quantities with non dimensional quantities to get heat equation for the particle phase.

$$\frac{\partial \theta_p}{\partial t} = -\delta(\theta_p - \theta).$$

(24)

where

$$\alpha = \frac{KN\nu}{\rho U_0^2} = \frac{f}{\lambda}, \quad \beta = \frac{\rho_p C_s}{\rho C_p} \frac{1}{\tau_T} \frac{\nu}{U_0^2} = \frac{2f}{3\lambda}, \quad \gamma = \frac{K\nu}{mU_0^2} = \frac{1}{\lambda}, \quad \delta = \frac{\nu}{U_0^2 \tau_T} = \frac{2}{3\varphi \lambda}.$$

Boundary conditions are

$$u(0, t) = 1, \quad u(y, 0) = 0$$

$$\theta(0, t) = \cos \omega t, \quad \theta(y, 0) = \cos \omega t.$$

The symbols \bar{u} , \bar{u}_p , $\bar{\theta}$, $\bar{\theta}_p$ are the Laplace transformed of u , u_p , θ , θ_p

$$\bar{\theta}(y,s) = \frac{s}{s^2 + \omega^2} \frac{\sinh L(b-y)}{\sinh Lb} \quad (25)$$

$$\bar{\theta}_p = \frac{\delta \bar{\theta}}{s + \delta} \quad (26)$$

$$\bar{u}(y,s) = \frac{1}{s} \frac{\sinh M(b-y)}{\sinh Mb} \quad (27)$$

$$\bar{u}_p = \frac{\gamma \bar{u}}{s + \gamma} \quad (28)$$

where

$$L^2 = \frac{\text{Pr}(s^2 + (\beta + \delta)s)}{s + \delta} \bullet$$

$$M^2 = \frac{\text{Pr}(s^2 + (\alpha + \gamma)s)}{s + \gamma}$$

Taking inverse Laplace Transform, the temperature and the velocity of the fluid and particles phase is given by,

$$\begin{aligned} \theta(y,t) = & \frac{(AC + BD)\cos \omega t - (BC - AD)\sin \omega t}{C^2 + D^2} \\ & + \sum_{n=1}^{\infty} \frac{2n\pi m_1 \sin\left(\frac{n\pi y}{b}\right) (m_1 + \delta)^2 e^{m_1 t}}{b^2(m_1^2 + \omega^2)(m_1^2 + 2m_1\delta + \delta(\beta + \delta))} \\ & + \sum_{n=1}^{\infty} \frac{2n\pi m_2 \sin\left(\frac{n\pi y}{b}\right) (m_2 + \delta)^2 e^{m_2 t}}{b^2(m_2^2 + \omega^2)(m_2^2 + 2m_2\delta + \delta(\beta + \delta))} \end{aligned} \quad (29)$$

$$\begin{aligned} \theta_p(y,t) = & \frac{\delta}{\delta^2 + \omega^2} \left(\frac{((AC + BD)\delta + (BC - AD)\omega)\cos \omega t}{C^2 + D^2} + \frac{((AC + BD)\omega + (BC - AD)\delta)\sin \omega t}{C^2 + D^2} \right) \\ & + \sum_{n=1}^{\infty} \frac{2\delta n\pi m_1 \sin\left(\frac{n\pi y}{b}\right) (m_1 + \delta) e^{m_1 t}}{b^2(m_1^2 + \omega^2)(m_1^2 + 2m_1\delta + \delta(\beta + \delta))} \end{aligned}$$

$$\begin{aligned}
 & + \sum_{n=1}^{\infty} \frac{2\delta n \pi m_2 \sin\left(\frac{n\pi y}{b}\right) (m_2 + \delta) e^{m_2 t}}{b^2 (m_2^2 + \omega^2) (m_2^2 + 2m_2 \delta + \delta(\beta + \delta)) \text{Pr}} \\
 (30)
 \end{aligned}$$

$$\begin{aligned}
 u(y,t) = \frac{b-y}{b} + \sum_{n=1}^{\infty} \frac{2n\pi \sin\left(\frac{n\pi y}{b}\right) (m_3 + \gamma)^2 e^{m_3 t}}{b^2 m_3 (m_3^2 + 2m_3 \gamma + \gamma(\gamma + \alpha))} + \sum_{n=1}^{\infty} \frac{2n\pi \sin\left(\frac{n\pi y}{b}\right) (m_4 + \gamma)^2 e^{m_4 t}}{b^2 m_4 (m_4^2 + 2m_4 \gamma + \gamma(\gamma + \alpha))} \\
 (31)
 \end{aligned}$$

$$\begin{aligned}
 u_p(y,t) = \frac{b-y}{b} + \sum_{n=1}^{\infty} \frac{2n\pi \gamma \sin\left(\frac{n\pi y}{b}\right) (m_3 + \gamma) e^{m_3 t}}{b^2 m_3 (m_3^2 + 2m_3 \gamma + \gamma(\gamma + \alpha))} + \sum_{n=1}^{\infty} \frac{2n\pi \gamma \sin\left(\frac{n\pi y}{b}\right) (m_4 + \gamma) e^{m_4 t}}{b^2 m_4 (m_4^2 + 2m_4 \gamma + \gamma(\gamma + \alpha))} \\
 (32)
 \end{aligned}$$

Where

$$A = \sinh \delta_1 (b - y) \cos \delta_2 (b - y)$$

$$B = \cosh \delta_1 (b - y) \sin \delta_2 (b - y)$$

$$C = \sinh \delta_1 b \cos \delta_2 b$$

$$D = \cosh \delta_1 b \sin \delta_2 b$$

$$\delta_1 = \frac{\sqrt{\alpha_1 + \sqrt{\alpha_1^2 + \alpha_2^2}}}{\sqrt{2}}$$

$$\delta_2 = \frac{\sqrt{-\alpha_1 + \sqrt{\alpha_1^2 + \alpha_2^2}}}{\sqrt{2}}$$

$$\alpha_1 = \frac{\text{Pr} \omega^2 \beta}{\omega^2 + \delta^2}$$

$$\alpha_2 = \frac{\text{Pr}(\omega \delta(\beta + \delta) + \omega^3)}{\omega^2 + \delta^2}$$

$$E = \beta + \delta + \frac{n^2 \pi^2}{b^2 \text{Pr}}$$

$$F = E^2 - \frac{4n^2 \pi^2 \delta}{b^2 \text{Pr}}$$

$$m_1 = \frac{-E + \sqrt{F}}{2}$$

$$m_1 = \frac{-E - \sqrt{F}}{2}$$

$$G = \alpha + \gamma + \frac{k^2 \pi^2}{b^2},$$

$$H = G^2 - \frac{4\gamma k^2 \pi^2}{b}$$

$$m_3 = \frac{-G + \sqrt{H}}{2}$$

$$m_4 = \frac{-G - \sqrt{H}}{2}$$

where n and k is any integer.

Results and Discussion

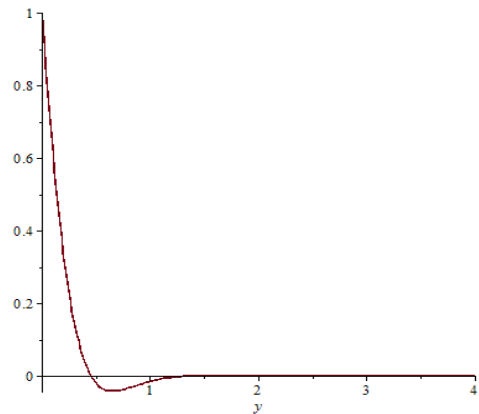


Figure 4: Temperature Profile in a Fluid Phase

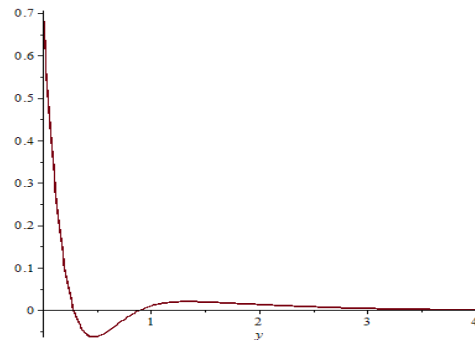


Figure 5: Temperature Profile in a Particle Phase

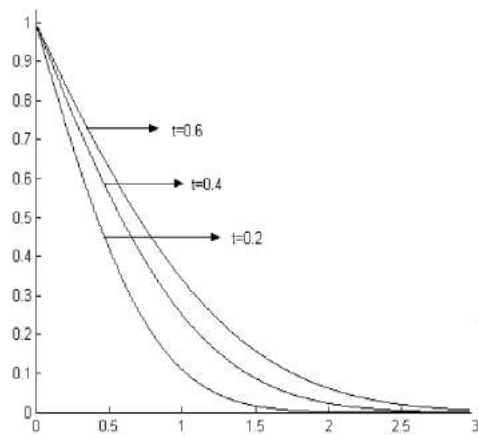


Figure 6: The Velocity Profile of the Fluid Phase

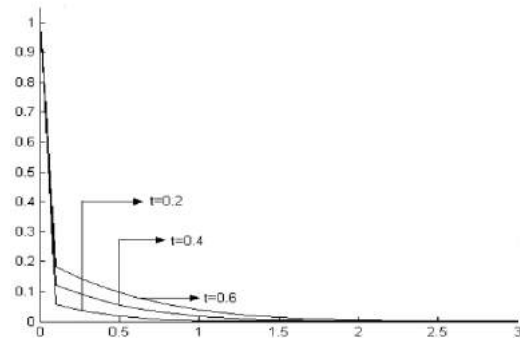


Figure 7: The Velocity Profile of the particle phase

From the Figure 4 to 7, we can observed that the temperature and the velocity of the fluid and particle decrease. As y increases, all the profiles maintain a decreasing trend and gradually tend to zero.

Conclusions

The heat transfer effects on the flow of the dusty fluid past the vertical plate has been studied. The derivation of the governing equation such as continuity, momentum and energy equation of fluid flow is well derived from fundamental physical principal with the help of some illustration in methodology. Laplace transform technique can be used to solve the differential equations. This study had encountered some problem such as the technique used to solve the equation using Laplace transform and how to plot a graph from the solved equation. So in the next study, the other method should be considered to use in solving the equations perhaps numerical method.

References

B.C. Sakiadis. (1961). *Boundary Layer Behavior on Continuous Solid Surface: III. The Boundary Layer on a Continuous Cylindrical Surface*, E. I. Du Pont de Nemours and Company, Incorporated, Wilmington, Delaware.

E.G. Tulapurkara. (2005). *Hundred years of the boundary layer*, Indian Institute of Technology Madras, Chennai.

H.D. Beggs, J.P. Brill. (1973). *A Study of Two-Phase Flow in Inclined Pipes*, American Institute of Mining, Metallurgical, and Petroleum Engineers, Inc, San Antonio, Tex.

J.D. Anderson, JR. (1995). *Computational Fluid Dynamics The Basic With Applications*, McGraw-Hill International Editions, Singapore

M.Mageswari.(2010). *Study on Two Phase Fluid Flows Involving Porous Medium, Stagnation Point and MHD*, SRM University, Kattankulathur.

P.G. Saffmann (1962). *On the Stability of Laminar Flow of Dusty Gas*. Journal of Fluid Mechanics 13.

T.T. Romeo.(2007). *Fundamentals of Food Process Engineering*, University of Georgia, Athens.

MULTIVARIATE ANALYSIS OF VARIANCE (MANOVA) AND CONCENTRATION GRID TEST

Mohammad Faris bin Suhaimi & Muhammad Fauzee Hamdan

Abstract

The purpose of the present study was to investigate relationships between mood and performance. We tested the notion that feelings of depressed mood are central to the overall mood response and influence the functional impact of anger and tension on performance. Athlete in Universiti Teknologi Malaysia (UTM) (n=60) completed a measure of anger, confusion, depression, fatigue, tension, vigour before completing a self-report of 10x10 squares of Concentration Grid Test (CGT) within one minute duration. Multivariate Analysis of Variance (MANOVA) was adopted to explore the association between mood and CGT and whether any differences exist between the depression and no-depression groups. Result indicated that only vigour and score of CGT had no difference between depression and no-depression groups. We suggest that future research should specify an appropriate condition for the participants during the data is taken.

Keyword: MANOVA, BRUMS.

Introduction

Multivariate Analysis of Variance (MANOVA) is a multivariate extension of Analysis of Variance (ANOVA) when there are two or more dependent variables. We only use MANOVA when there is a good rationale for analyzing several dependent variables together and they should be biologically sound and theoretically related. For this research, we have depressed mood group of athletes and no depressive symptoms group of athletes as our dependent variables.

This study focused on performance of athlete among depressed group. The data is obtained by distributing BRUMS questionnaires and concentration grid test result from athletes. All the obtained data we will keep confidential. The data obtain will be analyse

using SPSS software along with MANOVA analysis. Mood can be predictive especially when we are dealing high degree situation. Thus, the findings of this research hopefully will uncover the main problem that cause the performance of athletes based on their mood.

Literature Review

Brunel Mood scale (BRUMS) (formerly called The Profile of Mood States–Adolescent (POMS–Terry, Lane, & Fogarty, 2003). The BRUMS is a 24-item inventory that assesses the mood dimensions of Anger, Confusion, Depression, Fatigue, Tension, and Vigour. Although the BRUMS assesses the same mood dimensions as the POMS (Terry et al., 1999) argued that there was need to develop a new inventory for two reasons. First, the original POMS was developed and validated for use with psychiatric outpatients, hence its validity for use in achievement settings is unknown. Second, the original POMS has been criticized for having items not easily understood by other cultures than the North American, something that is problematic in achievement research environments where brevity is important. The POMS has items such as ‘blue’ and ‘grovelly’ that are not immediately understood by UK participants. (Terry et al., 1999) comprehensively validated the BRUMS. Multisampling confirmatory factor analysis has demonstrated factorial invariance among samples of adult students, adult athletes, young athletes, and school children (Terry et al., 2003). Correlations between scores on the BRUMS and the Positive and Negative Affect Schedule (PANAS; Watson, Clark, & Tellegen, 1988) and the State-Trait Anger-expression Inventory (STAXI; Spielberger, 1991) provide evidence of concurrent validity. Lane and Terry (2000) developed a conceptual model to explain these effects as shown in Appendix B. A key part of Lane and Terry’s model is the assumption that different dimension of mood interact to influence performance. They also proposed that individuals in a depressed mood tend to direct feelings of anger internally, leading to suppression, self-blame and, ultimately, performance decrements.

Moran (2000) argues that despite their proliferation, and testaments to their efficacy in applied sport psychology texts, many of the concentration exercises that have been proposed are based neither on a firm theoretical underpinning nor on sufficient empirical research. One such exercise that may fit into this category is the concentration grid exercise (Harris & Harris, 1984)

Methodology

We used the 24-item Brunel Mood Scale (BRUMS) that has six factors with four items in each factor to measure mood of the athletes. Examples of tension items include “worried” and “anxious”; anger items include “furious” and “bad-tempered”. Examples of fatigue items include “worn out” and “exhausted”; vigour items include “lively” and “energetic”. Examples of confusion items include “mixed-up” and “uncertain”, and depression items include “miserable” and “downhearted”. Items were rated on 5-point scale anchored by “not at all” (0) to “extremely” (4). The participants answered the self-guided questionnaire 10 minutes before they are completing Concentration Grid Test.

The concentration grid test was used as a measure of performance score of the athletes. It is modified from the concentration grid exercise (Harris & Harris, 1984). The concentration grid test was used in this study consists of 10 horizontal and 10 vertical squares arranged in a grid of 100 squares altogether. A unique two digit-number (from 00 to 99) was placed randomly in the centre of each square.

In the concentration grid task, the participants were instructed to mark as many consecutive number (starting from 00) as possible within 1-min period. The resultant number of correctly processed items were used as performance score.

MANOVA is useful in experimental situations where at least some of the independent variables are manipulated. It has several advantages over ANOVA. First, by measuring several dependent variables in a single experiment, there is a better chance of discovering which factor is truly important. Second, it can protect against Type I errors that might occur if multiple ANOVA's were conducted independently. Additionally, it can reveal differences not discovered by ANOVA tests.

However, there are several cautions as well. It is substantially more complicated design than ANOVA, and therefore there can be some ambiguity about which independent variable affects each dependent variable (Carey, 1998). Thus, the observer must make many potentially subjective assumptions. Moreover, one degree of freedom is lost for each dependent variable that is added. The gain of power obtained from decreased SS error may offset by the loss in these degrees of freedom. Finally, the dependent variables should be largely uncorrelated. If the dependent variables are highly correlated, there is little advantage in including more than one in the test given the resultant loss in degrees of freedom.

There is a potential benefit of MANOVA is that interpretation of results may be enhanced by considering criterion variables simultaneously. One way of conceptualizing MANOVA is that it forms a new criterion for each subject, which is that linear combination of the p variables that maximally separates the groups. In other words, when $p=2$ (for simplicity), MANOVA finds a criterion of the form:

$$V_{ij} = k_1 Y_1 + k_2 Y_2 \tag{1}$$

where, k_1 is the weight for variable Y_1 and k_2 is the weight for variable Y_2 . This is new criterion has the property that mean differences are maximized relative to within-group variance on this variable. Any other linear combination of Y_1 and Y_2 would produce more overlap between the distributions. Because the linear combination found by MANOVA maximizes group differences, it is often informative to interpret MANOVA results based on the magnitude of the weights derived for each of the dependent variables.

In particular, the null hypothesis to be tested as an equality of vectors is

$$H_0: \mu_1 = \mu_2 = \dots = \mu_k \tag{2}$$

For purposes of generality, we will let p represent the number of dependent variables in the study. We will let μ_{mj} represent the population mean on variable m for group j . Notice that m ranges from 1 to p , while j ranges from 1 to k . The null hypothesis can be written much more compactly by using matrix algebra notation. Specifically, we can let μ_j be a column vector of population means for group j :

$$\mu_j = \begin{pmatrix} \mu_{1j} \\ \mu_{2j} \\ \vdots \\ \mu_{pj} \end{pmatrix} \tag{3}$$

The multivariate test considers not just $SS_{between}$ and SS_{within} for the two dependent variables (or, in general, p variables), but also the relationship between variables. This relationship is captured in the product of e_1 times e_2 for each model. Whereas the univariate approach compares $\sum_j \sum_i e_1 (F)$ versus $\sum_j \sum_i e_1 (R)$, the multivariate approach also compares $\sum_j \sum_i e_1 e_2 (F)$ versus $\sum_j \sum_i e_1 e_2 (R)$

Two points merit further consideration. The $\sum_j \sum_i e_1 e_2$ term for a model is closely related to the correlation between the 2 variables. In particular,

$$r_{Y_1 Y_2}(\text{within groups}) = \sum_j \sum_i e_1 e_2 (F) / \left(\sum_j \sum_i e_1^2 (F) \sum_j \sum_i e_2^2 (F) \right)^{1/2} \tag{4}$$

and

$$r_{Y_1Y_2}(\text{total sample}) = \frac{\sum_j \sum_i e_1 e_2 (R)}{\left(\sum_j \sum_i e_1^2 (R) \sum_j \sum_i e_2^2 (R) \right)^{1/2}} \quad (5)$$

where the first correlation is a pooled within-groups correlation between the two variables, and the second correlation is a measure of relationship ignoring group membership.

In MANOVA the comparison is based on two matrices. To see how this is done, consider first the errors of the full model. We can represent $\sum_j \sum_i e_1^2 (F)$, $\sum_j \sum_i e_2^2 (F)$, $\sum_j \sum_i e_1 e_2 (F)$ in matrix form as

$$\mathbf{E} = \begin{bmatrix} \sum_j \sum_i e_1^2 (F) & \sum_j \sum_i e_1 e_2 (F) \\ \sum_j \sum_i e_1 e_2 (F) & \sum_j \sum_i e_2^2 (F) \end{bmatrix} \quad (6)$$

This matrix is referred to as a sum of squares and cross-products (SSCP) matrix, and is closely related to a covariance matrix and a correlation matrix. (Dividing each element of \mathbf{E} by $N-k$ would yield a covariance matrix. Corresponding correlations could be found by dividing each covariance by the product of the square roots of the variances of the two variables.) similarly, for the reduced model information regarding the errors can be written in matrix form as

$$\mathbf{R} = \begin{bmatrix} \sum_j \sum_i e_1^2 (R) & \sum_j \sum_i e_1 e_2 (R) \\ \sum_j \sum_i e_1 e_2 (R) & \sum_j \sum_i e_2^2 (R) \end{bmatrix} \quad (7)$$

The difference between the two models can be represented as the difference between the \mathbf{T} and \mathbf{E} matrices. The resulting matrix, usually represented \mathbf{H} for hypothesis sum of squares and cross-product matrix is thus given by

$$\mathbf{H} = \mathbf{T} - \mathbf{E} \quad (8)$$

It can be shown that in general case of k groups and $p=2$ variables, \mathbf{H} equals

$$\mathbf{H} = \begin{bmatrix} \sum_j n_j (\bar{Y}_{1j} - \bar{Y}_1)^2 & \sum_j n_j (\bar{Y}_{1j} - \bar{Y}_1)(\bar{Y}_{2j} - \bar{Y}_2) \\ \sum_j n_j (\bar{Y}_{1j} - \bar{Y}_1)(\bar{Y}_{2j} - \bar{Y}_2) & \sum_j n_j (\bar{Y}_{2j} - \bar{Y}_2)^2 \end{bmatrix} \quad (9)$$

The elements on the main diagonal are just the between-group- sum of squares for each variable, while the off-diagonal element represents the between-group relationship between the two variables.

In testing the multivariate null hypothesis is to ascertain how large the s eigenvalues are. In other words, we must compare their values to what we would expect to occur if the null hypothesis is true. It turns out that there are 4 reasonable ways of combining the information is the s eigenvalues, and each of these ways leads to a unique test statistic. We will follow standard notation by letting λ_i represent the i th eigenvalue of \mathbf{HE}^{-1} . Notice then that λ_1 refers to the ratio of SS_{between} to SS_{within} for V_1 , which is the variate for which this ratio is a maximum.

The four multivariate test statistics are Wilks' lambda, the Pillai-Bartlett trace, Roy's greatest characteristic root, and the Hotelling trace. The formula for Wilks' lambda is

$$U = \prod_{i=1}^s \frac{\lambda_i}{1 + \lambda_i}$$

Recalling that λ_i is $SS_{between} / SS_{within}$, it follows that $1/(1 + \lambda_i)$ equals SS_{within} / SST . Thus, Wilks' lambda is a product of the unexplained variances on each of the discriminant variates. The formula for Pillai-Bartlett trace is given by

$$V = \sum_{i=1}^s \frac{\lambda_i}{1 + \lambda_i}$$

It can be shown that $1/(1 + \lambda_i)$ equal $SS_{between} / SST$. Thus, the Pillai-Bartlett trace is the sum of explained variances on the discriminat variates. The formula for Roy's greatest characteristic root is

$$GCR = \frac{\lambda_1}{1 + \lambda_1}$$

which is $SS_{between} / SST$ for V_1 alone. Thus, Roy's test is based only on the first discriminant variate. Finally, the formula for the Hotelling trace is

$$T = \sum_{i=1}^s \lambda_i$$

which is the sum of $SS_{between} / SS_{within}$ for each of the discriminant variates.

Any of these 4 statistics might be used to test the multivariate null hypothesis. Only in the special case of $s=1$ (i.e. either $k=2$ or $p=1$) do the 4 approaches necessarily agree with one another.

Whenever $s>1$, it is possible that 4 approaches will disagree as to whether the null hypothesis should be rejected at a specified alpha level.

Results and Discussion

All 4 test statistics are produced and all are significant. Hence, we reject the null hypothesis for the overall MANOVA.

H_0 : There is no mean difference between depressed group and not depressed group for all dependent variables.

H_1 : There is mean difference between depressed group and not depressed group at least one dependent variable.

Table 4.2 and Table 4.3 show the estimated mean for anger, confusion, fatigue, tension, vigour, and score of CGT among depressed group and no-depressive symptom group respectively.

Table 4.2: Estimated Mean, Standard Deviation, and 95% Confidence Interval (CI) of Anger, Confusion, Fatigue, Tension, Vigour, and Score of CGT among Depressed Group

Variables	Estimated	Standard	95% CI	
	Mean	Deviation	Lower bound	Upper bound
Anger	5.00	0.510	3.980	6.020
Confusion	5.837	0.477	4.883	6.792
Fatigue	8.023	0.572	6.879	9.1668
Tension	5.302	0.504	4.294	6.310
vigour	7.907	0.608	6.690	9.124
Score of CGT	15.791	0.382	15.026	16.555

Table 4.3: Estimated Mean, Standard Deviation, and 95% Confidence Interval (CI) of Anger, Confusion, Fatigue, Tension, Vigour, and Score of CGT among No-depressive Symptom Group

Variables	Estimated	Standard	95% CI	
	Mean	Deviation	Lower bound	Upper bound
Anger	0.647	0.811	-0.976	6.020
Confusion	0.765	0.758	-0.753	6.792
Fatigue	5.471	0.909	3.650	9.1668
Tension	0.706	0.801	-0.897	6.310
vigour	7.412	0.967	5.476	9.124
Score of CGT	16.824	0.607	15.608	18.039

Table 4.4 below shows the mean difference between depressed group and no-depressive symptom group among dependent variables with 95% confidence interval (CI), standard deviation (SD), and p -value for all dependent variables. We can see that p -value of anger ($p=0.001$), confusion ($p=0.001$), fatigue ($p=0.021$), and tension ($p=0.001$) are less than 0.05. Therefore, there is a difference in mean between depression and no-depression for anger, confusion, fatigue, and tension. Meanwhile, vigour and score of CGT have no difference in mean between depressed group and no-depressive symptom group since the p -values greater than 0.05. Anger, confusion, fatigue, and tension have significantly positive mean

differences which means depressed group for anger, confusion, fatigue, and tension have higher mean than no-depressive symptom group. While, vigour has a positive mean difference between depression and no-depression but not significant. The score of CGT has a negative mean difference between depressed group and no-depressive symptom group but not significant. The mean difference for score of CGT explains that the depressed group has higher score than the no-depressive symptom group.

Table 4.4: Mean Difference between Depression Group and No-depression Group among Anger, Confusion, Fatigue, Tension, Vigour, and Score of CGT

Variables	Mean Difference	SD	p-value	95% CI	
				Lower Bound	Upper Bound
Anger	4.353	0.958	0.001	2.436	6.270
Confusion	5.073	0.896	0.001	3.280	6.865
Fatigue	2.553	1.074	0.021	0.403	4.703
Tension	4.596	0.946	0.001	2.702	6.490
Vigour	0.495	1.142	0.666	-1.791	2.781
Score of CGT	-1.033	0.717	0.155	-2.469	0.403

Conclusions

The athletes in UTM reach peak performance when they have no-depression. There are a few weakness in this study, first, the athletes did not really understand the word used in 24-items of BRUMS questionnaire. This will lead to misunderstanding the true meaning of the word in the BRUMS would show inaccurate mood by them at that time. The athletes were also distracted during completing the CGT might affected the score. This will cause the score of CGT did not show their real performance. So in the next study, multilingual questionnaire for BRUMS should be considered to use in helping the participants who is weak in English. An appropriate environment during taking the CGT should be considered too such as doing the BRUMS and CGT at a place where less interference to get an accurate data on mood and score of CGT.

References

- Abernethy, B. (2001). Attention. In R. Singer, H. A. Hausenblas, & C. M. Janelle (Eds), *Handbook of Sport Psychology* (2nd Ed). (pp. 53-85). New York: Wiley.
- Bless, H. (2001). Mood and the Use of General Knowledge Structures. In L. Martin & G. L. Clore (Eds.), *Theories of mood and cognition*. (pp. 9-26). London: Erlbaum.

[Bray, J. H., & Maxwell, S. E. \(1985\). *Multivariate Analysis of Variance*. United State of America: Sage Publications.](#)

Carey, G. (1998). Introduction to MANOVA [Online]. Available: <http://ibgwww.colorado.edu/%7Ecarey/p7291dir/handouts/manova1.pdf> [Accessed 20/04/2015].

Diment, G. M., & Terry, P. C. (2003). Mood variability, personality, and swimming performance. *Australian Journal of Psychology*, 55, S176 [abstract].

Gendolla, G. H. E., & Kruske, J. (2000). The Joint Effect of Informational Mood Impact and Performance-Contingent Consequences on Effort-Related Cardiovascular Response. *Journal of Personality and Social Psychology*, 83, (pp. 271-283).

Harris, D. V., & Harris, B. L. (1984). *The Athlete's Guide To Sport Psychology: Mental Skills for Physical People*. New York: Leisure Press.

Lane, A. M., & Terry, P. C. (2000). The Nature of Mood: Development of a Theoretical Model with a Focus on Depression. *Journal of Applied Sport Psychology*, 12, (pp. 16-33).

Mahoney, M. J., & Avenier, M. (1997). Psychology of the Elite Athlete: An Exploratory Study. *Cognitive Therapy and Research*, 1, (pp. 135-141)

Martin, L. L. (2001). Mood as Input: a Configural View of Mood Effects. In Martin, L. L., & Clore, G. L. (Eds.), *Theories of mood and cognition*, (pp 135-158). Mahwah, NJ: Lawrence Erlbaum.

Moran, A. P. (2000). Improving Sporting Abilities: Training Concentration Skills. In J. Hartley, & A. Branthwaite (Eds), *The Applied Psychologist* 2nd Ed. (pp. 92-110). Buckingham: Open University Press.

Terry, P. C., Lane, A. M., & Fogarty, G. (2003). Construct Validity for the Profile of Mood States-A for use with adults. *Psychology of Sport and Exercise*, 4, (pp. 125-139).

Terry, P. C., Lane, A. M., Lane, H. J., & Keohane, L. (1999). Development and Validation of a Mood Measure for Adolescents: POMS-A. *Journal of Sports Sciences*, 17, (pp. 861-872).

Schmid, A., & Peper, E. (1998). Training Strategies for Concentration. In J. M. Williams (Ed), *Applied Sport Psychologist*, 8, (pp. 73-86)

Spielberger, C. D. (1991). *Manual for the State-Trait Anger Expression Inventory*. Odessa, FL: Psychological Assessment Resources.

Watson, D., Clark, L. A., & Tellegen, A. (1988). Development and Validation of Brief Measures of Positive and Negative Affect: The PANA scales. *Journal of Personality and Social Psychology*, 54, (pp. 1063-1070)

SOLVING FIRST ORDER WAVE EQUATION USING FINITE DIFFERENCE METHODS

Muhammad Fadzli Bin Hussein & Tuan Hj. Hamisan Bin Rahmat

Abstract

This research was conducted to solve one dimensional wave equations using Finite Difference Methods. Five Finite Difference Methods were chosen to solve hyperbolic Partial Differential Equation which is Leapfrog method, Upwind method, Forward Euler method, Lax Fredrids method and Lax Wendroff method. The algorithm for each method has been expanded and the solution of the problem is simplified using Microsoft Excel. Difference value of the step size had been chosen in order to get more accurate result. Based on result obtained, it can be conclude that Leapfrog method and Forward Euler method are the poor choice for solving hyperbolic PDEs. Meanwhile, the Upwind method, Lax Fredrids method and Lax Wendroff were selected as the best methods for solving the problem indicates with hyperbolic PDEs.

Keywords: :(Leapfrog method, Upwind method, Forward Euler method, Lax Fredrids method and Lax Wendroff method).

Introduction

Finite difference method divided into many branches, but in this case only applied leapfrog method, forward euler method, upwind method, lax friedrichs and lax wendroff for solving this problem.

The simplest of a hyperbolic equation is

$$(1) \quad u_t = cu_x \quad c = \text{constant} > 0$$

Given sufficiently smooth initial data $u(x, 0) = u_0(x)$ has the solution $u(x, t) = u_0(x + t)$

Finite different method used for solve hyperbolic equation by substituting difference time and difference space into finite difference approximation (FDAs). In order to solve hyperbolic equation, finite difference method was chosen for solve hyperbolic equation. It is important for understand the algorithm contained in leapfrog method. The concepts and theory must be clearly and real for leapfrog method.

The study of the FDMs is important to solving hyperbolic equation because this method is easy to be applied. Furthermore, form this research, the technique used to solve the problem by using Microsoft Excel can be learnt.

The objectives of this research study is (i) to study and understand the selected type of FDMs; (ii) to solve first order wave equation using FDMs with different equation (iii) to solve one dimensional wave equation problems by using manually and by using Microsoft Excel (iv) .To find the best method using comparison between error.

The scope of study is solving the first order wave equation using leapfrog, Forward Euler, Upwind, Lax-Friedrichs and Lax- Wendroff methods. The scope of this study can be used in scientific and engineering with extended the branches of the study and can be applied in the large area of study

Literature Review

According Mattheji(2005) Partial Differential Equation was known as a relation between an unknown function and its partial derivatives. Partial differential equation usually mostly applied in physical and engineering. Besides that, this method also used in biology, chemistry, computer science and in economics.

Debnath (1997) states that the partial differential equation most important in many branches, especially in areas sciences and engineering because there is more than one independent variable involved in a solution. On the 1960, Peter Lax and Burton Wendroff had introduced Lax- wendroff for solving hyperbolic Partial Differential Equation. Then follows by Richtmyer (1963), he divide this method into two types which Lax- Wendroff one step and Lax Wendroff two step methods. While a predictor-corrector Lax Wendroff had been produced by MacCromack (1969). It plays an important role in the development of computational fluid dynamics. According Abarbanel and Zwas (2014), the present of an interactive finite different method scheme for initial value problems is applied to the quasi-linear hyperbolic system representing the one dimensional time dependent flow of a compressible polytrophic gas. Based on Yalcin Kaya and Noakes (2008) the leapfrog algorithm mostly proposes for solving a class of optimal control problem. Based on Akollermo (1979) a technique for the complete error analysis of finite difference schemes for hyperbolic initial boundary values problems is developed and well applied to several choses or initial approximations and boundary for leapfrog with second and fourth order accuracy in space.

Methodology

First and foremost, the derivation of the equation will be replacing the time and space derivatives in PDE by using FDMs. The result obtained may produce the truncation error due to the using of the approximation of the exact value. The truncation error is known as the difference between a truncated value and the actual value which is represented by a numeral with a fixed number of allowed digits with any excess digits.

To derive the leapfrog method equation must be replacing first order partial derivative into finite difference formula.

From the equation, Eq. (1) replaces the first order partial derivative $\left(\frac{\delta u}{\delta t}\right)_{i,j}$ centred difference formula.

$$\left(\frac{\delta u}{\delta t}\right)_{i,j} = \frac{1}{2k} (u_{i,j+1} - u_{i,j-1}) \quad (2)$$

The first order partial derivative for $\left(\frac{\delta u}{\delta x}\right)_{i,j}$ replaced by centred difference formula.

$$\left(\frac{\delta u}{\delta x}\right)_{i,j} = \frac{1}{2h} (u_{i+1,j} - u_{i-1,j}) \quad (3)$$

Replace the both Eq. (2) and Eq. (3) into the Eq. (1):

$$\frac{1}{2k} (u_{i,j+1} - u_{i,j-1}) = \frac{c}{2h} (u_{i+1,j} - u_{i-1,j}) \quad (4)$$

Solving the equation, Eq.(3) to obtain value $u_{i,j+1}$.

$$(5) \quad u_{i,j+1} = u_{i,j-1} + cr(u_{i+1,j} - u_{i-1,j})$$

$$\text{wherer} = \frac{k}{h}$$

To derive the upwind method equation must be replacing first order partial derivative into finite difference formula.

Replace the partial derivative using forward $\left(\frac{\delta u}{\delta t}\right)_{i,j}$ by forward difference formula.

$$\left(\frac{\delta u}{\delta t}\right)_{i,j} = \frac{u_{i,j+1} - u_{i,j}}{k} \quad (6)$$

And partial derivative using forward $\left(\frac{\delta u}{\delta x}\right)_{i,j}$ by forward difference formula

$$(7) \quad \left(\frac{\delta u}{\delta x}\right)_{i,j} = \frac{u_{i+1,j} - u_{i,j}}{h}$$

Replace the both Eq. (6) and Eq. (7) into the Eq. (1):

$$\frac{u_{i,j+1} - u_{i,j}}{k} = c \left(\frac{u_{i+1,j} - u_{i,j}}{h} \right) \quad (8)$$

From the equation, Eq. (8) Solving to obtain $u_{i,j+1}$

$$u_{i,j+1} = u_{i,j} + cr(u_{i+1,j} - u_{i,j}) \quad (9)$$

$$\text{wherer} = \frac{k}{h}$$

To derive the forward Euler methods, substituting equation, Eq. (2) and Eq. (6) into wave equation, Eq. (1.1).

$$(10) \quad \frac{u_{i,j+1} - u_{i,j}}{k} = c \left(\frac{u_{i+1,j} - u_{i-1,j}}{2h} \right)$$

From the equation, Eq. (10) Solving to obtain $u_{i,j+1}$

$$(11) \quad u_{i,j+1} = u_{i,j+1} + \frac{cr}{2} (u_{i+1,j} - u_{i-1,j})$$

$$\text{wherer} = \frac{k}{h}$$

To derive the Lax- Friedrichs method from forward euler method equation can be made stable by replacing $u_{i,j}$ with the average term $\frac{u_{i+1,j} + u_{i-1,j}}{2}$..

$$\frac{u_{i,j+1} - (u_{i+1,j} + u_{i-1,j})/2}{k} = \frac{u_{i+1,j} - u_{i-1,j}}{2h}$$

$$(12)$$

From the equation, Eq. (12) Solving to obtain $u_{i,j+1}$

$$u_{i,j+1} = \frac{(u_{i+1,j}+u_{i-1,j})}{2} + r \frac{(u_{i+1,j}-u_{i-1,j})}{2}$$

(13)

where $r = \frac{k}{h}$

To derive the Lax Wendroffmethod equation must be derived from a Taylor- series expansion in the following manner.

$$u_{i,j+1} = u_{i,j} + \Delta t u_t + \frac{(\Delta t)^2(u_{tt})}{2} + O[(\Delta t)^3]$$

(14)

Using the wave equation, Eq. (1) differentiate respect to t .

$$u_{tt} = c^2 u_{xx}$$

(15)

Substitute Eq. (15) into Eq. (14)

$$u_{i,j+1} = u_{i,j} + c\Delta t u_x + \frac{c^2(\Delta t)^2 u_{xx}}{2} + O[(\Delta t)^3]$$

(16)

From the Eq. (16) replaces the second order partial derivative $\left(\frac{\delta^2 u}{\delta x^2}\right)_{i,j}$ centred difference formula.

$$\left(\frac{\delta^2 u}{\delta x^2}\right)_{i,j} = \frac{(u_{i+1,j}-2u_{i,j}+u_{i-1,j})}{\Delta x^2}$$

(17)

Finally, replaces Eq.(3) and Eq.(17) into Eq. (16) Solving the equation, Eq(16) to obtain value $u_{i,j+1}$.

$$u_{i,j+1} = u_{i,j} + \frac{r}{2}(u_{i+1,j} - u_{i-1,j}) + \frac{r^2}{2}(u_{i+1,j} - 2u_{i,j} + u_{i-1,j})$$

(18)

where $\left(\frac{\Delta t}{\Delta x}\right)^2 = r^2$

Analysis and Discussion

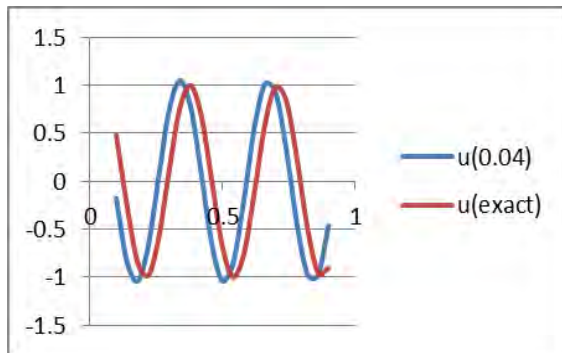


Figure 1 Result Leapfrog method for $\Delta x = 0.005$

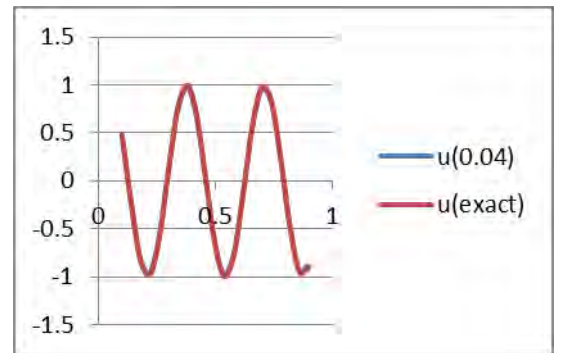


Figure 2 Result Leapfrog method for $\Delta x = 0.002$

Figure 1 and 2 shows the comparison for leapfrog methods with different Δx . In Figure 4.1 the value of Δx is 0.005 while in Figure 4.2 the value of Δx reduced to 0.002. The comparison for these both figures above is shown by comparing the numerical value with exact solution. Figure 4.1 shows the significant differences between graph forms for numerical solution with exact solutions. When the value of Δx reduced to the 0.002 as shown figure 4.2, the graph form obtained for numerical solution is exactly same as the graph form for exact solution. The overlapped between the graph form for numerical solution and exact solution are produced.

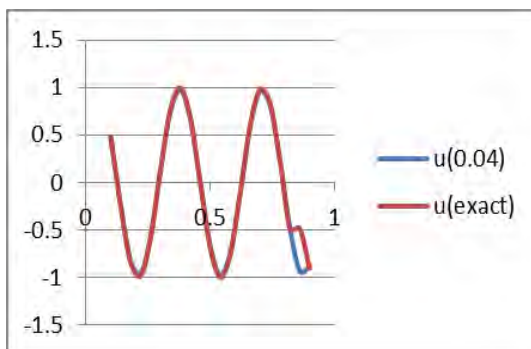


Figure 3 Result Upwind methods for $\Delta x = 0.005$

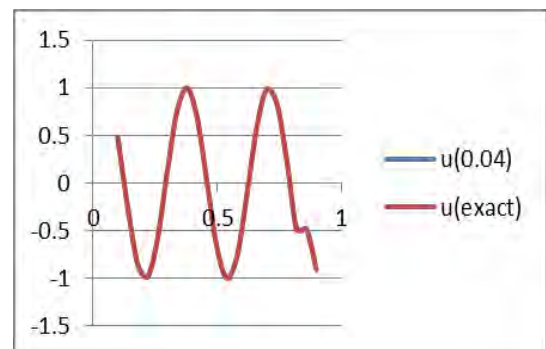


Figure 4 Result Upwind methods for $\Delta x = 0.002$

Figure 3 and 4 shows the comparison for Upwind methods with different values of Δx . The value of Δx used in figure 3 is 0.005, while the Δx is reduced to 0.002 in figure 4. This method shows the comparison between numerical solution with exact value when reduce the Δx . Figure 3 presented the graph form for $\Delta x = 0.005$. In this Figure, the graph form for numerical solution almost the same with exact solution but there are still have very small difference when comparing with the exact solution. When the value of Δx reduced, the result for numerical solution same with the exact value. The graph form shows like in

figure 4. The blue line in the graph depicts the numerical value while the red line depicts the exact value.

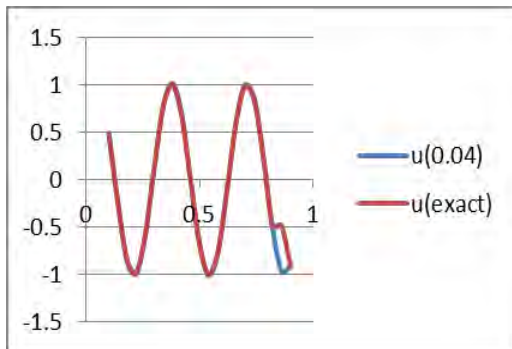


Figure 5 Result Forward Euler methods $\Delta x = 0.005$

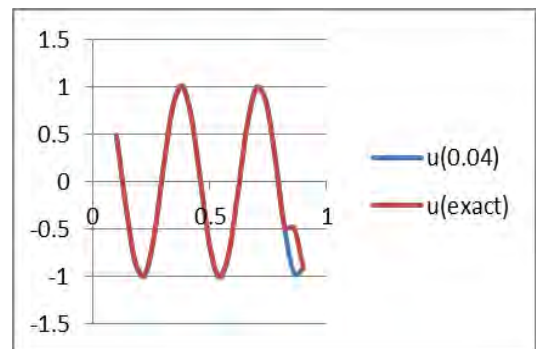


Figure 6 Result Forward Euler method for $\Delta x = 0.002$

The Figure 5 and 6 shows comparison for Forward Euler method with different values of Δx . Figure 4.5 shows the graph form for value of $\Delta x = 0.005$, while figure 6 shows the graph form for value of $\Delta x 0.002$. There is slightly different between the values of at 0.04 and the exact value at $\Delta x = 0.005$. When the value of Δx is reduced to 0.002, the graph produced the same form as in Figure 5. There is no difference obtained between both figures.

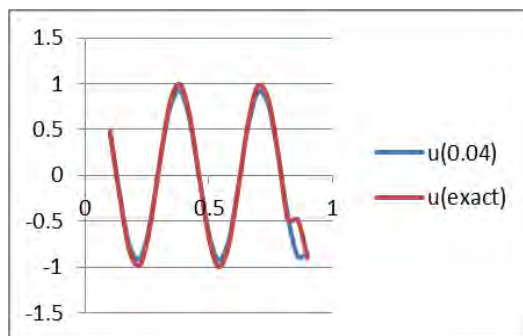


Figure 7 Result Lax- Friedrichs methods $\Delta x = 0.005$

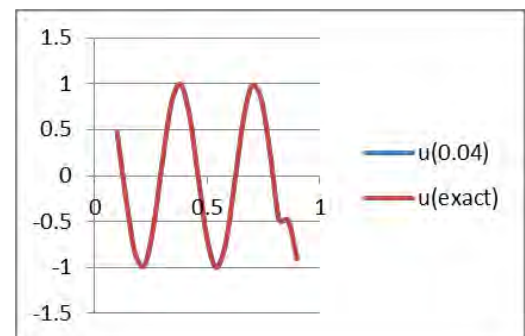


Figure 8 Result Lax -Friedrichs methods $\Delta x = 0.002$

Figure 7 and 8 shows the results Lax- Friedrichs methods in graph form. The figures above made by comparing the value of u at 0.04 with exact value. Figure 7 using the value of $\Delta x = 0.005$ while Δx is reduced to 0.002 in the figure 8. From the figure 7, there are differences between graph forms for numerical value with exact value. There are significant changes in graph form when the value of Δx is decrease to 0.002 as in figure 8. The overlapped between the graph form of numerical value and the exact value is occurred. It shows that there is no difference between the numerical solution and the exact value.

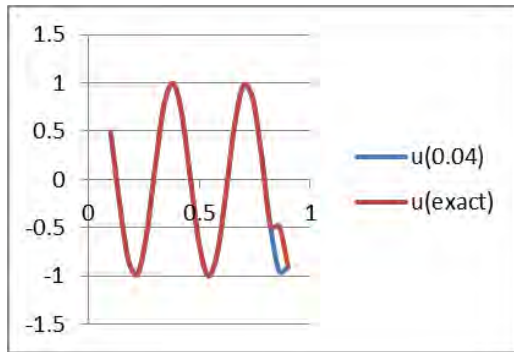


Figure 9 Result Lax- Wendroff

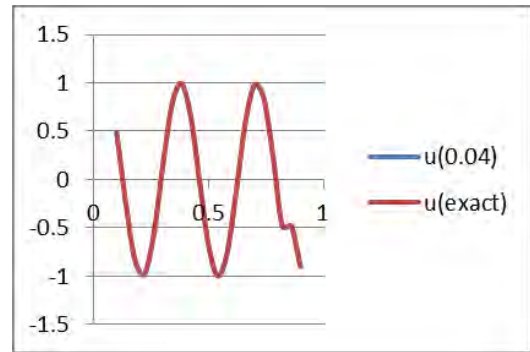


Figure 10 Result Lax- Wendroff method for $\Delta x = 0.005$

Wendroff method for $\Delta x = 0.005$

Figure 9 and 10 shows the comparison for Lax -Wendroff methods with difference values of Δx . For the Figure9, the value of $\Delta x = 0.005$ is used while the value of Δx is reduced to 0.002 for Figure 10. This methods shows the comparison between numerical solution with exact solution when reduce the value of Δx . The graph form produced at $\Delta x = 0.005$ is shown in Figure9. There is small difference founded when the numerical value is comparing with the exact value. When the value of Δx is reduced as in Figure 10, the result for numerical solution is exactly same with the exact value since the errors obtained are approximately zero.

Conclusion

Form the result obtained for the Leapfrog method, the significant difference occurred when the values of Δx had been decreases compared to Forward Euler method, the slightly difference occurred even though the values Δx had been decreases. Besides that, for the Upwind method, Lax- Friedrichs and Lax Wendroff the error approximately zero when the smaller step size are used. In conclusion, from the analysis, it is proved that the Leapfrog method and Forward Euler method are the not suitable for solving the wave equation in one dimensional hyperbolic equation. Meanwhile, the Upwind method, Lax- Friedrichs method and Lax Wendroff were selected as the best methods because it gives the significant difference when the step size is decrease.

References

Akai, T.J.(1994). Applied Numerical Methods for Engineers. New York: John Wiley & son, Inc.

Gary, J. ,“ On Certain Finite Difference Schemes for the Equation of Hydrodynamics, AEC Report, NYO -9188,1962.

Dennis. J. E. Jr., and R. B. Schnabel, Numerical Methods For Unconstrained Optimization and Nonlinear Equations, SIAM, Philadelphia, 1996.

BURSTEIN, S.Z. Numerical Calculations of Multidimensional Shocked Flows, N.Y.U.Courant Inst. Math. Sci. Res. Dep. N.Y.O.-10, 433, 1963.

Iserles, A. A First Course in the Numerical Analysis of Differential Equations. Cambridge University Press, 1996

Dautray, R. and J.L. Lions, Mathematical analysis and numerical methods for science and technology,

Approximate Analytical Solutions of Burgers' Equation via Homotopy Analysis Method (HAM)

¹Muhammad Hanif Khairuddin, ²Prof. Dr. Zainal Abdul Aziz,

Abstract: Nonlinear equations are very difficult to solve for analytical solutions in most physical and engineering phenomena. Homotopy Analysis Method (HAM) is an approximate analytical technique which provides a new way to obtain series solution of nonlinear problem. In this research, HAM is applied to obtain the approximate analytical solution of nonlinear Burgers' equation. HAM contains the auxiliary parameter \hbar , which gives way to adjust and control convergence region of the series solution. Mathematica software is used to solve the nonlinear equation. The graphical outputs of the solutions are generated. The approximate analytical solution at 6th order approximation is compared with the exact solution of Burgers' equation and shown to be in good agreement with the least of absolute error.

Keywords: Approximate Analytical Solution, Burgers' equation, Homotopy Analysis Method (HAM).

INTRODUCTION

Nonlinear equations are much more difficult to solve than linear ones, especially by means of analytical methods. The Homotopy Analysis Method (HAM) [1, 2] is an analytical technique to solve nonlinear equations which was first introduced by Liao in 1992. This method already successfully applied in real nonlinear problem especially in engineering and science, such as the magneto hydrodynamics flows of non-Newtonian fluids over a stretching sheet [3], boundary layer flows over an impermeable stretch plate [4], nonlinear model of combined convective and radiative cooling of a spherical body [5], and unsteady boundary layer flows over a stretching flat plate [6]. Thus the validity, effectiveness, and flexibility of the HAM are verified via all of these successful applications. Also, many types of nonlinear problems were solved with HAM by others [7-10].

The Burgers' equation is a fundamental partial differential equation from fluid mechanics. It occurs in various areas of applied mathematics, such as modeling of gas dynamics and traffic flow. The first steady-state solution of Burgers' equation was given by Bateman [11] in 1915. Although the equation gets its name from immense research of Burgers' [12] beginning in 1939. The study of the general properties of the Burgers' equation can be used as a model for any nonlinear wave diffusion problem subject to destruction [13]. Depending on the problem being modeled, this destruction may result from elasticity, gas dynamics, heat conduction, chemical reaction, or other.

The paper layout is as follows: in Section 2, basic idea of HAM is presented. In Section 3, the Burgers' equation is approximately solved by HAM. In Section 4, HAM results are compared and discussed. Section 5 provides a brief conclusion.

IDEAS OF HAM

Consider a nonlinear equation in a general form,

$$\mathcal{N}[u(r, t)] = 0, \tag{1}$$

where \mathcal{N} indicates a nonlinear operator, $u(r, t)$ an unknown function. Suppose $u_0(r, t)$ denotes an initial guess of the exact solution $u(r, t)$, $H(r, t) \neq 0$ an auxiliary function, \mathcal{L} an auxiliary parameter, and $q \in [0,1]$ as an embedding parameter. By means of HAM, we construct the so-called zeroth-order deformation equation

$$(1 - q)\mathcal{L}[\phi(r, t; q) - u_0(r, t)] = q\hbar H(r, t)\mathcal{N}[\phi(r, t; q)]. \tag{2}$$

It should be noted, that the auxiliary parameter attributes in HAM are chosen with freedom. Obviously, when $q = 0,1$ it holds

$$\phi(r, t; 0) = u_0(r, t), \quad \phi(r, t; 1) = u(r, t)$$

respectively. Then as long as q increase from 0 to 1, the solution $\phi(r, t; q)$ varies from initial guess $u_0(r, t)$ to the exact solution $u(r, t)$.

Liao[5] by Taylor theorem expanded $\phi(r, t; q)$ in a power series of q as follows

$$\phi(r, t; q) = \phi(r, t; q) + \sum_{m=1}^{\infty} u_m(r, t)q^m, \tag{3}$$

where

$$u_m(r, t) = \frac{1}{m!} \left. \frac{\partial^m \phi(r, t; q)}{\partial q^m} \right|_{q=0}. \tag{4}$$

The convergence of the series in Equation (3) depends upon the auxiliary function $H(r, t)$, auxiliary parameter \hbar , auxiliary linear operator \mathcal{L} and initial guess $u_0(r, t)$. If these are selected properly, the series in Equation (3) is convergence at $q = 1$, and one has

$$u(r, t) = u_0(r, t) + \sum_{m=1}^{\infty} u_m(r, t). \tag{5}$$

Based on Equation (2), the governing equation can be derived from the zeroth-order deformation in Equation (5) and the exact solution can be defined in vector form

$$\overrightarrow{u_n(r, t)} = \{u_0(r, t), u_1(r, t), \dots, u_n(r, t)\}.$$

Differentiating m -times of zeroth order deformation Equation (2) with respect to $q = 0$, the result will be so-called m th-order deformation equation

$$\mathcal{L}[u_m(r, t) - \chi_m u_{m-1}(r, t)] = \hbar H(r, t) R_m(u_{m-1}, r, t),$$

(6)

where

$$\chi_m = \begin{cases} 0, & m \leq 1 \\ 1, & m > 1 \end{cases} \quad (7)$$

$$R_m(u_{m-1}, r, t) = \frac{1}{(m-1)!} \left\{ \frac{\partial^{m-1}}{\partial q^{m-1}} \mathcal{N} \left[\sum_{m=0}^{\infty} u_m(r, t) q^m \right] \right\} \Bigg|_{q=0}$$

(8)

THEOREM 1 (Liao [5]):

The series solution (5) is convergent to the exact solution of Equation (1) as long as it is convergent.

HAM SOLUTION OF BURGERS' EQUATION

The Burgers' equation is described by

$$u_t + uu_x - u_{xx} = 0, \quad x, t \in R \quad (9)$$

subjects to the initial condition

$$u(x, 0) = f(x) \quad (10)$$

and the exact solution of this equation is [14]

$$u(x, t) = \frac{1}{2} - \frac{1}{2} \tanh \frac{1}{4} \left(x - \frac{1}{2} t \right). \quad (11)$$

For HAM solution of Burgers' equation we choose

$$u_0(x, t) = \frac{1}{2} - \frac{1}{2} \tanh \frac{1}{4}(x)$$

(12)

as the initial guess and

$$\mathcal{L}[u(x, t; q)] = \frac{\partial u(x, t; q)}{\partial t}$$

(13)

as the auxiliary linear operator satisfying

$$\mathcal{L}[C] = 0 \tag{14}$$

where C is a constant and consider the auxiliary function

$$H(x, t) = 1 \tag{15}$$

and the zeroth-order deformation problem is given by

$$(1 - q)\mathcal{L}[u(x, t; q) - u_0(x, t)] = q\hbar\mathcal{N}[u(x, t; q)], \tag{16}$$

$$\mathcal{N}[u(x, t; q)] = \frac{\partial u(x, t; q)}{\partial t} + u(x, t; q) \frac{\partial u(x, t; q)}{\partial x} - \frac{\partial^2 u(x, t; q)}{\partial x^2}$$

(17)

the m th-order deformation problem is

$$\mathcal{L}[u_m(x, t) - \chi_m u_{m-1}(x, t)] = \hbar \left[\frac{\partial u_{m-1}(x, t)}{\partial t} + \sum_{i=0}^{m-1} u_i(x, t) \frac{\partial u_{m-1-i}(x, t)}{\partial x} - \frac{\partial^2 u_{m-1}(x, t)}{\partial x^2} \right],$$

(18)

$$u_m(x, t) = 0, \quad (m \geq 1).$$

It is found that the HAM solution in a series form is given by

$$u(x, t) = \frac{1}{2} - \frac{1}{2} \tanh\left(\frac{x}{4}\right) - \frac{1}{16} \hbar t \operatorname{sech}\left(\frac{x}{4}\right)^2 + \dots \tag{19}$$

RESULT AND DISCUSSION

The approximate analytical solutions of Burgers' equation by HAM given by (19) containing auxiliary parameter \hbar , which influences the convergence region and rate of approximation for the HAM solutions. In figure 1 the \hbar -curves is plotted for $u(x, t)$ of Burgers' for HAM solutions.

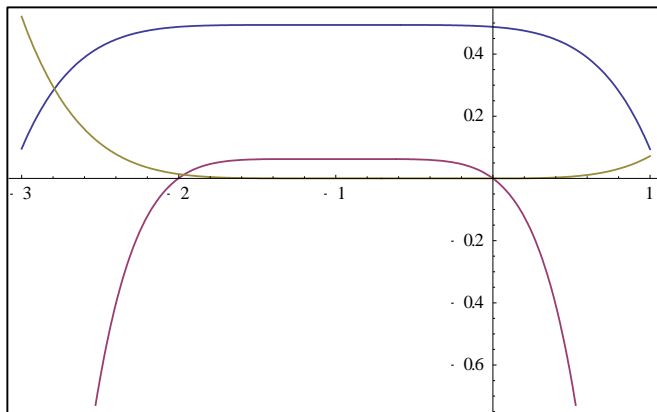
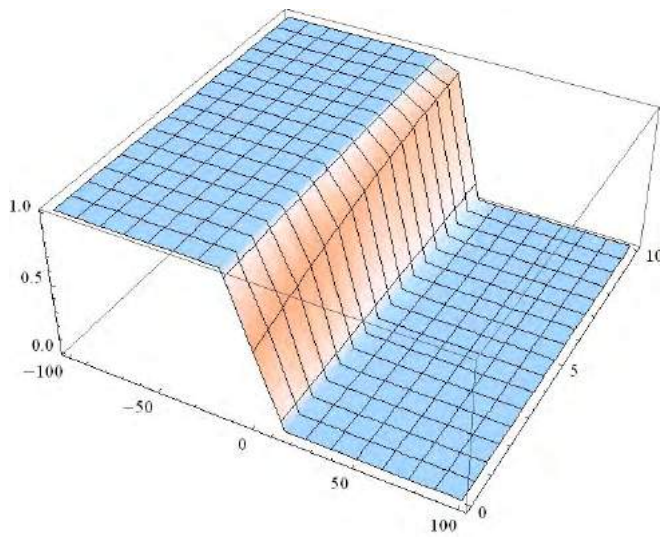


Figure 1 The \hbar -curves of 6th order approximation, blue line $u(0.1,0.1)$; red line $\dot{u}(0.1,0.1)$; yellow line $\ddot{u}(0.1,0.1)$.

As pointed out by Liao [4], the valid region of \hbar is a horizontal line segment. It is clear that the valid region for Burgers' case is $-1.4 < \hbar < -0.4$. According to theorem 1, the series solution (19) must be exact solution as long as it is convergent. In this case, for $0 < t < 10$ and $\hbar = -0.5$, the result exact solution and HAM solution are shown to be in good agreement with the least of absolute error, as shown in Figure 2. The obtained numerical results are summarized in Table 1.

(a) Exact solution



(b) HAM solution

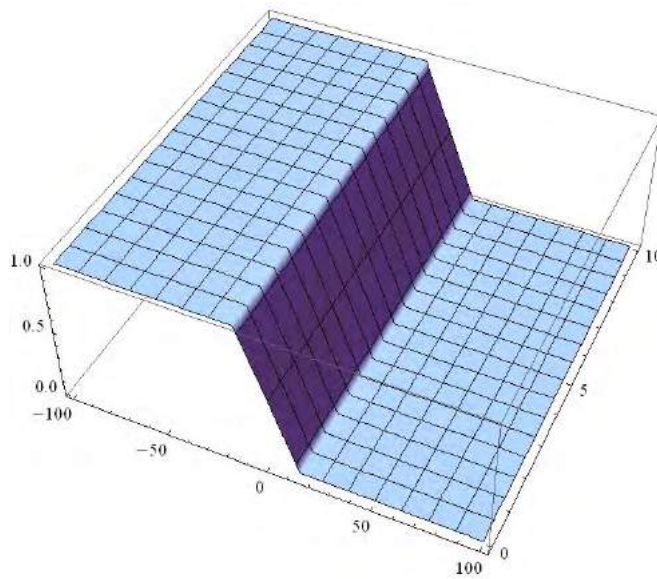


Figure 2 Comparison of the exact solution with HAM of Burgers' equation, when $\hbar = -0.5$

Table 1 Comparison of HAM solution with exact solution of Burgers' equation, when $\hbar = -0.5$

t	x	Absolute error of exact and HAM
	-100	0.
	-50	$5.5511151231 \times 10^{-17}$
	-20	$5.5511151231 \times 10^{-17}$

0	0	0.
	20	0.
	50	0.
	100	0.
	-100	0.
	-50	$1.0880185641 \times 10^{-14}$
	-20	$3.5251310315 \times 10^{-8}$
0.25	0	$7.8080485704 \times 10^{-3}$
	20	$5.4682595285 \times 10^{-8}$
	50	$1.6708856520 \times 10^{-14}$
	100	0.
	-100	0.
	-50	$1.6764367671 \times 10^{-14}$
	-20	$5.4662331883 \times 10^{-8}$
0.5	0	$1.558945190 \times 10^{-3}$
	20	$1.3284220051 \times 10^{-7}$
	50	$4.0689673852 \times 10^{-14}$
<i>t</i>	<i>x</i>	Absolute error of exact and HAM
	100	0.
	-100	0.
	-50	$1.8873791418 \times 10^{-14}$

	-20	$6.1406564499 \times 10^{-8}$
0.75	0	$2.331779443 \times 10^{-2}$
	20	$2.3901915940 \times 10^{-7}$
	50	$7.3108186171 \times 10^{-14}$
	100	0.
	-100	0.
	-50	$1.7819079545 \times 10^{-14}$
	-20	$5.8274747971 \times 10^{-8}$
1	0	$3.096711597 \times 10^{-2}$
	20	$3.7829115812 \times 10^{-7}$
	50	$1.1568523916 \times 10^{-13}$
	100	0

CONCLUSION

In this paper, the Homotopy Analysis Method (HAM) [2] is applied to obtain the solitary solution of Burgers' equation. HAM provides us with a convenient way to control the convergence of approximation series, which is a fundamental qualitative difference in analysis between HAM and other methods. The solution of Burgers' equation by HAM when $\hbar = -0.5$ at 6th order approximation has been compared with the exact solution of Burgers' equation. The resulted HAM solution at 6th order approximation is then compared with that of the exact soliton solution of Burgers' equation and shown to be in good agreement. The numerical results show that the HAM solution of Burgers' equation is approximate to exact solution of Burgers' equation with the least value of absolute error.

References

- [1] S. J. Liao, *The proposed homotopy analysis technique for the solution of nonlinear problems [Ph.D. thesis]*, Shanghai Jiao University, 1992.
- [2] S. J. Liao, Ed., *Beyond Perturbation: Introduction to the Homotopy Analysis Method* Boca Raton, Chapman & Hall, Boca Raton, Fla, USA, 2003
- [3] S. J. Liao, "On the analytic solution of magnetohydrodynamic flows of non-Newtonian fluids over a stretching sheet," *Journal of Fluid Mechanics*, vol. 488, pp. 189–212, 2003.

- [4] S. J. Liao, "A new branch of solutions of boundary-layer flows over an impermeable stretched plate," *International Journal of Heat and Mass Transfer*, vol. 48, no. 12, pp. 2529–2539, 2005.
- [5] S. J. Liao, J. Su, and A. T. Chwang, "Series solutions for a nonlinear model of combined convective and radiative cooling of a spherical body," *International Journal of Heat and Mass Transfer*, vol. 49, no.15-16, pp. 2437–2445, 2006.
- [6] S. J. Liao, "Series solutions of unsteady boundary-layer flows over a stretching flat plate," *Studies in Applied Mathematics*, vol. 117, no. 3, pp. 239–263, 2006.
- [7] S. Abbasbandy, "The application of homotopy analysis method to nonlinear equations arising in heat transfer," *Physics Letters A*, vol. 360, no. 1, pp. 109–113, 2006.
- [8] S. Abbasbandy, "The application of homotopy analysis method to solve a generalized Hirota-Satsuma coupled KdV equation," *Physics Letters A*, vol. 361, no. 6, pp. 478–483, 2007.
- [9] S. Abbasbandy, "Homotopy analysis method for heat radiation equations," *International Communications in Heat and Mass Transfer*, vol. 34, no. 3, pp. 380–387, 2007.
- [10] M. Ayub, A. Rasheed, and T. Hayat, "Exact flow of a third grade fluid past a porous plate using homotopy analysis method," *International Journal of Engineering Science*, vol. 41, no. 18, pp. 2091–2103, 2003.
- [11] H. Bateman, "Some recent researches on the motion of fluids," *Monthly Weather Review*, vol. 43, pp. 163–170, 1915.
- [12] J. M. Burgers, *Mathematical Examples Illustrating Relations Occurring in the Theory of Turbulent Fluid Motion*, vol. 17, Transitions of Royal Netherlands Academy of Arts and Sciences, Amsterdam, TheNetherlands, 1939, Reprinted in F. T. M. Nieuwstadt and J. A. Steketee, Selected papers of J. M. Burgers, Kluwer Academic, Dordrecht, The Netherlands, pp. 281–334, 1995.
- [13] C. A. J. Fletcher, "Burgers' equation: a model for all reasons," in *Numerical Solutions of Partial Differential Equations*, North-Holland, Amsterdam, The Netherlands, 1982.
- [14] Nazari, M., F. Salah, Z. A. Aziz, M. Nilashi. 2012. Approximate Analytic Solution for the Kdv and Burger Equations with the Homotopy Analysis. *Journal of Applied Mathematics*. Article ID 878349, 13 pages.

MANOVA ON PRINT ADVERTISING

Ng Siew Hui, Dr. Norazlina Ismail

Abstract

Print advertising is a common form of marketing communication used for the purpose of solicitation, marketing or promoting. With the presence of print ad elements, the advertisement is enhanced. The objective of the research is to determine the effect of different print ad copy elements on attitude towards product and intention to buy. Data were obtained from 100 subjects which are divided into 25 subjects per cell. Data were analyzed using simple 2x2 balanced design full factorial between subjects' multivariate analysis of variance and some necessary univariate analysis. Both competitive claim and uniqueness claim shown significant main effect on the dependent variables. The univariate tests shown significance of uniqueness claim on the likelihood on buying the product, whereas competitive claim on the liking of the product. It is concluded that the inclusion of print ad elements can affect the attitude towards product and intention to buy.

Keywords: MANOVA, print ad, SPSS, competitive claim, uniqueness claim.

Introduction

Advertising is a form of marketing communication used to persuade audience or consumers to take or continue some action, usually with respect to a commercial offering, or political or ideological support. Any advertisement printed on paper, be it newspapers, magazines, flyers, booklets or other medias that could be considered as a portable printed medium is called print advertising.

In this research, we want to test the effects of different print ad copy elements on attitude toward product and intention to buy by using MANOVA. MANOVA, Multivariate Analysis of Variance is a type of multivariate analysis used to assess the statistical significance of differences that involves more than one independent variable in one time. The null hypothesis tested in MANOVA is the equality of vectors of means on multiple dependent variables across groups.

Literature Review

A study was carried out by Keith P. Gennuso, *et al.* (2014) on the smokers' physical activity and weight gain one year after a successful versus unsuccessful quit attempt to examine whether smokers' physical activity is related to their weight changed following a quit attempt. Data were analysed by using *t*-tests and *chi-square* analyses. In a study conducted by FilizFatmaColakoglu, *et al.*(2014) examining the aggression levels and emphatic tendency levels of secondary school students who involve or do not involve in sports, both ANOVA and MANOVA is used to analyse the data. Aghajanihashtchintahmores (2011) investigated on the role of play in social skills and intelligence of children in three groups, kindergarden (3-5 years old), pre-school (6-7 years old), and school (8-12 years old) focusing on two factors, which is intelligence profile and social skill with data analysed by two-way MANOVA. William Flores, *et al.* (2013) explored on the effect of variations in banner ad, type of product, website context, language of advertising on Internet users' attitudes. The main goal of the study by Yu-Chen Hsieh, *et al.* (2010) was to verify different influences of the information types on advertising attention. Previous studies relevant to

internet advertising focused on the form, colour, size and location, while this study focused on how the information types and the webpage structure influenced the viewers' attention on banner advertising.

Methodology

Multivariate Analysis of variance (MANOVA) is a statistical test procedure for comparing multivariate (population) means of several groups. The one-way MANOVA is modelled as $[y_{ij}^{(1)} \ y_{ij}^{(2)} \ \dots \ y_{ij}^{(p)}] = [\mu^{(1)} \ \mu^{(2)} \ \dots \ \mu^{(p)}] + [\alpha_j^{(1)} \ \alpha_j^{(2)} \ \dots \ \alpha_j^{(p)}] + [\varepsilon_{ij}^{(1)} \ \varepsilon_{ij}^{(2)} \ \dots \ \varepsilon_{ij}^{(p)}]$ for p measures. $y_{ij}^{(k)}$ is the score for the subject ij on the dependent variable Y_k ; $\mu^{(k)}$ and $\alpha_j^{(k)}$ are parameters for Y_k (Finn, 1974).

We explored the multivariate effect and univariate effect for each MANOVA, where multivariate effect is how the independent variables have an impact on the combination of dependent variable and univariate effects is how the mean scores for each dependent variable differ across the independent variable groups. . It describes the effect of the independent variables upon the combined dependent variables.

A few assumptions have to be met to use MANOVA. All dependent variables must be distributed normally. Linear combinations of dependent variables must be distributed normally. All subsets of the variables must have a multivariate normal distribution (Statistics, L., 2013). In MANOVA, each one of dependent variables is required to have equal variances. Also, it is required in MANOVA that the covariance matrices are homogeneous. The variance shared between any two variables need to be equal across all levels of independent variable. Box's M test is used to test the hypothesis that the covariance matrices of the dependent variables are significantly different across levels of the independent variable. The assumption of MANOVA is violated when the Box's M test is significant (Zaiontz C., 2015). The subjects' scores on the dependent measures should not be influenced by or related to scores of other subjects in the condition or level. If it is suspected that the observations are lack of independence, it can be tested with an interclass correlation coefficient.

The dependent variables in MANOVA should not be too strongly correlated. When there are moderate correlations between the dependent variables, MANOVA works well. If the dependent variables are too correlated, there is not enough variance left over after the first dependent variable is fit. On the other hand, if the dependent variables are not correlated, the multivariate test will lack of power. Hence, the acceptable limits are positive correlation should not exceed $r=0.90$, while negative correlation should not exceed $r = -0.40$ (Andrew Mayers, 2013).

When we run the MANOVA analysis in SPSS, several lines of multivariate outcome are presented. Each reports different significance. The four options are: Wilks' Lambda, Hotelling's Trace, Pillai's Trace and Roy's Largest Root. Wilk's Lambda is used when the independent variable has more than two groups. It explores outcomes using a method similar to F ratios in univariate ANOVAs. The larger the dispersion between groups, the smaller the value of Wilk's Lambda, the greater the implied significance. Hotelling's Trace should be used only when the independent variables are represented by two groups. Pillai's Trace and Roy's Largest Root can be used with any number of independent variable groups. Pillai's Trace is most probably the most powerful option when the samples are equal in size. Roy's largest Root used similar calculations as Pillai's Trace, but it focused on the first factor in the analysis. The best measure to be used is the one most immune to the violations of the assumptions underlying MANOVA yet maintains the greatest power (Mayers, 2013).

When the MANOVA null hypothesis is rejected, we look into the main effect and interaction effect by using univariate tests, ANOVA. Analysis of Variance (ANOVA) is used to analyse the differences between group means and their associated procedures, such as variation among and between groups. In ANOVA, the null hypothesis is that all groups are random samples of the same population, implying that the treatments have the same effect on the samples. There are three assumptions to be satisfied for ANOVA test. The observations are obtained independently and randomly from the populations. The population at each factor level is (approximately) following normal distribution and these normal populations have a common variance, σ^2 .

Findings and Discussion

Correlations were found to meet the acceptable limits for MANOVA. Box's M test was used to test for the equality of variance-covariance matrices and was found that the assumptions were satisfied. From Table 1, the multivariate outcome showed no interaction effect, however response measures were found to be significantly dependent on the uniqueness and competitive claim. Univariate tests were run since the MANOVA null hypothesis is rejected. Homogeneity of between group variance for all dependent variables was found using Levene's test. ANOVA tests in Table 2 shown that uniqueness claim only effect the likelihood of buying the product while competitive claim effect 'How much do you like this product?' and 'I like this product'. The interaction effect in the univariate test shows that all the response measure are significantly dependent on the inclusion of both claims.

Effect		Sig.
Intercept	<u>Pillai's Trace</u>	.000
	<u>Wilks' Lambda</u>	.000
	<u>Hotelling's Trace</u>	.000
	Roy's Largest Root	.000
Uniqueness	<u>Pillai's Trace</u>	.001
	<u>Wilks' Lambda</u>	.001
	<u>Hotelling's Trace</u>	.001
	Roy's Largest Root	.001
Competitive	<u>Pillai's Trace</u>	.014
	<u>Wilks' Lambda</u>	.014
	<u>Hotelling's Trace</u>	.014
	Roy's Largest Root	.014
Uniqueness * Competitive	<u>Pillai's Trace</u>	.150
	<u>Wilks' Lambda</u>	.150
	<u>Hotelling's Trace</u>	.150
	Roy's Largest Root	.150

Table 1: Multivariate tests result.

Source	Dependent Variable	Sig.
Corrected Model	Y1	.016
	Y2	.025
	Y3	.025
	Y4	.002
Intercept	Y1	.000
	Y2	.000
	Y3	.000
	Y4	.000
Uniqueness	Y1	.963
	Y2	.885
	Y3	.148
	Y4	.001
Competitive	Y1	.017
	Y2	.032
	Y3	.201
	Y4	.877
Uniqueness*Competitive	Y1	.030
	Y2	.027
	Y3	.016
	Y4	.034

Table 2: Univariate Test Result

Conclusion

Our main objective is to test the effects of different print ad elements on the attitude toward the product and intention to buy. The multivariate tests showed that the response measures were significantly dependent on both the claims at significance level $\alpha=0.05$. This shows that the claims have an effect on the measures implying the addition of the claims gives positive result on the attitude towards the product and intention to buy. From the univariate test, the experimental effects that are significant at level $\alpha=0.05$ are Y4, 'What is the likelihood you would buy this product?', for uniqueness claim and Y1, 'I like this product', and Y2, 'I would buy this product', for competitive claim. Hence, we conclude that both the claims had effects on the attitude towards the product and intention to buy.

References

Gennuso, K. P., Thraen-Borowski, K. M., Schlam, T. R., LaRowe, T. L., Fiore, M. C., Baker, T. B., & Colbert, L. H. (2014). Smokers' physical activity and weight gain one year after a successful versus unsuccessful quit attempt. *Preventive medicine*, 67, 189-192.

Colakoglu, F. F., & Solak, N. (2014). Examination of aggression levels and empathic tendency levels of secondary school students who involve or not involve in sports. *Procedia-Social and Behavioral Sciences*, 152, 415-420.

tahmores, A. H. (2011). Role of play in social skills and intelligence of children. *Procedia-Social and Behavioral Sciences*, 30, 2272-2279.

Flores, W., Chen, J. C. V., & Ross, W. H. (2014). The effect of variations in banner ad, type of product, website context, and language of advertising on Internet users' attitudes. *Computers in Human Behavior*, 31, 37-47.

Hsieh, Y. C., & Chen, K. H. (2011). How different information types affect viewer's attention on internet advertising. *Computers in Human Behavior*, 27(2), 935-945.

Finn, J. D. (1974). *A general model for multivariate analysis*. Holt, Rinehart & Winston.

Statistics, L. (2013). One-way ANOVA in SPSS. Retrieved December, 21, 2013.

Zaiontz C. (2015) Real Statistics Using Excel. www.real-statistics.com

Mayers, A. (2013). *Introduction to statistics and SPSS in psychology*. Pearson.

GENETIC ALGORITHMS AND JOHNSON'S RULE FOR FLOW SHOP SCHEDULING PROBLEM

Noor Harlinda Hariati Mohd Othman, Syarifah Zyurina Nordin

2.0 INTRODUCTION

Scheduling is an act of defining priorities or arranging activities to meet certain requirements, constraints or objectives. Since time always been major constraint scheduling are needed in manufacturing industry as process of allocating each job for a machine in order to complete a task in the shortest possible time. In order to have a better understanding of flow shop scheduling problem, the Genetic Algorithms and Johnson's Rule are used.

The objectives of this research study comprises of (i) to solve three machines flow shops problem using Genetic Algorithms; (ii) to solve two machines flow shops scheduling problem using Johnson's Rule; and (iii) to extend Johnson's Rule to solve three machines flow shops scheduling problem.

1.1 STUDY AREA

This study will look into the concepts in flow shop scheduling while understanding its application in the real life to find the minimum makespan. The concepts will be used to minimize the time used to finish the last job using Genetic Algorithms and Johnson's rule which will be represented by using Gantt chart. The methods of Genetic Algorithms and Johnson's rule will be used to solve the flow shop scheduling problem with the objective of minimizing the makespan.

1.2 LITERATURE REVIEW

Scheduling can be defined as the allocation of resources over time to perform a collection task. In real life problem, the resources have a limit. Scheduling consists of planning and prioritizing activities that need to be performed in an orderly sequence of operation [1]. Scheduling also play the role as decision maker that has a goal of the optimization for one or more objective. There are many kinds of field that need scheduling process such as manufacturing and production systems as well as most information-processing environment [2]. It also exists in transportation and distribution setting and in other types of service industries. For example, in gate assignment at the airport need scheduling in assign planes to suitable gates that have to be free at the respective arrival times. Scheduling also helps at the construction site by assign each crew at each stages in construction project so that the project can accomplish on time. Based on the above scenario,

we can say that in scheduling objectives can take many different forms, such as minimizing the time to complete all activities, minimizing the number of activities that are completed after the committed due date, and so on [3].

The shop scheduling is one of the most challenging scheduling problems. It can be classified into four main categories: single machine scheduling, flow shop scheduling, job shop scheduling and open shop scheduling. Generally speaking, scheduling problem is described by a triplet $\alpha | \beta | \gamma$ (Pinedo, 2002). First, the α field described the machine environment which contains a single machine or multiple machine. Then, the β field is job characteristics that can categorize in general four attribute: whether or not a job can be interrupted, whether or not precedence ordering is imposed on the job, whether or not job dependent release time is given and final specification regarding job duration time. The γ field described the optimality that used to specifying measure of performance.

1.3 METHODOLOGY

The overall structure of GA can be described as follows:

1. *Coding*: The genes of the chromosomes describe the jobs and the order in which they appear in the chromosome describes the sequence of jobs. Each chromosome represents a solution for the problem.
2. *Initial population*: The initial chromosomes are obtained by a random dispatching rule for sequencing.
3. *Fitness evaluation*: The sum of earliness and tardiness cost is computed for each chromosome in the current generations.
4. *Selection*: In any iteration, chromosomes are chosen randomly for crossover and mutation.
5. *Offspring generation*: The new generation is obtained by changing the sequencing of operations (reproduction, enhanced order crossover and mutation). These rules preserve feasibility of new individuals. New individuals are generated until a fixed maximum number of individual is reached.
6. *Stop criterion*: Fixed number of generations is reached. If the stop criterion is satisfied, the algorithm ends and the best chromosome, together with the corresponding schedule, are given as output. Otherwise, the algorithm iterates again step 3-5.

Based on bypass consideration GA is adapted to consider operation with zero processing time on some machines.

The Johnson's Rule method can be described as follows:

The two machine problem is the simplest form of a flow shop arrangement which each job must be processed successively on these two machines. The job process must follow the flow, the first operation on the first machine and the second operation on the second machine. Keep in mind that the second operation only can be start after operation first for each job is done. In this section we will see how Johnson's rule being applies for solving the two machines problem. Johnson (1954) has developed a scheduling procedure that gives a minimum makespan for the jobs on which the procedure is applied. For making the procedure general, we define $A_i = P_{i1}$ and $B_i = P_{i2}$. First, the jobs must be in sequenced, by determine the minimum times for all A_i and B_i . If the minimum is associated with A_i , place the corresponding job in the earliest possible position in the sequence. If the minimum is

associated with B_i , place the corresponding job in the latest possible position in sequence. We identify the job that had been sequence by marking the job as being sequence and scratch the associated A_i and B_i values. If all job are placed in the sequence, thus we have obtain the optimal sequence. If not, we must repeat the step until all the jobs a placed in sequence. Lastly, for the three machines problem, some modification is needed before we proceed with Johnson's Rule algorithm by develop two factors $A_i = P_{i1} + P_{i2}$ and $B_i = P_{i2} + P_{i3}$. These two factors we treat as machine 1 and machine 2 respectively. Hence, the three machine problem has become two machine problems.

1.4 RESULTS AND DISCUSSION

Genetic Algorithms in solving 3 machines flow shop problem are as below:

Table 1: Three Machines Problem

Job	Machine 1	Machine 2	Machine 3
1	5	1	1
2	1	2	4
3	9	4	3
4	3	6	2
5	10	3	1

We start with an initial population of six solutions which are generated randomly. Each solution is represented by the Gantt chart and the makespan (fitness function value) is calculated using the longest path. The longest makespan for Schedule 1, Schedule 2, Schedule 3, Schedule 4, Schedule 5 and Schedule 6 are 35, 32, 33, 35, 35 and 32 respectively.

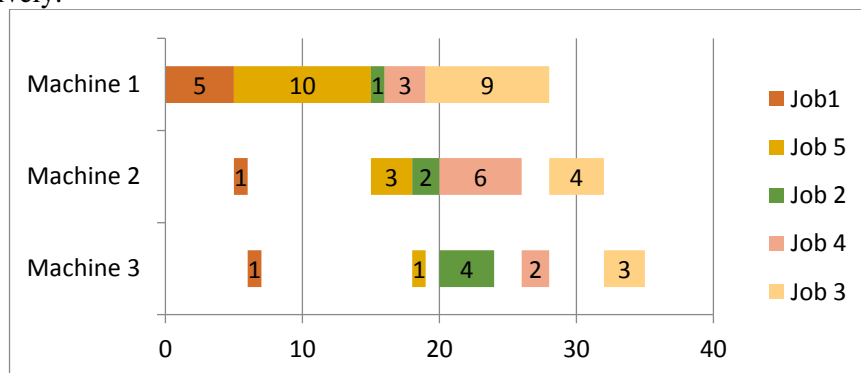


Figure 1: Solution of Schedule 1

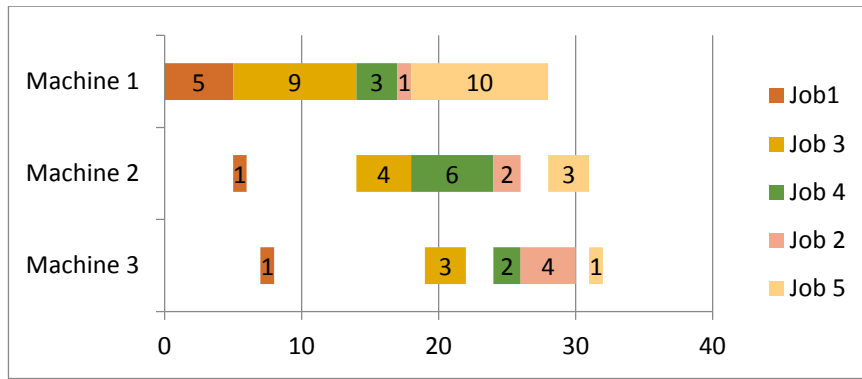


Figure2: Solution of Schedule 2

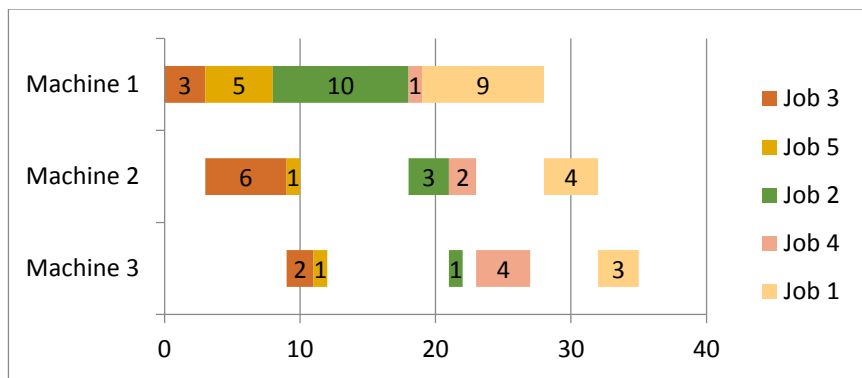


Figure 3: Solution of Schedule 3

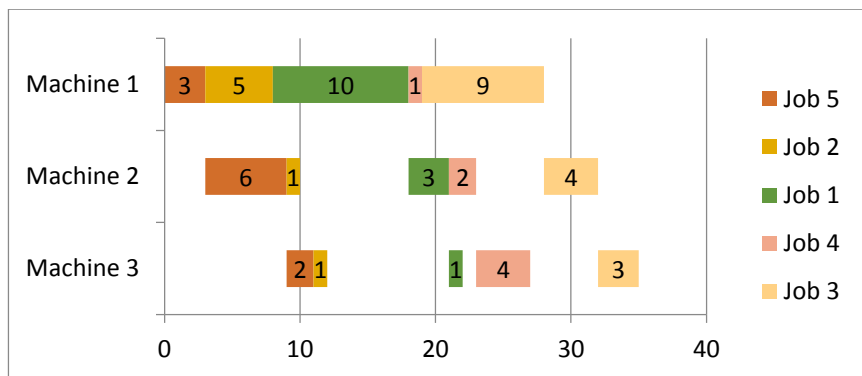


Figure 4: Solution of Schedule 4

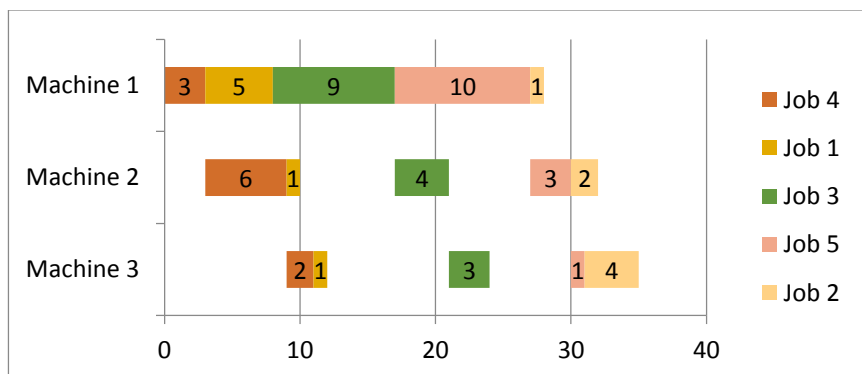


Figure 5: Solution of Schedule 5

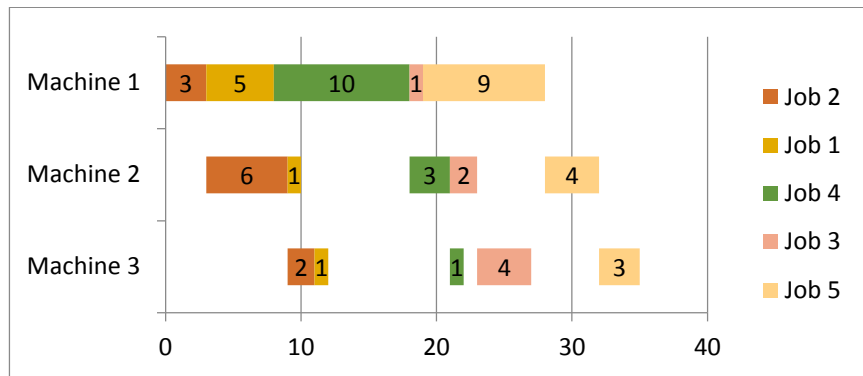


Figure 6: Solution of Schedule 6

For the selection of parents, There are many selection methods, for example fitness-based selection, rank- based selection, tournament-based selection and spatially-oriented selection. In this work, two selection methods are chosen, namely bias selection and random selection. For the first type of selection, job fitness is randomly chosen from the current population of breeding. In the second selection method, the best pair of parents from each population is chosen to produce two children. Then, the children and the other four unchosen schedules will be carried forward for the next population. The process of crossover is continuing with the best pair of schedule chosen as the parents for the crossover operation and the other is the random pair of parent for crossover operation.

The summary of the Genetic Algorithm produce for the best pair crossover and the random pair crossover selection methods are shown in Table 2:

Table 2: Result of GA problem

	Best Pair Crossover	Random Pair Crossover
Best Makespan	32	35
Job Sequence	1-3-2-4-5	3-5-1-4-2
	2-1-3-4-5	4-1-5-2-3

Table 2 shows that the best pair crossover selection is better compared to the random pair crossover selection.

Johnson’s Rule in solving 2 machines flow shop problem are as below:

Table 3: Two Machines Problem

Job	Work Center I	Work Center II
1	5	2
2	1	6
3	9	7
4	3	8
5	10	4

Consider a company is faced with five tasks that have to be processed through two work centers. We have five jobs that need to be processed. The above data show the time required for each job for each machine. The objective is to determine the optimum sequence in order to minimize the makespan. By using the Johnson’s rule algorithm we can obtain the optimum sequence.

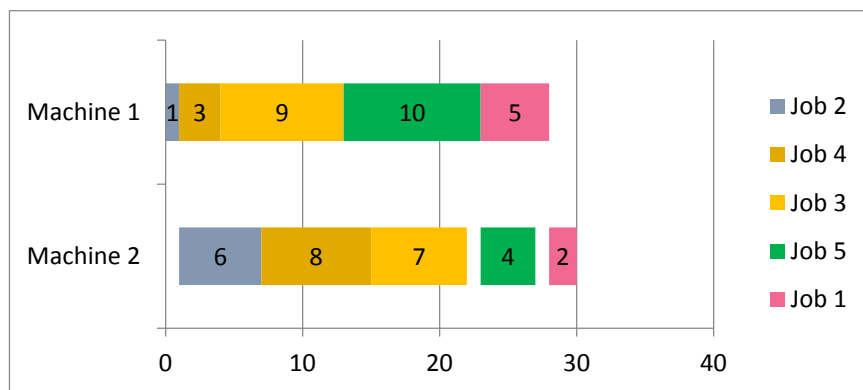


Figure 7: Optimal schedule for two machines problem

Figure 7 shows that the optimal schedule for two machine problem (2-4-3-5-1) with the makespan of 30.

Unfortunately, Johnson’s rule cannot be extended to n machines or facilities. However, it can be extended to a three machines flow shop provided the second machine is not a “bottleneck” machine. For a machine not to be a bottleneck, it should not delay any job; in other word, as a job is released from the first machine. If such is the case, develop the following two factors for each job i : $A_i = P_{i1} + P_{i2}$ and $B_i = P_{i2} + P_{i3}$. Then apply the Johnson’s rule procedure described, but treat factors A_i as machine 1 time and factors B_i as machine 2 time.

Table 4: Three Machines Problem

Job	Work Center I	Work Center II	Work Center III
1	5	1	1
2	1	2	4
3	9	4	3
4	3	6	2
5	10	3	1

The table above shows the processing time for each job that will process on three machines which are work center I, II and III. We need to develop factor A_i and B_i . This modification is to change this 3 machines problem into 2 machines problem so that the Johnson's rule can work. The table below shows the value of the both factors.

Table 5: Value of factor A and B for three machines

Job	$A_i = P_{i1} + P_{i2}$	$B_i = P_{i2} + P_{i3}$
1	6	2
2	3	6
3	13	7
4	9	8
5	13	4

On 3 machine problem, Johnson's rule can only give the minimum makespan if the second machine is not a bottleneck machine. According to Dileep R. Sule if the first number is greater than the second number, the job is waiting on the machine and if the second number is larger than the first, the machine is waiting for the job.

$$\text{Machine } k \text{ idle time} = \sum (C_{i-1,k} - C_{i,k-1}) \text{ for } C_{i-1,k} - C_{i,k-1} < 0$$

$$\text{Total waiting time on machine } k = \sum C_{i-1,k} - C_{i,k-i} \text{ for } C_{i-1,k} - C_{i,k-i} \geq 0$$

In this problem, machine 2 is not a bottleneck because machine 2 idle time is $(4 - 3) + (13 - 10) + (23 - 17) + (28 - 26) = 12$, while total waiting for jobs on machine 2 is zero. Hence, the sequence that we get by applying the modification of Johnson's rule is optimum.

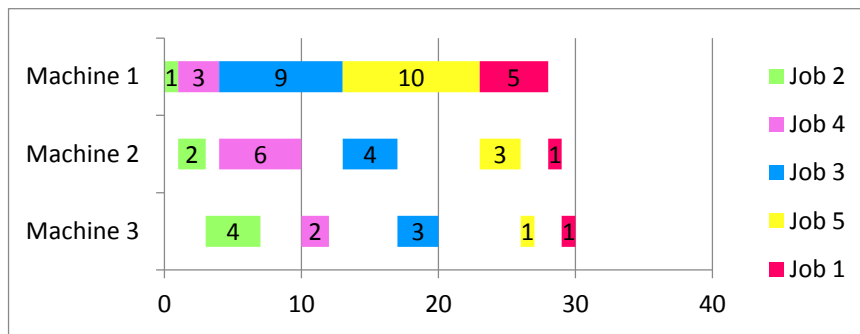


Figure 8: Optimal schedule for three machines problem

1.5 CONCLUSION

In this study, a general flow shops problem was founded with n jobs which are to be processed by m machine for each operation. The task will be processed in the unique sequence in order to get the minimum makespan. The sequence is generated by following the steps of the Johnson's rule. For machine 2 problem, there is no modification need to the problem or the algorithm. Johnson's rule can straightly use to get the optimal solution. For the two machines problem, we get the optimal schedule is 2-4-3-5-1 with minimum makespan is 30.

We continue our discussion with solving three machines problem. For this problem, we need to modify the problem or the algorithm before we can apply Johnson's rule. The optimal sequence for three machines problem is 2-4-3-5-1 with 30 minimum makespan.

We also solve the three machines problem by using the Genetic Algorithm method. The initial schedules are generated randomly and the makespan (fitness function value) is calculated using the Gantt chart. We proceed with the crossover process by using two selection methods which are the best pair crossover and the random pair crossover. From the experimental result, it can be seen that the best pair crossover selection is better compared to the random pair crossover selection with the makespan of 32 and 35 respectively.

REFERENCES

1. Sule, D.R. (Dileep R.), Louisiana Tech University . *Industrial Scheduling*. PWS Publishing Company.
2. Pinedo, M. L. Columbia University. *Scheduling: theory, algorithm and systems*. Prentice Hall international series in industrial and systems engineering.
3. Pinedo, M. L. *Planning and scheduling in Manufacturing and Services*.
United State of Amerika: Springer, 2005.
4. Colin R. Reeve. *Modern Heuristic technique for combinatorial problems* Halsted press.
5. Holland, J.H., *Adaptation in natural and artificial systems*, Ann Arbor: University of Michigan Press, 1975.
6. Joanna Jozefowska. *Just in time scheduling: Models and algorithms for computer and manufacturing systems*. Springer.
7. M. R. Garey and D. S. Johnson, *Computers and Intractability: A guide to the Theory of NP-Completeness*, Freeman, San Francisco, CA, 1979.
8. L. Davis, *Handbook of Genetic Algorithms*, 1991, New York, Van Nostrand Reinhold.
9. Nadia N, A. A. and Luiza, M. M. *Genetic Systems Programming*. (13th ed.).
Berlin Hidelberg, N. Y.: Springer, 2006.
10. Zbigniew, M. (1996). *Genetic Algorithms+Data Data Structures=Evolution Programs*.(3rd ed.). Berlin Heidelberg, NY.: Springer.
11. Peter, B. *Scheduling Algorithms*. (5th ed.). Berlin Heidelberg, N. Y.: Springer, 2007.
12. R. G. Parker. *Deterministic Scheduling Theory*. (1st ed.). Boundary Row, London, UK.: Chapman & Hall, 1995.

THE EFFECT OF PARAMETER SETTING ON CLASSIFICATION OF DOMESTIC WATER CONSUMPTION USING SIMPLIFIED FUZZYQSBA

Nor Aina Mohmud, Munira Ismailand Khairul Anwar Rasmani

Abstract:

Water is essential in human daily life and it is renewable. However, the resources of water are reducing due to climate and other factors. Hence many researches were conducted to predict the water consumption and applying many different approaches to solve this problem. Therefore the aim of this research is to enhance an existing method for producing a better and reliable technique with more accurate results. The proposed method is FuzzyQSBA and the parameter settings of the membership function are manipulated to investigate its effect on the accuracy of the method. Here, simplified FuzzyQSBA is used for the classification of domestic water. There are four different parameter settings, the performances of each setting are compared and it shows that parameter setting does effects the final results. Next, the result of the best parameter setting is then compared with other existence fuzzy method using a software name WEKA. Results claimed that the proposed method is compatible with other method in terms of it accuracy.

Key Words: Domestic water consumption, Simplified FuzzyQSBA

Introduction

We are considering the simplified FuzzyQSBA method for classification of domestic water consumption. This method only been used for classification of medical data set by Garibaldi et al. [1] and not yet applied in other field. There are also many investigation related to classification of domestic water consumption such as Altunkaynak et al [2], Corona-Nakamura et al [3] and Nezhad et al. [4]. All of these researchers used fuzzy and non-fuzzy approach but none of them are applying quantifier-based algorithm.

In this paper, we proposed the simplified FuzzyQSBA method for classification of the domestic water consumption. Simplified FuzzyQSBA is a compressed version of FuzzyQSBA which is more simple and easy to be used. In addition the parameter of membership function is set for four different setting to investigate the best parameter to obtain higher classification accuracy. Since this quantifier-based algorithm is new for classification of water consumption, hence its performance will be compared with other methods.

The structure of this paper is defined as follows. The second section presents the domestic water consumption data set and brief detail about the data set used in this research. Section 3 contains the method of this study, the steps for simplified FuzzyQSBA and Section

4 presents the accuracy results and its analysis. The last Section 5 gives the main conclusions about this study.

Domestic Water Consumption Data Set

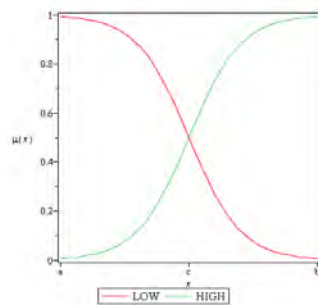
The consumer data that will be used for this study was previously used in research reported in [5]. This data set is obtained from internet surveyed for a month water usage in a household. The original consumer data, DWL consists of 439 instances with 11 attributes that are size of household, number of toilet, brushing teeth, washing face, showering, flushing toilet, washing clothes by hand and by machine, used for cooking, car washing and total used based on the meter reading and were classified into 2 different classes, likely and unlikely. “Likely” class will refer to excessive water used or a leakage and “unlikely” refer to no water leakage or no excessive used.

Since there is only 1 set of original data which will be used as the training data, so the testing data will be generated from the original data using 10-fold cross validation by using Microsoft excel. Here, the data with 439 instances is divided into 10 set training data and 10 set testing data where each training dataset consists of 395 or 396 instances while each testing dataset consists of 44 or 43 instances.

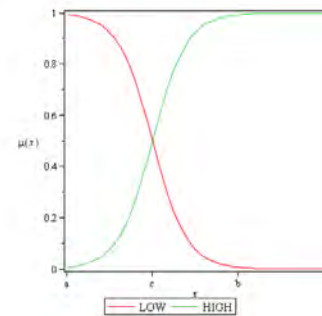
Simplified FuzzyQSBA

A. Fuzzification

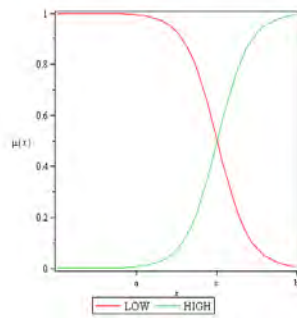
Fuzzification is a process of transforming the crisp values into the grade of membership. This can be done by assigning the suitable membership function for the problem. Sigmoid function will be applied for this data. The following step is required for fuzzification. First, the partition is formed for each of attributes by try and error technique. Next, this partition will be used to set the parameter setting. There were four parameter settings that will be set and this parameter setting affect the sigmoid membership function. The following below are the figure sigmoid function for each parameter setting.



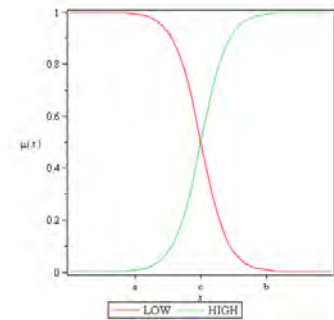
Parameter setting 1



Parameter setting 2



Parameter setting 3



Parameter setting 4

B. Fuzzy Subsethood Measures

In this research, it is define as the degree of subsethood for the linguistic terms which are the attribute M to a decision class N . Consider an attributes $\{M_1, M_2, \dots, M_n\} \in M$ and $(M, N) \subseteq X$, the fuzzy subsethood values are calculated as follow :

$$S(N, M_i) = \frac{\sum_{x \in X} \nabla[\mu_N(x), \mu_{M_i}(x)]}{\sum_{x \in X} \mu_N(x)} \quad (1)$$

Where $S(N, M_i) \in [0,1]$ and ∇ can be any t-norm operator [1].

C. Fuzzy Quantifier

Fuzzy quantification techniques can be based on the generalisation of first order logic quantifiers, where the quantification mechanism involves the definition of the existential quantifier, \exists and of the universal quantifier, \forall [6]. The truth values of the existential quantifier $T_{\exists, A/M}$ and the universal quantifier $T_{\forall, A/M}$ are as follows :

$$T_{\exists, A/M} = \Delta_{k=1}^N \mu(a_k) \nabla \mu(m_k)$$

$$T_{\forall, A/M} = \nabla_{k=1}^N (1 - \mu(m_k)) \Delta \mu(a_k)$$

where a_k and m_k are the membership functions of fuzzy sets A and M respectively, ∇ represents the t-norm and Δ represents the t-conorm [1].

The quantifier is defined as a linear interpolation:

$$T_{Q, \frac{A}{M}}(\lambda_Q) = (1 - \lambda_Q)T_{\nabla, \frac{A}{M}} + \lambda_Q T_{\exists, \frac{A}{M}}$$

Where Q is the quantifier for fuzzy set A relative to fuzzy set M and λ_Q is the degree of the neighbourhood of the two extreme quantifiers.

D. FuzzyQSBA rule generation

Rule set generated from FuzzyQSBA can be represented by :

$$R_k = \nabla_{i=1 \dots p} \left(\Delta_{j=1 \dots q} \left(Q(A_{ij}, M_k) \nabla \mu_{A_{ij}}(x) \right) \right), k = 1, 2, \dots, n$$

where $Q(A_{ij}, M_k)$ are fuzzy quantifiers of linguistic proposition and $\mu_{A_{ij}}(x)$ are fuzzy linguistic terms modified by the weights, with ∇ and Δ denotes the logical conjunction and disjunction operators respectively [6].

E. Simplify FuzzyQSBA rule

The rule simplification process is based on fuzzy quantifier where fuzzy quantifier will be as fuzzy threshold. Rule simplification will use the following fuzzy quantifiers and fuzzy antonym quantifiers respectively :

$$T_Q(\eta) = \begin{cases} 1 & \text{if } T_Q(\lambda) \geq \eta, \\ \frac{T_Q(\lambda)}{\eta} & \text{if } T_Q(\lambda) < \eta \end{cases}$$

$$T_{antQ}(\eta) = \begin{cases} 1 & \text{if } T_Q(\lambda) \leq 1 - \eta \\ \frac{1 - T_Q(\lambda)}{\eta} & \text{if } T_Q(\lambda) > 1 - \eta \end{cases}$$

Where $T_Q(\eta)$ is truth value of quantifier for each linguistic term and η is a threshold value such that :

$$\eta = p \times \omega$$

where p is a multiplication factor for the maximum truth value quantifier (TVQ), ω [6]. The following technique is proposed in [6] to perform the rule simplification:

1. Choose maximum truth value quantifier and calculate $T_Q(\eta)$ and $T_{antQ}(\eta)$ for each linguistic term of each variable.
2. For $i = 1, 2, \dots, k$ where k is number of linguistic terms for a variable and for $m \neq n$, calculate :

$$\delta(T_{Q_i}(\eta)) = |T_{Q_m}(\eta) - T_{Q_n}(\eta)|$$

$$\delta(T_{antQ_i}(\eta)) = |T_{antQ_m}(\eta) - T_{antQ_n}(\eta)|$$

3. Run a test such that if $\min_i \{ \delta(T_{Q_i}(\eta)) \geq \delta(T_{antQ_i}(\eta)) \}$ then choose the negation of terms with the lowest truth value of quantifier to represent the conditional attribute, else choose the term with highest truth value.
4. Create a simplified rule using accepted linguistic terms.

Performance of Simplified FuzzyQSBA on Domestic Water Consumption

A. Performance of Simplified FuzzyQSBA with Different parameter Settings

Table 1 present results obtained by simplified FuzzyQSBA method with four different parameter setting showing the classification accuracy (%) of domestic water consumption. Third parameter setting, Fuzval 3 gives the best results while parameter setting Fuzval 4 produces the lowest accuracy. Based on the difference, clearly that the parameter setting does effects the performance of fuzzyQSBA method. In this research, Fuzval 4 is the worst option on choosing the parameter setting. However, it only valid for this study since it might not be the same if different dataset is used.

Table 1 Classification accuracy (%) of simplified FuzzyQSBA for different setting

SET	Fuzval 1	Fuzval 2	Fuzval 3	Fuzval 4
1	90.91	90.91	97.73	84.09
2	90.91	90.91	95.45	77.27
3	90.91	90.91	95.45	81.82
4	95.45	95.45	93.18	65.91
5	90.91	90.91	86.36	68.18
6	95.45	90.91	93.18	81.82

7	88.64	88.64	93.18	77.27
8	90.91	90.91	88.64	75.00
9	90.69	90.69	93.02	81.40
10	86.36	86.36	86.36	77.27
Av.	91.11	90.63	92.03	77.00

B. Performance of Simplified FQSBA compare to Other Methods

The fuzzy methods that will be compared using with simplified FuzzyQSBA using software WEKA are FuzzyRoughNN (FRNN), NN, FuzzyNN (FNN), FuzzyOwnershipNN (FONN), DiscernibilityClassifier (DC), QSBA1, QuickRules (QR) and VQRules (VQR). QSBA1 is Quantifier Subsethood-based Algorithm but the membership function used is trapezoidal.

Table 2 is the classification accuracy (%) results for other fuzzy methods and results of fuzzyQSBA using Fuzval 4. The best result is produce by FuzzyRoughNN, FRNN, however the proposed method, simplified FuzzyQSBA with Fuzval 3 also give a good performance with 92.03 percent of accuracy. In addition, it gives better performance than fuzzyQSBA with trapezoidal membership function, QSBA1.

Table 2 Classification accuracy (%) of simplified FuzzyQSBA with other methods

SET	FRNN	NN	FNN	FONN	DC	QSBA1	QR	VQR	SFQSBA
1	95.45	93.18	90.91	97.73	97.73	90.91	93.18	93.18	97.73
2	93.18	90.91	88.64	90.91	93.18	93.18	93.18	93.18	95.45
3	93.18	90.91	93.18	90.91	90.91	88.64	90.91	90.91	95.45
4	90.91	90.91	90.91	95.45	93.18	95.45	93.18	93.18	93.18
5	93.18	90.91	90.91	93.18	90.91	68.18	93.18	93.18	86.36
6	97.73	95.45	93.18	86.36	95.45	88.64	95.45	95.45	93.18
7	93.18	93.18	93.18	95.45	93.18	97.73	95.45	93.18	93.18
8	100.00	92.66	100	100.00	96.20	79.55	99.24	99.24	88.64
9	93.02	90.69	90.69	90.69	90.69	95.35	93.02	93.02	93.02

10	93.18	90.91	88.64	90.91	90.91	84.09	88.64	93.18	86.36
Av.	94.30	91.97	92.02	93.18	93.23	88.17	93.54	93.77	92.03

Conclusion

This paper offers a new method for classification of domestic water consumption by using simplified FuzzyQSBA. The result in Table 1 reveal the effect of different parameter setting on the classification accuracy (%) and it shows that Parameter Setting 3 produced the best result among the four setting with higher classification accuracy. However, this parameter setting is only valid for domestic water consumption data set.

Table 2 presents the classification accuracy (%) of other methods together with the simplified FuzzyQSBA. It shown simplified fuzzyQSBA method is compatible with other existence techniques with equivalent accuracy.

References

- [1] K. A. Rasmani, *et al.*, "Linguistic rulesets extracted from a quantifier-based fuzzy classification system," in *Fuzzy Systems, 2009. FUZZ-IEEE 2009. IEEE International Conference on*, 2009, pp. 1204-1209.
- [2] A. Altunkaynak, *et al.*, "Water Consumption Prediction of Istanbul City by Using Fuzzy Logic Approach," *Water Resources Management*, vol. 19, pp. 641-654, 2005/10/01 2005.
- [3] M. A. Corona-Nakamura, *et al.*, "Classification of domestic water consumption using an Anfis model," in *Automation Congress, 2008. WAC 2008. World*, 2008, pp. 1-9.
- [4] M. Z. Nezhad, *et al.*, "Estimation of domestic water demand function in Ahvaz, Iran," 2013.
- [5] H. M. Hanif, *et al.*, "Detecting Residential Household Water Leakage and Wastage Using the Individual Hotelling T^2 control chart," presented at the IJAS American-Canadian International Conference on Academic Disciplines Toronto, Canada, 2013.
- [6] J. M. Garibaldi, *et al.*, "Consensus Clustering And Fuzzy Classification For Breast Cancer Prognosis," presented at the 24th European Conference on Modelling and Simulation (ECMS2010), Kuala Lumpur, Malaysia, 2010.

SOME NUMERICAL SCHEMES FOR SPRAY DRYING DIC MODELING USING PARTIAL DIFFERENTIAL EQUATION

Norhadhilah Mohd Hussain & Che Rahim CheTeh

Abstract

A new technology of drying process called spray drying by using instant control pressure drop (DIC) technique is considered high potential to maintain the nutrient in a *food*. DIC is also used to process the fruit waste into organic fertilizers, feeding to livestock or been disposed of either by composting or dumping in the landfills. Based on this advance, the project focuses on governing the mathematical modelling for visualizing the parameters involved in DIC technique during the drying and dehydration processes. The function of DIC technique is to transform the liquid form into powder or natural dye material. The mathematical modelling of the spray DIC was governed by computational fluid dynamics (CFD) equations based on the partial differential equation (PDE). Some parameter identification involves are continuity and energy. The parameters are investigating to improve the dehydration process in term of viscosity of the liquid, temperature behaviors and liquid contents. PDE was discretized by using Finite Difference Method (FDM). The linear system of the FDM has been solved via Jacobi method and Gauss Seidel method. The simulation of the discretization has been implemented in MATLAB 7.12.0 (R2011a). It can be concluded that the CFD equation is the alternative modelling to improve the dehydration process of DIC. Gauss Seidel is the superior method for solving the linear system of the FDM. It will enhance the inexpensive cost of the drying and maintain the quality nutrient in *food* products.

Keywords: Mathematical modeling, DIC technique, Parabolic equation, Numerical schemes, Finite difference method

Introduction

There were two types of waste which are organic and municipal wastes. Organic waste is the food waste and municipal waste is the other left over or sewage water that comes from housing, trade or commercial and industrial. Then, DIC technique was chosen to solve the problem of the dehydration process for fruit waste because DIC has high potential in solving the problem, low cost, low energy consumption, low equipment price and environmental friendly. The spray drying process will transform the fruit waste into powder and natural dye.

Many of drying process efforts using DIC only focusing on the mathematical model involving parameters pressure, temperature and water contents. Therefore, in this study we are focusing on the mathematical modeling involving liquid contents, the viscosity of the liquid, pressure and temperature behaviour. The objective of this study is to govern mathematical model for spray drying DIC by using the partial differential equation (PDE) based on the computational fluid dynamics (CFD). Then, use finite difference method (FDM) to discretize the PDE. The sequential algorithm is developed by using the discretized PDE based on the numerical schemes for implementation in the MATLAB. Numerical schemes that used to solve the PDE were Jacobi and Gauss Seidel schemes. This scope of the study will provide the useful information to the other researchers for their study or further study this topic.

Literature Review

Instant control drop pressure (DIC) technique was the most common method with the potential for the dehydration process that could be maintained the nutrition and gave the high quality for food storage (Alias *et al.*, 2012). An axisymmetric numerical model was used to simulate the velocity, temperature, humidity pattern and trajectories in pilot-scale spray dryer (Frydman *et al.*, 2007). The governing partial differential equation for their study can be expressed as

Continuity balance:

$$\frac{\partial \rho}{\partial t} + \vec{\nabla} \cdot \rho \vec{V}_g = S_M$$

where S_M is the additional mass to the continuous phase that comes from the dispersed phase due to droplet evaporation.

Momentum balance:

$$\frac{\partial \rho \vec{V}_g}{\partial t} + \vec{\nabla} \cdot (\rho \vec{V}_g \vec{V}_g) = -\vec{\nabla} P + \rho \vec{g} + \vec{F} \cdot \vec{\nabla} \cdot \tau$$

where τ is the stress tensor, \vec{g} and \vec{F} are gravitational acceleration and external body forces respectively.

Energy balance:

$$\begin{aligned} \frac{\partial \rho H_g}{\partial t} \cdot \vec{\nabla} \cdot (\rho \vec{V}_g H_g) \\ = \lambda_g \lambda^2 T_g + \frac{\partial P}{\partial t} + \vec{V}_g \vec{\nabla} \cdot P + \tau \cdot \vec{\nabla} \vec{V}_g - \left(\frac{\partial (J_{ij} H_i)}{\partial x} + \frac{1}{r} \frac{\partial (r J_{ij} H_i)}{\partial r} + \frac{1}{r} \frac{\partial (J_{ij} H_i)}{\partial \theta} \right) \\ + S_H \end{aligned}$$

where T_g is the temperature of the gas, J_{ij} is the diffusive mass flux of the i species (air or steam) in the j direction and λ_g is the thermal conductivity of the continuous phase. S_H is the heat transfer between the continuous and dispersed phases.

Computational fluid dynamics (CFD) were applied in a pilot-scale spray dryer study to solve the governing equation of the flow field, heat and mass transfer, and particle trajectory (Sadripour *et al.*, 2014). The governing equation involved in their study consists of continuity, momentum and energy balance equations.

Methodology

The aim of this study is to describe the parameters liquid contents, pressure, temperature behaviour and viscosity of the liquid of the mathematical modeling for spray drying DIC in partial differential equation (PDE) form. Partial differential equation can describe the most of the phenomenon that appear in mathematical physics and engineering (Abdul-Majid Wazwaz, 2002). A linear second-order partial differential equation can be classified into elliptic, parabolic and hyperbolic types. In this study, we only use parabolic type for first order PDE in two-dimensional. Finite difference method (FDM) is a method for looking an approximation to the solution of a boundary value problem at a finite number of points in the grid points (Knabner *et al.*, 2003). Then, FDM was used in this study to discretize the PDE of the mathematical model.

The PDE of the continuity and energy equations are written as a two-dimensional parabolic type:

Continuity:

$$\frac{\partial(\rho A)}{\partial t} + \left(\rho A \frac{\partial V}{\partial x} + \rho A \frac{\partial V}{\partial y}\right) + \left(\rho V \frac{\partial A}{\partial x} + \rho V \frac{\partial A}{\partial y}\right) + \left(V A \frac{\partial \rho}{\partial x} + V A \frac{\partial \rho}{\partial y}\right) = \cos(P) + Sc \quad (1)$$

where $\cos(P)$ is a function of pressure and Sc is a Schmidt number for the viscosity of the liquid. The Schmidt number formula

$$Sc = \frac{\mu}{\rho D}$$

where μ is dynamic viscosity (Pa.s or N.s/m² or kg/m.s)

ρ is density of the liquid (kg/m³)

D is the mass diffusivity (m²/s)

Energy:

$$\rho c_v \frac{\partial T}{\partial t} + \rho V c_v \left(\frac{\partial T}{\partial x} + \frac{\partial T}{\partial y}\right) = -\rho RT \left[\left(\frac{\partial V}{\partial x} + \frac{\partial V}{\partial y}\right) + V \left(\frac{\partial(\ln A)}{\partial x} + \frac{\partial(\ln A)}{\partial y}\right)\right] \quad (2)$$

The PDE was expressed in terms of non-dimensional variables as preferred by the fluid dynamicists that frequently use these non-dimensional terms when dealing with nozzle flows. Then, the non-dimensional PDE's are as follows:

Continuity:

$$\frac{\partial \rho}{\partial t} = -\rho \left(\frac{\partial V}{\partial x} + \frac{\partial V}{\partial y}\right) - \rho V \left(\frac{\partial(\ln A)}{\partial x} + \frac{\partial(\ln A)}{\partial y}\right) - V \left(\frac{\partial \rho}{\partial x} + \frac{\partial \rho}{\partial y}\right) + \cos(P) + Sc \quad (3)$$

where the function for parameter pressure and Schmidt number for parameter viscosity of the liquid was added to the continuity equation.

Energy:

$$\frac{\partial T}{\partial t} = -V \left(\frac{\partial T}{\partial x} + \frac{\partial T}{\partial y}\right) - (\gamma - 1)T \left[\left(\frac{\partial V}{\partial x} + \frac{\partial V}{\partial y}\right) + V \left(\frac{\partial(\ln A)}{\partial x} + \frac{\partial(\ln A)}{\partial y}\right)\right] \quad (4)$$

The finite difference method was used to discretize the non-dimensional variables of the PDE based on the Jacobi and Gauss Seidel numerical schemes. The discretization of the PDE based on the Gauss Seidel scheme for each parameter is as follows:

Liquid contents parameter:

$$\rho_{i,j,k+1} = \frac{\Delta t}{\Delta x} \left[-\rho_{i,j,k}(V_{i+1,j,k+1} - V_{i,j,k}) - \rho_{i,j,k}V_{i,j,k}(A_{i+1,j,0} - A_{i,j,0}) - V_{i,j,k}(\rho_{i+1,j,k+1} - \rho_{i,j,k})\right] + \frac{\Delta t}{\Delta y} \left[-\rho_{i,j,k}(V_{i,j+1,k+1} - V_{i,j,k}) - \rho_{i,j,k}V_{i,j,k}(A_{i,j+1,0} - A_{i,j,0}) - V_{i,j,k}(\rho_{i,j+1,k+1} - \rho_{i,j,k})\right] + \rho_{i,j,k} + \Delta t[\cos(P_{i,j,k}) + Sc] \quad (5)$$

by assuming Sc as a constant in this study.

Temperature behaviour parameter:

$$T_{i,j,k+1} = \frac{\Delta t}{\Delta x} \left[-V_{i,j,k}(T_{i+1,j,k+1} - T_{i,j,k}) - (\gamma - 1)T_{i,j,k}(V_{i+1,j,k+1} - V_{i,j,k}) + V_{i,j,k}(\ln A_{i+1,j,0} - \ln A_{i,j,0})\right] + \frac{\Delta t}{\Delta y} \left[-V_{i,j,k}(T_{i,j+1,k+1} - T_{i,j,k}) - (\gamma - 1)T_{i,j,k}(V_{i,j+1,k+1} - V_{i,j,k}) + V_{i,j,k}(\ln A_{i,j+1,0} - \ln A_{i,j,0})\right] + T_{i,j,k} \quad (6)$$

The discretization of the PDE based on the Jacobi scheme for each parameter is as follows:

Liquid contents parameter:

$$\rho_{i,j,k+1} = \frac{\Delta t}{\Delta x} [-\rho_{i,j,k}(V_{i+1,j,k+1} - V_{i,j,k}) - \rho_{i,j,k}V_{i,j,k}(A_{i+1,j,0} - A_{i,j,0}) - V_{i,j,k}(\rho_{i+1,j,k+1} - \rho_{i,j,k})] + \frac{\Delta t}{\Delta y} [-\rho_{i,j,k}(V_{i,j+1,k+1} - V_{i,j,k}) - \rho_{i,j,k}V_{i,j,k}(A_{i,j+1,0} - A_{i,j,0}) - V_{i,j,k}(\rho_{i,j+1,k+1} - \rho_{i,j,k})] + \rho_{i,j,k} + \Delta t[\cos(P_{i,j,k}) + Sc] \tag{7}$$

by assuming Sc as a constant in this study.

Temperature behaviour parameter:

$$T_{i,j,k+1} = \frac{\Delta t}{\Delta x} [-V_{i,j,k}(T_{i+1,j,k+1} - T_{i,j,k}) - (\gamma - 1)T_{i,j,k}(V_{i+1,j,k+1} - V_{i,j,k}) + V_{i,j,k}(\ln A_{i+1,j,0} - \ln A_{i,j,0})] + \frac{\Delta t}{\Delta y} [-V_{i,j,k}(T_{i,j+1,k+1} - T_{i,j,k}) - (\gamma - 1)T_{i,j,k}(V_{i,j+1,k+1} - V_{i,j,k}) + V_{i,j,k}(\ln A_{i,j+1,0} - \ln A_{i,j,0})] + T_{i,j,k} \tag{8}$$

The sequential algorithm based on the both numerical schemes was developed for MATLAB computing. The implementation of the sequential algorithm in the MATLAB was as followed:

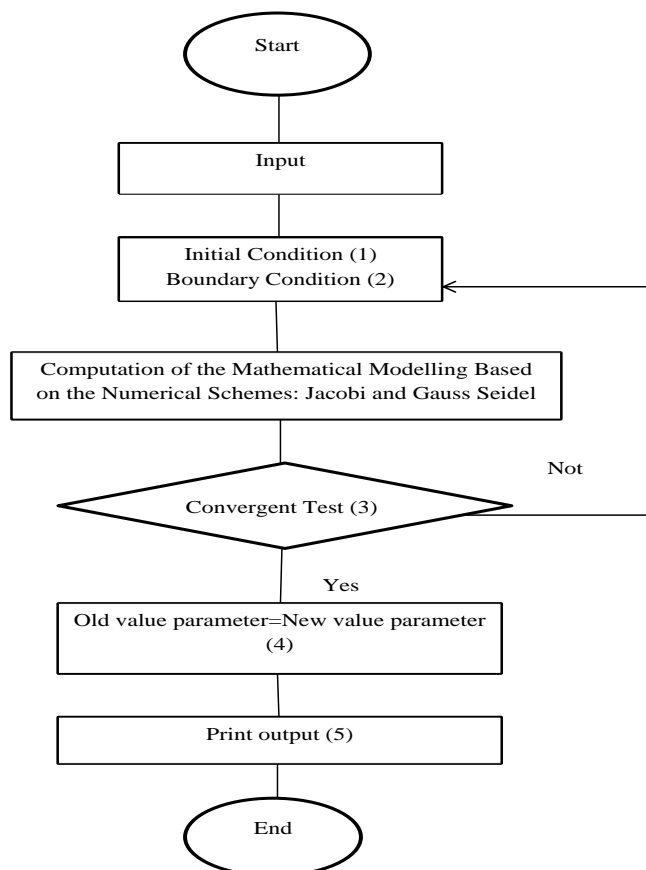


Figure 1: Sequential algorithm

Figure 1 shows that the simulation of the spray drying DIC during the drying and dehydration process by using Gauss Seidel and Jacobi scheme. The simulation starts by putting in the input. The initial and boundary conditions were declared in order to start the computation of the mathematical modeling. Then, the output such as parameters liquid

contents and temperature behaviour of the computation can be printed if the computation is converged.

Result and Discussion

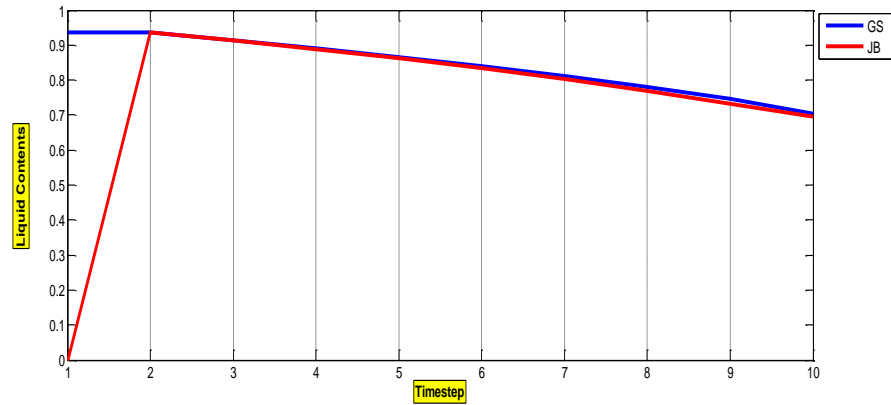


Figure 2: Graph of the liquid contents by using Gauss Seidel and Jacobi schemes

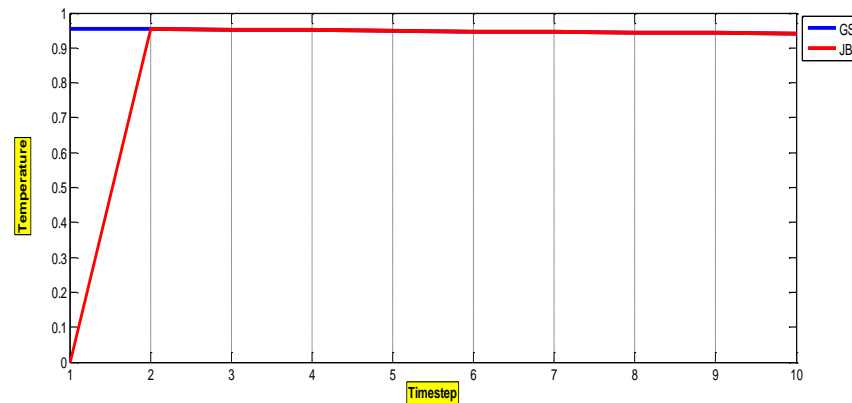


Figure 3: Graph of the temperature behaviour by using Gauss Seidel and Jacobi schemes

Figure 2 and Figure 3 indicate the graph of the liquid contents and temperature behaviour during the drying and dehydration process by using Gauss Seidel and Jacobi schemes respectively. Each graph from the both figures were captured at the space point (2,4) for 10 time steps. As we can see, the graph in the Figure 2 shows the liquid contents by using Gauss Seidel scheme was slightly decreased as the time step increasing compared to the liquid contents by using Jacobi scheme. The temperature by using Gauss Seidel scheme was slightly decreased as the time step for the drying and dehydration increasing compared to the temperature by using Jacobi scheme that slowly decreasing. The temperature of this study was decreased during the drying and dehydration process because of the steam pressure used in the spray drying.

Table 1: Numerical analysis from MATLAB computing

PDE	Continuity		Energy	
Numerical Schemes	Gauss Seidel	Jacobi	Gauss Seidel	Jacobi
Iteration	8	8	8	8
Running Time	0.327619	0.359136	0.312307	0.375064
Convergence	Fast	Slow	Fast	Slow
Computer Complexity	Complicated to set up and program	Simple to set up and program	Complicated to set up and program	Simple to set up and program

The table indicates that the number of iterations for both numerical schemes and PDE was all the same with 8 iterations. From the table, the MATLAB computing result shown that the running time for Gauss Seidel scheme was slower than the Jacobi scheme, though the difference from the running time between the two schemes was small.

From the table, convergence of the Gauss Seidel schemes was faster than Jacobi scheme for the both continuity and energy PDE. The Gauss Seidel scheme was complicated to set up and program compared to the Jacobi scheme which more simple to set up and program.

Conclusion

The Gauss Seidel scheme is more on advantages in order to solve the mathematical model for spray drying DIC. Based on the numerical analysis, we can see that the Gauss Seidel scheme was the suitable scheme to solve the mathematical model in this study compare to Jacobi scheme. According to the running time and convergence, it was proved that Gauss Seidel scheme was the better and efficient scheme to use in the actual experiment so that the risk and computing error can be minimized. Although the Gauss Seidel scheme was complicated to set up and program than Jacobi scheme, the efficiency of the scheme is more important.

Reference

Abdul-Majid Wazwaz. (2002). Partial Differential Equations Method and Applications.

Alias N, Hafizah F. S. S, Ghani A. C. A (2012). Chronology of DIC Technique Based on the Fundamental Mathematical Modeling and Dehydration Impact. *J Food Science Technology*.

Besombes C, B. B. Z, Allaf K (2010). Instant Controlled Pressure Drop Extraction of Lavandin Essential Oils: Fundamentals and Experimental Studies. 6807-6815.

Frydman A, Vasseur J, Moureh J, Sionneau M & Tharrault P (2007). Comparison of Superheated Steam and Air Operated Spray Dryers Using Computational Fluid Dynamics.

Knabner P and Angermann L (2003). Numerical Methods for Elliptic and Parabolic Partial Differential Equations.

Sadripour M, Rahimi A, and Hatamipour M. S (2014). CFD Modeling and Experimental Study of a Spray Dryer Performance. *Chemical Product and Process Modeling* 2014; 9(1): 15–24.

FRACTIONAL-ORDER DIFFERENTIAL EQUATION OF TUMOR-IMMUNE SYSTEM INTERACTION

Norliza Binti Mohd Zain & Anati Binti Ali

Abstract

The purpose of this study is to derive and describe the model for the tumor-immune system interaction using fractional-order differential equations (FODEs) which are naturally related to systems with memory; approximate the numerical solutions of FODEs; evaluate the equilibrium point and stability of the model. Many mathematical model have been proven valuable in understanding the dynamics of the biological systems. However, problem arise since the behaviour of most biological system has memory which is always being neglected. Hence, FODEs are more appropriate to model this biological system. Numerical solution of the resulting systems is being solved using Caputo fractional derivative of order α and implicit Euler's approximation which provide an unconditionally stable method. Numerical simulation using MATLAB software shows the stability and nonstability conditions for disease-free equilibrium and positive equilibrium obtained in terms of a threshold parameter, \mathcal{R}_0 (minimum tumor-clearance parameter or minimum infection free) for each cases. Results obtained confirmed that solution of FODEs plotted for $0.6 \leq \alpha \leq 0.9$ are as stable as their integer-order counterpart which continuously depends on all the previous state.

Keywords : Fractional-Order Differential Equation, Tumor-Immune System.

1. Introduction

Immune system is one of the most fascinating schemes from the point of view of biology and mathematics. It is known to be multifunctional and multipathway, so most immune effectors do more than one job. So thus each function of the immune system is typically done by more than one effector, which make it more robust. That is the reason why we are using FODEs to represent the interaction between tumor and immune system. FODEs are naturally related to systems with memory which exists in this interaction.

Previous study with mathematical modelling using ordinary differential equations with integer order have been proven valuable in understanding the dynamics of biological system [9]. However, the behaviour of most biological systems has memory or aftereffects in which such effects are neglected in the classical integer-order mathematical modeling. In other words, there are some busted points in the surface of the cells where the ordinary (classical) derivative cannot explain [12]. In this kind of domain, FODEs can be used. Apart from that, all the points in a neighborhood of that point are used for the solution of FODEs which indicate that this kind of solution give more accurate result [11, 12]. Hence, there is a growing need to study and use fractional-order differential equations in mathematical modelling of this biological systems. The objectives of this research study comprises of (i) to derive and describe the model for tumor-immune system interaction using fractional-order differential equations (FODEs); (ii) to approximate the numerical solutions of FODEs using implicit Euler's method; and (iii) to evaluate the equilibrium points and the stability of the model. The scope of study include model that are derive using Caputo fractional derivative of order α . And since most of the FODEs do not have an exact analytic solutions, approximation and numerical techniques must be used. Here's for the scope of our study we implement implicit Euler's approximation to solve the FODEs model of tumor-immune system interaction.

2. Literature Review

Fathalla A.Rihan [9] has proposed a model of fractional-order differential equation which includes two effector cells in the immune system $E_1(t), E_2(t)$ which is cytotoxic T cells and natural killer cells interact with cancer tumor cells $T(t)$ represented with a Holling function of type III. This model takes the form of

$$D^\alpha T = aT - r_1TE_1 - r_2TE_2, \tag{2.1a}$$

$$D^\alpha E_1 = -d_1E_1 + \frac{T^2E_1}{T^2 + k_1}, \quad 0 < \alpha \leq 1 \tag{2.1b}$$

$$D^\alpha E_2 = -d_2E_2 + \frac{T^2E_2}{T^2 + k_2}. \tag{2.1c}$$

In this study, we will modify this model of equation (2.1a), (2.1b) and (2.1c) to include three populations of the activated immune system cells, $E(t)$ the tumor cells $T(t)$ and the concentration of IL-2 in the single tumor-site compartment, $I_L(t)$.

Mehdi Shahbazi *et al.* [12] proposed a similar type of mathematical modeling for the circulating lymphocyte population which represents patient health. According to [12], FODEs is chosen to model their systems of interaction to obtain the more accurate results in optimally control application of chemotherapy and to minimize the total tumor while constraining the immune state to stay above a specified threshold. E. Ahmed *et al.* [7] also study the fractional-order model of two immune effectors interacting with the cancer cells due to just a similar reason as stated by [12].

3. Research Methodology

3.1 Fractional Model of Tumor-Immune System

To obtain the fractional-order differential model which include three populations of the activated immune system cells, $E(t)$ the tumor cells $T(t)$ and the concentration of IL-2 in the single tumor-site compartment, $I_L(t)$ we modify equation (2.1a), (2.1b), and (2.1c). We consider the classic bilinear model that includes Holling function of type I. Hence, obtain the interactions of the three populations as follow :

$$D^{\alpha_1} E = s_1 + p_1ET - p_2E + p_3EI_L, \tag{3.1a}$$

$$D^{\alpha_2} T = p_4T(1 - p_5T) - p_6ET, \tag{3.1b}$$

$$0 < \alpha_i \leq 1, \quad i = 1, 2, 3,$$

$$D^{\alpha_3} I_L = s_2 + p_7ET - p_8I_L, \tag{3.1c}$$

with initial conditions

$$E(0) = E_0, T(0) = T_0, I_L(0) = I_{L_0}. \tag{3.2}$$

From a research conducted by [9], the parameters used in equations (3.1a), (3.1b) and (3.1c) and its interpretation are as represented by **Table 3.1**:

Table 3.1. Variables and parameter values used in equation (3.1a), (3.1b), (3.1c)

Variable / Parameters	Interpretation
s_1	External source of the effector cells
s_2	External input of IL-2 into the system
p_1	Antigenicity rate of the tumor (immune response to the appearance of the tumor)
p_2	Rate of death
p_4	Incorporates both multiplication and death of tumor cells
p_5^{-1}	Maximal carrying capacity of the biological environment for tumor cell
p_3	Cooperation rate of effector cells with interleukin-2 parameter
p_6	Rate of tumor cells
p_7	Competition rate between the effector cells and the tumor cells
p_8	Rate loss of parameter of IL-2 cells

In the absence of immunotherapy with IL-2, we have

$$D^{\alpha_1}E = s_1 + p_1ET - p_2E, \quad 0 < \alpha_i \leq 1, \quad i = 1, 2, \tag{3.3a}$$

$$D^{\alpha_2}T = p_4T(1 - p_5T) - p_6ET. \tag{3.3b}$$

3.2 Non-Dimensionalization Of The Bilinear System

We non-dimesionalize the bilinear system by taking the rescaling:

$$\begin{aligned} x &= \frac{E}{E_o}, & y &= \frac{T}{T_o}, & \omega &= \frac{P_4T_o}{t_s}, \\ \theta &= \frac{P_2}{t_s}, & \sigma &= \frac{s_1}{t_sE_o}, & a &= \frac{P_4}{t_s}, \\ b &= p_5T_o, & l &= \frac{P_6E_o}{t_s}, & \tau &= t_s t. \end{aligned} \tag{3.4}$$

Therefore, after the substitution of (3.4) into equation (3.3a) and (3.3b) and also by replacing τ by t , the model becomes

$$D^{\alpha_1}x = \sigma + \omega xy - \theta x, \tag{3.5a}$$

$$D^{\alpha_2}y = ay(1 - by) - xy. \tag{3.5b}$$

3.3 Equilibria and Local Stability of Model

The steady states of the reduced model (3.5a) and (3.5b) are again the intersection of the null clines $D^{\alpha_1}x = 0$ and $D^{\alpha_2}y=0$. If $y=0$, the tumor free equilibrium is at $\bar{\xi}_0 = (\bar{x}, \bar{y}) = (\frac{\sigma}{\theta}, 0)$ where this steady states is always exist, since $\frac{\sigma}{\theta} > 0$.

However, if $y \neq 0$, the steady states are obtained by solving

$$\omega aby^2 - a(\omega + \theta b)y + a\theta - \sigma = 0, \tag{3.6}$$

Where in this case, we have two endemic equilibria, $\bar{\xi}_1$ and $\bar{\xi}_2$:

$$\bar{\xi}_1 = (\bar{x}_1, \bar{y}_1) = \left(\frac{2ab\sigma}{a(b\theta - \omega) - \sqrt{\Delta}}, \frac{a(b\theta + \omega) + \sqrt{\Delta}}{2ab\omega} \right),$$

$$\bar{\xi}_2 = (\bar{x}_2, \bar{y}_2) = \left(\frac{2ab\sigma}{a(b\theta - \omega) + \sqrt{\Delta}}, \frac{a(b\theta + \omega) - \sqrt{\Delta}}{2ab\omega} \right).$$

3.4 Implicit Euler’s Scheme for FODEs

Consider biological models in the form of a system of FODEs of

$$D^\alpha X(t) = F(t, X(t), \mathbf{P}), \quad t \in [0, T], \quad 0 < \alpha \leq 1, \tag{3.7}$$

$$X(0) = X_0.$$

Here $X(t) = [x_1(t), x_2(t), \dots, x_n(t)]^T$, \mathbf{P} is the set of parameters appear in the model. Apply a fractional integral operator to the differential equation (3.7) and incorporate the initial conditions, thus converting the equation into the equivalent equation which gives

$$X(t) = X(0) + \frac{1}{\Gamma(\alpha)} \int_0^t (t - s)^{\alpha-1} F(s, X(s), \mathbf{P}) ds, \tag{3.8}$$

which is also a Volterra equation of the second kind. Define the operator \mathcal{Q} such that

$$\mathcal{Q}X(t) = X(0) + \frac{1}{\Gamma(\alpha)} \int_0^t (t - s)^{\alpha-1} F(s, X(s), \mathbf{P}) ds \tag{3.9}$$

Given model (3.7) and mesh points $T = \{t_0, t_1, \dots, t_N\}$ such that $t_0 = 0$ and $t_N = T$. Then a discrete approximation to the fractional derivative can be obtained by a simple quadrature formula, using the Caputo fractional derivative of order α , $0 < \alpha \leq 1$, and using implicit Euler’s approximation as follows

$$\begin{aligned} D_*^\alpha x_i(t_n) &= \frac{1}{\Gamma(1-\alpha)} \int_0^t \frac{dx_i(s)}{ds} (t_n - s)^{-\alpha} ds \\ &\approx \frac{1}{\Gamma(1-\alpha)} \sum_{j=1}^n \int_{(j-1)h}^{jh} \left[\frac{x_i^j - x_i^{j-1}}{h} + O(h) \right] (nh - s)^\alpha ds \\ &= \frac{1}{(1-\alpha)\Gamma(1-\alpha)} \\ &\times \sum_{j=1}^n \left\{ \left[\frac{x_i^j - x_i^{j-1}}{h} + O(h) \right] \times [(n-j+1)^{1-\alpha} - (n-j)^{1-\alpha}] \right\} h^{1-\alpha} \\ &= \frac{1}{(1-\alpha)\Gamma(1-\alpha)} \frac{1}{h^\alpha} \\ &\times \sum_{j=1}^n [x_i^j - x_i^{j-1}] [(n-j+1)^{1-\alpha} - (n-j)^{1-\alpha}] + \frac{1}{(1-\alpha)\Gamma(1-\alpha)} \\ &\times \sum_{j=1}^n [x_i^j - x_i^{j-1}] [(n-j+1)^{1-\alpha} - (n-j)^{1-\alpha}] O(h^{2-\alpha}). \end{aligned}$$

Setting

$$\varrho(\alpha, h) = \frac{1}{(1-\alpha)\Gamma(1-\alpha)} \frac{1}{h^\alpha} = \frac{1}{\Gamma(2-\alpha)} \frac{1}{h^{\alpha'}}, \tag{3.10}$$

$$\omega_j^\alpha = j^{1-\alpha} - (j-1)^{1-\alpha},$$

(where $\omega_1^\alpha = 1$).

The first-order approximation method for the computation of Caputo's fractional derivative is then given by the expression

$$D_*^\alpha x_i(t_n) = \varrho(\alpha, h) \sum_{j=1}^n \omega_j^\alpha (x_i^{n-j+1} - x_i^{n-j}) + O(h). \tag{3.11}$$

3.5 Numerical Computation

After some replacement on the left hand side of equation (3.5a) with equation of (3.11), we have

$$x_n = \frac{\varrho(\alpha, h)\omega_1^\alpha x_{n-1} + \sigma - \varrho(\alpha, h) \sum_{j=2}^n \omega_j^\alpha (x_{n-j+1} - x_{n-j})}{\varrho(\alpha, h)\omega_1^\alpha - \omega y_{n-1} + \theta}, n \geq 2, \tag{3.12}$$

where, $\varrho(\alpha, h)\omega_1^\alpha - \omega y_{n-1} + \theta \geq 1$.

Hence, same goes to the second equation of (3.5b). After some replacement on the left hand side of equation (3.5b) with equation of (3.11), we get

$$y_n = \frac{ay_{n-1} + \varrho(\alpha, h)\omega_1^\alpha y_{n-1} - \sum_{j=2}^n \omega_j^\alpha (y_{n-j+1} - y_{n-j})}{\varrho(\alpha, h)\omega_1^\alpha + ab + x_n}, n \geq 2. \tag{3.13}$$

Numerical computation was performed using equation (3.12) and (3.13) using MATLAB software and the data was collected for 200 time steps for $0.6 \leq \alpha \leq 1$. Note that, for the numerical computation there is only initial condition for variables x and y provided. For interaction between tumor cells and effector cells, there is no boundary condition. Besides that, the stability and convergence were analysed for different value of α based on the graph illustrated.

4. Result and Discussion

1. Case 1 : Threshold Frequency \mathcal{R}_0 (Minimum Infection Free) < 1 .

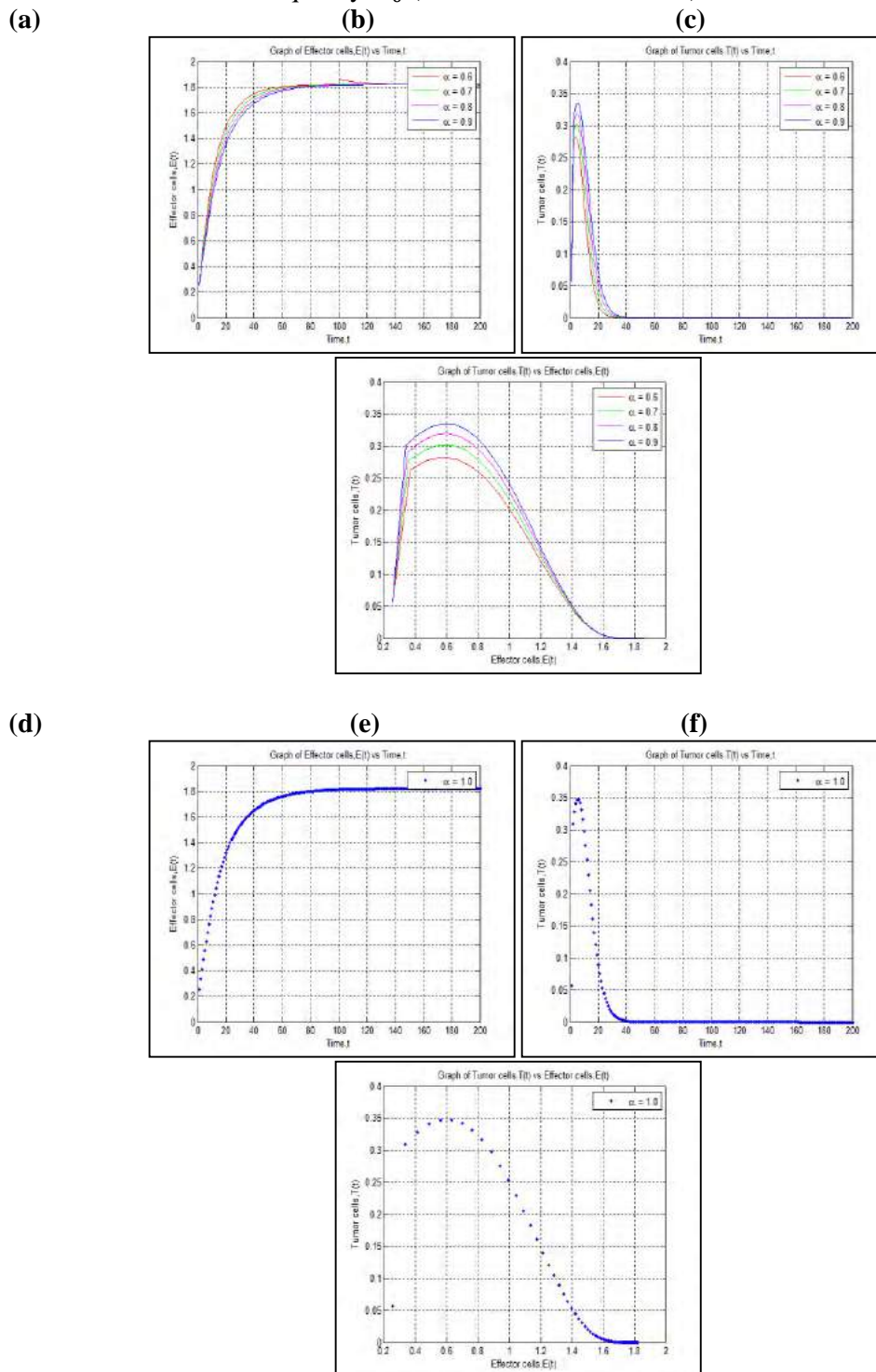


Figure 4.1 : Numerical simulation of the FODEs of (3.9a) and (3.9b) when $a = 0.636$, $b = 0.002$, $\omega = 0.1184$, $\theta = 0.1747$, and $\sigma = 0.3181$ for $0.6 \leq \alpha \leq 0.9$ and $\alpha = 1$.

For cases where $\mathcal{R}_0 = \frac{a\theta}{\sigma} < 1$, the endemic tumor does not exist since the whole tumor cells population is totally eradicated after 40 days. By referring to **Figure 4.1(a)-4.1(f)**, one of the observation that can be made is that the greater and the closer the value of α to its integer-order value of $\alpha = 1$ then the closer the solution to their integer-order

counterpart. Whereas, **Figure 4.1(c)** and **Figure 4.1(f)** shows clearly that the infection free steady state $\bar{\xi}_0 = (1.8208, 0)$ is locally asymptotically stable when $\mathcal{R}_0 = \frac{a\theta}{\sigma} < 1$ since all trajectories converge to a similar equilibrium point of $\bar{\xi}_0$ regardless of any value of α .

3. Case 2 : Threshold Frequency \mathcal{R}_0 (Minimum Infection Free) = 1.

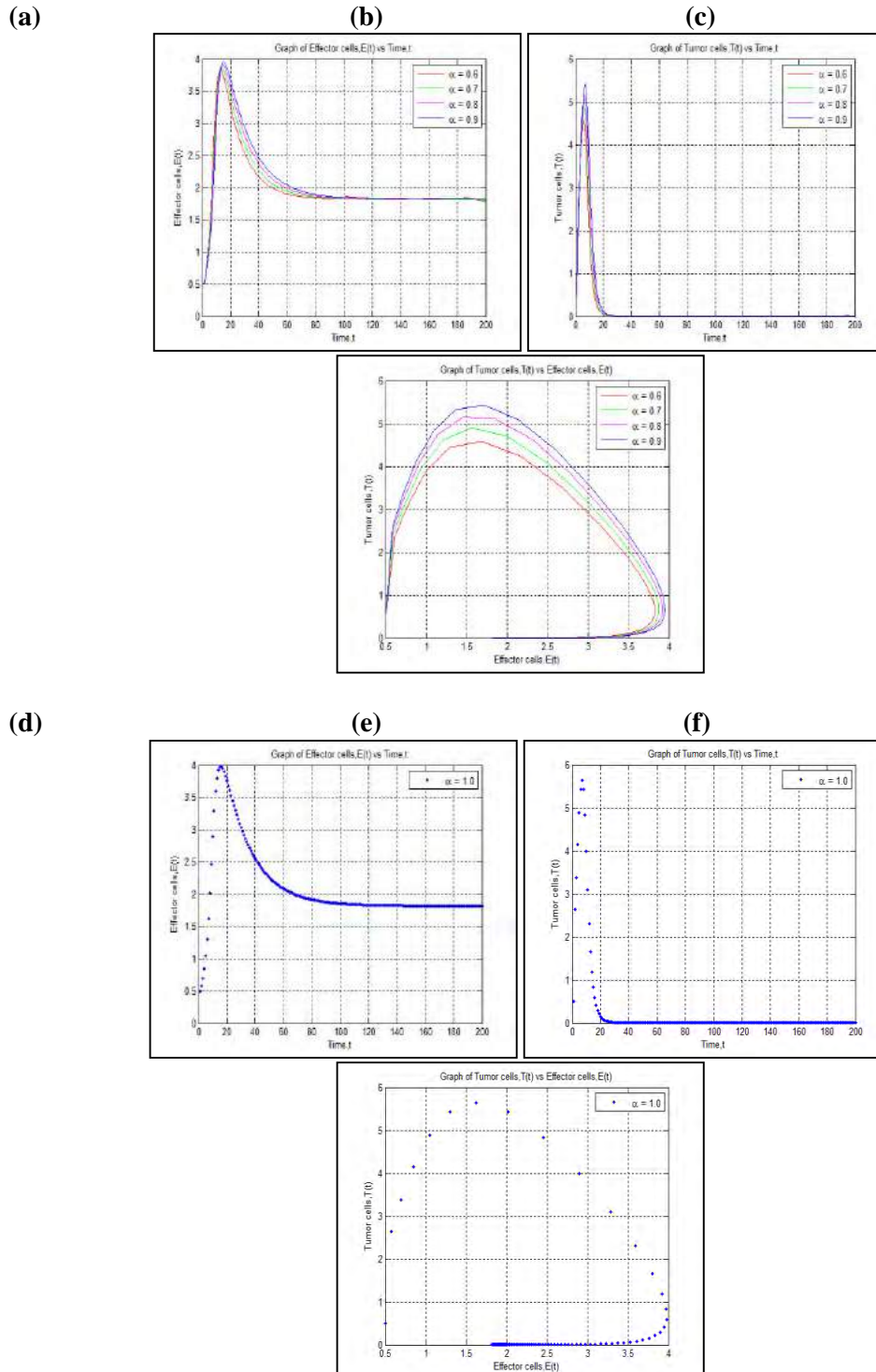
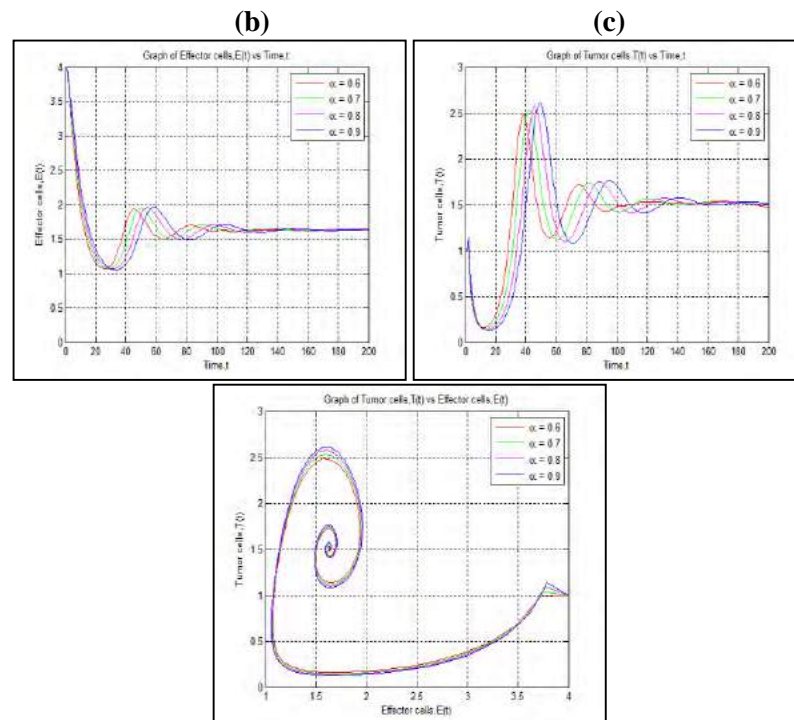


Figure 4.2: Numerical simulation of the FODEs of (3.9a) and (3.9b) when $a = 1.8209$, $b = 0.002$, $\omega = 0.1184$, $\theta = 0.1747$, and $\sigma = 0.3181$ for $0.6 \leq \alpha \leq 0.9$ and $\alpha = 1$.

For cases where $\mathcal{R}_0 = \frac{a\theta}{\sigma} = 1$, immune response by the effector cells does not fully eradicate the tumor cell population but it does reduce its population number. Thus, only a very small part of tumor cells survives. From **Figure 4.2(a)-4.2(f)** by comparison of the illustrated graph for both tumor cells and effector cells plotted for $0.6 \leq \alpha \leq 0.9$ and $\alpha = 1$ we can see that for any value of α the solution is stable since it does converge to a similar steady state value. As fractional-order of α getting closer to its integer-order of $\alpha = 1$, so does the solution also getting closer to its integer-order solution. From **Figure 4.2(c)** and **Figure 4.2(f)**, we can see clearly that $\bar{\xi}_2 = (1.8209, 0.0001)$ is a stable node equilibrium point since all trajectories regardless of any value of α converge to a similar steady state value and this mean that the endemic state persist. However, it exist in terms of a very small controllable number of tumor cells as represented in the illustrated figure.

3. Case 3 : Threshold Frequency \mathcal{R}_0 (Minimum Infection Free) > 1 .

(a)



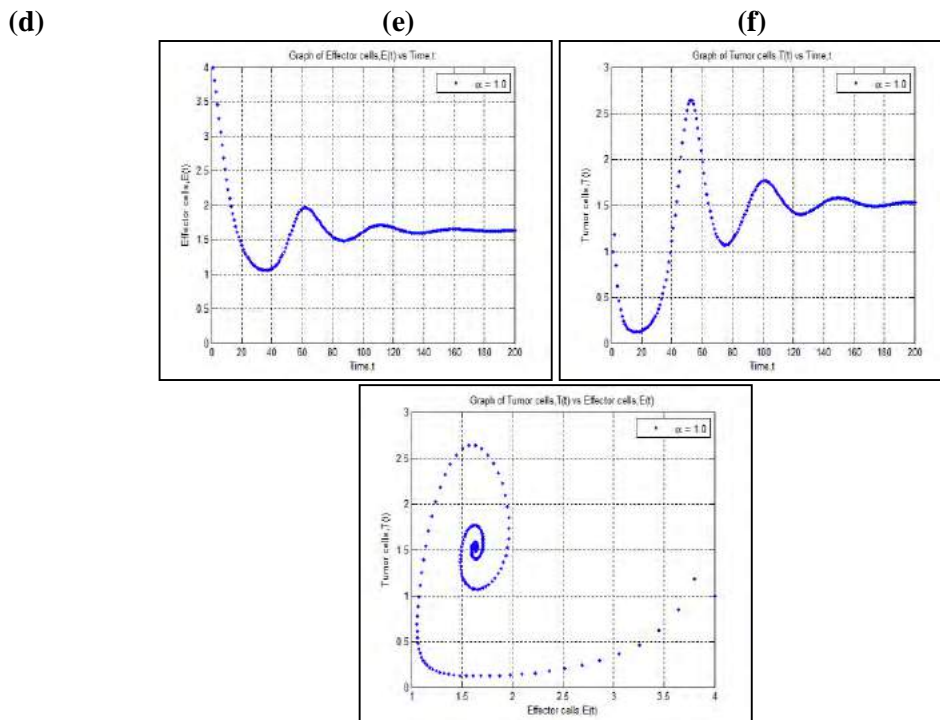


Figure 4.3 : Numerical simulation of the FODEs of (3.9a) and (3.9b) when $a = 1.636$, $b = 0.002$, $\omega = 0.1184$, $\theta = 0.3747$, and $\sigma = 0.3181$ for $0.6 \leq \alpha \leq 0.9$ and $\alpha = 1$.

For cases where $\mathcal{R}_0 = \frac{a\theta}{\sigma} > 1$, its indicates that the tumor is persists. By referring to **Figure 4.3(a)-4.3(f)** where our system evolves towards a controllable population of tumor cells in a damped oscillating way until it reach its steady state approximately after 160 days. On the other hand, another result that can be drawn from **Figure 4.3(a)-4.3(f)** which illustrated the number of effector cells and tumor cells for $0.6 \leq \alpha \leq 1$ is that as value of fractional-order of α varied closer to its integer-order of $\alpha = 1$, the solutions for the number of effector cells and tumor cells are also getting closer and converge to its integer-order solution. From **Figure 4.3(c)-4.3(f)**, we can conclude that the endemic state $\bar{\xi}_2 = (1.6310, 1.5175)$ is locally asymptotically stable focus equilibrium point when $\mathcal{R}_0 = \frac{a\theta}{\sigma} > 1$ since regardless of any value of α , all the trajectories is converged to a similar point of steady state of $\bar{\xi}_2$.

5. Conclusion

Threshold parameter, $\mathcal{R}_0 = \frac{a\theta}{\sigma} < 1$ means that the endemic infected state does not exist. Whereas, threshold parameter, $\mathcal{R}_0 = \frac{a\theta}{\sigma} = 1$ represent a transition stage for tumor-immune interaction before it enter a condition of $\mathcal{R}_0 = \frac{a\theta}{\sigma} > 1$ which means that the endemic infected state persists. As a conclusion, all the three objectives has been fulfilled. The fractional-order differential equation can be used to describe the dynamics of the tumor-immune interaction. Certain threshold parameter describe by numerical simulation seems possible to reduce or even eliminate the tumor cells population. Hence, this results may give insight to the infectious disease specialist.

References

- 1 Oki K. Dzivenu, D. Phil., and Jill O'Donnell-Tomey (2003). "*Cancer and Immune System: The Vital Connection*". Doctor Philosophy. Cancer Research Institute.
- 2 Minaya Villasana, and Ami Radunskaya (2003). A Delay Differential Equation Model For Tumor Growth. *Mathematical Biology*. 47(2003), 270-294.
- 3 L. G. De Pillis, D. G. Mallet and A. E. Radunskaya (2006). Spatial Tumor-Immune Modeling. *Computational And Mathematical Methods In Medicine*.7(2-3), 159-176.
- 4 N.M. Berezhnaya (2010). Interaction Between Tumor And Immune System. *The Role Of Tumor Cell Biology*. 32(3), 159-166.
- 5 Carlo Cattani, and Armando Ciancio (2010). Second Order Models Of Tumor-Immune System Competition. *The International Conference "Differential Geometry-Dynamical Systems 2009"*. 8-11 October 2009. Burcharest-Romania, 31-40.
- 6 Raluca Eftimie, Jonathan L. Bramson, and David J.D. Earn (2010). Interaction Between The Immune System And Cancer. *A Brief Review Of Non-Spatial Mathematical Models*. 73(2011), 2-32.
- 7 E. Ahmed, A.H. Hashis, and F.A. Rihan (2012). On Fractional Order Cancer Model. *Journal Of Calculus and Applications*. 3(2), 1-6.
- 8 Urszula Ledzewicz, and Mozhdeh Sadat Faraji Mosalman (2013). Optimal Controls For A Mathematical Model Of Tumor-Immune Interactions Under Targeted Chemotherapy With Immune Boost. *Discrete And Continuous Dynamical Systems Series B*. 18(4), 1031-1051.
- 9 Fathalla A. Rihan (2013). Numerical Modelling of Fractional-Order Biological Systems. *Abstract and Applied Analysis*. 2013(816803), 1-11.
- 10 Senol Kartal (2014). Mathematical Modeling And Analysis Of Tumor-Immune System Interaction By Using Lotka-Volterra Predator-Prey Like Model With Piecewise Constants Arguments. *Periodicals Of Engineering And Natural Sciences*. 2(1), 7-12.
- 11 G.H. Erjaee, M.H. Ostadzad, S. Amanpour, and K.B. Lankarani (2013). Dynamical Analysis Of The Interaction Between Effector Immune And Cancer Cells And Optimal Control Of Chemotherapy. *Nonlinear Dynamics, Psychology, And Life Sciences*. 17(4), 449-463.
- 12 Mehdi Shahbazi, G Hussian Erjaee, and Hoda Erjaee (2014). Dynamical Analysis Of Chemotherapy Optimal Control Using Mathematical Model Presented By Fractional Differential Equations, Describing Effector Immune And Cancer Cells Interactions. *Journal Of Pharmacy And Pharmaceutical Sciences*. 3(3), 5-18.
- 13 N. Varalta, A.V. Gomes, and R.F. Camargo (2014). A Prelude To The Fractional Calculus Applied To Tumor Dynamic. *Tendencias Em Matematica Aplicada E Computacional*. 15(2), 211-221.
- 14 Eric Vivier et al. (2011). Innate or Adaptive Immunity? The Example of Natural Killer Cells. *Science*. 331(44), 44-49.
- 15 F. A. Rihan, D. H. Abdelrahman, and F. Al-Maskari (2014). Delay Differential Model for Tumour-Immune Response with Chemoimmunotherapy and Optimal Control. *Computational and Mathematical Methods in Medicine*. 2014(982978). 1-15.
- 16 M. Kolev, E. Kozłowska, and M.Lachowicz (2005). A Mathematical Model for Single Cell Cancer-Immune System Dynamics. *Mathematical and Computer Modelling*. 41(2005), 1083-1095.
- 17 Elena De Angelis, and Pierre-Emmanuel Jabin (2003). Qualitative Analysis of a Mean Field Model of Tumor-Immune System Competition. *Math. Models Meth. Appl. Sci.* 1-24.
- 18 Gurpreet Kaur, and Naseem Ahmad (2014). On Study of Immune Response to Tumor Cells in Prey-Predator System. *International Scholarly Research Notices*. 2014(346597), 1-8.

- 19 Manju Agarwal, and Archana S. Bhadauria (2013). A generalised Prey-Predator Type Model of Immunogenic Cancer with The Effect of Immunotherapy. *International Journal of Engineering Science and Technology*. 5(1), 66-84.
- 20 c. Mathematical Modeling of Interaction Between Tumor and Immune Cells. *International Journal of Engineering Science and Technology*. 6(4), 98-111.

Integral Equations with Degenerate Kernel and Some Applications

Norsharmila binti Osman & Assoc Prof Dr Mukhiddin Muminov

Abstract

The theory of integral equations has close contacts with many different areas of mathematics. This research are generally about the Fredholm integral equation with degenerate kernel and the spectral analysis of the lattice two-particle Schrödinger operator. Within this research, we obtained the existence of solutions of non-homogeneous integral equation. Also, we obtain the condition of existence of existing of solutions for homogeneous integral equations with degenerate kernel. Applying the obtained results we get the condition of existence of the eigenvalues for two particle Schrödinger operator. This study deal with linear integral equations that is, equation involving an unknown function with appears under an integral sign. Such equations occur widely in diverse areas of applied mathematics and physics. One obvious reason for using the integral equation rather than differential equations is that all the conditions specifying the initial value problems for a differential equation can often be condensed into a single integral equation. There are various methods to solve an integral problem but this study is focused on degenerate kernel method of Fredholm integral equation problem. We also used *Wolfram Mathematica 9.0 software* to solve some problems.

Keywords: Integral Equation with degenerate Kernel, two-particle Schrödinger operator.

Introduction

The theory of integral equations has close contacts with many different areas of mathematics. Many problems in the field of ordinary and partial differential equations can be recast as integral equations. Many existence and uniqueness results can then be derived from the corresponding result from integral equations. Many problems of mathematical physics

can be stated in the form of integral equations. In many ways one can view the subjects of integral equations as an extension of linear algebra and precursor of modern functional analysis. Especially in dealing with linear integral equations the fundamental concepts of linear vector spaces, eigenvalues, and eigenfunctions will play a significant role. The idea of an integral equation comes from differential equation. Some unknown function is defined in term of a relation between its derivatives. From this relation it is possible, in theory, to obtain the unknown function which is defined apart from a number or arbitrary constants for ordinary differential equations, or a number of arbitrary functions for partial differential equations. The function is completely defined by specifying that some relations hold for it, or its derivatives, or a mixture of them at some points or over some domain.

Literature review

The term integral equation was first used by Paul du Bois-Reymond in 1888. In general, an integral equation is an equation where an unknown function occurs under an integral.

$$g(x) = f(x) + \int_a^b k(x, y)f(y)dy, \quad (1)$$

where $k(x, y)$ is a function of two variables called the *Kernel* or *Nucleus* of an integral equation. We are given functions of $g(x), k(x, y), [a, b]$ and wish to determine $f(x)$. Some problems have their mathematical representations appear directly, and in every natural way, in term of integral equation. Other problems, whose direct representation is in differential equations and their auxiliary conditions, may also be reduced to integral equations.

Methodology

We consider the Fredholm integral equation of the second kind is defined as

$$f(x) = g(x) - \int_a^b K(x, y)f(y)dy$$

(2)

Definition :The kernel $K(x, y)$ is said to be degenerate (separable) if it can be written as a sum of terms, each being a product of a function of x and a function of y

$$\text{Thus, } K(x, y) = \sum_{j=1}^n u_j(x)v_j(y) \quad (3)$$

We substitute equation (3) into equation (2)

$$\begin{aligned} f(x) &= g(x) - \int_a^b \left[\sum_{j=1}^n u_j(x)v_j(y) \right] f(y) dy \\ &= g(x) - \sum_{j=1}^n \left[u_j(x) \int_a^b v_j(y) f(y) dy \right] \end{aligned} \quad (4)$$

Let,

$$c_j = \int_a^b v_j(y) f(y) dy$$

then,

$$f(x) = g(x) - \sum_{j=1}^n c_j u_j(x) \quad (5)$$

$$f(y) = g(y) - \sum_{j=1}^n c_j v_j(y)$$

$$c_j = \int_a^b v_j(y) [g(y) - \sum_{j=1}^n c_j v_j(y)]$$

After summarization,

$$c_1 = b_1 - [c_1 d_{11} + c_2 d_{12} + \dots c_n d_{1n}]$$

$$c_2 = b_2 - [c_1 d_{21} + c_2 d_{22} + \dots c_n d_{2n}]$$

⋮

$$c_n = b_n - [c_1 d_{n1} + c_2 d_{n2} + \dots c_{n-1} d_{n(n-1)} + c_n d_{nn}]$$

Where

$$d_{ij} = \int_a^b u_i(y)v_j(y) d(y), \text{ And } b_i = \int_a^b v_i(y)g(y)d(y)$$

Now, we let

$$\Delta = \det \begin{vmatrix} 1 + d_{11} & d_{12} & \dots d_{1n} \\ d_{21} & 1 + d_{22} & \dots d_{2n} \\ d_{n1} & \dots & 1 + d_{nn} \end{vmatrix} \neq 0$$

Where Δ is called Fredholm determinant of equation. If $\Delta = 0$, then non-homogeneous integral equation has no solution. So now, we let $\Delta \neq 0$ and by using Cramer's rule, we solve;

$$c_j = \frac{\Delta_j}{\Delta}, j = 1, 2, \dots, n$$

Therefore, equation (3) has unique solution.

Result and conclusion

Theorem 1

Let $z \notin [0, 2]$ and $\Delta_c(z)\Delta_s(z) \neq 0$ then, the resolvent $(h - zI)^{-1}$ of the operator h exist and has the form

$$(h - zI)^{-1}g(x) = \frac{g(x)}{1 - \cos x - z} + \sum_{k=0}^n [c_x \cos kx + s_x \sin kx]$$

Where (c_1, \dots, c_n) and (s_1, \dots, s_n) are the solutions of linear system equation determined by:

$$\Delta_c(z) = \begin{pmatrix} 1 - B_{11} & -B_{12} & \dots & -B_{1n} \\ B_{12} & 1 - B_{22} & \dots & -B_{2n} \\ \vdots & \vdots & \dots & \vdots \\ B_{n1} & + B_{n2} & \dots & 1 - B_{nn} \end{pmatrix} \quad (6)$$

$$\Delta_s(z) = \begin{pmatrix} 1 - D_{11} & -D_{12} & \dots & -D_{1n} \\ D_{12} & 1 - D_{22} & \dots & -D_{2n} \\ \vdots & \vdots & \dots & \vdots \\ D_{n1} & + D_{n2} & \dots & 1 - D_{nn} \end{pmatrix} \quad (7)$$

Theorem 2

The number of $z \notin [0,2]$ is an eigenvalue of the operator h if and only if $\Delta_c(z)\Delta_s(z)=0$

When $n = 2$,

$$\Delta_c(z) = \begin{vmatrix} 1 - B_{11} & -B_{12} \\ B_{21} & 1 - B_{22} \end{vmatrix}$$

$$\Delta_s(z) = \begin{vmatrix} 1 - D_{11} & -D_{12} \\ D_{21} & 1 - D_{22} \end{vmatrix}$$

Then, we can find the value of $\Delta_c(z)$ and $\Delta_s(z)$ by calculate the equation below for $l = 1,2$ and $k = 1,2$

$$B_{lk} = \int_0^{2\pi} \frac{\cos lx \cos kx}{1 - \cos x - Z} dx$$

$$D_{lk} = \int_0^{2\pi} \frac{\sin lx \sin kx}{1 - \cos x - Z} dx$$

From the calculation, we get

$$B_{11} = \frac{2\pi}{\sqrt{(1-Z)^2 - 1}} - \frac{2\pi}{(1-Z) + \sqrt{(1-Z)^2 - 1}}$$

$$B_{22} = -12\pi + 28\pi z - 24\pi z^2 + 8\pi z^3 - \frac{6\pi}{\sqrt{(z-1)^2 - 1}} + \frac{8\pi(z-1)^4}{\sqrt{(z-1)^2 - 1}} - \frac{8\pi}{(z-1) + \sqrt{(z-1)^2 - 1}}$$

$$B_{12} = B_{21} = -4\pi + 8\pi z - 4\pi z^2 - \frac{4\pi(z-1)^3}{\sqrt{(z-1)^2 - 1}} + \frac{2\pi(z-1)}{\sqrt{(z-1)^2 - 1}}$$

and

$$D_{11} = \frac{2\pi}{(z-1) + \sqrt{(z-1)^2 - 1}}$$

$$D_{22} = 12\pi - 28\pi z + 24\pi z^2 - 8\pi z^3 - \frac{8\pi}{(z-1) + \sqrt{(z-1)^2 - 1}} + \frac{8\pi}{\sqrt{(z-1)^2 - 1}} - \frac{8\pi(z-1)^4}{\sqrt{(z-1)^2 - 1}}$$

$$D_{12} = D_{21} = -10\pi + 8\pi z - 4\pi z^2 - \frac{4\pi(z-1)}{\sqrt{(z-1)^2 - 1}} - \frac{4\pi(z-1)^3}{\sqrt{(z-1)^2 - 1}}$$

Therefore, we can proceed to find $\Delta_c(z)$ and $\Delta_s(z)$

$$\Delta_c(z) = \begin{vmatrix} 1 - B_{11} & -B_{12} \\ B_{21} & 1 - B_{22} \end{vmatrix} = (1 - B_{11})(1 - B_{22}) - (-B_{12})(B_{21}).$$

Since $B_{12} = B_{21}$, we have

$$\begin{aligned} \Delta_c(z) &= (1 - B_{11})(1 - B_{22}) - (B_{12})^2, \\ &= 1 - B_{22} - B_{11} + (B_{11}) \cdot (B_{22}) - (B_{12})^2, \\ &= 1 - \left(-12\pi + 28\pi z - 24\pi z^2 + 8\pi z^3 - \frac{6\pi}{\sqrt{(z-1)^2 - 1}} + \frac{8\pi(z-1)^4}{\sqrt{(z-1)^2 - 1}} \right. \\ &\quad \left. - \frac{8\pi}{(z-1) + \sqrt{(z-1)^2 - 1}} \right) \\ &\quad - \left(\frac{2\pi}{\sqrt{(z-1)^2 - 1}} - \frac{2\pi}{(z-1) + \sqrt{(z-1)^2 - 1}} \right) \\ &\quad + \left(\frac{2\pi}{\sqrt{(z-1)^2 - 1}} - \frac{2\pi}{(z-1) + \sqrt{(z-1)^2 - 1}} \right) \\ &\quad \cdot \left(-12\pi + 28\pi z - 24\pi z^2 + 8\pi z^3 - \frac{6\pi}{\sqrt{(z-1)^2 - 1}} \right. \\ &\quad \left. + \frac{8\pi(z-1)^4}{\sqrt{(z-1)^2 - 1}} - \frac{8\pi}{(z-1) + \sqrt{(z-1)^2 - 1}} \right) \\ &\quad - \left(-4\pi + 8\pi z - 4\pi z^2 - \frac{4\pi(z-1)^3}{\sqrt{(z-1)^2 - 1}} + \frac{2\pi(z-1)}{\sqrt{(z-1)^2 - 1}} \right)^2, \end{aligned}$$

By using *Maple 12.0* software, we get the value of z as

$$z = 0.4810484559.$$

Then

$$\Delta_s(z) = \begin{vmatrix} 1 - D_{11} & -D_{12} \\ D_{21} & 1 - D_{22} \end{vmatrix} = (1 - D_{11})(1 - D_{22}) - (-D_{12})(D_{21}).$$

Since $D_{12} = D_{21}$, we have

$$\begin{aligned} \Delta_s(z) &= 1 - D_{22} - D_{11} + (D_{11}) \cdot (D_{22}) - (D_{12})^2, \\ &= 1 - \left(12\pi - 28\pi z + 24\pi z^2 - 8\pi z^3 - \frac{8\pi}{(z-1) + \sqrt{(z-1)^2 - 1}} + \frac{8\pi}{\sqrt{(z-1)^2 - 1}} \right. \\ &\quad \left. - \frac{8\pi(z-1)^4}{\sqrt{(z-1)^2 - 1}} \right) - \left(\frac{2\pi}{(z-1) + \sqrt{(z-1)^2 - 1}} \right) \\ &\quad + \left(\frac{2\pi}{(z-1) + \sqrt{(z-1)^2 - 1}} \right) \\ &\quad \cdot \left(12\pi - 28\pi z + 24\pi z^2 - 8\pi z^3 - \frac{8\pi}{(z-1) + \sqrt{(z-1)^2 - 1}} \right. \\ &\quad \left. + \frac{8\pi}{\sqrt{(z-1)^2 - 1}} - \frac{8\pi(z-1)^4}{\sqrt{(z-1)^2 - 1}} \right) \\ &\quad - \left(10\pi + 8\pi z - 4\pi z^2 - \frac{4\pi(z-1)}{\sqrt{(z-1)^2 - 1}} - \frac{4\pi(z-1)^3}{\sqrt{(z-1)^2 - 1}} \right)^2 \end{aligned}$$

By using *Maple 12.0* software, we get the value of z as

$$z = 2.171218478$$

Since z has numerical value, therefore our linear system equation has some solution.

Conclusion and Recommendation.

we presented more details about integral equation including the classification of integral equations and some example of its applications by using real problem. Also, we presented several definitions that we were used in applications. We discussed about the method to solve our problem. In general, we discussed how to solve Fredholm integral equation. We also presented some problems which are solved by using *Wolfram Mathematica 9.0 Software*. In addition, we presented the spectral analysis of the lattice two-particle Schrödinger operator. Theorem 4.1 is discussing about the spectral analysis whereas Theorem 4.2 is about eigenvalue problem. As the result, we found the value of z by using *Maple 12.0* software. This shown, our linear system equations has some solution. This study has achieved its objectives to study the Fredholm integral equation with degenerate kernel and to describe the condition existing of solutions in sense of Fredholm determinant. Since the study has only focused on the Fredholm integral equation, it is recommended that further studies to be carried out by others to solve the integral equation with another method. Furthermore, further research is required to explore the different types of integral equation and its wider applications in real life.

References

- F.Porter (2012), *Integral Equation*, PhysicsRevision 141223.
- H.Hochstadt. (1973) *Integral Equations*, United States of America, John Wiley & Sons, Ins.
- LI.G.Chambers. (1976) *Integral Equations: A Short Course*, East Kilbride, Scotland, Great Britain, Thomson Litho Ltd.
- G.Afken, and H.Weber. (2000) *Mathematical Methods for Physicists*, Harcourt, Academic Press.
- A.J.Jerry. (1985) *introduction to integral equations with applications*, New York and Basel, Marcell Dekker, INC.
- William J.Parnell (2013). *Greens Functions, integral equations and applications*, Spring.
- P.Kamal.(1971).*Linear Integral Equations:Theory and Technique*, Academic Press inc. (London) LTD.

I.Shingareva, C.Lizarraga-Celeya. (2007,2009) *Maple and mathematica*, Germany, Springer-Verlag.

S.Albeverio, S.N.Lakaev, K.A.Makarov,Z.I.Muminov, The threshold effects for the two particle Hamiltonians.Common.Math.Phys.262,91-115(2006).

M.I.Muminov,A.M.Khurramov. *Spectral Properties of A Two-Particle Hamiltonian on A Lattice*theoretical And Mathematical Physics,2013,177:3,pp.16931705.

M.I.Muminov,positivity of the two-particle Hamiltonian on a lattice.teoret.Mat.Fiz.,153:3(2007),381387.

Boutet de Monvel,A.,Sahbani,J.: On The Spectral Properties of Discrete *Schödinger operators: (the Multi-dimensional Case)*.Rev.Math.Phys. 11, 10611078 (1999)

H.Isozaki, E.Korotyaev.Inverseproblems,*Trace Formulae for Discrete Schödinger Operators*. Annales Henri Poincare, Volume 13, Issue 4 (2012), pp 751-788

M.I.Muminov,A M. Khurramov.*Multiplicity of virtual levels at the lower edge of the continuous spectrum of a two-particle Hamiltonian on a lattice*. Theoretical and Mathematical Physics, 180(3): 10401050(2014)

M.I.Muminov, A. M. khurramov. *Spectral Properties of Two Particle Hamiltonian on One-Dimensional Lattice*. Ufa Mathematical Journal. Volume 6. No 4(2014).Pp.102-110

P.R.HalmosandV.S.Sunder, *Bounded Integral Operators on L^2 Spaces*, Springer Verlag, New York. 1978.

H.Bristol Dwight. (1961). *Tables of Integrals and Other Mathematical Data*,United State of Amarica,The Macmillan Company.